

Cyclopropenium Ions Catalyzed Organic Transformations and Their Applications in the Total Synthesis of Resveratrol-based Natural Products

Pavit Kumar Ranga

*A thesis submitted for the partial fulfillment
of the degree of Doctor of Philosophy*



Department of Chemical Sciences

Indian Institute of Science Education and Research (IISER) Mohali

Sector 81, Knowledge City, S. A. S. Nagar, Manauli PO, Mohali, 140306 Punjab, India.

November 2023

Dedicated To
My beloved family
for their love and affection

Declaration

The work presented in this thesis titled **“Cyclopropenium Ions Catalyzed Organic Transformations and Their Applications in Total Synthesis of Resveratrol-based Natural Products”** has been carried out by me under the supervision of **Dr. R. Vijaya Anand** in the Department of Chemical Sciences, Indian Institute of Science Education and Research (IISER) Mohali, Punjab.

This work has not been submitted in part or full for a degree, diploma, or fellowship to any other university or institute.

Whenever contributions of others are involved, every effort is made to indicate this clearly with due acknowledgments of collaborative work and discussions. This thesis is a bonafide record of original work done by me, and all sources listed within have been detailed in the bibliography.

Pavit Kumar Ranga

In my capacity as the supervisor of the candidate's thesis work, I certify that the above statements by the candidate are true to the best of my knowledge.

Dr. R. Vijaya Anand

Acknowledgments

My Ph.D. journey was a great experience and learning phase for me personally and professionally. The most important thing I realized during the Ph.D. is to keep patience and consistency in work, even if it is not going well. I made unforgettable memories with the people of the **Indian Institute of Science Education and Research (IISER)**, Mohali.

First and foremost, I would like to acknowledge my Ph.D. supervisor **Prof. R. Vijaya Anand**, for giving me a chance to conduct my Ph.D. research in his Lab. I am thankful for his continued motivation, support, and scientific suggestions during my doctoral studies. It has been my fortune to work under his unwavering supervision, as a result of which I have developed a good attitude, diligence, and problem-solving skills. I appreciate his idea that working with a free mind will help us to finish our job more efficiently. He has enriched me with his kind-heartedness, imaginative thoughts, and enthusiasm towards science throughout my research period, which encouraged me to boost my growth as a researcher. I am grateful that he has given me the freedom to pursue my interests in research work. He motivated me to learn to do good research despite publishing the article. After this wonderful journey, I can see how much I've changed as a scholar under his guidance.

I would like to thank my Doctoral Committee Members, Dr. Sugumar Venkataramani, and Dr. S. Arulananda Babu, for their insightful comments and suggestions, and also for spending their precious time assessing my research improvement on an annual basis. I would also acknowledge Dr. Sripada S. V. Ramasastry for his valuable suggestions during my Ph.D.

I wish to thank our former Director, Professor N. Sathyamurthy, Prof. Debi P. Sarkar, and Director, Prof. J. Gowrishankar for providing the world-class infrastructure and facilities. I would like to thank our former Head of Department (HOD), Prof. K. S. Viswanathan, Dr. S. Arulananda Babu, and Head of Department (HOD), Dr. Sanjay Singh for valuable suggestions and for providing the facilities at the Department of Chemical Sciences. I am also thankful to IISER Mohali for NMR, HRMS, IR, departmental X-ray facilities, and other facilities.

I am very grateful to all the faculty members of the Department of Chemical Sciences for allowing me to use the departmental facilities.

Furthermore, I also owe this success to my brilliant labmates Dr. Vir Reddy, Dr. Panjab Arde, Dr. Mahesh Sriram, Dr. Abhijeet Jadhav, Dr. Prithwish Goswami, Dr. Dilip Kumar, Dr. Priya,

Dr. Akshi Tyagi, Mrs. Guddi Kant, Mr. Feroz Ahmad, Dr. Yogesh A. Pankhade, Dr. Gurdeep Singh, Dr. Rekha Yadav, Dr. Sonam Sharma, Dr. Rajat Pandey, Shaheen Fatma, Akshay, Arun, Shruthi, Athira for their valuable discussions, cooperation and for creating a healthy environment around me. I especially thank Divyanshu, Prabhat Singh Rana, Prashant Nagar, Vaibhav Kumar, Piyush Saini, Munnu Kumar, Pawan, Kanika, Aditya Garai, Vinod, Tarunjeet, and Shounak for their help and assistance during the projects. I am also obliged to Dr. Sandeep Thakur, Chanderkalan Negi, Vikram Singh, and Manu Adhikari for their help in solving the crystal structure. I also acknowledge all the summer trainees, especially Amisha, Suraj, Reena, Pusphit, Pushkar, Varnika, and others who worked for a short time in our lab.

I'm also grateful to Mr. Balbir and Mr. Triveni for their assistance. I'd like to thank the chemistry teaching lab assistants for their assistance during my research period. I am also grateful to all of my IISERM colleagues for their prompt assistance.

There aren't enough words to express my gratitude to my dear friends, especially Ankit, Bara, Prateek, Feroz, Arup, Prabhakar, Yogesh, Rishi, Ketan, J.P., Pravesh, Himanshu, Debpriya, Prashant, Radha, Akshi, Sunu Yadav, Nitin, and all my batchmates. They supported me through all of my difficult times and frequently experienced my joy and grief alongside me. I am thankful to Jaiveer, Pooja, Pallavi, Amit, Parveen, Kuljeet, Sapna, Akhila, Jyoti, Mamta, Neeshu, and Manpreet for their enjoyable and unforgettable negotiations (other than research) and chat during my journey. I am really lucky to have these friends in my life. I am grateful to the project supervisor Prof. Avinash Bajaj (RCB) and my senior Dr. Sandeep for encouraging my research interest. I am also grateful to all my teachers from the bottom of my heart for their guidance and inspiration.

I must also thank IISER Mohali for providing me with a research fellowship during my doctoral studies. Additionally, I would like to thank the Department of Science and Technology (DST), India, and IISER Mohali for supporting me and enabling me to finish my doctoral work. I also want to thank INST, Mohali for providing the XPS facility.

Last but the most significant, it gives me immense pleasure to express my gratitude to my beloved **parents (Mr. Omprakash and Mrs. Sarvati), wife (Jyoti), brothers (Mr. Hargyan and Mr. Neeraj), and all family members** who have always believed in me and supported me with unconditional love throughout my life.

Abstract

This thesis work primarily focuses on organocatalytic transformations using cyclopropenium ions as an organocatalyst. This work is organized into four chapters. Chapter 1 discusses the general introduction to the chemistry of cyclopropenium-based organic molecules. Chapter 2 illustrates the bis(amino)cyclopropenyliene (BACs) catalyzed intramolecular cyclization of 2-(2-formylaryl)aryl-substituted *p*-quinone methides via umpolung of aldehyde followed by 1,6-conjugate addition leading to phenanthrols and 7-membered carbocycles. Chapter 3 involves cyclopropenium cation-catalyzed conjugate addition reactions of *p*-QMs. Chapter 4 describes the tris-arylcyclopropenium carbocation as a highly promising organocatalyst in fundamental organic transformation such as Nazarov cyclization and other conjugate addition reactions.

Chapter 1: General introduction to the chemistry of cyclopropenium-based small molecules.

In this chapter, the structure, properties, and catalytic applications (Figure 1) of cyclopropenium-based small molecules are briefly discussed.

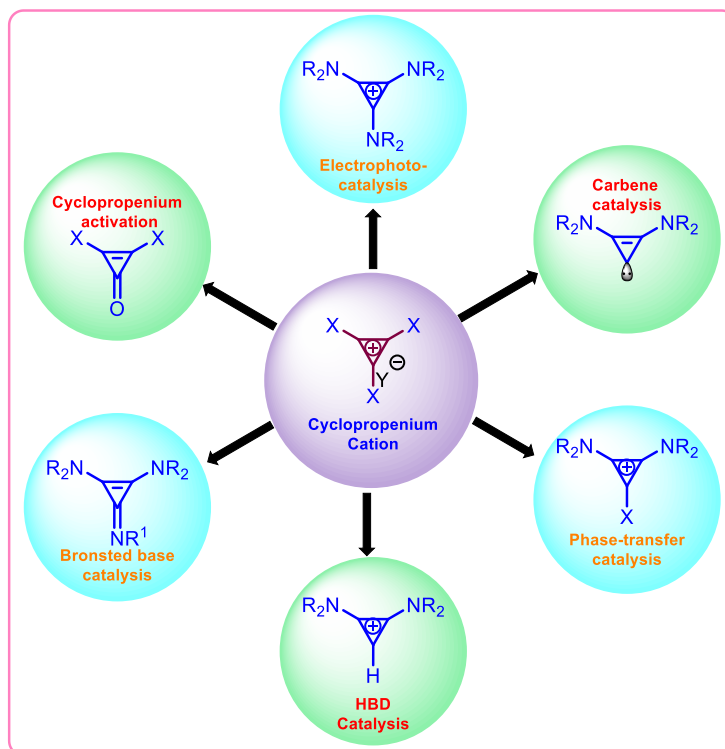


Figure 1. An overview of cyclopropenium ion-based catalysis.

Due to the unique structural and electronic properties of cyclopropenium salts, they have been

used in a wide range of applications such as organocatalysts (**Figure 1.**), potential materials for energy storage devices, electro-photocatalyst, ligands for catalytic metal complexes, ionic liquids, fluorescent materials, aromatic cations in hybrid halide perovskites, nanoparticles, redox-active polymers for redox flow batteries and as transfection agents.

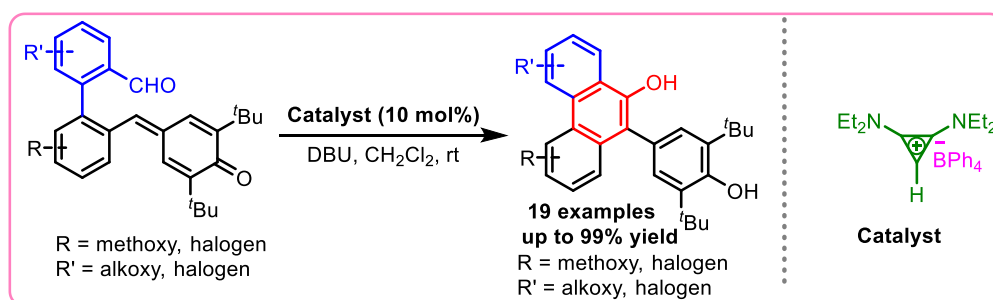
Chapter 2: Bis(amino)cyclopropenylidene catalyzed intramolecular cyclization of 2-(2-formylaryl)-phenyl-substituted *p*-quinone methides.

This Chapter is further divided into two parts namely, Part A and Part B.

Part A: Access to phenanthrols through a bis(amino)cyclopropenylidene catalyzed intramolecular cyclization of 2-(formylaryl)-aryl-substituted *p*-quinone methides.

The organocatalytic application of bis(amino)cyclopropenylidene (BAC) was unknown until Tamm and co-workers employed it for aldehyde umpolung reactions. It has been reported that carbene can readily react with an aldehyde to form a Breslow-type intermediate, which then can react with various electrophiles such as aldehydes (Benzoin reaction), enones (Stetter reaction), imines (aza-benzoin reaction), dienones (Rauhut-Currier reaction), etc. to form the corresponding acylated products.

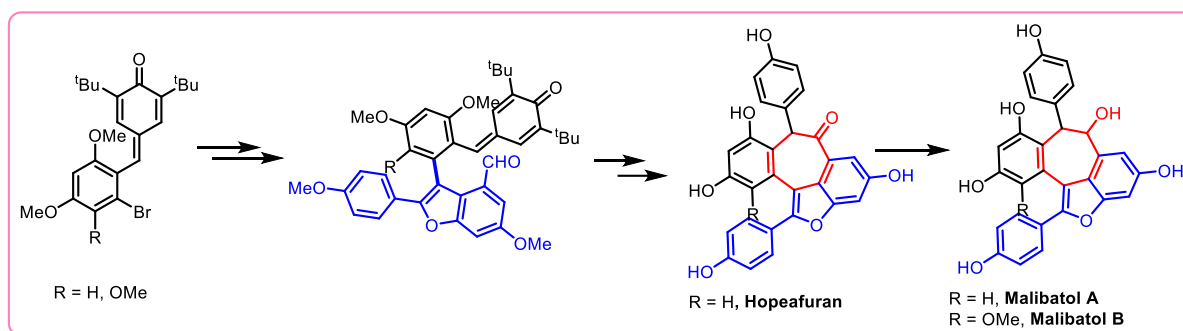
In line with this, we have developed a BAC-catalyzed intramolecular cyclization reaction of 2-(2-formylaryl)-phenyl-substituted *p*-quinone methides to access 10-(4-hydroxyphenyl)phenanthren-9-ol derivatives (Scheme 1). Additionally, this method was also elaborated for the synthesis of medium-sized rings, which are proven to possess antimicrobial and anticancer properties.



Scheme 1. Synthesis of 10-(4-hydroxyphenyl)phenanthren-9-ol derivatives through BACs catalyzed intramolecular cyclization reaction

Part B: Total syntheses of shoreaphenol, malibatol A, & B, parviflorol, and diptoindonesin A through a BAC catalyzed intramolecular cyclization reactions of 2-(formylaryl)-aryl-substituted *p*-quinone methides.

This part describes the synthesis of some of the recently discovered resveratrol-based natural products through BAC catalyzed intramolecular cyclization reactions of 2-(formylaryl)-aryl-substituted *p*-quinone methides. Resveratrol has been associated with a diverse range of biological functions including antioxidant, anticancer, anti-diabetic, anti-tumor, cardioprotective, and anti-aging characteristics. Malibatol A and B are two novel oligostilbenes that were isolated by Boyd and colleagues in 1998 and were derived from an organic extract of the leaves of *Hopea malibato*. Since then, several natural products in the same family have been isolated, and some articles on their total synthesis have been published. Hence, alternate methodologies for synthesizing these compounds are undoubtedly required as most previously known synthetic procedures involve multiple steps resulting in low overall yields.



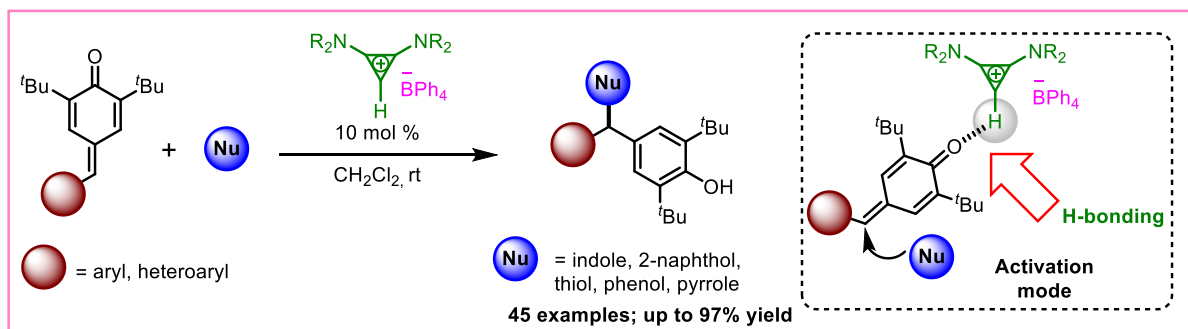
Scheme 2. Total synthesis of hopeafurane, malibatol A and B.

After establishing the strategy for the synthesis of the crucial core structure of 10-dihydro-11H-benzo[6,7]cyclohepta[1,2,3-cd]indol-11-one in part A, we turned our attention to synthesize some of the resveratrol and found that our methodology could be successfully applied to the total syntheses of malibatol A, malibatol B, hopeafurane, parviflorol E, and its epimer diptoindonesin D (Scheme 2).

Chapter 3: Bis(amino)cyclopropenium ion as a hydrogen-bond donor catalyst for 1,6-conjugate addition reactions.

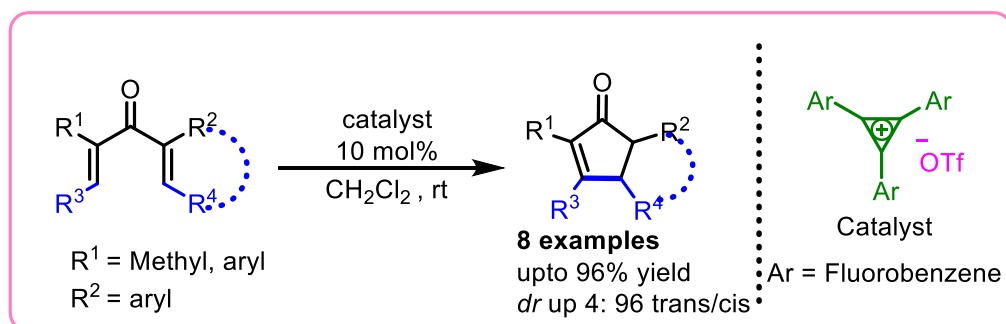
In this chapter, we have explored, for the first time, BAC precursor as a ‘Hydrogen Bond Donor’ catalyst in conjugate addition reactions of *p*-QMs with indoles and 2-naphthols. Deuterium isotope labeling experiments and spectroscopic investigations (^1H & ^{13}C NMR and UV-vis) were performed to prove the hypothesis; revealing that the C-H hydrogen atom in the cyclopropene ring of the catalyst is indeed responsible for the catalytic activity. This catalyst was also shown to be incredibly beneficial for the 1,6-conjugate addition of *p*-QMs with various nucleophiles such as 2-naphthols, phenols, and thiols. Later some of the indolyl

diarylmethanes were transformed into other valuable products to demonstrate the synthetic potential of this protocol (**Scheme 3**).



Chapter 4: Tris-arylcyclopropenium carbocation as an organic Lewis acid catalyst in Nazarov cyclization and conjugate addition reactions.

While working on the smallest aromatic Huckel moiety, widely recognized as cyclopropenium ion-based catalysis, we anticipated that it could behave as an organic Lewis acid catalyst in various organic transformations. In line with this, we have utilized, for the first time, tris-arylcyclopropenium carbocation as an organic Lewis acid catalyst in Nazarov cyclization reactions. The reactions worked very well under mild reaction conditions and the cyclopentenone derivatives could be obtained in excellent yields within a short reaction time. The same protocol was utilized for diversified reactions including 1,6/1,4 hydroolefinations and 1,2 addition of indoles to aromatic carboxaldehydes. The hypothesis was further supported by spectroscopic investigations (^1H & ^{13}C NMR and UV-vis) and the XPS technique. To show the Lewis acidity of the catalyst pK_a value of the cation was calculated using the Breslow method.



Abbreviations

ACN	Acetonitrile
Ac ₂ O	Acetic anhydride
acac	Acetylacetonate
a.t	Ambient temperature
Aq	Aqueous
AC	Adenylyl cyclase
BINAP	(2,2'-Bis(diphenylphosphine)-1,1'-binaphthyl)
brs	Broad singlet
CCl ₄	Carbon tetrachloride
clcd	Calculated
CSA	Camphorsulfonic acid
cm	Centimetre
δ	Chemical shift
CHCl ₃	Chloroform
CDCl ₃	Chloroform-D
<i>J</i>	Coupling constant
cy	Cyclohexyl
cod	1,5-cyclooctadiene
cAMP	Cyclic-Adenosine-3',5'-Monophosphate
CNS	Central nervous system
COPD	Chronic obstructive pulmonary disease
CP	Cyclopropenium Ion
CysA	Cyclophilin A
°C	Degree celsius
<i>dr</i>	Diastereomeric ratio
DBU	1,8-Diazabicyclo[5.4.0]undec-7-ene
DDQ	2,3-Dichloro-5,6-dicyano-1,4-benzoquinone
DCE	Dichloroethane
DCM	Dichloromethane
DMeO-BPY	4-4'-Dimethoxy-2-2'-bipyridine

DMA	Dimethylacetamide
DMSO	Dimethyl sulfoxide
d	Doublet
dd	Doublet of doublet
ddd	Doublet of doublet of doublet
dt	Doublet of triplets
dtbbpy	4,4'-Di- <i>tert</i> -butyl-2,2'-dipyridyl
DTBP	Di- <i>tert</i> -butyl peroxide
EWG	Electron withdrawing
E. C	Electrocyclic Reactions
ESI	Electrospray ionization
λ_{emi}	Emission maxima
<i>ee</i>	Enantiomeric excess
<i>er</i>	Enantiomeric ratio
EtOH	Ethanol
EtOAc	Ethylacetate
equiv	Equivalents
FT-IR	Fourier transform infrared spectroscopy
Hz	Hertz
HPLC	High-Pressure Liquid Chromatography
HRMS	High-resolution Mass Spectrum
h	Hour(s)
<i>i</i> -Pr	<i>iso</i> -Propyl
LED	Light-emitting diode
<i>m/z</i>	Mass/Charge
MHz	Megahertz
m.p.	Melting point
Mes	Mesityl
MeOH	Methanol
MsOH	Methane Sulfonic Acid
<i>m</i> CPBA	<i>meta</i> -Chloroperoxybenzoic acid
mg	Milligram(s)
mL	Milliliter(s)

mmol	Millimole(s)
min	Minute(s)
μL	Microliter (s)
μm	Micrometre (s)
M.S.	Molecular sieves
m	Multiplet
DMF	<i>N,N'</i> -Dimethyl formamide
NMP	<i>N</i> -Methyl-2-pyrrolidone
NMR	Nuclear Magnetic Resonance
<i>n</i> -Pr	Propyl
<i>P</i> -TSA	<i>p</i> -Toluene sulfonic acid
PDE4	Phosphodiesterase-4
PAH	Polycyclic aromatic hydrocarbons
q	Quartet
R_f	Retention factor
rt	Room temperature
sept	Septet
s	Singlet
^t Bu	<i>tert</i> -Butyl
<i>tert</i>	Tertiary
TBAB	Tetrabutylammonium bromide
THF	Tetrahydrofuran
TMS	Tetramethylsilane
TFA	Trifluoroacetic acid
t	Triplet
td	Triplet of doublets
tt	Triplet of triplet
UV	Ultraviolet
Vis	Visible
XPS	X-ray Photoelectron Spectroscopy

Contents

Declaration.....	i
Acknowledgements.....	ii
Abstract.....	iv
Abbreviations.....	viii

The thesis work is divided into four chapters, **Chapter 1, Chapter 2, Chapter 3, and Chapter 4.**

Chapter 1: General introduction to the chemistry of cyclopropenium-based small molecules.

1.1. Introduction.....	3
1.2. Organocatalytic transformations through ‘cyclopropenium’ activation.....	4
1.3. Phase-transfer catalysis (PTC) by cyclopropenium salts.....	6
1.4. Cyclopropenium-based Brønsted base organocatalysts in organic transformations..	8
1.5. Electrophotocatalysis with tris(amino)cyclopropenium (TAC) salts.....	10
1.6. References.....	14

Chapter 2: Bis(amino)cyclopropenylidene catalyzed intramolecular cyclization of 2-(2-formylaryl)-phenyl-substituted *p*-quinone methides.

This Chapter is further divided into two parts namely, **Part A** and **Part B**.

Part A: Access to phenanthrols through a bis(amino)cyclopropenylidene catalyzed intramolecular cyclization of 2-(formylaryl)-aryl-substituted *p*-quinone methides.

2.1.1 Introduction of Bis(amino)cyclopropenylidenes (BACs).....	17
2.1.2 A brief literature review on BACs.....	17
2.1.3 Background.....	21
2.1.4 Results and discussion.....	22
2.1.5 Conclusion.....	29
2.1.6 Experimental section.....	29
2.1.7 References.....	60

Part B: Total syntheses of shoreaphenol, malibatol A, & B, parviflorol, and diptoindonesin A through a BAC catalyzed intramolecular cyclization reactions of 2-(formylaryl)-aryl-substituted *p*-quinone methides.

2.2.1	Introduction.....	63
2.2.2	Literature reports on the formal synthesis of diptoindonesin D and parviflorol.....	64
2.2.3	Literature reports on total and formal synthesis of malibatol A and shoreaphenol/hopeafuran.....	65
2.2.4	Background.....	66
2.2.5	Our approach.....	66
2.2.6	Conclusion.....	68
2.2.7	Experimental section.....	69
2.2.8	References	80

Chapter 3: Bis(amino)cyclopropenium ion as a hydrogen-bond donor catalyst for 1,6-conjugate addition reactions

3.1.	Introduction.....	82
3.2.	Literature reports on the imidazolium salt-based H-bond donor catalysis.....	82
3.3.	Background.....	85
3.4.	Results and discussion	86
3.5.	Conclusion.....	99
3.6.	Experimental section.....	99
3.7.	References.....	130

Chapter 4: Tris-arylcyclopropenium carbocation as an organic Lewis acid catalyst in Nazarov cyclization and conjugate addition reactions.

4.1.	Introduction.....	135
4.2.	Literature reports on carbocation catalyzed organocatalysis.....	136
4.3.	Background.....	143
4.4.	Results and discussion.....	144
4.5.	Conclusion.....	160
4.6.	Experimental Section.....	160
4.7.	References.....	175

Curriculum Vitae.....	178
------------------------------	------------

General introduction to the chemistry of cyclopropenium-based small molecules.

1.1 Introduction

In 1957, Breslow reported the synthesis of cyclopropenium cation, called triphenyl cyclopropenium cation, which served as the first ‘non-benzenoid aromatic system having cyclic conjugation with less than six π -electrons.’¹ With this, a new class of carbon-centered cationic entities called cyclopropenium (CP) ions gained attention for their extraordinary aromatic stability, ring strain, and tuneable activity. Following that, several functionalized CP ions were developed. In 1970 Yoshida² and co-workers designed an amino-functionalized cation that has drawn the most interest. As the energy cost of an incomplete octet is decreased by the conjugation of an electron lone pair with a carbocation, incorporating the conjugative electron-donating amino group onto the cyclopropene ring may increase the degree of stability. Subsequently, in 1980, Stang and co-workers reported an oxy-bridged dication of CP, but it was only studied in solution.³ Phenyl cyclopropenium ions have a pK_R^+ value of 3.11; whereas all amino-cyclopropenium ions have a value greater than 10.⁴ The dialkyl-amino substituted cyclopropenium ion having pK_R^+ 13, was found to be very stable against the strongly alkaline medium. Tris(dialkylamino)cyclopropenium chloride salts have a higher thermal decomposition temperature (Tdec) [$>300\text{ }^\circ\text{C}$] than dialkyl imidazolium chloride salts (Td $250\text{ }^\circ\text{C}$).⁵ These molecules have various fascinating and practical features due to the amine group's affinity to donate its lone pair in conjugation with the cyclic core. The same effect also stabilizes the non-heterocyclic carbene species that correspond to amino substituents.⁶

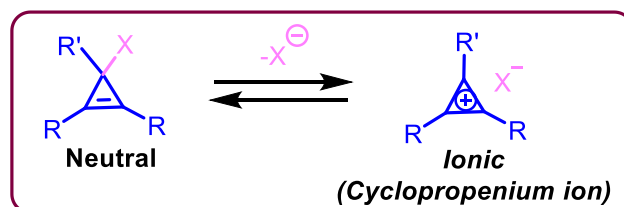


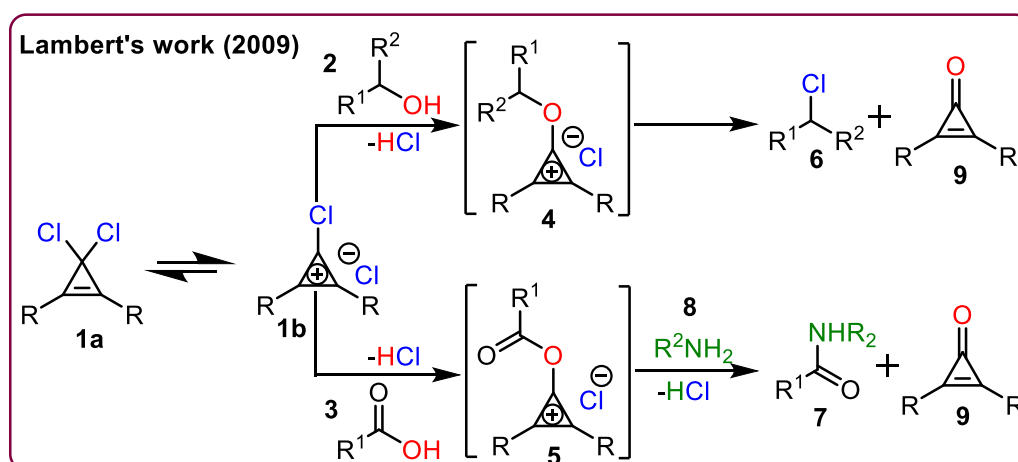
Fig.1 Equilibrium between ‘neutral’ and ‘ionic’ forms.

By reversible association with their anion or heteroatom lone pair, cyclopropenium ions can exist in both ‘*non-aromatic neutral*’ and ‘*aromatic charged*’ states. This is possible because of their dual qualities of aromatic stability and ionic charge (Fig.1).⁷ The balance between ionic and neutral forms is thought to be essential for promoting organic reactions. These ions have

been used for various applications because of their distinct structural and electronic characteristics. Some of these purposes are as promising materials for energy storage batteries⁸, nanoparticles,⁹ polyelectrolytes,¹⁰ ionic liquids and liquid crystals,¹¹⁻¹³ fluorescent materials,¹⁴ aromatic cations in hybrid halide perovskites,¹⁵ redox-active polymers (for redox flow batteries),¹⁶ gene therapy,¹⁷ persistent radical cations in redox reactions,¹⁸ ligands for transition metal complexes¹⁹⁻²² and redox-active organic cations in Na/Li batteries.^{23,24} Similarly, several cyclopropene derivatives and cyclopropenium salts have been explored in various fundamental chemical transformations due to their distinct reactivity profiles, resulting in diverse organocatalytic activities.²⁵⁻²⁸ Generally, the cyclopropene derivatives regenerate or change into other catalytically active species as the reaction progresses by forming a "temporary" and "comparatively- weak" covalent bond with the substrate(s) or reagent(s).^{27,28} Depending on the reaction or substrates/reagents, the cyclopropenium salts either engage noncovalently or covalently to activate the substrate(s) or reagent(s). The precursors to the catalytically active species in various organocatalytic reactions are the cyclopropenes and cyclopropenium salts.²⁵ The uses of such catalytically active cyclopropenes and cyclopropenium salts in organocatalysis are outlined below.

1.2 Organocatalytic transformations through ‘cyclopropenium’ activation

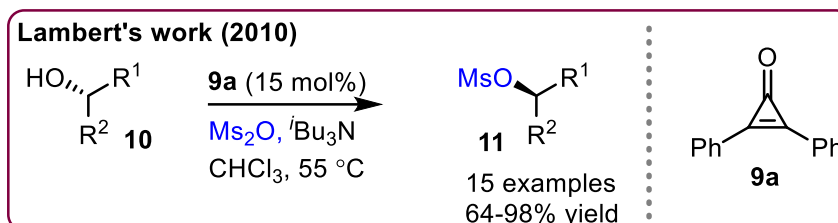
The cyclopropene and cyclopropenone analogs are well-known reagents explored in synthetic applications,^{27,29-31} and certain of their derivatives have been utilized as organocatalysts³²⁻³⁴ or stoichiometric activators³³ in several fundamental reactions.



Scheme 1. Reactions mediated by geminal di-chloro-substituted cyclopropene derivatives.

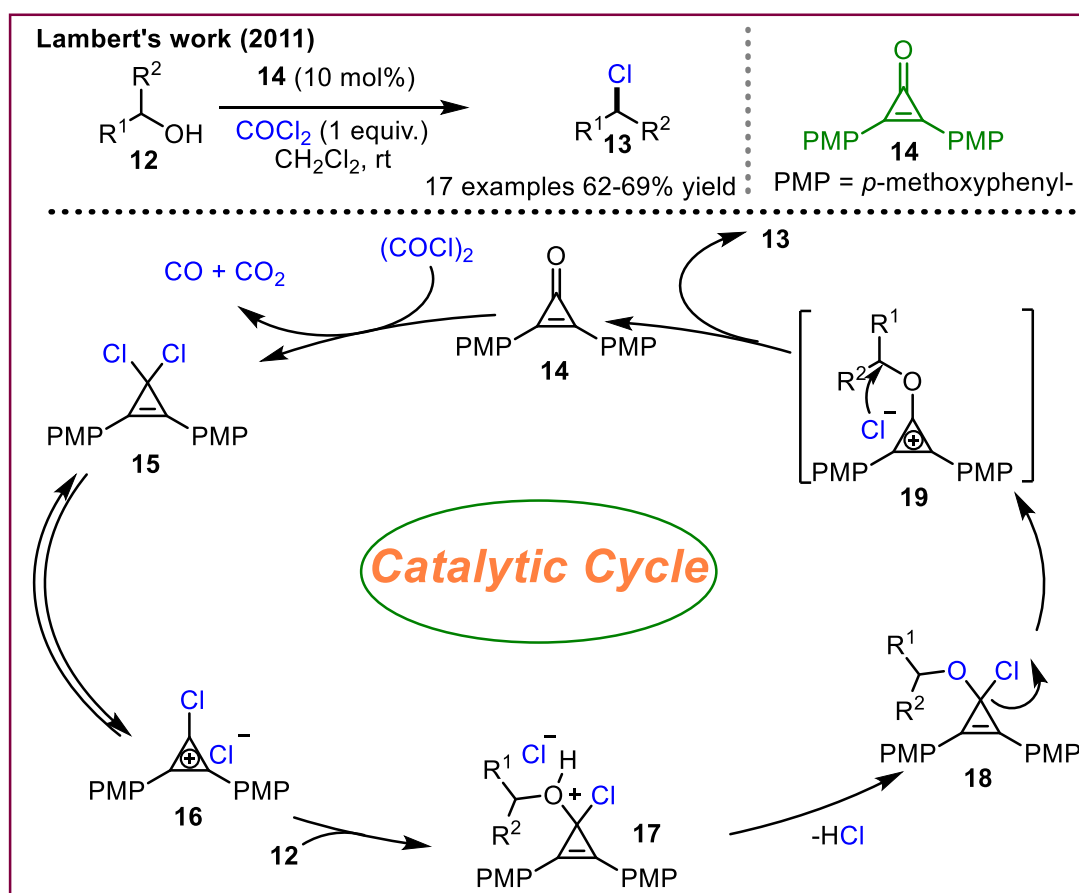
For the very first time in 2009, Lambert's research group introduced the concept of cyclopropenium activation in the transformation of alcohols **2** to alkyl chlorides **6**, alcohol

cyclodehydration, and nucleophilic acyl substitution of carboxylic acids **3** by employing 1-dichloro-2,3-diphenylcyclopropene **9** as a reagent (Scheme 1).⁷ Later, the groups of Lambert



Scheme 2. Cyclopropenium-catalyzed substitution of alcohols with mesylate anion

and Yadav has reported independently the Beckmann rearrangement of oximes to amides through cyclopropenium activation.^{35,36} Lambert and co-workers also developed an alternative to the Mitsunobu reaction using 2,3-diphenyl cyclopropenone **9a** as a catalyst and methane sulfonic anhydride as a reagent. Numerous enantiomerically enriched secondary alcohols (**10**) could be transformed into their respective mesylates (**11**) with opposite stereochemistry in high yields (Scheme 2).³⁷



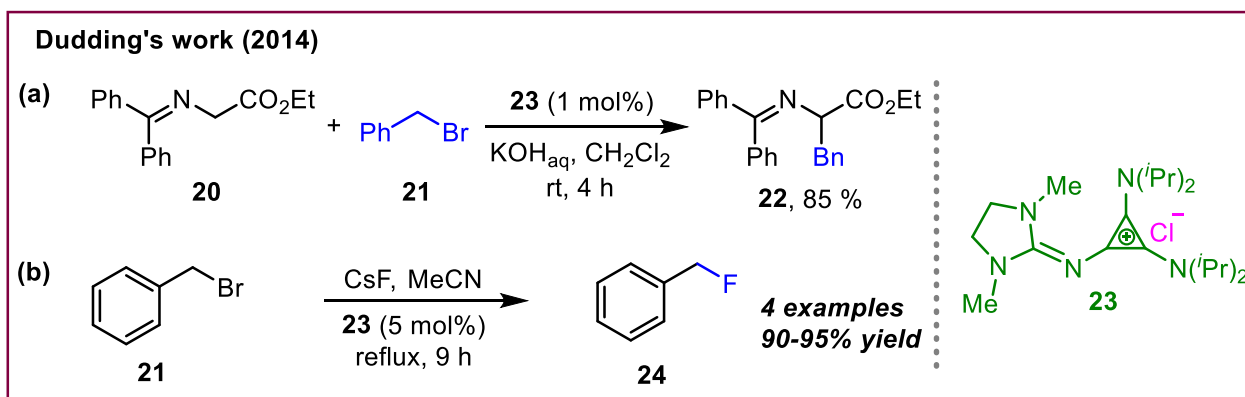
Scheme 3. Cyclopropenium-catalyzed chloro-dehydration of alcohol

To further show the catalytic applications of cyclopropenone derivatives, Lambert's group

developed the chlorination of alcohols (Scheme 3).³⁸ Here, 2,3-di-*p*-methoxyphenyl-cyclopropenone **14** acts as an organocatalyst, and oxalyl chloride serves as a stoichiometric chlorinating reagent, to generate the respective chlorinated compounds (**13**). Many alcohols, including optically pure secondary alcohols, could be converted to their corresponding alkyl chlorides in moderate to good yields under standard conditions. It has been proposed that catalyst **14** first interacts with oxalyl chloride to produce 1,1,-dichloro-2,3-di-*p*-methoxyphenyl-cyclopropene **13**, which is in equilibrium with cyclopropenium salt **16**. Then, alcohol **12** reacts with cyclopropenium salt **16** to produce an intermediate **17**, which after the elimination of HCl and a chloride ion gets converted to another cyclopropenium salt **19** through **18**. The nucleophilic displacement reaction between cyclopropenium salt **19** and a chloride ion generates the alkyl chloride **13** with the regeneration of **14** (Scheme 3).³⁸

1.3 Phase-transfer catalysis (PTC) by cyclopropenium salts

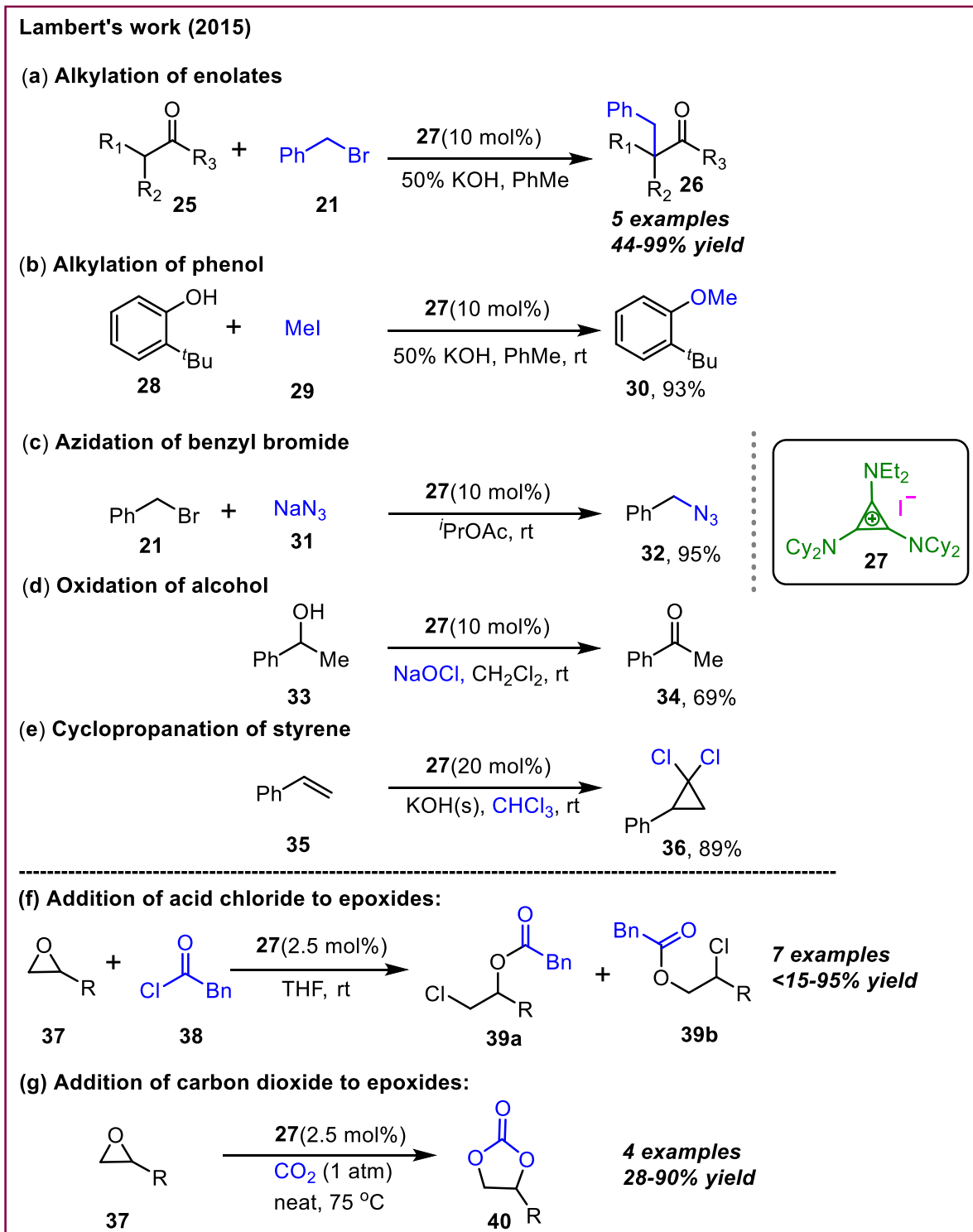
Phase transfer catalysis is a very important sub-class of organocatalysis, especially in enantioselective transformations.^{39,40} Recently, cyclopropenium salts have been utilized as promising phase transfer catalysts (PTCs), in several fundamental organic reactions. In 2014, Dudding and co-workers synthesized a mixed N(I) dicarbene complex **23** and utilized it in halogen exchange and C-alkylation reactions (Scheme 4). It was observed that when the benzylation of **20** was done under phase-transfer catalysis (PTC) conditions, the desired product **22** was isolated in an 85% yield. Additionally, the same catalyst was found to be very effective for the benzylic fluorination of benzyl bromides **21** using CsF as a fluoride source (Scheme 4).⁴¹



Scheme 4. Cyclopropenium-catalyzed benzylation and benzylic fluorination reactions

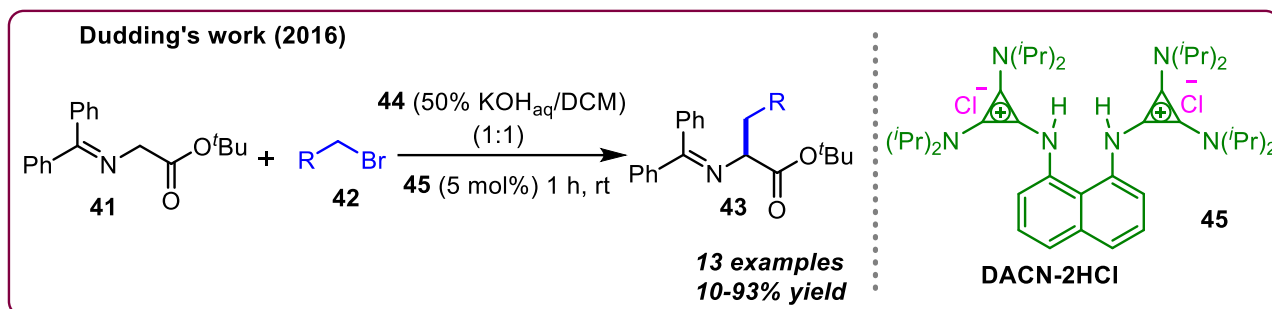
Lambert research group has used tris(dialkylamino)cyclopropenium (TDAC) salt **27** as a PTC in several organic transformations, including α -alkylation of carbonyl compounds (**25**), alkylation of phenols (**28**), azidation of benzyl bromide **21**, oxidation of alcohol **33** and

cyclopropanation of styrene **35**, etc. (a-e, Scheme 5).⁴² TDAC Catalyst **27** was also employed for the reaction of acid chloride **38** and epoxide **37** to obtain halohydrin ester adducts **39a** and **39b**, in good regioselectivity (f, Scheme 5). A similar methodology was also used for the synthesis of cyclic carbonates **40** by trapping CO₂ with epoxides (g, Scheme 5).⁴²



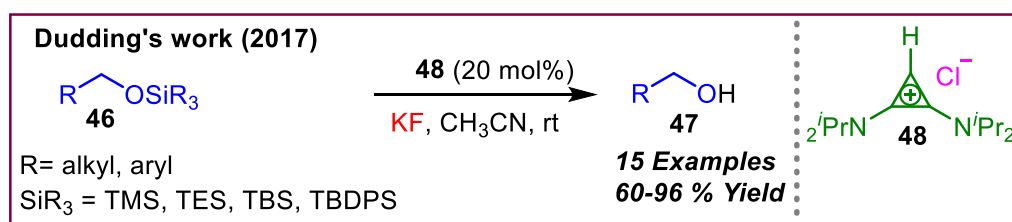
Scheme 5. Phase-transfer reactions catalyzed by TDAC salt **27**.

Dudding and co-workers reported the alkylation of O'Donnell's glycine imine **41** using a bis(diisopropylamine)cyclopropenimine-substituted bis-protonated proton sponge **45** as a bifunctional phase-transfer catalyst. The O'Donnell's glycine imine **41** reacted well with various alkyl halides (**42**) and produced the desired alkylated products (**43**) in good yields under optimal conditions. (Scheme 6).⁴³



Scheme 6. Phase-transfer catalyzed C-alkylation of O'Donnell's glycine imine (**41**).

Dudding's group also established yet another simple protocol for the deprotection of *O*-silyl ethers (**46**) utilizing a bis(dialkylamino)cyclopropenium (BDAC) salt **48** as a PTC (Scheme 13).⁴⁴

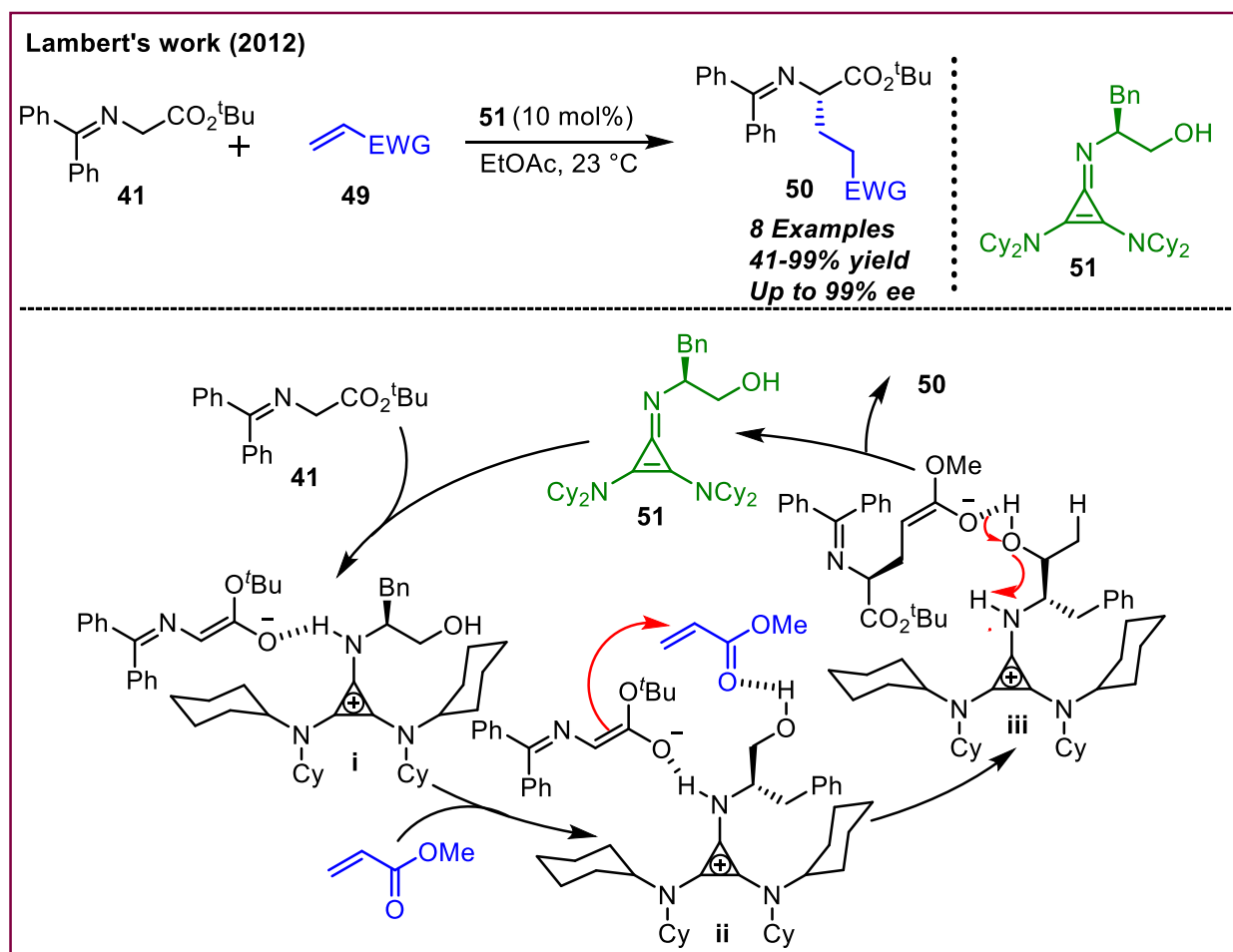


Scheme 7. BDAC salt catalyzed silyl-deprotection in *O*-silyl ethers

1.4 Cyclopropenium-based Brønsted base organocatalysts in organic transformations:

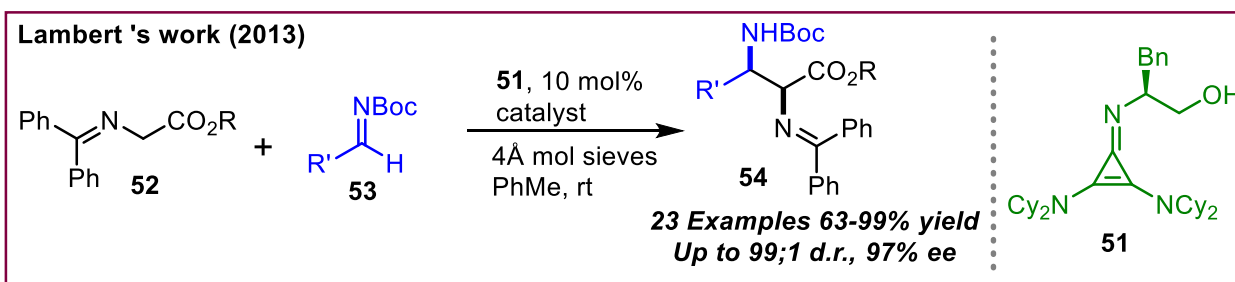
Lambert and workers were the first to establish the use of a chiral cyclopropenimine **51** as a Brønsted base to catalyze the enantioselective C-alkylation of *N*-protected glycineimine **41** with α,β -unsaturated compounds **49** under optimal conditions to synthesize enantiomerically pure derivatives of the higher order of amino acids (**50**) with very high enantioselectivity (up to 99% *ee*) [Scheme 08].⁴⁵ In the proposed mechanism, the glycineimine **41** is deprotonated by the catalyst **51** to produce a complex (**i**), which subsequently coordinates with **49** through H-bonding (TS **ii**). At this point, the enantioselective Michael addition occurs, resulting in the formation of a second complex **iii**, which then undergoes proton shuffle and

generates product **50** (Scheme 8). The mechanism was further supported by the DFT studies.⁴⁶



Scheme 8. Cyclopropenimine-catalyzed enantioselective Michael addition reaction.

Later in 2013, Lambert's team created a new, intriguing method for the production of enantiomerically pure 1,2-diamine derivatives (**54**) employing an enantioselective Mannich reaction, in which glycineimine **52** and aldimines (**53**) were utilized as substrates and **51** as a Brønsted base catalyst (Scheme 9).⁴⁷

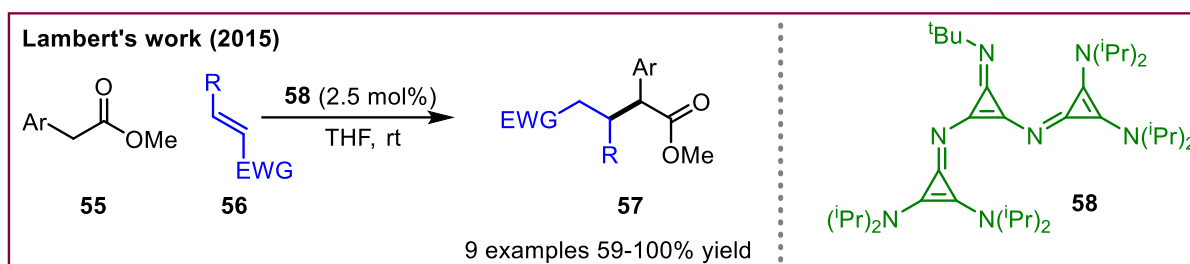


Scheme 09. Cyclopropenimine-catalyzed enantioselective Mannich reaction.

Under optimal conditions, it was feasible to produce a variety of chiral 1,2-diamine derivatives (**54**) with high yields (up to 99%) and diastereo-/enantio-selectivity (up to 97% *ee*).

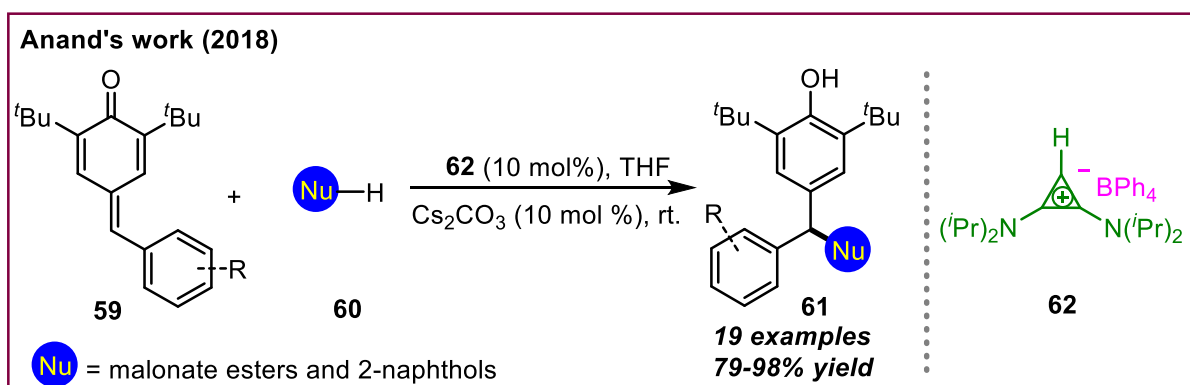
While exploring their research on cyclopropenimine-based Brønsted bases, Lambert's

group has also developed several higher-order bases, out of which **58** were found to be very effective for the Michael reaction of α -aryl esters (**55**) with enones (**56**) to generate α -alkylated α -aryl esters (**57**) with good to excellent yields (Scheme 10).⁴⁸



Scheme 10. Cyclopropenimine-based super base-catalyzed Michael reaction.

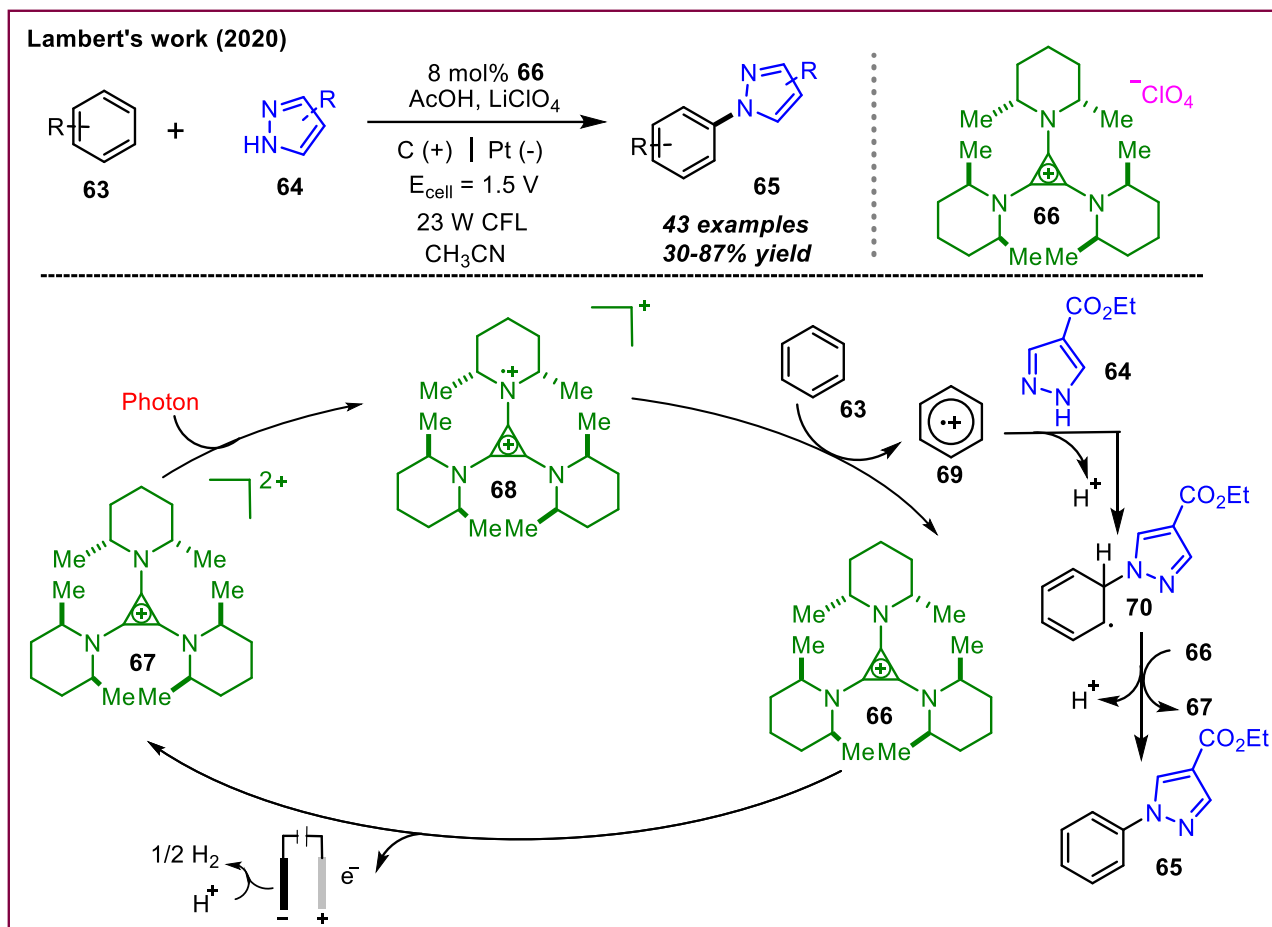
In 2018, Anand and co-workers reported the 1,6 conjugate addition of carbon nucleophiles to *p*-QMs (**59**) using bis(amino)cyclopropenylidene (BAC) **62** as a non-covalent Brønsted base catalyst (Scheme 11).⁴⁹ Various *p*-QMs (**59**) were treated with different nucleophiles (**60**) such as active methylene compounds and 2-naphthols to access the desired products (**61**) in excellent yields.



Scheme 11. BAC as a Brønsted base catalyst in conjugate addition reactions

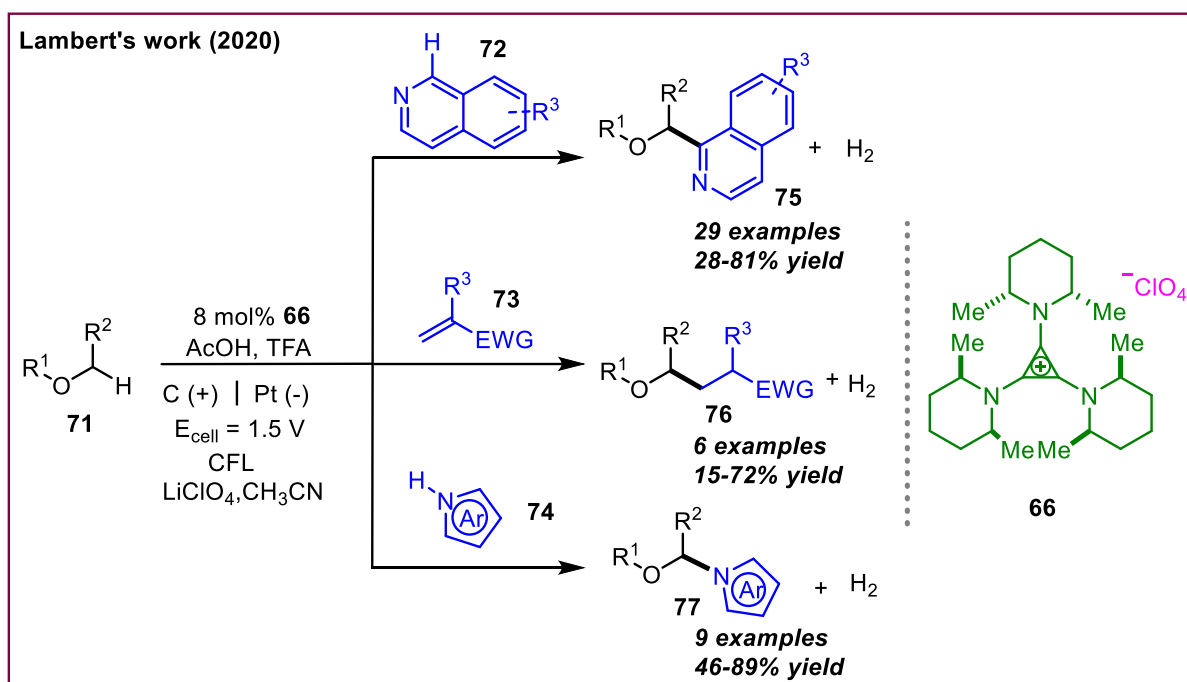
1.5 Electrophotocatalysis with tris(amino)cyclopropenium (TAC) salts

A new branch of synthetic chemistry known as "electrophotocatalysis" has been developed in recent years. This branch of chemistry combines "photocatalysis" and "electrocatalysis" in some way.



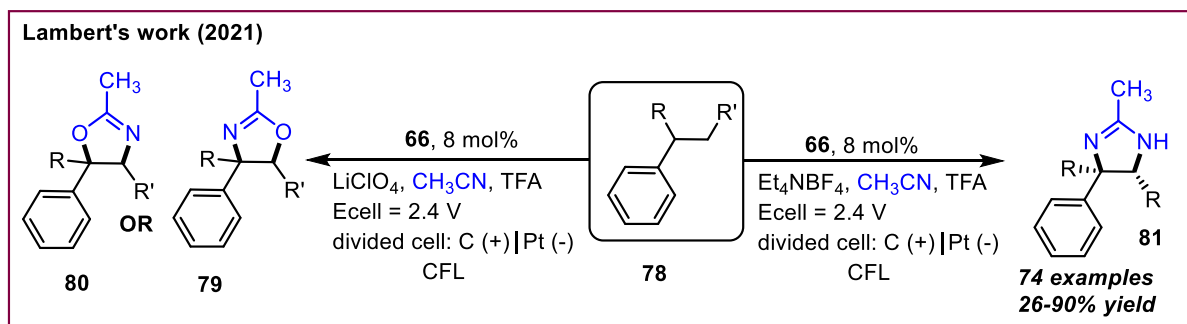
Scheme 12. TAC salt catalyzed electrophotocatalytic C-N coupling reaction

Although not many publications have appeared in this field of research till now, this idea has been used in certain fundamental organic transformations, including the oxidation of benzyl alcohols, acylation of olefins, alkylation of arenes, C-H amination, etc. Lambert and co-workers utilized TACs salt **66** for oxidative C-N coupling reaction with arenes (**63**) and pyrazoles (**64**) to synthesize various *N*-aryl pyrazoles (**65**) in excellent yields (Scheme 12). They have proposed that radical dication **67** is formed after the electrochemical oxidation of TAC salt **66**, which underwent photoexcitation to generate an intermediate **68**. This intermediate oxidizes the arene to form the radical cation **69**, which gets trapped by pyrazole **64** to form another radical **70**. At last, **70** undergoes oxidation with **66** to produce the final product **65** (Scheme 12).¹⁸ Moreover, by utilizing **66** as a catalyst at low electrochemical potential, Lambert's group developed an oxidant-free and highly regioselective C-H functionalization of ethers (**71**) with isoquinolines (**72**), alkenes (**73**), pyrrole **74**, etc., to form corresponding products **75**, **76**, and **77** respectively in good to excellent yield with the evolution of hydrogen gas as a side product (Scheme 13).⁵⁰



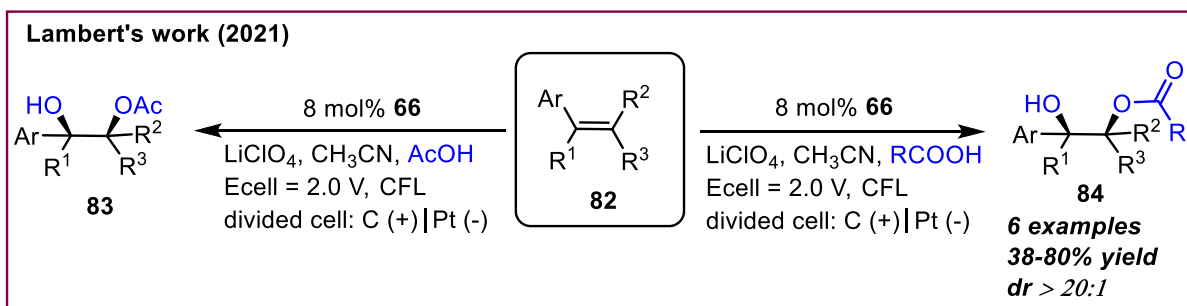
Scheme 13. TAC salt catalyzed electrophotocatalytic C–H functionalization of ethers.

Recently, Lambert's group has established a novel method for the Ritter-type C–H functionalization processes of alkanes (**78**) to access 3,4-dihydroimidazoles (**81**) employing **66** as an electrophotocatalyst and Et_4NBF_4 as an electrolyte (Scheme 14).⁵¹ The same group also developed a similar method for the benzylic C–H amidation reactions to generate cyclic carbamates (**79** and **80**) in excellent yield.⁵² For instance, here acetonitrile served the purpose of solvent as well as the nitrogen source.



Scheme 14. TAC salt catalyzed electrophotocatalytic Ritter type C–H functionalization.

Lambert's group has also explored the catalytic efficiency of TAC salts in the dioxygenation of aryl-substituted olefins (**82**) under electrophotocatalytic conditions (Scheme 15).⁵³ For cyclic, di-, and tri-substituted alkenes, this approach was found to be quite effective, and in the majority of those cases, moderate to good yields of the respective acetoxylated aliphatic alcohols (**83** and **84**) were obtained.



Scheme 15. TAC salt catalyzed deoxygenation of alkenes.

1.6 References:-

- (1) Breslow, R. *J. Am. Chem. Soc.* **1957**, 79, 5318.
- (2) Yoshida, Z.; Tawara, Y. *J. Am. Chem. Soc.* **1971**, 93, 2573.
- (3) Stang, P. J.; Maas, G.; Fisk, T. E. *J. Am. Chem. Soc.* **1980**, 102, 6361.
- (4) Kerber, R. C.; Hsu, C.-M. *J. Am. Chem. Soc.* **1973**, 95, 3239.
- (5) Curnow, O. J.; MacFarlane, D. R.; Walst, K. J. *Chem. Commun.* **2011**, 47, 10248.
- (6) Johnson, L. E.; DuPré, D. B. *J. Phys. Chem. A* **2008**, 112, 7448.
- (7) Kelly, B. D.; Lambert, T. H. *J. Am. Chem. Soc.* **2009**, 131, 13930.
- (8) Trahey, L.; Brushett, F. R.; Balsara, N. P.; Ceder, G.; Cheng, L.; Chiang, Y.; Hahn, N. T.; Ingram, B. J.; Minter, S. D.; Moore, J. S.; Mueller, K. T.; Nazar, L. F.; Persson, K. A.; Siegel, D. J.; Xu, K.; Zavadil, K. R.; Srinivasan, V.; Crabtree, G. W. *A Perspective from the Joint Center for Energy Storage Research.* **2020**, 117, 12550.
- (9) Killups, K. L.; Brucks, S. D.; Rutkowski, K. L.; Freyer, J. L.; Jiang, Y.; Valdes, E. R.; Campos, L. M. *Macromolecules* **2015**, 48, 2519.
- (10) Jiang, Y.; Freyer, J. L.; Cotanda, P.; Brucks, S. D.; Killups, K. L.; Bandar, J. S.; Torsitano, C.; Balsara, N. P.; Lambert, T. H.; Campos, L. M. *Nat. Commun.* **2015**, 6, 5950.
- (11) Griffin, P. J.; Freyer, J. L.; Han, N.; Geller, N.; Yin, X.; Gheewala, C. D.; Lambert, T. H.; Campos, L. M.; Winey, K. I. *Macromolecules* **2018**, 51, 1681.
- (12) Freyer, J. L.; Brucks, S. D.; Gobieski, G. S.; Russell, S. T.; Yozwiak, C. E.; Sun, M.; Chen, Z.; Jiang, Y.; Bandar, J. S.; Stockwell, B. R.; Lambert, T. H.; Campos, L. M. *Angew. Chem. Int. Ed.* **2016**, 55, 12382.
- (13) Litterscheidt, J.; Judge, P.; Bühlmeier, A.; Bader, K.; Bandar, J. S.; Lambert, T.; Laschat, S. *Liq. Cryst.* **2018**, 45, 1250.
- (14) Belding, L.; Guest, M.; Le Sueur, R.; Dudding, T. *J. Org. Chem.* **2018**, 83, 6489.
- (15) Kasel, T. W.; Murray, A. T.; Hendon, C. H. *J. Phys. Chem. C*, **2018**, 122, 2041.
- (16) Yan, Y.; Vaid, T. P.; Sanford, M. S. *J. Am. Chem. Soc.* **2020**, 142, 17564.
- (17) Steinman, N. Y.; Campos, L. M.; Feng, Y.; Domb, A. J.; Hosseinkhani, H. *Pharmaceutics* **2020**, 12, 768.
- (18) Strater, Z. M.; Rauch, M.; Jockusch, S.; Lambert, T. H. *Angew. Chem. Int. Ed.* **2019**, 58, 8049.
- (19) Bruns, H.; Patil, M.; Carreras, J.; Vázquez, A.; Thiel, W.; Goddard, R.; Alcarazo, M.

- Angew. Chem. Int. Ed.* **2010**, *49*, 3680.
- (20) Kozma, Á.; Rust, J.; Alcarazo, M. *Chem. Eur. J.* **2015**, *21*, 10829.
- (21) Kozma, Á.; Deden, T.; Carreras, J.; Wille, C.; Petuskova, J.; Rust, J.; Alcarazo, M. *Chem. Eur. J.* **2014**, *20*, 2208.
- (22) Alcarazo, M. *Acc. Chem. Res.* **2016**, *49*, 1797.
- (23) Ji, W.; Huang, H.; Zheng, D.; Zhang, X.; Ding, T.; Lambert, T. H.; Qu, D. *Energy Storage Mater.* **2020**, *32*, 190.
- (24) Ji, W.; Huang, H.; Huang, X.; Zhang, X.; Zheng, D.; Ding, T.; Chen, J.; Lambert, T. H.; Qu, D. *J. Mater. Chem. A*, **2020**, *8*, 17156.
- (25) Komatsu, K.; Kitagawa, T. *Chem. Rev.* **2003**, *103*, 1371.
- (26) Bandar, J. S.; Lambert, T. H. *Synthesis* **2013**, *45*, 2498.
- (27) An, J.; Denton, R. M.; Lambert, T. H.; Nacsa, E. D. *Org. Biomol. Chem.* **2014**, *12*, 3003.
- (28) Lyons, D. J. M.; Crocker, R. D.; Blümel, M.; Nguyen, T. V. *Angew. Chem. Int. Ed.* **2017**, *56*, 1484.
- (29) Komatsu, K.; Kitagawa, T. *Chem. Rev.* **2003**, *103*, 1428.
- (30) Bandar, J.; Lambert, T. *Synthesis*, **2013**, *45*, 2485.
- (31) Litterscheidt, J.; Bandar, J. S.; Ebert, M.; Forschner, R.; Bader, K.; Lambert, T. H.; Frey, W.; Bühlmeier, A.; Brändle, M.; Schulz, F.; Laschat, S. *Angew. Chem. Int. Ed.* **2020**, *59*, 10555.
- (32) Ranga, P. K.; Ahmad, F.; Singh, G.; Tyagi, A.; Anand, R. V. *Org. Biomol. Chem.* **2021**, *19*, 9541.
- (33) Wilson, R. M.; Lambert, T. H. *Acc. Chem. Res.* **2022**, *55*, 3057.
- (34) Xiao, W.; Wu, J. *Chin. Chem. Lett.* **2023**, *34*, 107637.
- (35) Vanos, C. M.; Lambert, T. H. *Chem. Sci.*, **2010**, *1*, 705.
- (36) Srivastava, V. P.; Patel, R.; Yadav, L. D. S. *Chem. Commun.*, **2010**, *2*, 5808.
- (37) Nacsa, E. D.; Lambert, T. H. *Org. Lett.* **2013**, *15*, 38.
- (38) Hardee, D. J.; Kovalchuk, L.; Lambert, T. H. *J. Am. Chem. Soc.* **2010**, *132*, 5002.
- (39) Shirakawa, S.; Maruoka, K. *Angew. Chem., Int. Ed.* **2013**, *52*, 4312.
- (40) Shiho k., Yusuke. K. and Shirakawa. S. *Org. Biomol. Chem.* **2016**, *14*, 5367.
- (41) Mirabdolbaghi, R.; Dudding, T.; Stamatatos, T. *Org. Lett.* **2014**, *16*, 2790.
- (42) Bandar, J. S.; Tanaset, A.; Lambert, T. H. *Chem. - Eur. J.* **2015**, *21*, 7365.
- (43) Belding, L.; Stoyanov, P.; Dudding, T. *J. Org. Chem.* **2016**, *81*, 553.
- (44) Mir, R.; Dudding, T. *J. Org. Chem.* **2017**, *82*, 709.
- (45) Bandar, J. S.; Lambert, T. H. *J. Am. Chem. Soc.* **2012**, *134*, 5552.

- (46) Bandar, J. S.; Sauer, G. S.; Wulff, W. D.; Lambert, T. H.; Vetticatt, M. J. *J. Am. Chem. Soc.* **2014**, *136*, 10700.
- (47) Bandar, J. S.; Lambert, T. H. *J. Am. Chem. Soc.* **2013**, *135*, 11799.
- (48) Nacsá, E. D.; Lambert, T. H. *J. Am. Chem. Soc.* **2015**, *137*, 10246.
- (49) Singh, G.; Goswami, P.; Anand, R. V. *Org. Biomol. Chem.* **2018**, *16*, 384.
- (50) Huang, H.; Strater, Z. M.; Lambert, T. H. *J. Am. Chem. Soc.* **2020**, *142*, 1698.
- (51) Shen, T.; Lambert, T. H. *Science* **2021**, *371*, 620.
- (52) Shen, T.; Lambert, T. H. *J. Am. Chem. Soc.* **2021**, *143*, 8597.
- (53) Huang, H.; *J. Am. Chem. Soc.* **2021**, *143*, 7247.

Chapter 2

Bis(amino)cyclopropenylidene catalyzed intramolecular cyclization of 2-(2-formylaryl)-phenyl-substituted *p*-quinone methides.

This Chapter is further divided into two parts namely, **Part A** and **Part B**.

Part A

Access to phenanthrols through a bis(amino)cyclopropenylidene catalyzed intramolecular cyclization of 2-(formylaryl)-aryl-substituted *p*-quinone methides.

2.1.1 Introduction on bis(amino)cyclopropenylidenes (BACs)

It has been observed that N-heterocyclic carbenes (NHCs) with a heterocyclic core, such as thiazole, triazole, imidazole, and others dominate in organocatalysis due to their immaculate nucleophilicity¹ and high stability.² However, the non-heterocyclic based carbenes, on the other hand, have been relatively less explored for umpolung-type activation of carbonyl compounds, despite the fact that their organometallic complexes are well investigated.³ Bis(amino)cyclopropenylidenes (BACs), another form of nucleophilic carbene generated from cyclopropenium salts, were discovered to be a promising non-heterocyclic-based candidate in terms of reactivity towards metals and carbonyl compounds. BACs, unlike N-heterocyclic carbenes, do not require the presence of a heteroatom(s) close to the electron-deficient carbene carbon center to be stable. Indeed, the push-pull effect of the two amino substituents linked to the ring could contribute to the stability of these cyclopropenylidenes.⁴ The sigma-aromaticity of the cyclopropene ring is another crucial feature that leads to carbene stability.⁴ Although the synthesis and structural features of bis(amino)cyclopropenylidene salts were independently exploited in the 1970s by Weiss and Yoshida, their applications⁵ have only lately been realized, particularly in organometallic chemistry.⁶

2.1.2 A brief literature review on BACs

Bertrand and co-workers reported the first isolation of bis(diisopropylamino)cyclopropenylidene **I** in his seminal work (Figure 1).⁷ This particular

BAC **I** was discovered to be very air-sensitive and to have reasonable thermal stability. NMR and X-ray methods were used to extensively characterize BAC **I**. It was reported that the reaction of a stoichiometric ratio mixture of bis(diisopropylamino)cyclopropenylidene tetraphenylborate salt **III** and $\text{KN}(\text{SiMe}_3)_2$ in dry Et_2O at 78°C resulted in the formation of

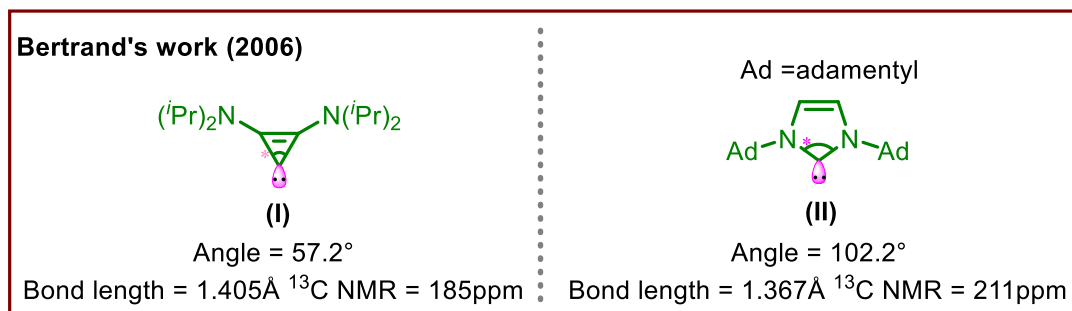
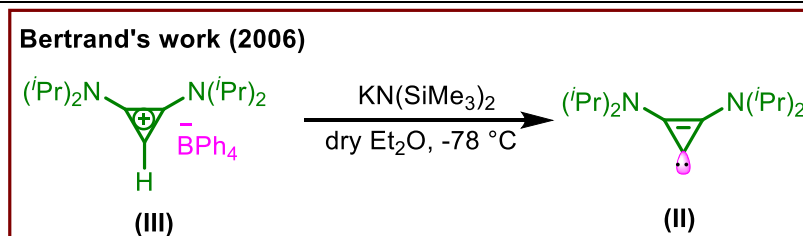
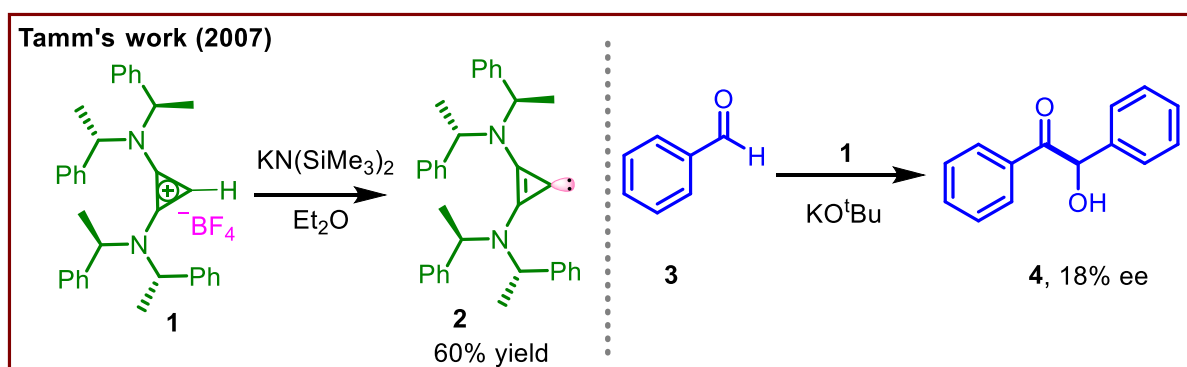


Figure 1. A general comparison between BAC (**I**) and NHC (**II**).



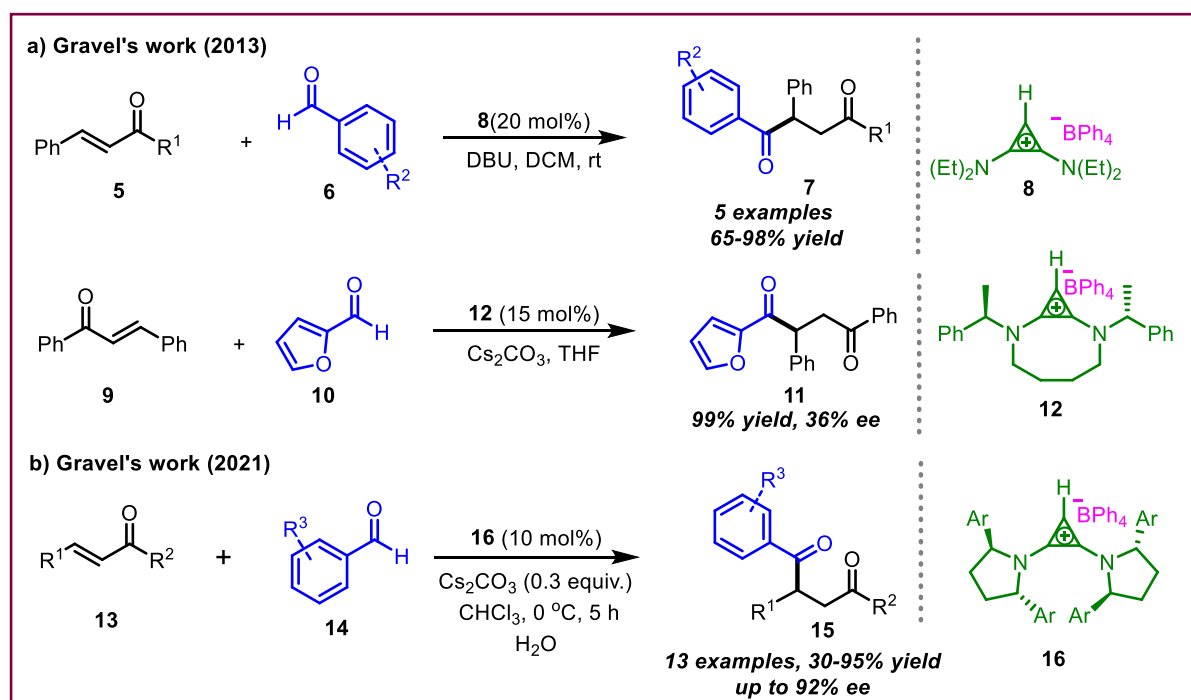
Scheme 1. First report on isolation of free BACs carbene

cyclopropenylidene **I** in 20% yield (Scheme 1).⁸ After the successful isolation of BACs by Bertrand's group, several reports appeared in the literature on the application of BACs as a catalyst in organometallic chemistry.³ In 2007, Tamm and co-workers reported the synthesis of the first chiral catalyst bis[bis(R-1-phenylethyl)amino]cyclopropenylidene **2** (prepared from the precursor **1**), that has been employed for an enantioselective benzoin reaction of aromatic aldehyde **3**. However, the product benzoin **4** was formed only in 18% *ee* (Scheme 2).⁹ The authors have explained that the low enantioselectivity was probably due to the rapid rotation of the chiral amino groups in **2**.



Scheme 2. Chiral BAC catalyzed benzoin reaction.

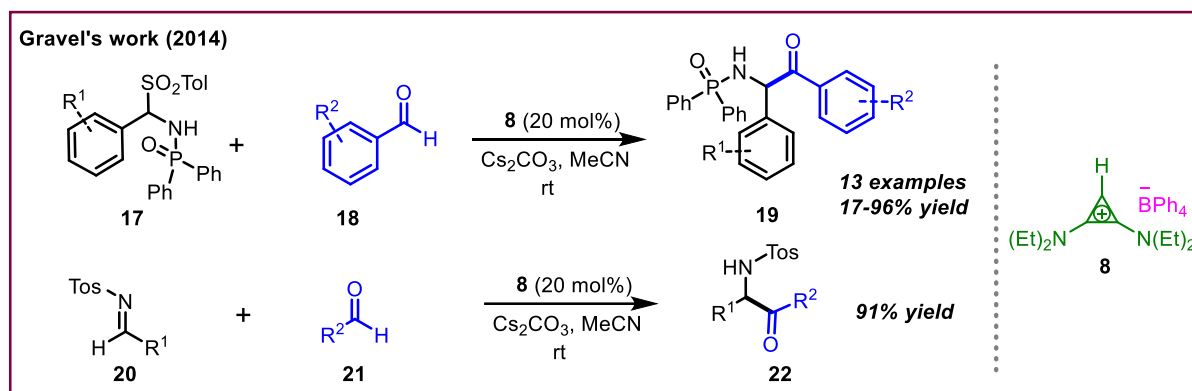
Later, Gravel and co-workers described bis(amino)cyclopropenyliidene salt **8** as a precatalyst for a highly chemo-selective intermolecular Stetter reaction between chalcones (**5**) and aldehydes (**6**) to produce a variety of 1,4 diketones (**7**). Interestingly, in those cases, the formation of benzoin products (**4**) was not observed during the reactions, which contrasted with analogous reactions using thiazolium and triazolium salts as precatalysts (**a**, Scheme 3).¹⁰ Gravel research group also worked on the failure of Tamm's enantioselective Stetter reaction by restricting the rotation of chiral amino group through constructing the cyclic ring in catalyst **12**; this catalyst was employed in an enantioselective Stetter reaction between furfural **10** and chalcone **9**. Although, in this case, the chemical yield of the Stetter product was excellent, the enantioselectivity of product **11** was only 36% (**a**, Scheme 3).¹⁰ Recently, in continuation of this work, the same group has developed a highly efficient enantioselective intramolecular Stetter reaction of chalcones (**13**) and aromatic aldehydes (**14**) by employing another chiral BAC precursor **16**, and accessed the enantiomerically enriched 1,4-diketones (**15**) with up to 92% *ee* (**b**, Scheme 3).¹¹



Scheme 3. BAC-catalyzed Stetter reaction

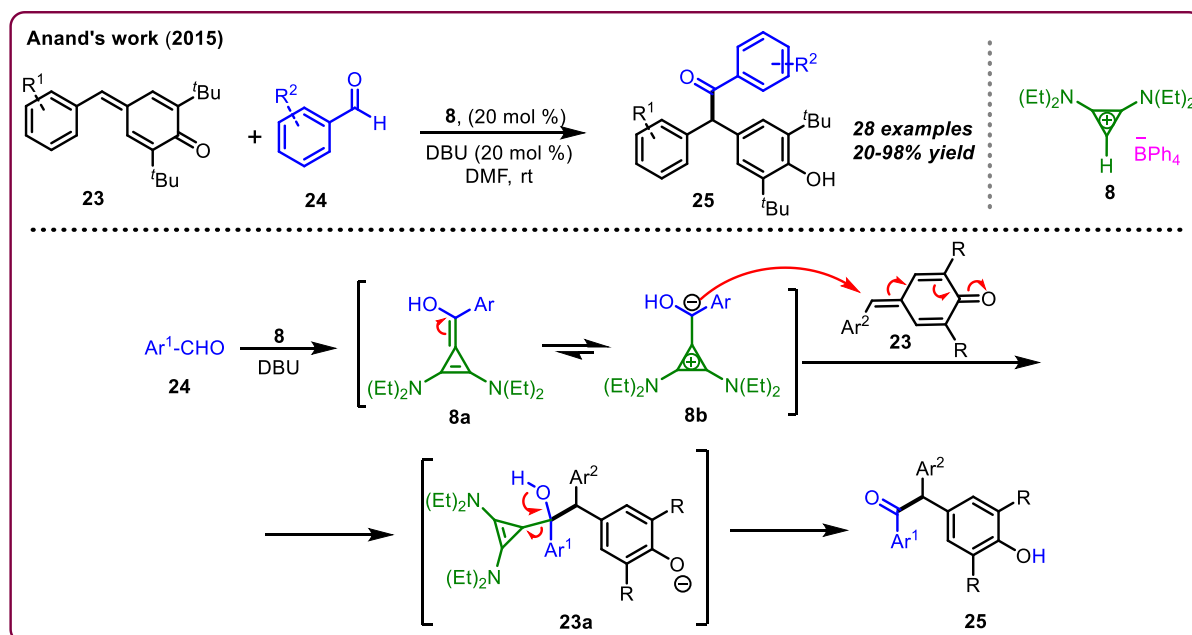
Apart from this, Gravel's group also developed an effective protocol for the synthesis of phosphinoylamino-ketone derivatives (**19**) under bis(amino)cyclopropenyliidene catalyzed aza-benzoin reaction between aldehydes (**18**) and imines (**17**). When the reaction was carried out between **18** and **17** using **8** as a precatalyst, the aza-benzoin products (**19**) were obtained

with very high chemoselectivity. Interestingly, in any of these cases, the homobenzoin product was not observed. The same strategy was used for the synthesis of α -amino ketones (**22**) by employing aldehydes (**21**) and *N*-protected imines (**20**) [Scheme 4].¹²



Scheme 4. BAC catalyzed Aza-benzoin reactions

While working on carbene-catalyzed organic transformations,¹³ Anand's research group has developed a bis(amino)cyclopropenylidene catalyzed vinylogous Stetter (1,6-conjugate addition reaction) reaction of aromatic/heteroaromatic aldehydes (**24**) to *para*-quinone methides (**23**) to isolate α,α' -diarylated ketones (**25**) in moderate to good yields (Scheme 5).¹⁴

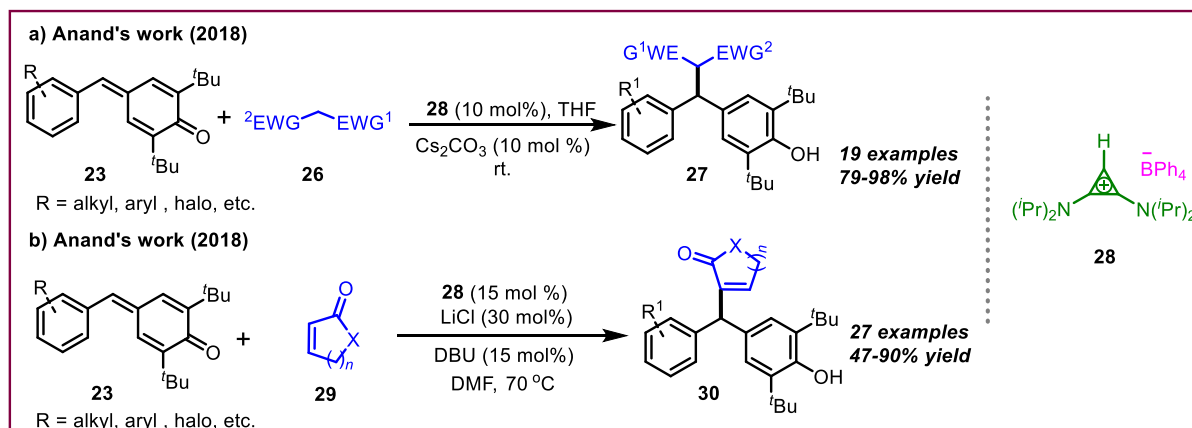


Scheme 5. BACs catalyzed intermolecular 1,6 addition reactions.

The author proposed that the reaction proceeds via the abstraction of a proton from **8** with a base (DBU) to produce carbene, which then reacts with **24** to generate the Breslow-type intermediate **8a/8b**. This intermediate **8a/8b** further reacted with *p*-QM **23** in a 1,6-fashion to

form another intermediate **23a**, which on proton transfer generates product **25** with the exclusion of carbene catalyst (Scheme 5).¹⁴

Recently, in 2018, Anand and co-workers disclosed the application of bis(amino)cyclopropenylidene (BAC) as a non-covalent Brønsted base catalyst in the conjugate addition of *p*-QMs (**23**) with carbon nucleophiles (**a**, Scheme 6).¹⁵ A wide range of *p*-QMs (**23**) were treated with 2-naphthols and active methylene compounds to afford the desired products (**27**) in excellent yields.



Scheme 6. BACs catalyzed 1,6 conjugated addition reaction of carbon nucleophiles.

Later, in the same year, Anand and co-workers established a BAC-promoted intermolecular Rauhut–Currier reaction of *p*-QMs (**23**) with enones (**29**) for the synthesis of unsymmetrical vinyl diarylmethane derivatives (**30**) in moderate to good yields (**b**, Scheme 6).¹⁶ Interestingly, the reaction worked only in the presence of LiCl.

2.1.3 Background

In recent years, the chemistry of *p*-quinone methides (*p*-QMs) has been explored in the synthesis of unsymmetrical diaryl-/triaryl-methanes, carbocycles, and heterocycles.¹³ Based on our previous experience in the carbene catalysis in *p*-QM chemistry (Scheme 5-6), we became interested in exploring the BAC catalysis in other transformations of *p*-QMs.

Phenanthrols, also known as hydroxy-substituted polycyclic aromatic hydrocarbons (PAHs), are abundant in natural products,¹⁷ alkaloids,¹⁸ and agrochemicals (Figure 2).¹⁹ They have a wide range of applications in material science²⁰ due to their special biomarker and smoke sensor properties.²¹ The phenolic hydroxy group in PACs can also be changed into several different functional groups.²² Over the past 20 years, many protocols have been developed to produce phenanthrene skeletons, including photocyclization reactions²³ of stilbene derivatives and intramolecular²⁴ and intermolecular benzannulation reactions of functionalized biphenyl

derivatives.²⁵ However, these methods typically require functionalized substrates²⁶, exogenous oxidants²³, ultraviolet (UV) irradiation²⁸, and other additional steps²⁹, which results in wasteful byproducts and unintended side reactions. Nevertheless, comprehensive research on the synthesis of hydroxy-substituted PACs is still limited, to the best of our literature serve, BACs catalyzed intramolecular cyclization reactions for the synthesis of PAHs are not known so far, this endorsed us for this organic transformation.

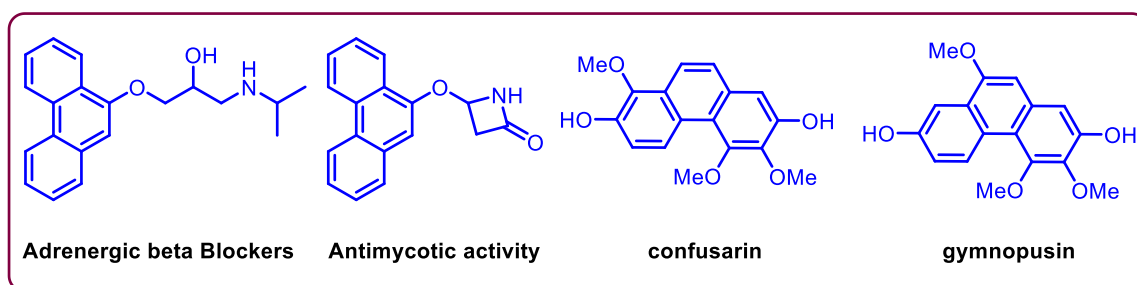


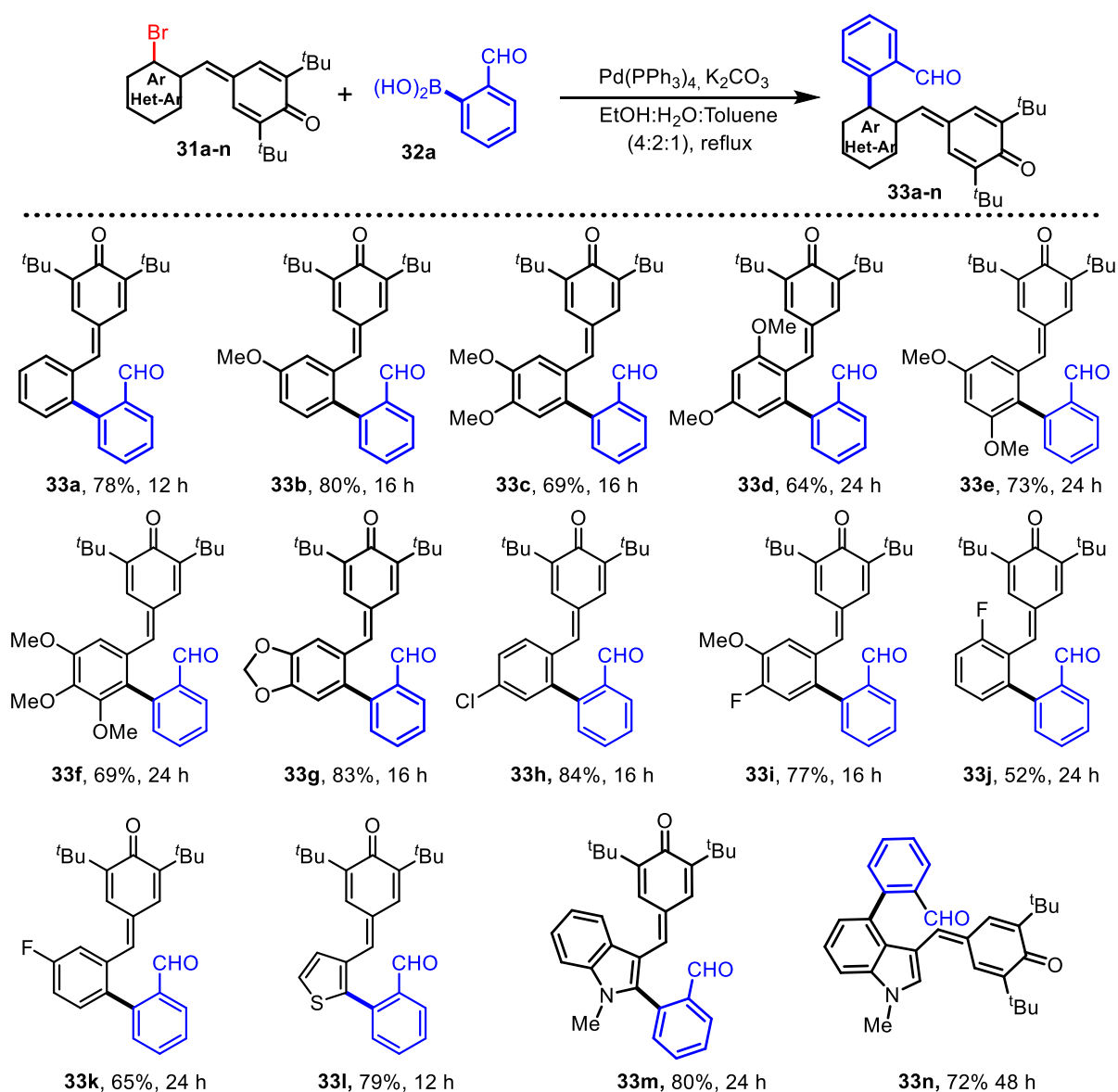
Figure 2. Phenanthrols-based natural products.

2.1.4 Result and discussion

With this concept in mind, we investigated the intramolecular 1,6-conjugate addition reaction of 2-(2-formylaryl)-phenyl-substituted *p*-quinone methides (*p*-QMs) under different reaction conditions. The 2-(2-formylaryl)-phenyl-substituted *p*-quinone methides **33a-m**, **33o-t** were synthesized by the Suzuki coupling between different 2-bromophenyl-substituted *para*-quinone methides and 2-formylphenylboronic acids as shown in the Scheme 7 & 8.³⁰

We began our optimization with a model substrate **33a** and used a wide range of NHC (**35a-c**) and BACs precursors (**36**, **28**, and **8**) [Table 1]. Our early experiment using triazolium-based NHC precatalyst **35a** and Cs₂CO₃ in dry THF did not produce a promising result as the anticipated product **34a** was not observed even after 24 hours (Entry 1). However, when the reaction was carried out using imidazolium-based NHC precursor **35b**, the desired product **34a** was obtained in a 71% yield after 24 hours (Entry 2). The thiazolium salt **35b**, however, could produce the product in 77% yield under the same reaction conditions within 12h (Entry 3). We observed a substantial improvement in yield of **34a** as well as in the rate of reaction, when BAC precursors **36**, **28**, and **8** were used as catalysts in dry THF (Entries 4-6).

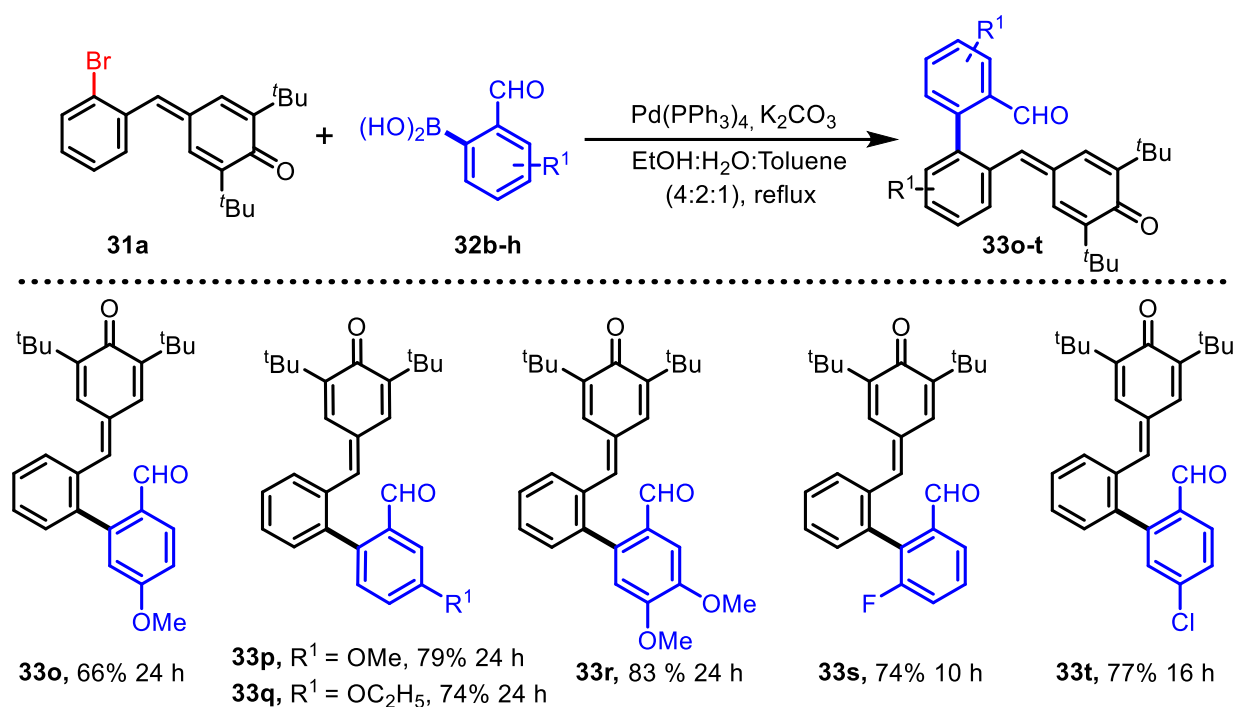
Scheme 7. Synthesis of 2-(2-formylaryl)-phenyl-substituted *p*-quinone methides.^a



^aReactions were carried out in 0.22-0.26 mmol scales of **31a-m**. Yields reported are isolated yields.

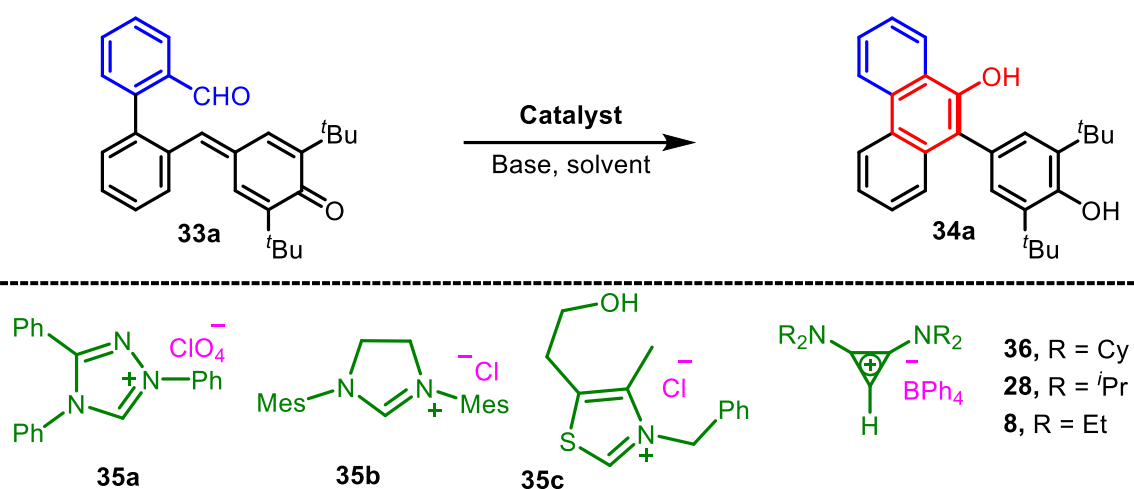
Our preliminary analysis showed that precursor **8** was marginally more effective and efficient than the other catalysts probably due to the lower steric effect (entry 6). Gratified by this result, we examined the reactions using carbene precursor **8** and different bases (Entries 7–13); it was noticed that when the reaction was carried out in Na_2CO_3 base, the yield of **34a** was dropped to 35% (Entry 7). Although in the case of NaH , the desired product **34a** was isolated in 67% yield (Entry 8), whereas the reaction produced only 37% of **34a** in the case of diisopropylethylamine (DIPEA) [Entry 9].

Scheme 08. Synthesis of 2-(2-formylaryl)-phenyl-substituted *p*-quinone methides.^a



^aReactions were carried out in 0.266 mmol scale of **31a**. Yields reported are isolated yields

Interestingly, the yield of **34a** was improved to 90% when DBU was used as a base (Entry 10). Encouraged by this result, optimization studies were elaborated using DBU as a base in other solvents including chlorinated and non-chlorinated solvents (Entries 11-14). In cases of chlorinated solvents such as CH_2Cl_2 and CHCl_3 , it was noticed that, although both the solvents were found to be very effective in driving this transformation with a considerable reduction in the reaction times (6 h to 1-3h), CH_2Cl_2 was found to be a bit superior to CHCl_3 in driving the reaction (Entry 11 vs 12). Other solvents such as 1,4-dioxane and *N,N*-dimethylformamide (DMF) were found to be less effective for this transformation (Entries 13 & 14). After screening bases and solvents, we were interested to know the catalyst loading effect. In line with this, a reaction was conducted using 5 mol % of **8**, and in this case, the reaction was found to be relatively slow and the product **34a** obtained in slightly lower yield (Entry 15).

Table 01. Catalyst screening and Optimization study^a

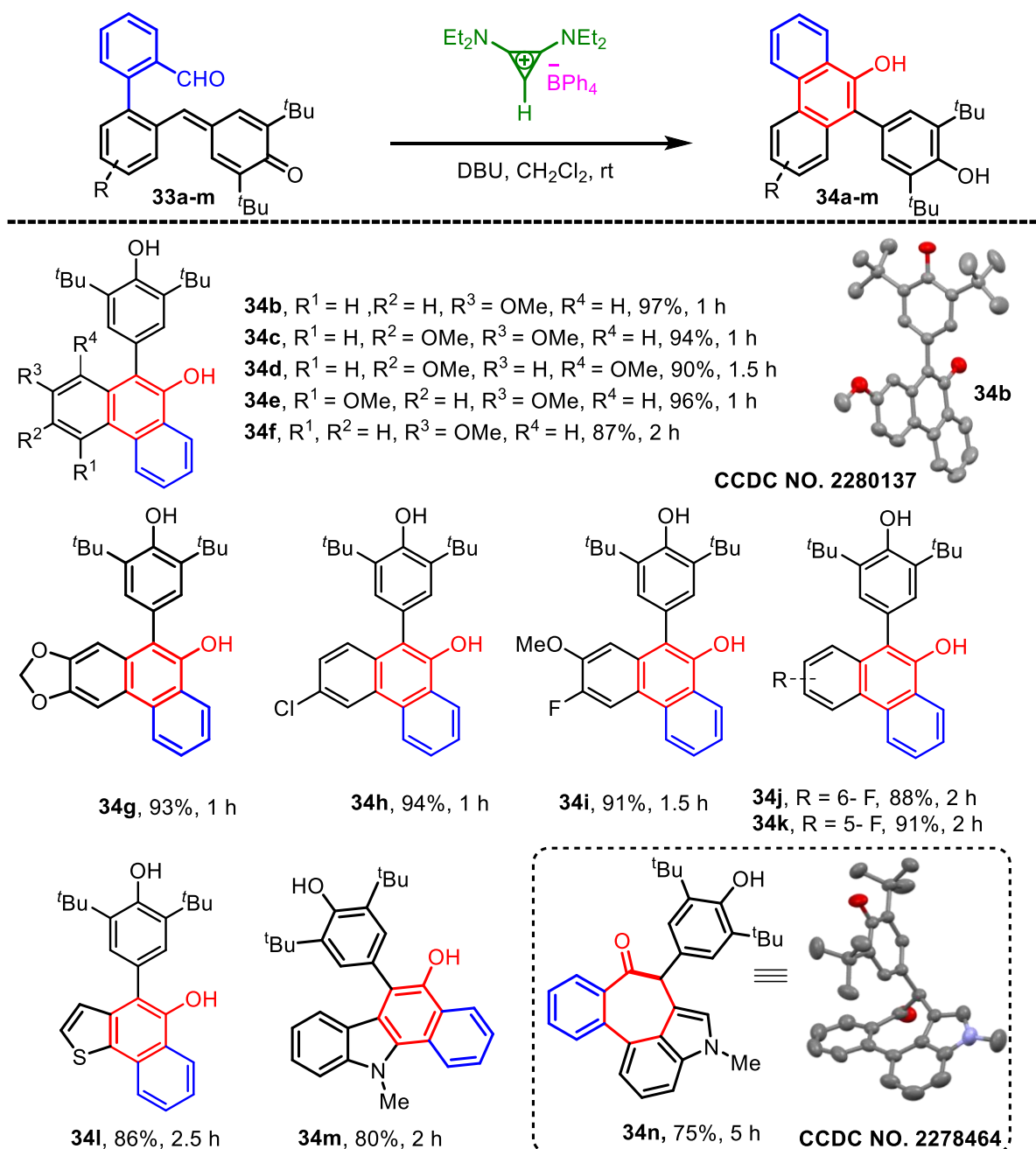
Entry	Catalyst	Base	Solvent	Time (h)	Yield ^b %
1	35a	Cs_2CO_3	THF	24	Trace
2	35b	Cs_2CO_3	THF	24	71
3	35c	Cs_2CO_3	THF	12	77
4	36	Cs_2CO_3	THF	10	78
5	28	Cs_2CO_3	THF	6	83
6	8	Cs_2CO_3	THF	6	85
7	8	Na_2CO_3	THF	24	35
8	8	NaH	THF	12	67
9	8	DIPEA	THF	24	37
10	8	DBU	THF	6	90
11 ^c	8	DBU	CH_2Cl_2	1	98
12	8	DBU	CHCl_3	3	92
13	8	DBU	1,4 Dioxane	24	57
14	8	DBU	DMF	24	39
15 ^d	8	DBU	CH_2Cl_2	2.5	95

All reactions were carried out with **33a** (0.10 mmol), and 10 mol % of catalyst **8** in 1.5 mL of solvent at room temperature. ^bIsolated yields. ^cOptimal condition. ^d5 mol % of catalyst was used.

2.1.4.1 Synthesis of 9-phenanthrols and their derivatives

Next, we looked at the generality of this transformation using various 2-(2-formylaryl)-phenyl-substituted *p*-quinone methides (*p*-QM) under optimal reaction conditions (Entry 11, Table 1). The structurally modified *p*-QMs **33b-m** underwent seamless conversion to their corresponding 10-(4-hydroxyphenyl)phenanthren-9-ol derivatives **34b-m** in exceptionally high yields, indicating that the electronic effects of the aryl substituents in the *p*-QMs had a little impact on the process (Chart 1).

Chart 1. Substrate scope^a

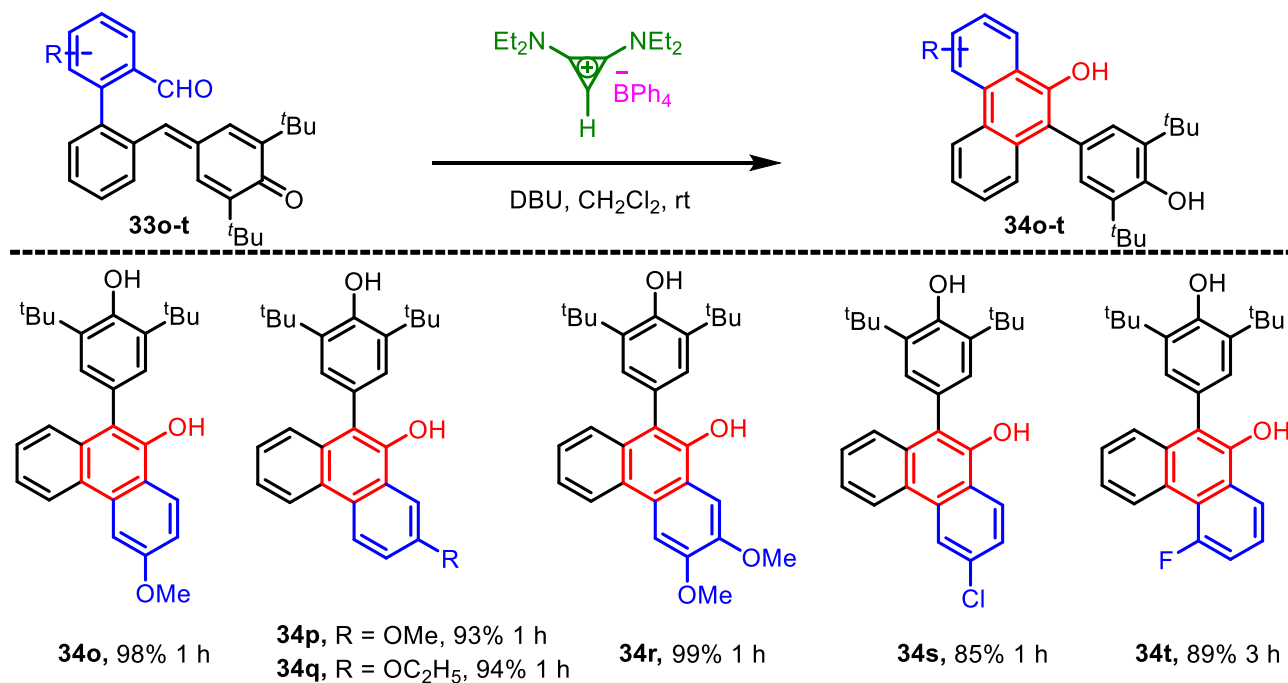


^aReactions were carried out in 0.69-79 mmol of **33a-l**. Yields reported are isolated yields.

In general, this protocol was effective for the preparation of 9-phenanthrol derivatives **34b-g** in excellent isolated yields (87-99%) from the respective precursors **33b-g**, derived from electron-rich aromatic aldehydes. This protocol was also found to be robust for the *p*-QMs containing halogen-substituted aromatic aldehydes. For instance, under the best-optimized condition, the *p*-QMs **33h-k** underwent umpolung followed by intramolecular 1,6-conjugate addition to produce the corresponding products **34h-k** in very high yields (88-94%). The *p*-QM **33l**, derived from 3-bromothiophene-2-carboxaldehyde, also underwent cyclization, and produced the desired product **34l** in 86% yield. Fascinatingly, the *p*-QM derived from indole **33n** produced a very interesting 1,3-dihydro-4H-benzo[4,5]cyclohepta[1,2,3-cd]indol-4-one compound based scaffold **34n**, which is found as a core in many natural products, in 75% yield. The structure of **34n** was unambiguously confirmed by X-ray crystallography.

To elaborate the substrate scope for this transformation, various other 2-(2-formylaryl)-phenyl-substituted *p*-quinone methides **33o-t** (derived from the 2-bromo *para*-quinone methide and different 2-formylphenylboronic acids) were subjected to this transformation under the optimal condition and in those cases, the respective products **34o-t** were obtained in 85-99% yields (Chart 2).

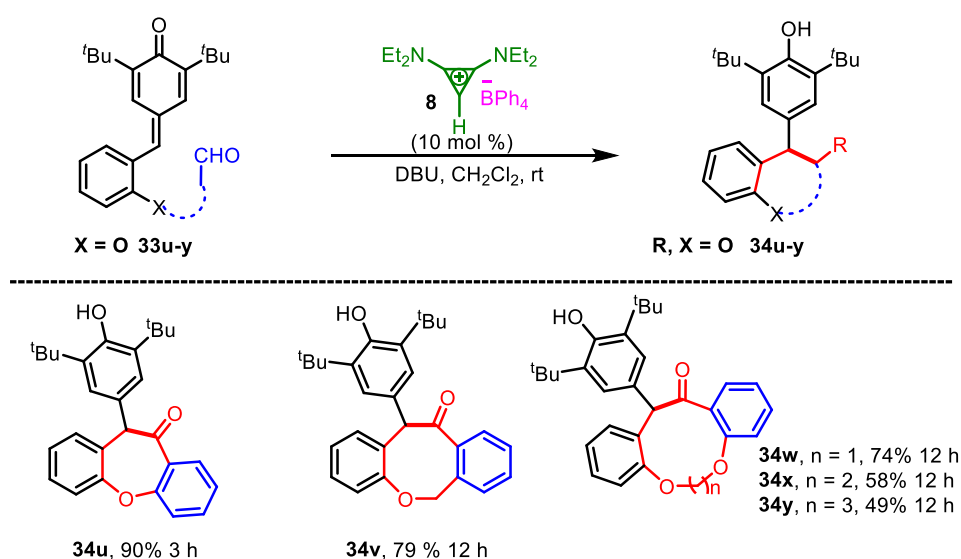
Chart 2. Substrate scope^a



^aReactions were carried out in 0.69-79 mmol of **33o-t**. Yields reported are isolated yields.

2.1.4.2 Synthesis of medium-sized carbocycles and heterocycles

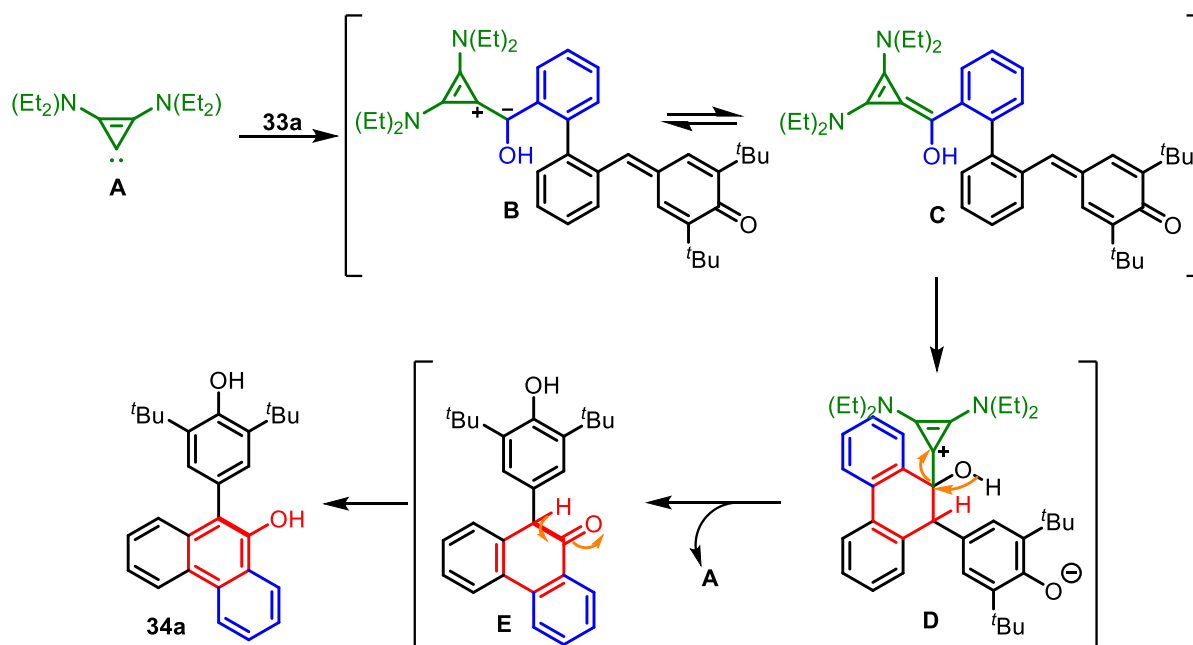
Compounds with cyclic molecular structures are attractive due to their availability and wide variety of applications. Medium-sized carbocycles and heterocycles are extremely prevalent in a wide range of natural products,³³ bioactive therapeutics,³⁴ and crucially essential synthetic chemicals.³⁵ The simplicity of preparation for each ring size varies greatly, though. Seven-membered and medium-sized rings (8–11-membered ring structures) are perhaps the hardest to prepare because they have less conformational stability than six-membered rings. Despite their success as pharmacological leads, compounds with MSRs are significantly underrepresented in screening libraries for drug development. To access medium-sized cyclic scaffolds using quick, modular, and practical methodologies, this problem has consistently motivated collective efforts toward a diversity-oriented synthesis.³⁶ However, the organocatalytic methodologies involving the construction of medium-sized carbocycles and heterocycles are still under represented. Based on the reaction of **33n**, which provided an interesting 7-membered carbocycle **34n** under the optimized reaction conditions (Chart 1), we hypothesized that it could be possible to prepare 7-membered and higher-order ring systems by suitably modifying the *p*-QMs. For this purpose, phenoxy- and various benzyloxy-substituted *p*-QMs were designed and synthesized. It was observed that phenoxy-substituted *p*-QM **37a** generated the corresponding cyclic compound **38a** in an excellent yield of 90% in a very short period of 3 h using **8** as a catalyst. However, in the cases of benzyloxy-substituted and other alkoxy-substituted *p*-QMs **37b-e**, the reactions were found to be sluggish; however, the expected higher-order cyclic compounds **38b-e** were obtained in the range of 79-49% yields (Scheme 11).



^aReactions were carried out in 0.69-79 mmol of **33 u-y**. Yields reported are isolated yields.

2.1.4.3 Plausible mechanism

A plausible mechanism has been hypothesized based on the outcomes of this transformation (Scheme 7). In the first stage, DBU removes the acidic proton from **8** and generates carbene **A**, which then combines with an aldehyde to form intermediate **B/C**, which then undergoes intramolecular 1,6-conjugate addition with **33a** to form another intermediate **D**. Elimination of the carbene **A** from **D** generates another intermediate **E**, which on aromatization gives the final product.



Scheme 7. Plausible Mechanism

2.1.5 Conclusion

In conclusion, we have established a BAC-catalyzed intramolecular cyclization reaction of 2-(2-formylaryl)-phenyl-substituted *p*-quinone methides to access 10-(4-hydroxyphenyl)phenanthren-9-ol derivatives. Additionally, this approach was also elaborated for the synthesis of medium-sized rings.

2.1.6 Experimental section:

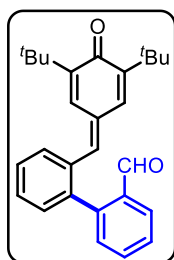
General Information. All other reactions were carried out under an argon atmosphere employing flame-dried glassware. Most of the reagents and starting materials were purchased

from commercial sources and used as such. 2-bromo *p*-quinone methide was prepared by following a literature procedure.¹³⁻¹⁵ The bis(amino)cyclopropenium salts **36**, **28**, and **8**,⁷⁻⁸ and the NHC precursor **35a-c** were prepared according to the literature procedure.³⁷ Melting points were recorded on the SMP20 melting point apparatus and are uncorrected. ¹H, ¹³C, and ¹⁹F spectra were recorded in CDCl₃, DMSO-*d*₆, and acetone-*d*₆ (400, 100, and 376 MHz, respectively) on a Bruker FT-NMR spectrometer. Chemical shift (δ) values are reported in parts per million (ppm) relative to TMS and the coupling constants (*J*) are reported in Hz. High-resolution mass spectra were recorded on Waters Q-TOF Premier-HAB213 spectrometer. FT-IR spectra were recorded on a Perkin–Elmer FT-IR spectrometer. Thin layer chromatography was performed on Merck silica gel 60 F₂₅₄ TLC plates. Column chromatography was carried out through a silica gel (100-200 mesh) column using a mixture of EtOAc/hexane as eluent.

General procedure for the synthesis of 2-(2-arylformyl)phenyl *p*-quinone methide derivatives (**33a-t**)

Procedure (For the preparation of **33a-m, and **33o-t**).** Nitrogen gas was purged through a mixture of an aqueous solution of sodium carbonate (1.6 mmol, 2 equiv.) and toluene (2:3) [10 mL] for 15 min, and then, to this mixture was added boronic acid [0.96 mmol, 1.2 equiv.], Pd(PPh₃)₄ [0.04 mmol, 5 mol%] and 4-(2-bromobenzylidene)-2,6-di-*tert*-butylcyclohexa-2,5-dienone [0.8 mmol, 1 equiv.] successively. The reaction mixture was stirred at 100 °C for 12 h. After completion of the reaction (monitored by TLC), the reaction mixture was diluted with ethyl acetate (30 mL) and water (10 mL). The organic layer was separated, and the aqueous layer was extracted with ethyl acetate (20 mL \times 2). The combined organic layer was dried over anhydrous sodium sulphate, filtered, and concentrated under reduced pressure. The residue was purified through neutral alumina column chromatography using hexane/EtOAc to obtain pure 2-formylarylphenyl *p*-quinone methide derivatives (**33a-t**).

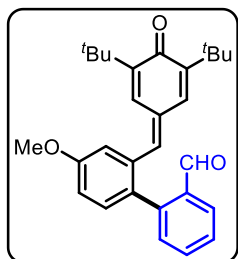
2'-((3,5-di-*tert*-butyl-4-oxocyclohexa-2,5-dien-1-ylidene)methyl)-[1,1'-biphenyl]-2-carbaldehyde (**33a**).



The reaction was performed at 0.268 mmol scale of 2-bromo *p*-quinone methide **31a**; *R_f* = 0.2 (10% EtOAc in hexane); orange gummy solid (83.5 mg, 78% yield); m. p. = 133-135 °C; ¹H NMR (400 MHz, CDCl₃) δ 9.77 (s, 1H), 8.05 (d, *J* = 7.7 Hz, 1H), 7.66 (t, *J* = 7.5 Hz, 1H), 7.56 (t, *J* = 8.4 Hz, 1H), 7.53–7.48 (m, 3H), 7.44 (s, 1H), 7.37 (d, *J* = 7.2 Hz, 1H), 7.33 (d, *J* = 7.6 Hz, 1H), 6.73 (s, 2H), 1.30 (s, 9H), 1.26 (s, 9H); ¹³C{¹H} NMR (100 MHz, CDCl₃) δ 191.5, 186.7, 149.9, 148.0, 143.9, 140.7, 138.7, 135.4, 134.6, 134.3, 133.8, 132.8, 131.7, 131.63, 131.60, 129.1, 128.7, 128.4, 128.0, 127.8, 35.6, 35.1, 29.7, 29.6; FT-IR

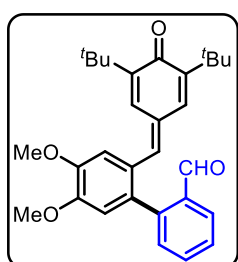
(neat): 2971, 2868, 1701, 1637, 1461, 1361, 1275, 750 cm^{-1} ; HRMS (ESI): m/z calcd for $\text{C}_{28}\text{H}_{31}\text{O}_2$ $[\text{M}+\text{H}]^+$: 399.2324; found: 399.2322.

2'-((3,5-di-tert-butyl-4-oxocyclohexa-2,5-dien-1-ylidene)methyl)-4'-methoxy-[1,1'-biphenyl]-2-carbaldehyde (33b).



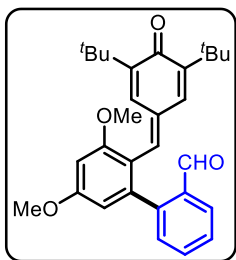
The reaction was performed at 0.249 mmol scale of corresponding 2-bromo phenyl substituted *p*-quinone methide **31b**; R_f = 0.4 (10% EtOAc in hexane); yellow solid (85.3 mg, 80% yield); m. p. = 129-130 $^{\circ}\text{C}$; ^1H NMR (400 MHz, CDCl_3) δ 9.78 (s, 1H), 8.03 (d, J = 7.6 Hz, 1H), 7.64 (t, J = 7.4 Hz, 1H), 7.54 (d, J = 7.6 Hz, 1H), 7.28 (d, J = 8.1 Hz, 1H), 7.06 – 7.03 (m, 2H), 6.74 (d, J = 2.0 Hz, 1H), 6.72 (s, 1H), 3.90 (s, 3H), 1.31 (s, 9H), 1.25 (s, 9H); $^{13}\text{C}\{^1\text{H}\}$ NMR (100 MHz, CDCl_3) δ 191.7, 186.7, 159.5, 149.9, 148.0, 143.7, 140.7, 136.4, 134.62, 134.56, 133.7, 132.9, 132.8, 132.1, 128.4, 127.9, 127.7, 116.4, 115.3, 56.7, 35.6, 35.1, 29.8, 29.6; FT-IR (neat): 2971, 2868, 1701, 1631, 1461, 1361, 1275, 750 cm^{-1} ; HRMS (ESI): m/z calcd for $\text{C}_{29}\text{H}_{33}\text{O}_3$ $[\text{M}+\text{H}]^+$: 429.2424; found: 429.2427.

2'-((3,5-di-tert-butyl-4-oxocyclohexa-2,5-dien-1-ylidene)methyl)-4',5'-dimethoxy-[1,1'-biphenyl]-2-carbaldehyde (33c).



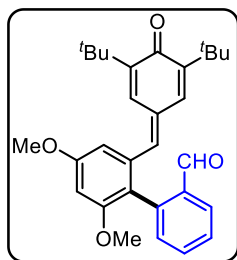
The reaction was performed at 0.23 mmol scale of corresponding 2-bromo phenyl substituted *p*-quinone methide **31c**; R_f = 0.3 (10% EtOAc in hexane); yellow solid (73.2 mg, 69% yield); m. p. = 282-284 $^{\circ}\text{C}$; ^1H NMR (400 MHz, CDCl_3) δ 9.80 (s, 1H), 8.04 (d, J = 7.6 Hz, 1H), 7.65 (t, J = 7.5 Hz, 1H), 7.56 (d, J = 7.5 Hz, 1H), 7.54 – 7.53 (m, 1H), 7.34 (d, J = 7.5 Hz, 1H), 7.08 (s, 1H), 6.85 (s, 1H), 6.73 (d, J = 2.2 Hz, 1H), 6.68 (s, 1H), 3.97 (s, 3H), 3.93 (s, 3H), 1.30 (s, 9H), 1.24 (s, 9H); $^{13}\text{C}\{^1\text{H}\}$ NMR (100 MHz, CDCl_3) δ 191.7, 186.5, 149.7, 149.6, 148.8, 147.5, 143.7, 140.8, 134.9, 134.5, 133.8, 132.3, 131.9, 131.6, 128.6, 127.83, 127.80, 114.2, 114.1, 56.3, 56.2, 35.6, 35.1, 29.8, 29.5; FT-IR (neat): 2971, 2868, 1701, 1634, 1461, 1361, 1275, 750 cm^{-1} HRMS (ESI): m/z calcd for $\text{C}_{28}\text{H}_{31}\text{O}_2$ $[\text{M}+\text{H}]^+$: 458.2457; found: 458.2451.

2'-((3,5-di-tert-butyl-4-oxocyclohexa-2,5-dien-1-ylidene)methyl)-3',5'-dimethoxy-[1,1'-biphenyl]-2-carbaldehyde (33d).



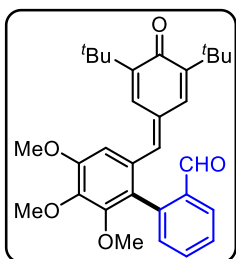
The reaction was performed at 0.23 mmol scale of corresponding 2-bromo phenyl substituted *p*-quinone methide **31d**; $R_f = 0.5$ (10% EtOAc in hexane); yellow solid (67.9 mg, 64% yield); m. p. = 193-195 °C; ^1H NMR (400 MHz, CDCl_3) δ 9.81 (s, 1H), 7.92 (d, $J = 7.6$ Hz, 1H), 7.61 – 7.57 (m, 1H), 7.45 (t, $J = 7.6$ Hz, 1H), 7.35 (d, $J = 7.4$ Hz, 1H), 6.80 (d, $J = 2.2$ Hz, 1H), 6.71 (d, $J = 2.2$ Hz, 1H), 6.61 – 6.60 (m, 1H), 6.52 (d, $J = 2.2$ Hz, 1H), 3.88 (s, 3H), 3.86 (s, 3H), 1.22 (s, 9H), 1.17 (s, 9H); $^{13}\text{C}\{^1\text{H}\}$ NMR (100 MHz, CDCl_3) δ 191.6, 186.8, 161.1, 158.4, 147.6, 147.0, 144.1, 140.4, 134.4, 133.82, 133.75, 133.3, 131.4, 129.0, 128.4, 127.6, 117.7, 108.2, 98.5, 55.79, 55.76, 35.2, 35.0, 29.6, 29.5; FT-IR (neat): 2971, 2868, 1701, 1634, 1461, 1361, 1275, 750 cm^{-1} ; HRMS (ESI): m/z calcd for $\text{C}_{28}\text{H}_{31}\text{O}_2$ $[\text{M}+\text{H}]^+$: 458.2457; found: 458.2451.

2'-((3,5-di-tert-butyl-4-oxocyclohexa-2,5-dien-1-ylidene)methyl)-4,6'-dimethoxy-[1,1'-biphenyl]-2-carbaldehyde (33e).



The reaction was performed at 0.23 mmol scale of corresponding 2-bromo phenyl substituted *p*-quinone methide **31e**; $R_f = 0.4$ (10% EtOAc in hexane); yellow solid (77.6 mg, 73% yield); m. p. = 196-198 °C; ^1H NMR (400 MHz, CDCl_3) δ 9.75 (s, 1H), 8.04 – 8.02 (m, 1H), 7.19 – 7.17 (m, 1H), 7.55 (d, $J = 2.2$ Hz, 1H), 7.50 (t, $J = 7.6$ Hz, 1H), 7.65 – 7.60 (m, 1H), 6.71 (d, $J = 2.3$ Hz, 1H), 6.68 (d, $J = 2.2$ Hz, 1H), 6.66 (s, 1H), 6.61 (d, $J = 2.2$ Hz, 1H), 3.89 (s, 3H), 3.72 (s, 3H), 1.31 (s, 9H), 1.25 (s, 9H); $^{13}\text{C}\{^1\text{H}\}$ NMR (100 MHz, CDCl_3) δ 192.3, 186.7, 160.5, 158.3, 149.7, 147.9, 141.4, 139.4, 137.1, 134.7, 133.8, 133.1, 132.6, 128.3, 127.3, 120.2, 107.8, 99.6, 55.9, 55.7, 35.6, 35.1, 29.8, 29.6; FT-IR (neat): 2971, 2868, 1701, 1634, 1461, 1361, 1275, 750 cm^{-1} ; HRMS (ESI): m/z calcd for $\text{C}_{28}\text{H}_{31}\text{O}_2$ $[\text{M}+\text{H}]^+$: 458.2457; found: 458.2451.

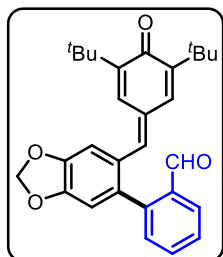
6'-((3,5-di-tert-butyl-4-oxocyclohexa-2,5-dien-1-ylidene)methyl)-2',3',4'-trimethoxy-[1,1'-biphenyl]-2-carbaldehyde (33f).



The reaction was performed at 0.22 mmol scale of corresponding 2-bromo phenyl substituted *p*-quinone methide **31f**; $R_f = 0.2$ (10% EtOAc in hexane); gummy orange solid (72.8 mg, 69% yield); ^1H NMR (400 MHz, CDCl_3) δ 9.81 (s, 1H), 8.11 – 8.06 (m, 1H), 7.67 – 7.63 (m, 1H), 7.57 – 7.54 (m, 1H), 7.25 – 7.23 (m, 1H), 6.88 (s, 1H), 6.71 (d, $J = 2.2$ Hz, 1H), 6.60 (s, 1H), 3.98 (s, 3H), 3.95 (s, 3H), 3.56 (s, 3H), 1.33 (s, 9H), 1.25 (s, 9H); $^{13}\text{C}\{^1\text{H}\}$ NMR (100 MHz, CDCl_3) δ 191.9, 186.6, 153.4, 151.7, 149.7, 147.8, 143.1, 141.0, 139.1, 134.8, 134.5, 133.7, 132.8, 132.1, 130.8, 128.5, 127.8, 127.7, 126.0, 120.2, 110.9, 61.4, 68.8, 56.3, 35.7, 35.1, 29.8, 29.6; FT-IR (neat): 2971, 2868, 1701, 1642, 1461, 1361, 1275, 750 cm^{-1} ;

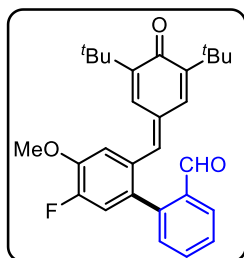
HRMS (ESI): m/z calcd for $C_{31}H_{37}O_5$ $[M+H]^+$: 489.2636; found 489.2635.

2-((3,5-di-tert-butyl-4-oxocyclohexa-2,5-dien-1-ylidene)methyl)benzo[d][1,3]dioxol-5-yl)benzaldehyde (33g).



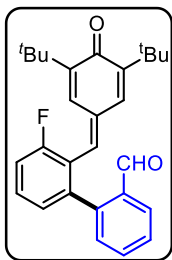
The reaction was performed at 0.24 mmol scale of corresponding 2-bromo phenyl substituted *p*-quinone methide **31g**; R_f = 0.4 (10% EtOAc in hexane); yellow solid (88 mg, 83% yield); m. p. = 137-139 °C; 1H NMR (400 MHz, $CDCl_3$) δ 9.80 (s, 1H), 8.04 – 8.02 (m, 1H), 7.67 – 7.63 (m, 1H), 7.55 (t, J = 7.6 Hz, 1H), 7.45 (d, J = 2.2 Hz, 1H), 7.31 (d, J = 7.0 Hz, 1H), 7.03 (s, 1H), 6.85 (s, 1H), 6.67 (d, J = 2.3 Hz, 1H), 6.58 (s, 1H), 6.13 (s, 2H), 1.32 (s, 9H), 1.24 (s, 9H); $^{13}C\{^1H\}$ NMR (100 MHz, $CDCl_3$) δ 191.5, 186.6, 149.7, 148.6, 148.2, 147.7, 143.6, 140.6, 134.8, 134.6, 133.9, 133.8, 131.87, 131.84, 129.4, 128.7, 128.0, 127.5, 111.6, 110.9, 102.2, 35.6, 35.1, 29.7, 29.6; FT-IR (neat): 2971, 2868, 1701, 1639, 1461, 1361, 1275, 750 cm^{-1} ; HRMS (ESI): m/z calcd for $C_{28}H_{33}O$ $[M+H]^+$: 385.2531; found: 385.2541.

2'-((3,5-di-tert-butyl-4-oxocyclohexa-2,5-dien-1-ylidene)methyl)-5'-fluoro-4'-methoxy-[1,1'-biphenyl]-2-carbaldehyde (33h).



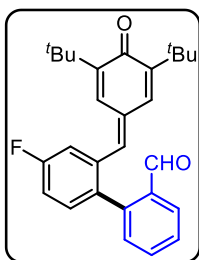
The reaction was performed at 0.24 mmol scale of corresponding 2-bromo phenyl substituted *p*-quinone methide **31h**; R_f = 0.3 (10% EtOAc in hexane); yellow solid (82.4 mg, 77% yield); m. p. = 200-202 °C; 1H NMR (400 MHz, $CDCl_3$) δ 9.79 (s, 1H), 8.03 (d, J = 7.7 Hz, 1H), 7.68 – 7.64 (m, 1H), 7.57 (t, J = 7.6 Hz, 1H), 7.44 (d, J = 2.2 Hz, 1H), 7.31 (d, J = 7.6 Hz, 1H), 7.13 (d, J = 7.8 Hz, 1H), 7.11 (d, J = 5.0 Hz, 1H), 6.72 (d, J = 2.3 Hz, 1H), 6.63 (s, 1H), 3.98 (s, 3H), 1.30 (s, 9H), 1.25 (s, 9H); $^{13}C\{^1H\}$ NMR (100 MHz, $CDCl_3$) δ 191.2, 186.6, 152.3 (d, J_{C-F} = 251 Hz), 150.2, 148.1, 147.6 (d, J_{C-F} = 10.9 Hz), 142.3, 139.5, 134.5 (d, J_{C-F} = 9.3 Hz), 133.9, 132.8, 132.0 (d, J_{C-F} = 6.5 Hz), 131.8, 131.7 (d, J_{C-F} = 3.9 Hz), 128.9, 128.3, 127.4, 119.2 (d, J_{C-F} = 19.1 Hz), 116.3 (d, J_{C-F} = 1.4 Hz), 56.5 (d, J_{C-F} = 3.3 Hz), 56.2, 35.7, 35.2, 29.8, 29.6; ^{19}F NMR (376 MHz, $CDCl_3$) δ -132.5; FT-IR (neat): 2971, 2868, 1721, 1634, 1461, 1361, 1275, 750 cm^{-1} ; HRMS (ESI): m/z calcd for $C_{29}H_{32}FO_3$ $[M+H]^+$: 447.2330; found: 447.2330.

2'-((3,5-di-tert-butyl-4-oxocyclohexa-2,5-dien-1-ylidene)methyl)-3'-fluoro-[1,1'-biphenyl]-2-carbaldehyde (33i).



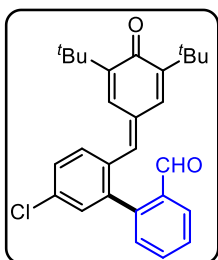
The reaction was performed at 0.255 mmol scale of corresponding 2-bromo phenyl substituted *p*-quinone methide **31i**; $R_f = 0.4$ (10% EtOAc in hexane); orange solid (55.3 mg, 52% yield); m. p. = 197-199 °C; ^1H NMR (400 MHz, CDCl_3) δ 9.77 (s, 1H), 8.05 – 8.03 (m, 1H), 7.69 – 7.65 (m, 1H), 7.57 (t, $J = 7.6$ Hz, 1H), 7.40 (d, $J = 2.2$ Hz, 1H), 7.36 – 7.33 (m, 1H), 7.31 – 7.30 (m, 1H), 7.26 – 7.18 (m, 2H), 6.70 (d, $J = 2.2$ Hz, 1H), 6.62 (s, 1H), 1.31 (s, 9H), 1.25 (s, 9H); $^{13}\text{C}\{^1\text{H}\}$ NMR (100 MHz, CDCl_3) δ 191.2, 186.6, 162.3 (d, $J_{\text{C-F}} = 247.4$ Hz), 150.5, 148.4, 142.7, 138.7, 136.2 (d, $J_{\text{C-F}} = 8.0$ Hz), 134.4, 134.3, 133.9, 133.5, 133.1 (d, $J_{\text{C-F}} = 8.2$ Hz), 131.8, 128.9, 128.4, 127.1, 118.0 (d, $J_{\text{C-F}} = 226$ Hz), 116.0 (d, $J_{\text{C-F}} = 212$ Hz), 35.7, 35.2, 29.7, 29.6; ^{19}F NMR (376 MHz, CDCl_3) δ -109.6; FT-IR (neat): 2971, 2868, 1713, 1639, 1461, 1361, 1275, 750 cm^{-1} ; HRMS (ESI): m/z calcd for $\text{C}_{28}\text{H}_{30}\text{FO}_2$ $[\text{M}+\text{H}]^+$: 417.2224; found: 417.2224.

2'-((3,5-di-tert-butyl-4-oxocyclohexa-2,5-dien-1-ylidene)methyl)-4'-fluoro-[1,1'-biphenyl]-2-carbaldehyde (33j).



The reaction was performed at 0.255 mmol scale of corresponding 2-bromo phenyl substituted *p*-quinone methide **31j**; $R_f = 0.4$ (10% EtOAc in hexane); yellow solid (69.2 mg, 65% yield); m. p. = 186-188 °C; ^1H NMR (400 MHz, CDCl_3) δ 9.75 (s, 1H), 8.05 – 8.03 (m, 1H), 7.68 – 7.66 (m, 1H), 7.57 (t, $J = 7.6$ Hz, 1H), 7.40 (d, $J = 2.2$ Hz, 1H), 7.36 – 7.33 (m, 1H), 7.31 – 7.30 (m, 1H), 7.26 – 7.18 (m, 2H), 6.70 (d, $J = 2.2$ Hz, 1H), 6.62 (s, 1H), 1.31 (s, 9H), 1.25 (s, 9H); $^{13}\text{C}\{^1\text{H}\}$ NMR (100 MHz, CDCl_3) δ 191.2, 186.6, 162.3 (d, $J_{\text{C-F}} = 247.4$ Hz), 150.5, 148.4, 142.7, 138.7, 136.2 (d, $J_{\text{C-F}} = 8.0$ Hz), 134.4, 134.3, 133.9, 133.5, 133.1 (d, $J_{\text{C-F}} = 8.2$ Hz), 131.8, 128.9, 128.4, 127.1, 118.0 (d, $J_{\text{C-F}} = 226$ Hz), 116.0 (d, $J_{\text{C-F}} = 212$ Hz), 35.7, 35.2, 29.7, 29.6; ^{19}F NMR (376 MHz, CDCl_3) δ -109.1; FT-IR (neat): 2971, 2868, 1715, 1639, 1461, 1361, 1275, 750 cm^{-1} ; HRMS (ESI): m/z calcd for $\text{C}_{28}\text{H}_{30}\text{FO}_2$ $[\text{M}+\text{H}]^+$: 417.2224; found: 417.2224.

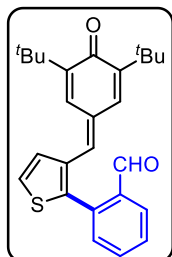
5'-chloro-2'-((3,5-di-tert-butyl-4-oxocyclohexa-2,5-dien-1-ylidene)methyl)-[1,1'-biphenyl]-2-carbaldehyde (33k).



The reaction was performed at 0.245 mmol scale of corresponding 2-bromo phenyl substituted *p*-quinone methide **31k**; $R_f = 0.6$ (10% EtOAc in hexane); yellow solid (89.2 mg, 84% yield); m. p. = 169-171 °C; ^1H NMR (400 MHz, CDCl_3) δ 9.77 (s, 1H), 8.05 – 8.03 (m, 1H), 7.69 – 7.65 (m, 1H), 7.58 (t, $J = 7.6$ Hz, 1H), 7.53 (d, $J = 2.2$ Hz, 1H), 7.48 – 7.46 (m, 1H), 7.39 (d, $J = 2.2$ Hz, 1H), 7.32 – 7.29 (m, 2H), 6.70 (d, $J = 2.0$ Hz, 1H), 6.60 (s, 1H), 1.31 (s, 9H), 1.25 (s, 9H); $^{13}\text{C}\{^1\text{H}\}$ NMR (100 MHz, CDCl_3) δ 191.1, 186.6, 150.4, 148.5, 142.5, 138.5,

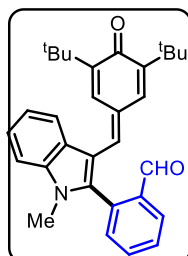
137.1, 136.9, 134.5, 134.3, 134.0, 133.6, 132.6, 131.6, 131.3, 129.0, 128.9, 128.5, 127.2, 35.7, 35.2, 29.7, 29.6; FT-IR (neat): 3642, 3070, 2953, 1597, 1434, 1390, 1233, 1152, 912, 746 cm^{-1} ; HRMS (ESI): m/z calcd for $\text{C}_{32}\text{H}_{33}\text{O}_2$ $[\text{M}+\text{H}]^+$: 433.1929; found: 433.1925.

2-(3-((3,5-di-tert-butyl-4-oxocyclohexa-2,5-dien-1-ylidene)methyl)thiophen-2-yl)benzaldehyde (33l).



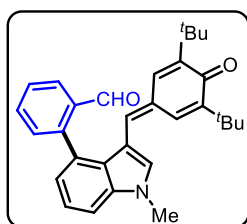
The reaction was performed at 0.247 mmol scale of 4-((2-bromothiophen-3-yl)methylene)-2,6-di-tert-butylcyclohexa-2,5-dien-1-one **31l**; R_f = 0.4 (5% EtOAc in hexane); gummy orange solid (79.3 mg, 79% yield); ^1H NMR (400 MHz, CDCl_3) δ 9.88 (s, 1H), 8.11 – 8.09 (m, 1H), 7.94 (d, J = 2.2 Hz, 1H), 7.74 – 7.70 (m, 1H), 7.65 (d, J = 5.2 Hz, 1H), 7.61 (t, J = 7.6 Hz, 1H), 7.40 (d, J = 7.5 Hz, 1H), 7.14 (d, J = 5.2 Hz, 1H), 6.74 (s, 1H), 6.72 (d, J = 2.2 Hz, 1H), 1.38 (s, 9H), 1.25 (s, 9H); $^{13}\text{C}\{^1\text{H}\}$ NMR (100 MHz, CDCl_3) δ 191.5, 186.3, 150.0, 147.8, 142.6, 139.1, 136.5, 135.2, 134.9, 134.1, 131.9, 131.7, 131.1, 130.4, 129.9, 129.1, 128.2, 126.9, 35.9, 35.2, 29.8, 29.6; IR (neat): 2956, 1730, 1638, 1458, 1261, 1360, 821, 764 cm^{-1} ; HRMS (ESI): m/z calcd for $\text{C}_{28}\text{H}_{29}\text{O}_2\text{S}$ $[\text{M}+\text{H}]^+$: 405.1883; found: 405.1886.

2-(3-((3,5-di-tert-butyl-4-oxocyclohexa-2,5-dien-1-ylidene)methyl)-1-methyl-1H-indol-2-yl)benzaldehyde (33m).



The reaction was performed at 0.266 mmol scale of 2-bromo *p*-quinone methide **31m**; R_f = 0.4 (15% EtOAc in hexane); orange solid (82 mg, 88% yield); m. p. = 246–248 $^{\circ}\text{C}$; ^1H NMR (400 MHz, CDCl_3) δ 9.92 (s, 1H), 7.99 (d, J = 7.6 Hz, 1H), 7.66 – 7.62 (m, 1H), 7.54 (d, J = 7.9 Hz, 2H), 7.46 – 7.37 (m, 3H), 7.23 – 7.19 (m, 1H), 6.94 (d, J = 6.2 Hz, 2H), 6.81 (s, 1H), 3.85 (s, 3H), 1.29 (s, 9H), 1.02 (s, 9H); $^{13}\text{C}\{^1\text{H}\}$ NMR (100 MHz, CDCl_3) δ 192.2, 186.5, 149.9, 148.5, 138.8, 134.7, 134.4, 134.3, 134.2, 133.9, 132.6, 128.5, 128.3, 128.1, 127.9, 121.9, 115.5, 35.3, 35.2, 29.6, 29.4; FT-IR (neat): 2971, 2868, 1701, 1631, 1461, 1361, 1275, 750 cm^{-1} ; HRMS (ESI): m/z calcd for $\text{C}_{31}\text{H}_{34}\text{NO}_2$ $[\text{M}+\text{H}]^+$: 452.2584; found: 452.2584.

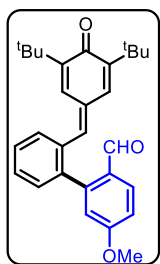
4-(2-((3,5-di-tert-butyl-4-oxocyclohexa-2,5-dien-1-ylidene)methyl)phenyl)-1-methyl-1H-indole-3-carbaldehyde (33n).



The reaction was performed at 0.266 mmol scale of 2-bromo *p*-quinone methide **31n**; R_f = 0.4 (5% EtOAc in hexane); orange solid (264 mg, 78% yield); m. p. = 179–181 $^{\circ}\text{C}$; ^1H NMR (400 MHz, CDCl_3) δ 9.75 (s, 1H), 8.10 – 8.08 (m, 1H), 7.71 – 7.67 (m, 1H), 7.61 (t, J = 7.6 Hz, 1H), 7.53 (d, J = 2.2 Hz, 1H), 7.49 – 7.46 (m, 2H), 7.42 – 7.38 (m, 2H), 7.14 (d, J = 6.8 Hz, 1H), 6.29 (d, J = 6.2 Hz, 2H), 6.18 (s, 1H), 3.96 (s, 3H), 1.33 (s, 9H), 1.28 (s, 9H);

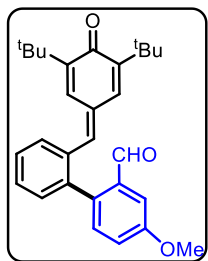
$^{13}\text{C}\{^1\text{H}\}$ NMR (100 MHz, CDCl_3) δ 192.1, 186.7, 148.2, 145.8, 144.7, 137.3, 136.1, 135.4, 133.7, 132.4, 131.4, 131.1, 128.3, 127.8, 127.5, 127.3, 126.7, 124.0, 123.0, 112.9, 110.2, 35.5, 34.8, 29.8, 29.5; FT-IR (neat): 2971, 2868, 1701, 1631, 1461, 1361, 1275, 750 cm^{-1} ; HRMS (ESI): m/z calcd for $\text{C}_{31}\text{H}_{34}\text{NO}_2$ $[\text{M}+\text{H}]^+$: 452.2584; found: 452.2584.

2'-((3,5-di-tert-butyl-4-oxocyclohexa-2,5-dien-1-ylidene)methyl)-5-methoxy-[1,1'-biphenyl]-2-carbaldehyde (33o).



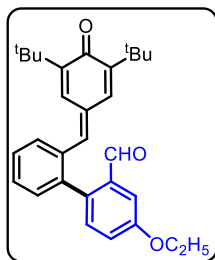
The reaction was performed at 0.266 mmol scale of 2-bromo *p*-quinone methide **31a**; R_f = 0.4 (10% EtOAc in hexane); orange solid (75.3 mg, 66% yield); m. p. = 199-206 $^{\circ}\text{C}$; ^1H NMR (400 MHz, CDCl_3) δ 9.57 (s, 1H), 8.02 (d, J = 8.7 Hz, 1H), 7.83 (d, J = 8.6 Hz, 1H), 7.54 – 7.46 (m, 3H), 7.42 (d, J = 2.2 Hz, 1H), 7.37 (d, J = 7.2 Hz, 1H), 7.06 – 7.03 (m, 1H), 6.99 (d, J = 8.6 Hz, 1H), 6.78 (d, J = 2.2 Hz, 1H), 6.75 – 6.74 (m, 2H), 3.88 (s, 3H), 1.29 (s, 9H), 1.25 (s, 9H); $^{13}\text{C}\{^1\text{H}\}$ NMR (100 MHz, CDCl_3) δ 191.1, 186.7, 163.7, 149.8, 147.9, 146.3, 140.5, 138.8, 135.2, 134.6, 132.8, 132.1, 131.4, 131.0, 130.3, 129.0, 128.4, 127.8, 116.2.7, 114.4, 55.8, 35.6, 35.1, 29.6, 29.5; FT-IR (neat): 2971, 2868, 1701, 1631, 1461, 1361, 1275, 750 cm^{-1} ; HRMS (ESI): m/z calcd for $\text{C}_{29}\text{H}_{33}\text{O}_3$ $[\text{M}+\text{H}]^+$: 429.2424; found: 429.2427.

2'-((3,5-di-tert-butyl-4-oxocyclohexa-2,5-dien-1-ylidene)methyl)-4-methoxy-[1,1'-biphenyl]-2-carbaldehyde (33p).



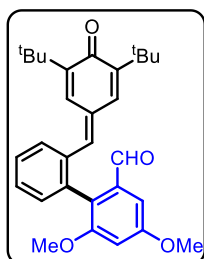
The reaction was performed at 0.266 mmol scale of 2-bromo *p*-quinone methide **31a**; R_f = 0.4 (10% EtOAc in hexane); orange solid (75.3 mg, 66% yield); m. p. = 199-206 $^{\circ}\text{C}$; ^1H NMR (400 MHz, CDCl_3) δ 9.57 (s, 1H), 8.02 (d, J = 8.7 Hz, 1H), 7.83 (d, J = 8.6 Hz, 1H), 7.54 – 7.46 (m, 3H), 7.42 (d, J = 2.2 Hz, 1H), 7.37 (d, J = 7.2 Hz, 1H), 7.06 – 7.03 (m, 1H), 6.99 (d, J = 8.6 Hz, 1H), 6.78 (d, J = 2.2 Hz, 1H), 6.75 – 6.74 (m, 2H), 3.88 (s, 3H), 1.29 (s, 9H), 1.25 (s, 9H); $^{13}\text{C}\{^1\text{H}\}$ NMR (100 MHz, CDCl_3) δ 191.1, 186.7, 163.7, 149.8, 147.9, 146.3, 140.5, 138.8, 135.2, 134.6, 132.8, 132.1, 131.4, 131.0, 130.3, 129.0, 128.4, 127.8, 116.2.7, 114.4, 55.8, 35.6, 35.1, 29.6, 29.5; FT-IR (neat): 2971, 2868, 1701, 1631, 1461, 1361, 1275, 750 cm^{-1} ; HRMS (ESI): m/z calcd for $\text{C}_{29}\text{H}_{33}\text{O}_3$ $[\text{M}+\text{H}]^+$: 429.2424; found: 429.2427.

2'-((3,5-di-tert-butyl-4-oxocyclohexa-2,5-dien-1-ylidene)methyl)-4-ethoxy-[1,1'-biphenyl]-2-carbaldehyde (33q).



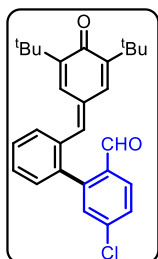
The reaction was performed at 0.266 mmol scale of 2-bromo *p*-quinone methide **31a**; $R_f = 0.5$ (5% EtOAc in hexane); orange solid (69.5 mg, 59% yield); m. p. = 187-189 °C; ^1H NMR (400 MHz, CDCl_3) δ 9.71 (s, 1H), 7.52 – 7.45 (m, 5H), 7.35 (d, $J = 6.7$ Hz, 1H), 7.24 – 7.22 (m, 1H), 7.21 – 7.18 (m, 1H), 6.76 – 6.75 (m, 2H), 4.16 (q, $J = 7.0$ Hz, 2H), 1.47 (t, $J = 7.0$ Hz, 3H), 1.30 (s, 9H), 1.26 (s, 9H); $^{13}\text{C}\{^1\text{H}\}$ NMR (100 MHz, CDCl_3) δ 191.4, 186.7, 159.1, 149.8, 147.9, 141.0, 138.6, 136.6, 135.7, 135.2, 134.7, 133.0, 132.6, 132.0, 131.7, 129.0, 128.2, 127.9, 121.7, 110.9, 64.1, 35.6, 35.1, 29.7, 29.6, 14.9; FT-IR (neat): 2971, 2868, 1701, 1631, 1461, 1361, 1275, 750 cm^{-1} ; HRMS (ESI): m/z calcd for $\text{C}_{30}\text{H}_{35}\text{O}_3$ $[\text{M}+\text{H}]^+$: 443.2581; found: 443.2571.

2'-((3,5-di-tert-butyl-4-oxocyclohexa-2,5-dien-1-ylidene)methyl)-4,5-dimethoxy-[1,1'-biphenyl]-2-carbaldehyde (33r).



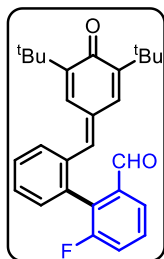
The reaction was performed at 0.266 mmol scale of 2-bromo *p*-quinone methide **31a**; $R_f = 0.5$ (10% EtOAc in hexane); orange solid (204 mg, 60% yield); m. p. = 197-199 °C; ^1H NMR (400 MHz, CDCl_3) δ 9.57 (s, 1H), 8.02 (d, $J = 8.7$ Hz, 1H), 7.83 (d, $J = 8.6$ Hz, 1H), 7.54 – 7.46 (m, 3H), 7.42 (d, $J = 2.2$ Hz, 1H), 7.37 (d, $J = 7.2$ Hz, 1H), 7.06 – 7.03 (m, 1H), 6.99 (d, $J = 8.6$ Hz, 1H), 6.78 (d, $J = 2.2$ Hz, 1H), 6.75 – 6.74 (m, 2H), 3.88 (s, 3H), 1.29 (s, 9H), 1.25 (s, 9H); $^{13}\text{C}\{^1\text{H}\}$ NMR (100 MHz, CDCl_3) δ 191.1, 186.7, 163.7, 149.8, 147.9, 146.3, 140.5, 138.8, 135.2, 134.6, 132.8, 132.1, 131.4, 131.0, 130.3, 129.0, 128.4, 127.8, 116.2.7, 114.4, 55.8, 35.6, 35.1, 29.6, 29.5; FT-IR (neat): 2971, 2868, 1701, 1631, 1461, 1361, 1275, 750 cm^{-1} ; HRMS (ESI): m/z calcd for $\text{C}_{28}\text{H}_{31}\text{O}_2$ $[\text{M}+\text{H}]^+$: 458.2457; found: 458.2451.

5-chloro-2'-((3,5-di-tert-butyl-4-oxocyclohexa-2,5-dien-1-ylidene)methyl)-[1,1'-biphenyl]-2-carbaldehyde (33s).



The reaction was performed at 0.266 mmol scale of 2-bromo *p*-quinone methide **31a**; $R_f = 0.4$ (5% EtOAc in hexane); orange solid (88.7 mg, 77% yield); m. p. = 179-181 °C; ^1H NMR (400 MHz, CDCl_3) δ 9.70 (s, 1H), 8.02 (d, $J = 2.3$ Hz, 1H), 7.65 – 7.62 (m, 1H), 7.59 – 7.50 (m, 3H), 7.44 (d, $J = 2.2$ Hz, 1H), 7.37 (d, $J = 7.3$ Hz, 1H), 7.32 (d, $J = 8.2$ Hz, 1H), 6.77 (d, $J = 2.2$ Hz, 1H), 6.72 (s, 1H), 1.31 (s, 9H), 1.28 (s, 9H); $^{13}\text{C}\{^1\text{H}\}$ NMR (100 MHz, CDCl_3) δ 190.0, 186.6, 150.0, 148.1, 142.0, 140.0, 137.4, 135.4, 135.3, 135.2, 133.7, 133.09, 133.06, 131.8, 131.5, 129.2, 128.8, 127.7, 127.6, 35.6, 35.1, 29.6, 29.5; FT-IR (neat): 3642, 3070, 2953, 1597, 1434, 1390, 1233, 1152, 912, 746 cm^{-1} ; HRMS (ESI): m/z calcd for $\text{C}_{32}\text{H}_{33}\text{O}_2$ $[\text{M}+\text{H}]^+$: 433.1929; found: 433.1925.

2'-((3,5-di-tert-butyl-4-oxocyclohexa-2,5-dien-1-ylidene)methyl)-6-fluoro-[1,1'-biphenyl]-2-carbaldehyde (33t).

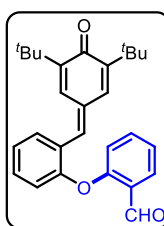


The reaction was performed at 0.266 mmol scale of 2-bromo *p*-quinone methide **31a**; R_f = 0.3 (5% EtOAc in hexane); orange gummy solid (82.8 mg, 74% yield); m. p. = 173-175 °C; ^1H NMR (400 MHz, CDCl_3) δ 9.97 (s, 1H), 7.63 – 7.58 (m, 1H), 7.54 – 7.45 (m, 3H), 7.34 (s, 1H), 7.29 (d, J = 7.4 Hz, 1H), 7.23 (d, J = 9.1 Hz, 1H), 7.09 (d, J = 7.6 Hz, 1H), 6.75 (s, 1H), 6.72 (s, 1H), 1.29 (s, 9H), 1.27 (s, 9H); $^{13}\text{C}\{^1\text{H}\}$ NMR (100 MHz, CDCl_3) δ 188.2, 186.7, 163.4 (d, $J_{\text{C-F}}$ = 261 Hz), 149.8, 148.0, 144.4, 140.5, 138.8 (d, $J_{\text{C-F}}$ = 2.2 Hz), 135.0 (d, $J_{\text{C-F}}$ = 3.4 Hz), 123.1 (d, $J_{\text{C-F}}$ = 6.9 Hz), 116.6 (d, $J_{\text{C-F}}$ = 21 Hz), 35.6, 35.2, 29.7, 29.6; ^{19}F NMR (376 MHz, CDCl_3) δ -109.8; FT-IR (neat): 2971, 2868, 1715, 1639, 1461, 1361, 1275, 750 cm^{-1} ; HRMS (ESI): m/z calcd for $\text{C}_{28}\text{H}_{30}\text{FO}_2$ $[\text{M}+\text{H}]^+$: 417.2224; found: 417.2224.

General procedure for synthesis of 33u & 33y.

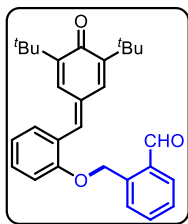
In a Dean-Stark apparatus, a mixture of aldehyde (1 equiv.) and 2,6-di-tertbutylphenol (1 equiv.) in toluene (0.25 M) was placed and refluxed. Piperidine (3 equiv.) was added to this reaction mixture in a drop-wise manner within an hour and the resultant mixture was stirred at reflux temperature for 12 h. The reaction mixture was cooled to 100 °C and acetic anhydride (2 equiv.) was added and the resulting solution was stirred for 30 more minutes at the same temperature, then concentrated under reduced pressure. The residue was purified by silica gel column chromatography to obtain a pure *p*-quinone methide **33u & 33y**.

2'-((3,5-di-tert-butyl-4-oxocyclohexa-2,5-dien-1-ylidene)methyl)-4'-methoxy-[1,1'-biphenyl]-2-carbaldehyde (33u).



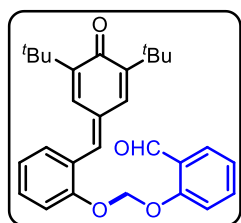
The reaction was performed at 0.240 mmol scale of 2,2'-oxydibenzaldehyde; R_f = 0.4 (10% EtOAc in hexane); yellow solid (85.3 mg, 85% yield); m. p. = 129-130 °C; ^1H NMR (400 MHz, CDCl_3) δ 10.50 (s, 1H), 7.97 – 7.96 (m, 1H), 7.55 – 7.52 (m, 2H), 7.47 (d, J = 3.0 Hz, 1H), 7.41 – 7.37 (m, 1H), 7.29 – 7.22 (m, 2H), 7.00 (d, J = 3.4 Hz, 1H), 6.97 – 6.95 (m, 1H), 6.89 (d, J = 8.3 Hz, 1H), 1.30 (s, 9H), 1.28 (s, 9H); $^{13}\text{C}\{^1\text{H}\}$ NMR (100 MHz, CDCl_3) δ 189.2, 186.7, 159.4, 155.4, 149.7, 148.1, 136.4, 136.1, 135.0, 133.0, 132.5, 131.0, 129.0, 127.9, 127.8, 127.0, 124.5, 124.1, 119.2, 118.8, 35.6, 35.2, 29.7; FT-IR (neat): 2971, 2868, 1701, 1631, 1461, 1361, 1275, 750 cm^{-1} HRMS (ESI): m/z calcd for $\text{C}_{28}\text{H}_{31}\text{O}_3$ $[\text{M}+\text{H}]^+$: 415.2268; found: 415.2269.

4-(3,9-dimethoxy-11*H*-benzo[*a*]fluoren-11-yl)phenol (33v).



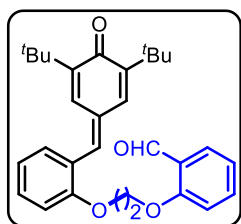
The reaction was performed at 0.234 mmol scale of 2'-((2-formylbenzyl)oxy)benzaldehyde; $R_f = 0.1$ (15% EtOAc in hexane); gummy orange solid (94.5 mg, 94% yield); ^1H NMR (400 MHz, CDCl_3) δ 10.42 (s, 1H), 7.84 – 7.82 (m, 1H), 7.60 – 7.57 (m, 1H), 7.40 – 7.33 (m, 6H), 7.22 (s, 1H), 7.18 – 7.13 (m, 2H), 6.91 (d, $J = 2.2$ Hz, 1H), 4.23 (s, 2H), 1.32 (s, 9H), 1.27 (s, 9H); $^{13}\text{C}\{^1\text{H}\}$ NMR (100 MHz, CDCl_3) δ 191.3, 186.7, 159.1, 149.1, 147.0, 137.1, 136.0, 135.0, 132.2, 131.1, 128.9, 128.0, 126.6, 125.8, 123.2, 123.0, 115.2, 115.1, 91.5, 35.5, 35.1, 29.6; FT-IR (neat): 2971, 2868, 1701, 1631, 1461, 1361, 1275, 750 cm^{-1} HRMS (ESI): m/z calcd for $\text{C}_{29}\text{H}_{33}\text{O}_3$ $[\text{M}+\text{H}]^+$: 429.2424; found: 429.2429.

2'-((3,5-di-tert-butyl-4-oxocyclohexa-2,5-dien-1-ylidene)methyl)-[1,1'-biphenyl]-2-carbaldehyde (33w).



The reaction was performed at 0.225 mmol scale of 2,2'-(methylenebis(oxy))dibenzaldehyde; $R_f = 0.2$ (5% EtOAc in hexane); orange gummy solid (79.4 mg, 79% yield); m. p. = 133-135 $^\circ\text{C}$; ^1H NMR (400 MHz, CDCl_3) ^1H NMR (400 MHz, CDCl_3) δ 10.42 (s, 1H), 7.84 – 7.82 (m, 1H), 7.62 – 7.57 (m, 1H), 7.42 – 7.33 (m, 6H), 7.24 (s, 1H), 7.18 – 7.12 (m, 2H), 6.92 (d, $J = 2.2$ Hz, 1H), 5.93 (s, 2H), 1.32 (s, 9H), 1.27 (s, 9H); $^{13}\text{C}\{^1\text{H}\}$ NMR (100 MHz, CDCl_3) δ 189.3, 186.7, 159.0, 149.4, 147.7, 137.8, 136.0, 135.0, 132.2, 131.1, 128.9, 128.0, 126.6, 125.8, 123.2, 123.0, 115.2, 115.1, 91.5, 35.5, 35.1, 29.6; FT-IR (neat): 2971, 2868, 1701, 1631, 1461, 1361, 1275, 750 cm^{-1} ; HRMS (ESI): m/z calcd for $\text{C}_{29}\text{H}_{32}\text{O}_4$ $[\text{M}+\text{H}]^+$: 445.2373; found: 445.2373.

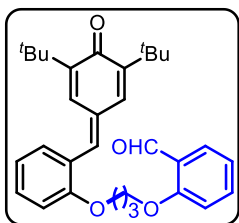
2'-((3,5-di-tert-butyl-4-oxocyclohexa-2,5-dien-1-ylidene)methyl)-[1,1'-biphenyl]-2-carbaldehyde (33x).



The reaction was performed at 0.218 mmol scale of 2,2'-(ethane-1,2-diylbis(oxy))dibenzaldehyde; $R_f = 0.2$ (5% EtOAc in hexane); orange gummy solid (68.1 mg, 68% yield); m. p. = 133-135 $^\circ\text{C}$; ^1H NMR (400 MHz, CDCl_3) ^1H NMR (400 MHz, CDCl_3) δ 10.46 (s, 1H), 7.84 – 7.82 (m, 1H), 7.57 – 7.55 (m, 1H), 7.43 (d, $J = 2.2$ Hz, 1H), 7.41 – 7.37 (m, 5H), 7.24 (s, 1H), 7.10 – 7.08 (m, 2H), 6.95 (d, $J = 2.2$ Hz, 1H), 4.70 (m, 4H), 1.32 (s, 9H), 1.27 (s, 9H); $^{13}\text{C}\{^1\text{H}\}$ NMR (100 MHz, CDCl_3) δ 189.4, 186.6, 159.2, 155.9, 149.4, 147.8, 137.2, 136.1, 135.0, 132.6, 131.3, 128.5, 128.0, 126.6, 125.8, 123.2, 122.8, 115.2, 115.1, 74.2, 74.1, 35.5, 35.1, 29.6; FT-IR (neat): 2971, 2868, 1701, 1631, 1461, 1361, 1275, 750 cm^{-1} HRMS (ESI): m/z calcd for $\text{C}_{30}\text{H}_{34}\text{O}_4$ $[\text{M}+\text{H}]^+$: 459.3530; found: 459.3533;

2'-((3,5-di-tert-butyl-4-oxocyclohexa-2,5-dien-1-ylidene)methyl)-[1,1'-biphenyl]-2-

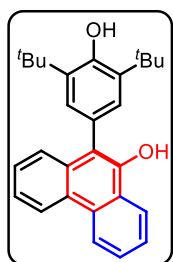
carbaldehyde (33y).



The reaction was performed at 0.210 mmol scale 2,2'-(propane-1,3-diylbis(oxy))dibenzaldehyde; $R_f = 0.2$ (5% EtOAc in hexane); orange gummy solid (65.1 mg, 65% yield); m. p. = 133-135 °C; ^1H NMR (400 MHz, CDCl_3) δ 10.50 (s, 1H), 7.84 – 7.82 (m, 1H), 7.55 – 7.51 (m, 1H), 7.45 (d, $J = 2.2$ Hz, 1H), 7.40 – 7.36 (m, 3H), 7.06 – 6.98 (m, 5H), 4.33-4.27 (m, 4H), 1.32 (s, 9H), 1.27 (s, 9H); $^{13}\text{C}\{^1\text{H}\}$ NMR (100 MHz, CDCl_3) δ 189.6, 186.8, 161.1, 157.5, 149.0, 147.5, 138.7, 136.1, 135.3, 132.2, 131.7, 131.0, 128.7, 128.5, 125.2, 125.0, 121.0, 120.9, 112.5, 111.9, 65.0, 64.8, 35.5, 35.1, 29.7; FT-IR (neat): 2971, 2868, 1701, 1631, 1461, 1361, 1275, 750 cm^{-1} HRMS (ESI): m/z calcd for $\text{C}_{31}\text{H}_{36}\text{O}_4$ $[\text{M}+\text{H}]^+$: 476.2686; found: 476.2686

General procedures for the synthesis of 9-phenanthrols (34a-u).

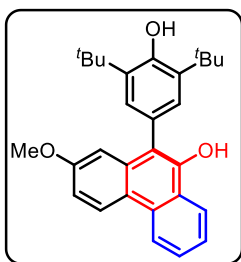
An oven-dried Schlenk tube with a magnet stir bar was applied full Schlenk conditions and charged with BACs precursor **8** (0.2 equiv.) and 2-(2-formylaryl)-phenyl-substituted *p*-quinone methides (*p*-QMs) (1 equiv.). The tube was undergone deaeration cycles for three times. followed by addition of DBU (0.2 equiv.) and CH_2Cl_2 (1 ml) under argon. The mixture was sealed and stirred at the room temperature. Reaction was monitored by TLC, and the reaction mixture was concentrated under reduced pressure and directly loaded onto a silica-gel column and was purified using EtOAc in hexane as an eluent to provide pure 9-phenanthrol derivatives.



2,6-di-tert-butyl-4-(9H-fluoren-9-yl)phenol (34a).

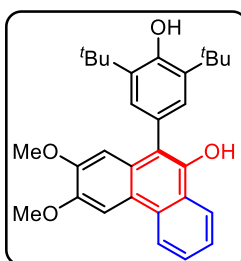
The reaction was performed at 0.101 mmol scale of **33a**; $R_f = 0.4$ (10% EtOAc in hexane); colourless solid (39.1 mg, 98 % yield); m. p. = 135-137 °C; ^1H NMR (400 MHz, CDCl_3) δ 8.75 (d, $J = 8.0$ Hz, 1H), 8.71 (d, $J = 8.2$ Hz, 1H), 8.43 (d, $J = 7.6$ Hz, 1H), 7.73 – 7.68 (m, 2H), 7.55 – 7.47 (m, 3H), 7.28 (s, 2H), 5.71 (s, 1H), 5.45 (s, 1H), 1.52 (s, 18H); $^{13}\text{C}\{^1\text{H}\}$ NMR (100 MHz, CDCl_3) δ 152.2, 146.4, 137.5, 133.3, 130.9, 128.0, 127.1, 126.9, 126.7, 126.5, 125.7, 125.1, 124.9, 123.9, 123.3, 122.7, 122.6, 118.3, 34.7, 30.5; FT-IR (neat): 3637, 3074, 2956, 1621, 1597, 1434, 1390, 1233, 1152, 746 cm^{-1} ; HRMS (ESI): m/z calcd for $\text{C}_{28}\text{H}_{31}\text{O}_2$ $[\text{M}+\text{H}]^+$: 399.2319; found : 399.2320;.

2,6-di-tert-butyl-4-(2-(tert-butyl)-9H-fluoren-9-yl)phenol (34b).



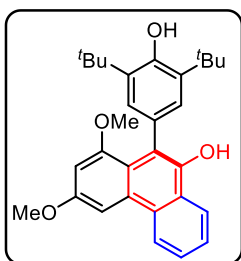
The reaction was performed at 0.093 mmol scale of **34b**; Rf = 0.4 (10% EtOAc in hexane); colorless solid (38.8 mg, 97 % yield); m. p. = 134-136 °C; ^1H NMR (400 MHz, CDCl_3) δ 8.60 (d, J = 8.0 Hz, 1H), 8.38 – 8.35 (m, 1H), 7.70 – 7.66 (m, 1H), 7.63 – 7.59 (m, 1H), 7.73 – 7.68 (m, 2H), 7.27 (s, 2H), 7.15 (dd, J = 6.34, 2.7 Hz, 1H), 6.91 (d, J = 2.7 Hz, 1H), 5.72 (s, 1H), 5.44 (s, 1H), 3.78 (s, 3H), 1.50 (s, 18H); $^{13}\text{C}\{^1\text{H}\}$ NMR (100 MHz, CDCl_3) δ 158.5, 154.1, 146.9, 137.5, 134.6, 131.0, 127.9, 127.2, 125.7, 124.9, 124.3, 124.0, 123.1, 122.1, 120.9, 117.9, 113.3, 107.3, 55.3, 34.7, 30.5; FT-IR (neat): 3631, 3070, 2952, 1620, 1593, 1424, 1390, 1239, 1150, 736 cm^{-1} ; HRMS (ESI): m/z calcd for $\text{C}_{29}\text{H}_{33}\text{O}_3$ $[\text{M}+\text{H}]^+$: 429.2424; found: 429.2427.

2,6-di-tert-butyl-4-(2-methoxy-9H-fluoren-9-yl)phenol (**34c**).



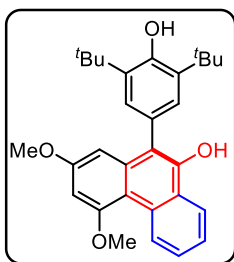
The reaction was performed at 0.087 mmol scale of **33c**; Rf = 0.4 (20% EtOAc in hexane); colourless solid (37.5mg, 94 % yield); m. p. = 145-147 °C; ^1H NMR (400 MHz, CDCl_3) δ 8.54 (d, J = 8.2 Hz, 1H), 8.37 – 8.35 (m, 1H), 8.02 (s, 1H), 7.67 – 7.58 (m, 2H), 7.28 (s, 2H), 6.89 (s, 1H), 5.65 (s, 1H), 5.43 (s, 1H), 4.10 (s, 3H), 3.78 (s, 3H), 1.49 (s, 18H); $^{13}\text{C}\{^1\text{H}\}$ NMR (100 MHz, CDCl_3) δ 154.4, 149.4, 147.4, 137.5, 130.2, 127.9, 126.8, 125.7, 125.2, 124.2, 123.2, 122.2, 120.7, 117.8, 106.4, 103.8, 56.2, 55.7, 34.8, 30.6; FT-IR (neat): 3647, 3016, 2942, 1579, 1431, 1393, 1254, 1237, 1129, 747 cm^{-1} ; HRMS (ESI): m/z calcd for $\text{C}_{28}\text{H}_{31}\text{O}_2$ $[\text{M}+\text{H}]^+$: 458.2457; found: 458.2451.

2,6-di-tert-butyl-4-(2-phenyl-9H-fluoren-9-yl)phenol (**34d**).



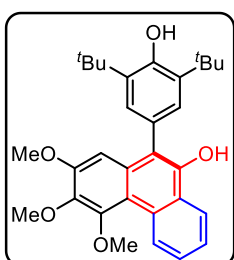
The reaction was performed at 0.087 mmol scale of **33d**; Rf = 0.4 (20% EtOAc in hexane); colourless solid (35.9 mg, 90 % yield); m. p. = 152-154 °C; ^1H NMR (400 MHz, CDCl_3) δ 8.62 – 8.60 (m, 1H), 8.35 – 8.33 (m, 1H), 7.72 (d, J = 2.4 Hz, 1H), 7.67 – 7.64 (m, 2H), 7.13 (s, 2H), 6.57 (d, J = 2.3 Hz, 1H), 5.70 (s, 1H), 5.27 (s, 1H), 4.01 (s, 3H), 3.37 (s, 3H), 1.47 (s, 18H); $^{13}\text{C}\{^1\text{H}\}$ NMR (100 MHz, CDCl_3) δ 157.6, 156.9, 153.0, 145.3, 136.1, 130.2, 129.0, 128.9, 126.9, 126.7, 126.6, 125.3, 123.2, 123.1, 118.4, 116.5, 99.9, 96.5, 55.6, 34.6, 30.6; FT-IR (neat): 3640, 3012, 2940, 1577, 1434, 1390, 1255, 1233, 1154, 749 cm^{-1} ; HRMS (ESI): m/z calcd for $\text{C}_{29}\text{H}_{33}\text{O}_4$ $[\text{M}+\text{H}]^+$: 458.2457; found: 458.2451.

2,6-di-tert-butyl-4-(4-methyl-9H-fluoren-9-yl)phenol (**34e**).



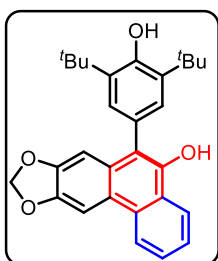
The reaction was performed at 0.087 mmol scale of **33e**; Rf = 0.5 (20% EtOAc in hexane); colourless solid (38.4 mg, 96 % yield); m. p. = 144–147 °C; ^1H NMR (400 MHz, CDCl_3) δ 9.60 (d, J = 8.7 Hz, 1H), 8.40 – 8.37 (m, 1H), 7.68 – 7.56 (m, 2H), 7.24 (s, 2H), 6.67 (d, J = 2.5 Hz, 1H), 6.52 (d, J = 2.4 Hz, 1H), 5.66 (s, 1H), 5.42 (s, 1H), 4.12 (s, 3H), 3.72 (s, 3H), 1.49 (s, 18H); $^{13}\text{C}\{^1\text{H}\}$ NMR (100 MHz, CDCl_3) δ 160.3, 158.1, 154.1, 147.2, 137.5, 136.6, 131.1, 128.0, 127.6, 127.0, 125.5, 125.0, 124.2, 122.4, 118.0, 111.9, 99.9, 96.6, 55.9, 55.1, 34.7, 30.5; FT-IR (neat): 3642, 3015, 2943, 1583, 1427, 1378, 1236, 1220, 1159, 743 cm^{-1} ; HRMS (ESI): m/z calcd for $\text{C}_{28}\text{H}_{31}\text{O}_4$ $[\text{M}+\text{H}]^+$: 458.2457; found: 458.2451.

2,6-di-tert-butyl-4-(4-iso-propoxy-1-methyl-9H-fluoren-9-yl)phenol (34f).



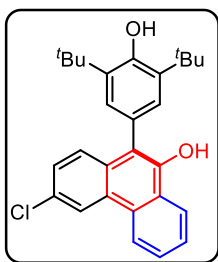
The reaction was performed at 0.101 mmol scale of **33f**; Rf = 0.4 (10% EtOAc in hexane); colourless solid (39.1 mg, 98 % yield); m. p. = 135–137 °C; ^1H NMR (400 MHz, CDCl_3) δ 9.59 (d, J = 7.8 Hz, 1H), 8.40 – 8.37 (m, 1H), 7.70 – 7.59 (m, 2H), 7.25 (s, 2H), 6.70 (s, 1H), 5.64 (s, 1H), 5.44 (s, 1H), 4.40 (s, 3H), 4.01 (s, 3H), 3.73 (s, 3H), 1.49 (s, 18H); $^{13}\text{C}\{^1\text{H}\}$ NMR (100 MHz, CDCl_3) δ 154.1, 152.7, 152.3, 146.2, 140.7, 137.6, 131.0, 130.5, 128.0, 127.3, 126.7, 125.6, 125.2, 124.5, 122.6, 117.8, 115.1, 103.0, 61.4, 60.5, 55.5, 34.7, 30.5; FT-IR (neat): 3623, 3007, 2929, 1567, 1427, 1389, 1236, 1205, 1220, 1159, 748 cm^{-1} ; HRMS (ESI): m/z calcd for $\text{C}_{31}\text{H}_{37}\text{O}_5$ $[\text{M}+\text{H}]^+$: 489.2636; found: 489.2635.

2,6-di-tert-butyl-4-(2-methyl-9H-fluoren-9-yl)phenol (34g).



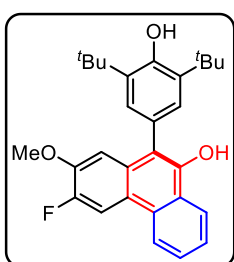
The reaction was performed at 0.090 mmol scale of **33g**; Rf = 0.4 (10% EtOAc in hexane); colourless solid (36.0 mg, 98 % yield); m. p. = 139–141 °C; ^1H NMR (400 MHz, CDCl_3) δ 8.49 (d, J = 8.2 Hz, 1H), 8.34 – 8.32 (m, 1H), 8.03 (s, 1H), 7.67 – 7.57 (m, 2H), 7.20 (s, 2H), 6.82 (s, 1H), 6.04 (s, 2H), 5.49 (s, 1H), 5.42 (s, 1H), 1.48 (s, 18H); $^{13}\text{C}\{^1\text{H}\}$ NMR (100 MHz, CDCl_3) δ 154.2, 147.8, 146.0, 145.5, 137.5, 130.5, 129.6, 127.8, 126.8, 125.8, 125.1, 124.0, 123.1, 122.4, 121.9, 118.7, 103.8, 101.2, 101.0, 34.7, 30.5; FT-IR (neat): 3637, 3074, 2956, 1625, 1597, 1575, 1434, 1390, 1204, 1039, 777 cm^{-1} ; HRMS (ESI): m/z calcd for $\text{C}_{29}\text{H}_{31}\text{O}_4$ $[\text{M}+\text{H}]^+$: 343.2217; found: 343.2211.

4-(2-bromo-9H-fluoren-9-yl)-2,6-di-tert-butylphenol (34h).



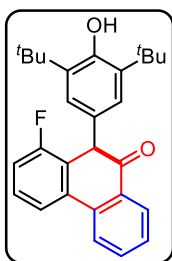
The reaction was performed at 0.093 mmol scale of **33h**; Rf = 0.5 (10% EtOAc in hexane); colourless solid (37.6 mg, 94 % yield); m. p. = 129-131 °C; ¹H NMR (400 MHz, CDCl₃) δ 8.62 (t, *J* = 9.8 Hz, 2H), 8.37 (d, *J* = 1.9 Hz, 1H), 7.66 – 7.63 (m, 1H), 7.53 – 7.49 (m, 3H), 7.24 (s, 2H), 5.68 (s, 1H), 5.45 (s, 1H), 1.50 (s, 18H); ¹³C{¹H} NMR (100 MHz, CDCl₃) δ 154.3, 145.5, 137.5, 133.0, 132.8, 129.3, 127.8, 127.5, 127.2, 126.2, 126.1, 125.9, 124.5, 124.34, 124.32, 122.6, 119.4, 34.7, 30.5; FT-IR (neat): 3642, 3070, 2953, 1597, 1434, 1390, 1233, 1152, 912, 746 cm⁻¹; HRMS (ESI): m/z calcd for C₂₈H₃₀ClO₂ [M+H]⁺: 447.1324; found: 447.1339.

2,6-di-tert-butyl-4-(9H-fluoreno[2,3-d][1,3]dioxol-9-yl)phenol (**34i**).



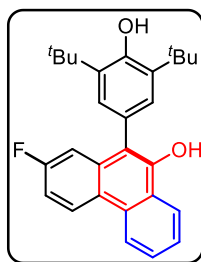
The reaction was performed at 0.090 mmol scale of **33i**; Rf = 0.3 (20% EtOAc in hexane); colourless solid (36.1 mg, 91 % yield); m. p. = 132-134 °C; ¹H NMR (400 MHz, CDCl₃) δ 8.46 (d, *J* = 8.0 Hz, 1H), 8.37 – 8.35 (m, 1H), 8.29 (d, *J* = 13.3 Hz, 1H), 7.70 – 7.60 (m, 2H), 7.27 (s, 2H), 6.95 (d, *J* = 8.8 Hz, 1H), 5.70 (s, 1H), 5.45 (s, 1H), 3.79 (s, 3H), 1.50 (s, 18H); ¹³C{¹H} NMR (100 MHz, CDCl₃) δ 154.2, 150.8 (d *J*_{C-F} = 248 Hz), 147.6 (d *J*_{C-F} = 12.4 Hz), 146.2, 137.6, 130.3 (d *J*_{C-F} = 4.2 Hz), 127.9, 127.2, 126.2, 124.8, 124.3, 123.2, 122.4, 120.6 (d *J*_{C-F} = 6.8 Hz), 117.5, 109.1 (d *J*_{C-F} = 19.3 Hz), 108.1, 56.0, (d *J*_{C-F} = 3.2 Hz), 34.8, 30.5; ¹⁹F NMR (376 MHz, CDCl₃) δ -138.7; FT-IR (neat): 3701, 3015, 2976, 1434, 1390, 1227, 1182, 765 cm⁻¹; HRMS (ESI): m/z calcd for C₂₉H₃₂FO₃ [M+H]⁺: 447.2330; found: 447.2337.

2,6-di-tert-butyl-4-(2-chloro-9H-fluoren-9-yl)phenol (**34j**).



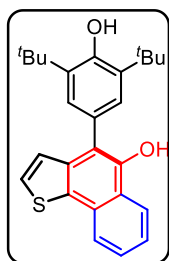
The reaction was performed at 0.096 mmol scale of **33j**; Rf = 0.3 (10% EtOAc in hexane); colourless solid (33.1 mg, 83 % yield); m. p. = 90-91 °C; ¹H NMR (400 MHz, CDCl₃) δ 8.64 – 8.61 (m, 1H), 8.55 (d, *J* = 7.8 Hz, 1H), 7.64 – 7.58 (m, 1H), 7.53 – 7.48 (m, 3H), 7.36 – 7.30 (m, 1H), 7.24 (s, 2H), 6.24 (d, *J* = 6.9 Hz, 1H), 5.42 (s, 1H), 1.50 (s, 18H); ¹³C{¹H} NMR (100 MHz, CDCl₃) δ 159.9 (d *J*_{C-F} = 249.5 Hz), 154.0, 145.5 (d *J*_{C-F} = 3.5 Hz), 137.1, 133.8 (d *J*_{C-F} = 3.1 Hz), 133.6, 128.0, 127.6, 127.0 (d *J*_{C-F} = 9.6 Hz), 126.0, 125.6 (d *J*_{C-F} = 2.4 Hz), 124.7, 124.4, 123.1, 120.6 (d *J*_{C-F} = 2.3 Hz), 119.1 (d *J*_{C-F} = 3.4 Hz), 114.6, (d *J*_{C-F} = 8.1 Hz), 113.0 (d *J*_{C-F} = 23.3 Hz) 34.7, 30.5; ¹⁹F NMR (376 MHz, CDCl₃) δ -114.6; FT-IR (neat): 3630, 3079, 2943, 1597, 1434, 1390, 1233, 1152, 765 cm⁻¹; HRMS (ESI): m/z calcd for C₂₈H₃₀FO₂ [M+H]⁺: 417.2224; found: 417.2224.

2,6-di-tert-butyl-4-(2-fluoro-9H-fluoren-9-yl)phenol (**34k**).



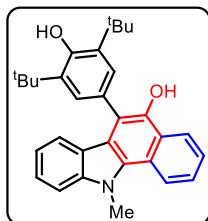
The reaction was performed at 0.096 mmol scale of **33k**; Rf = 0.3 (10% EtOAc in hexane); colourless solid (35.2 mg, 88 % yield); m. p. = 99-101 °C; ^1H NMR (400 MHz, CDCl_3) δ 8.63 (t, J = 8.6 Hz, 2H), 8.38 (d, J = 8.0 Hz, 1H), 7.73 – 7.63 (m, 2H), 7.25 – 7.20 (m, 3H), 7.10 (dd, J = 8.5, 2.6 Hz, 1H), 5.72 (s, 1H), 5.45 (s, 1H), 1.49 (s, 18H); ^{13}C {1H} NMR (100 MHz, CDCl_3) δ 161.9 (d $J_{\text{C-F}}$ = 242.8 Hz), 154.4, 147.4, 137.7, 135.0 (d $J_{\text{C-F}}$ = 8.8 Hz), 130.8, 127.5, 126.5, 125.0, 124.9, 124.4 (d $J_{\text{C-F}}$ = 9.0 Hz), 123.2 (d $J_{\text{C-F}}$ = 1.7 Hz), 122.5, 117.9 (d $J_{\text{C-F}}$ = 3.9 Hz), 112.6 (d $J_{\text{C-F}}$ = 23.9 Hz), 110.3 (d $J_{\text{C-F}}$ = 22.3 Hz), 34.7, 30.5; ^{19}F NMR (376 MHz, CDCl_3) δ -114.3; FT-IR (neat): 3636, 3071, 2958, 1434, 1390, 1235, 1159, 745 cm^{-1} ; HRMS (ESI): m/z calcd for $\text{C}_{28}\text{H}_{30}\text{FO}_2$ $[\text{M}+\text{H}]^+$: 417.2224; found: 417.2224.

4-(11H-benzo[a]fluoren-11-yl)-2,6-di-tert-butylphenol (**34l**).



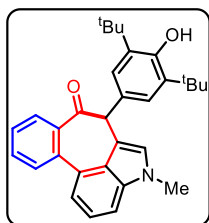
The reaction was performed at 0.099 mmol scale of **33l**; Rf = 0.4 (10% EtOAc in hexane); colourless solid (34.4 mg, 86 % yield); m. p. = 123-125 °C; ^1H NMR (400 MHz, CDCl_3) δ 8.36 (d, J = 8.1 Hz, 1H), 8.31 (d, J = 8.2 Hz, 1H), 7.95 (d, J = 5.4 Hz, 1H), 7.64 – 7.57 (m, 2H), 7.45 (s, 2H), 7.37 (d, J = 5.4 Hz, 1H), 6.50 (s, 1H), 5.80 (s, 1H), 5.44 (s, 1H), 1.50 (s, 18H); ^{13}C {1H} NMR (100 MHz, CDCl_3) δ 158.1, 154.4, 145.4, 140.1, 137.6, 130.0, 129.2, 126.9, 126.5, 126.5, 125.8, 125.1, 123.6, 123.4, 123.2, 122.3, 116.9, 34.7, 30.5; FT-IR (neat): 3637, 3074, 2956, 1597, 1458, 1390, 1233, 1152, 746 cm^{-1} ; HRMS (ESI): m/z calcd for $\text{C}_{28}\text{H}_{29}\text{O}_2\text{S}$ $[\text{M}+\text{H}]^+$: 405.1883; found: 405.1886.

6-(3,5-di-tert-butyl-4-hydroxyphenyl)-11-methyl-11H-benzo[a]carbazol-5-ol (**34m**).



The reaction was performed at 0.89 mmol scale of **34a**; Rf = 0.3 (20% EtOAc in hexane); colourless solid (36.8 mg, 92 % yield); m. p. = 135-137 °C; ^1H NMR (400 MHz, CDCl_3) δ 8.81 (d, J = 8.4 Hz, 1H), 8.55 (d, J = 7.7 Hz, 1H), 8.41 (d, J = 8.2 Hz, 1H), 7.73 (t, J = 7.3 Hz, 1H), 7.50 (t, J = 7.7 Hz, 1H), 7.41 – 7.34 (m, 3H), 7.32 (s, 2H), 5.70 (s, 1H), 5.50 (s, 1H), 3.29 (s, 3H), 1.50 (s, 18H); ^{13}C {1H} NMR (100 MHz, CDCl_3) δ 154.7, 148.5, 140.6, 137.64, 137.60, 129.9, 128.5, 127.5, 123.8, 123.7, 123.0, 122.9, 122.7, 121.1, 120.1, 120.0, 110.2, 109.5, 108.9, 34.7, 31.8, 30.5; FT-IR (neat): 3637, 3054, 2950, 2816, 1685, 1597, 1434, 1390, 1233, 1152, 746 cm^{-1} ; HRMS (ESI): m/z calcd for $\text{C}_{31}\text{H}_{34}\text{NO}_2$ $[\text{M}+\text{H}]^+$: 452.2584; found: 452.2584.

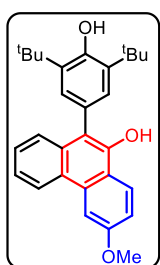
3-(3,5-di-tert-butyl-4-hydroxyphenyl)-1-methyl-1,3-dihydro-4H-benzo[4,5]cyclohepta[1,2,3-cd]indol-4-one (**34n**).



The reaction was performed at 0.089 mmol scale of **33n**; Rf = 0.6 (20% EtOAc in hexane); colourless solid (29.9 mg, 75 % yield); m. p. = 178-189 °C; ^1H NMR (400 MHz, CDCl_3) δ 8.01 (d, J = 8.0 Hz, 1H), 7.51 (t, J = 4.3 Hz, 1H), 7.43 – 7.36 (m, 3H), 7.19 – 7.14 (m, 2H), 6.87 (s, 2H), 5.38 (s, 1H), 5.00 (s, 1H), 3.83 (s, 3H), 1.23 (s, 18H); ^{13}C {1H} NMR (100 MHz, CDCl_3)

δ 201.8, 152.7, 140.4, 137.8, 135.7, 135.0, 131.0, 130.3, 129.6, 127.4, 126.9, 125.0, 124.3, 122.5, 119.8, 110.5, 109.6, 60.0, 34.3, 30.3; FT-IR (neat): 3637, 3074, 2956, 1621, 1597, 1434, 1390, 1233, 1152, 746 cm^{-1} ; HRMS (ESI): m/z calcd for $\text{C}_{31}\text{H}_{34}\text{NO}_2$ $[\text{M}+\text{H}]^+$: 452.2584; found: 452.2584.

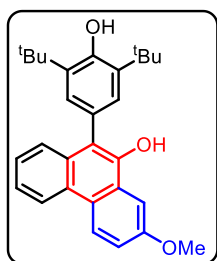
4-(7H-benzo[c]fluoren-7-yl)-2,6-di-tert-butylphenol (40o).



The reaction was performed at 0.101 mmol scale of **34a**; Rf = 0.4 (10% EtOAc in hexane); colourless solid (39.3 mg, 98 % yield); m. p. = 135-137 °C; ^1H NMR (400 MHz, CDCl_3) δ 8.65 (d, J = 9.1 Hz, 1H), 8.61 (d, J = 8.1 Hz, 1H), 7.88 (d, J = 2.8 Hz, 1H), 7.51 – 7.46 (m, 3H), 7.37 (dd, J = 6.3, 2.8 Hz, 1H), 7.28 (s, 2H), 5.69 (s, 1H), 5.46 (s, 1H), 4.03 (s, 3H), 1.52 (s, 18H); ^{13}C {1H} NMR (100 MHz, CDCl_3)

δ 158.6, 154.2, 145.9, 137.4, 133.9, 127.9, 128.0, 126.6, 126.3, 125.9, 125.7, 125.3, 125.0, 124.4, 124.0, 122.1, 117.8, 103.1, 55.6, 34.7, 30.5; FT-IR (neat): 3637, 3078, 2952, 1597, 1434, 1390, 1233, 1152, 748 cm^{-1} ; HRMS (ESI): m/z calcd for $\text{C}_{32}\text{H}_{33}\text{O}_3$ $[\text{M}+\text{H}]^+$: 429.2424; found: 429.2424.

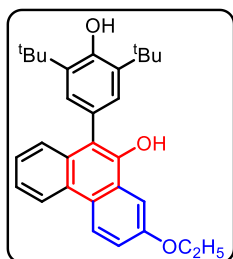
2,6-di-tert-butyl-4-(1-methoxy-7H-benzo[de]anthracen-7-yl)phenol (40p).



The reaction was performed at 0.101 mmol scale of **34a**; Rf = 0.4 (10% EtOAc in hexane); colourless solid (39.1 mg, 98 % yield); m. p. = 154-156 °C; ^1H NMR (400 MHz, CDCl_3) δ 8.61 – 8.59 (m, 1H), 8.31 (d, J = 9.0 Hz, 1H), 8.09 (d, J = 2.6 Hz, 1H), 7.50 – 7.46 (m, 3H), 7.32 (dd, J = 6.6, 2.4 Hz, 1H), 7.24 (s, 2H), 5.64 (s, 1H), 5.42 (s, 1H), 4.06 (s, 3H), 1.50 (s, 18H);

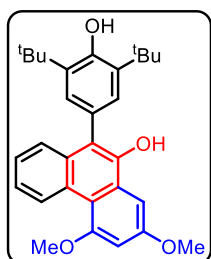
^{13}C {1H} NMR (100 MHz, CDCl_3) δ 159.0, 154.1, 146.5, 137.4, 133.7, 132.5, 128.1, 127.0, 125.9, 125.8, 125.0, 124.8, 123.5, 122.7, 119.6, 116.5, 104.2, 55.6, 34.7, 30.5; FT-IR (neat): 3637, 3074, 2956, 1621, 1597, 1434, 1390, 1233, 1152, 746 cm^{-1} ; HRMS (ESI): m/z calcd for $\text{C}_{32}\text{H}_{33}\text{O}_3$ $[\text{M}+\text{H}]^+$: 429.2424; found: 429.2424.

2,6-di-tert-butyl-4-(1,3-dimethoxy-9H-fluoren-9-yl)phenol (34q).



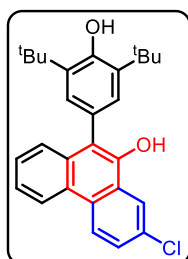
The reaction was performed at 0.101 mmol scale of **34a**; Rf = 0.4 (10% EtOAc in hexane); colourless solid (39.1 mg, 98 % yield); m. p. = 131-133 °C; ^1H NMR (400 MHz, CDCl_3) δ 8.62 (d, J = 9.1 Hz, 1H), 8.58 (d, J = 8.2 Hz, 1H), 7.74 (d, J = 2.6 Hz, 1H), 7.50 – 7.39 (m, 3H), 7.33 (dd, J = 6.4, 2.6 Hz, 1H), 7.24 (s, 2H), 5.65 (s, 1H), 5.43 (s, 1H), 4.25 (q, J = 7.0 Hz, 2H), 1.54 (t, J = 7.3 Hz, 3H), 1.50 (s, 18H); $^{13}\text{C}\{^1\text{H}\}$ NMR (100 MHz, CDCl_3) δ 158.0, 154.1, 145.9, 137.4, 131.9, 127.9, 126.6, 126.3, 125.8, 125.7, 125.2, 124.4, 124.0, 123.3, 122.1, 118.8, 118.3, 103.8, 63.8, 34.7, 30.5, 15.0; FT-IR (neat): 3637, 3576, 3074, 2956, 1597, 1434, 1390, 1233, 1152, 746 cm^{-1} ; HRMS (ESI): m/z calcd for $\text{C}_{30}\text{H}_{35}\text{O}_3$ $[\text{M}+\text{H}]^+$: 443.2581; found: 443.2571.

2,6-di-tert-butyl-4-(2,3-dimethoxy-9H-fluoren-9-yl)phenol (**34r**).



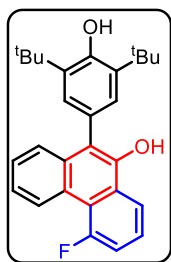
The reaction was performed at 0.101 mmol scale of **34a**; Rf = 0.4 (10% EtOAc in hexane); colourless solid (39.1 mg, 98 % yield); m. p. = 162-164 °C; ^1H NMR (400 MHz, CDCl_3) δ 8.53 – 8.51 (m, 1H), 8.00 (s, 1H), 7.72 (s, 1H), 7.48 – 7.41 (m, 3H), 7.24 (s, 2H), 5.64 (s, 1H), 5.42 (s, 1H), 4.16 (s, 3H), 4.08 (s, 3H), 1.49 (s, 18H); $^{13}\text{C}\{^1\text{H}\}$ NMR (100 MHz, CDCl_3) δ 154.0, 149.8, 149.5, 145.8, 137.4, 132.4, 128.1, 125.9, 125.8, 125.76, 125.0, 123.6, 122.2, 119.7, 117.0, 103.4, 103.1, 56.1, 34.7, 30.5; FT-IR (neat): 3637, 3074, 2956, 1621, 1597, 1434, 1390, 1233, 1152, 746 cm^{-1} ; HRMS (ESI): m/z calcd for $\text{C}_{29}\text{H}_{33}\text{O}_3$ $[\text{M}+\text{H}]^+$: 458.2457; found: 58.2451.

2,6-di-tert-butyl-4-(1-methoxy-7H-benzo[de]anthracen-7-yl)phenol (**34s**).



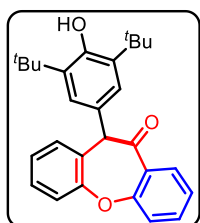
The reaction was performed at 0.101 mmol scale of **34a**; Rf = 0.4 (10% EtOAc in hexane); colourless solid (34.1 mg, 85 % yield); m. p. = 135-137 °C; ^1H NMR (400 MHz, CDCl_3) δ 8.62 (d, J = 9.1 Hz, 2H), 8.37 (d, J = 1.9 Hz, 1H), 7.66 – 7.63 (m, 1H), 7.53 – 7.49 (m, 3H), 7.24 (s, 2H), 5.68 (s, 1H), 5.45 (s, 1H), 1.50 (s, 18H); $^{13}\text{C}\{^1\text{H}\}$ NMR (100 MHz, CDCl_3) δ 154.3, 145.5, 137.6, 133.0, 132.8, 129.3, 127.8, 127.5, 127.1, 126.2, 126.1, 125.9, 124.5, 124.34, 124.32, 122.6, 119.4, 34.7, 30.5; FT-IR (neat): 3642, 3070, 2953, 1597, 1434, 1390, 1233, 1152, 912, 746 cm^{-1} ; HRMS (ESI): m/z calcd for $\text{C}_{32}\text{H}_{33}\text{O}_2$ $[\text{M}+\text{H}]^+$: 433.1929; found: 433.1925.

2,6-di-tert-butyl-4-(3-methoxy-11H-benzo[a]fluoren-11-yl)phenol (**34t**).



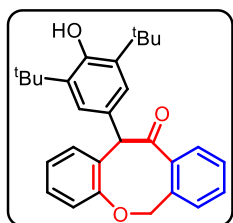
The reaction was performed at 0.101 mmol scale of **34a**; Rf = 0.4 (10% EtOAc in hexane); colourless solid (35.6 mg, 89 % yield); m. p. = 85-87 °C; ^1H NMR (400 MHz, CDCl_3) δ 8.63 (t, J = 8.6 Hz, 2H), 8.38 (d, J = 8.0 Hz, 1H), 7.73 – 7.63 (m, 2H), 7.25 – 7.20 (m, 3H), 7.10 (dd, J = 8.5, 2.6 Hz, 1H), 5.72 (s, 1H), 5.45 (s, 1H), 1.49 (s, 18H); ^{13}C {1H} NMR (100 MHz, CDCl_3) δ 161.9 (d $J_{\text{C-F}}$ = 242.8 Hz), 154.4, 147.4, 137.7, 135.0 (d $J_{\text{C-F}}$ = 8.8 Hz), 130.8, 127.5, 126.5, 125.0, 124.9, 124.4 (d $J_{\text{C-F}}$ = 9.0 Hz), 123.2 (d $J_{\text{C-F}}$ = 1.7 Hz), 122.5, 117.9 (d $J_{\text{C-F}}$ = 3.9 Hz), 112.6 (d $J_{\text{C-F}}$ = 23.9 Hz), 110.3 (d $J_{\text{C-F}}$ = 22.3 Hz), 34.7, 30.5; ^{19}F NMR (376 MHz, CDCl_3) δ -114.3; FT-IR (neat): 3636, 3071, 2958, 1434, 1390, 1235, 1159, 745 cm^{-1} ; HRMS (ESI): m/z calcd for $\text{C}_{28}\text{H}_{30}\text{FO}_2$ $[\text{M}+\text{H}]^+$: 417.2224; found: 417.2224.

11-(3,5-di-tert-butyl-4-hydroxyphenyl)dibenzo[b,f]oxepin-10(11H)-one (**34u**).



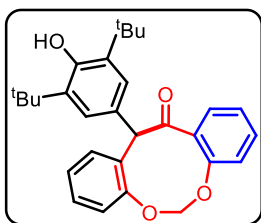
The reaction was performed at 0.064 mmol scale of **33u**; Rf = 0.3 (10% EtOAc in hexane); colourless solid (36.1 mg, 90 % yield); m. p. = 168-169 °C; ^1H NMR (400 MHz, CDCl_3) δ 7.78 – 7.76 (m, 1H), 7.43 – 7.40 (m, 3H), 7.33 (d, J = 7.6 Hz, 1H), 7.18 (d, J = 4.3 Hz, 1H), 7.13 (s, 2H), 7.03 – 7.01 (m, 2H), 6.72 (s, 1H), 5.66 (s, 1H), 1.39 (s, 18H); ^{13}C {1H} NMR (100 MHz, CDCl_3) δ 201.8, 154.1, 152.2, 151.0, 138.2, 138.1, 136.0, 132.2, 127.9, 126.9, 126.0, 124.7, 124.6, 123.4, 122.3, 121.7, 120.8, 117.8, 116.5, 60.0, 34.7, 30.6; FT-IR (neat): 3637, 3074, 2956, 1680, 1597, 1434, 1390, 1233, 1152, 746 cm^{-1} ; HRMS (ESI): m/z calcd for $\text{C}_{28}\text{H}_{31}\text{O}_3$ $[\text{M}+\text{H}]^+$: 415.2268; found: 415.2269.

12-(3,5-di-tert-butyl-4-hydroxyphenyl)-6H-dibenzo[b,f]oxocin-11(12H)-one (**34v**).



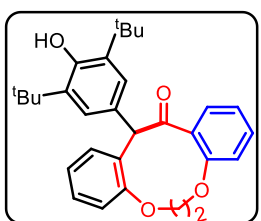
The reaction was performed at 0.089 mmol scale of **33v**; Rf = 0.6 (20% EtOAc in hexane); colourless solid (31.7 mg, 79 % yield); m. p. = 177-179 °C; ^1H NMR (400 MHz, CDCl_3) δ 7.83 (d, J = 9.0 Hz, 1H), 7.68 – 7.66 (m, 1H), 7.52 (d, J = 5.4 Hz, 1H), 7.45 – 7.42 (m, 2H), 7.16 (s, 2H), 6.98 – 6.90 (m, 3H), 6.72 (s, 1H), 5.48 (s, 1H), 5.20 (s, 2H), 1.43 (s, 18H); ^{13}C {1H} NMR (100 MHz, CDCl_3) δ 201.8, 157.8, 152.2, 138.1, 137.6, 132.9, 132.1, 129.2, 127.8, 126.5, 126.2, 125.0, 124.7, 121.6, 117.4, 112.8, 74.8, 51.2, 35.3, 30.4; FT-IR (neat): 3637, 3074, 2956, 1690, 1597, 1434, 1390, 1233, 1152, 746 cm^{-1} ; HRMS (ESI): m/z calcd for $\text{C}_{29}\text{H}_{33}\text{O}_3$ $[\text{M}+\text{H}]^+$: 429.2424; found: 429.2429.

13-(3,5-di-tert-butyl-4-hydroxyphenyl)dibenzo[d,h][1,3]dioxonin-12(13H)-one (**34w**).



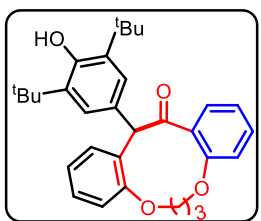
The reaction was performed at 0.089 mmol scale of **33w**; Rf = 0.6 (20% EtOAc in hexane); colourless solid (29.5 mg, 74 % yield); m. p. = 188-191 °C; ^1H NMR (400 MHz, CDCl_3) δ 7.59 – 7.56 (m, 1H), 7.48 (t, J = 7.0 Hz, 1H), 7.24 – 7.20 (m, 3H), 7.13 – 7.06 (m, 2H), 6.85 (d, J = 6.7 Hz, 1H), 6.0 (s, 1H), 5.59 (d, J = 6.2 Hz, 1H), 5.32 (d, J = 4.3 Hz, 1H), 5.17 (s, 1H), 1.40 (s, 18H); $^{13}\text{C}\{^1\text{H}\}$ NMR (100 MHz, CDCl_3) δ 202.1, 156.9, 155.5, 153.3, 135.8, 133.1, 130.4, 129.84, 129.80, 128.8, 127.51, 127.45, 127.40, 125.6, 125.4, 122.7, 122.5, 102.5, 102.4, 58.6, 34.5, 30.5; FT-IR (neat): 3637, 3074, 2956, 1706, 1597, 1434, 1390, 1233, 1152, 746 cm^{-1} ; HRMS (ESI): m/z calcd for $\text{C}_{29}\text{H}_{32}\text{O}_4$ $[\text{M}+\text{H}]^+$: 445.2373; found: 445.2373.

14-(3,5-di-tert-butyl-4-hydroxyphenyl)-6,7-dihydrodibenzo[e,i][1,4]dioxecin-13(14H)-one (34x).



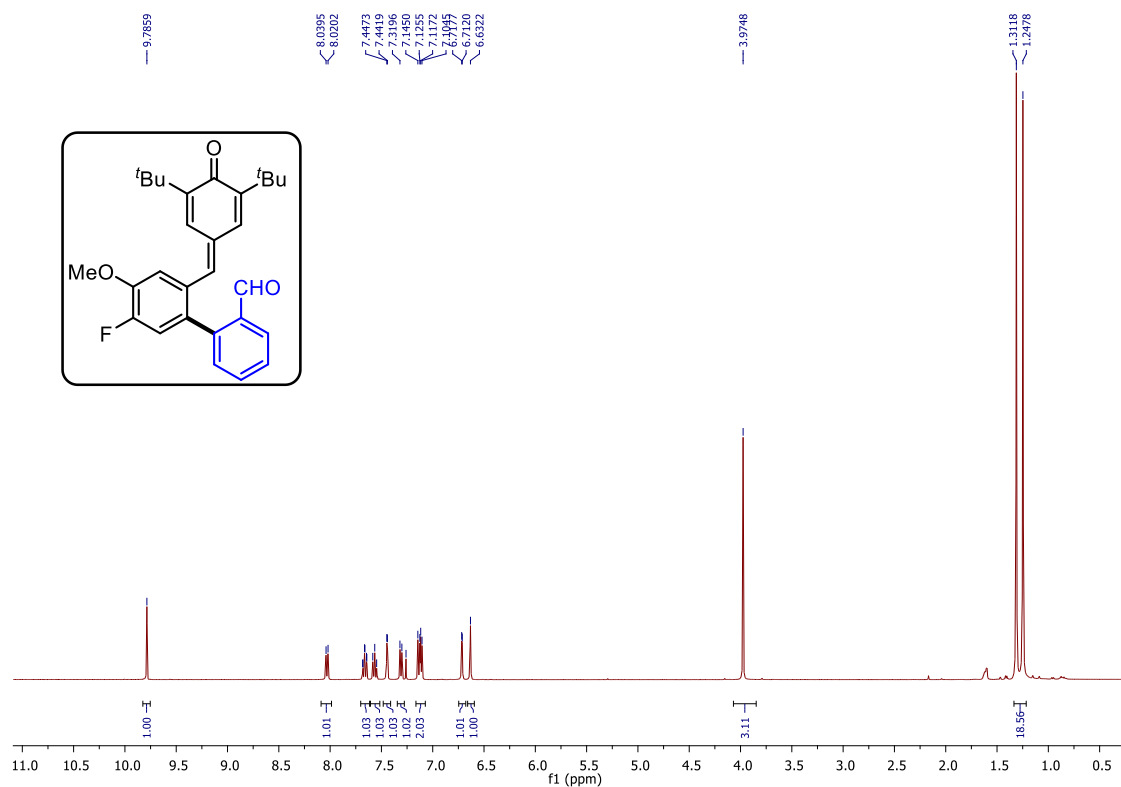
The reaction was performed at 0.089 mmol scale of **33x**; Rf = 0.6 (20% EtOAc in hexane); colourless solid (23.3 mg, 58 % yield); m. p. = 193-194 °C; ^1H NMR (400 MHz, CDCl_3) δ 7.62 – 7.61 (m, 1H), 7.51 (t, J = 7.0 Hz, 1H), 7.26 – 7.23 (m, 3H), 7.17 – 7.5 (m, 2H), 6.98 (d, J = 6.7 Hz, 1H), 6.10 (s, 1H), 5.17 (s, 1H), 4.01 – 3.97 (m, 4H), 1.39 (s, 18H); $^{13}\text{C}\{^1\text{H}\}$ NMR (100 MHz, CDCl_3) δ 201.6, 157.2, 154.5, 151.8, 135.1, 133.0, 130.2, 129.8, 129.6, 128.0, 127.5, 127.3, 126.9, 125.6, 125.4, 122.9, 122.6, 102.7, 102.1, 58.1, 34.7, 30.3; FT-IR (neat): 3637, 3074, 2956, 1701, 1597, 1434, 1390, 1233, 1152, 746 cm^{-1} ; HRMS (ESI): m/z calcd for $\text{C}_{30}\text{H}_{34}\text{O}_4$ $[\text{M}+\text{H}]^+$: 459.3530; found: 459.3533;

15-(3,5-di-tert-butyl-4-hydroxyphenyl)-7,8-dihydro-6H-dibenzo[f,j][1,5]dioxacycloundecin-14(15H)-one (34y).

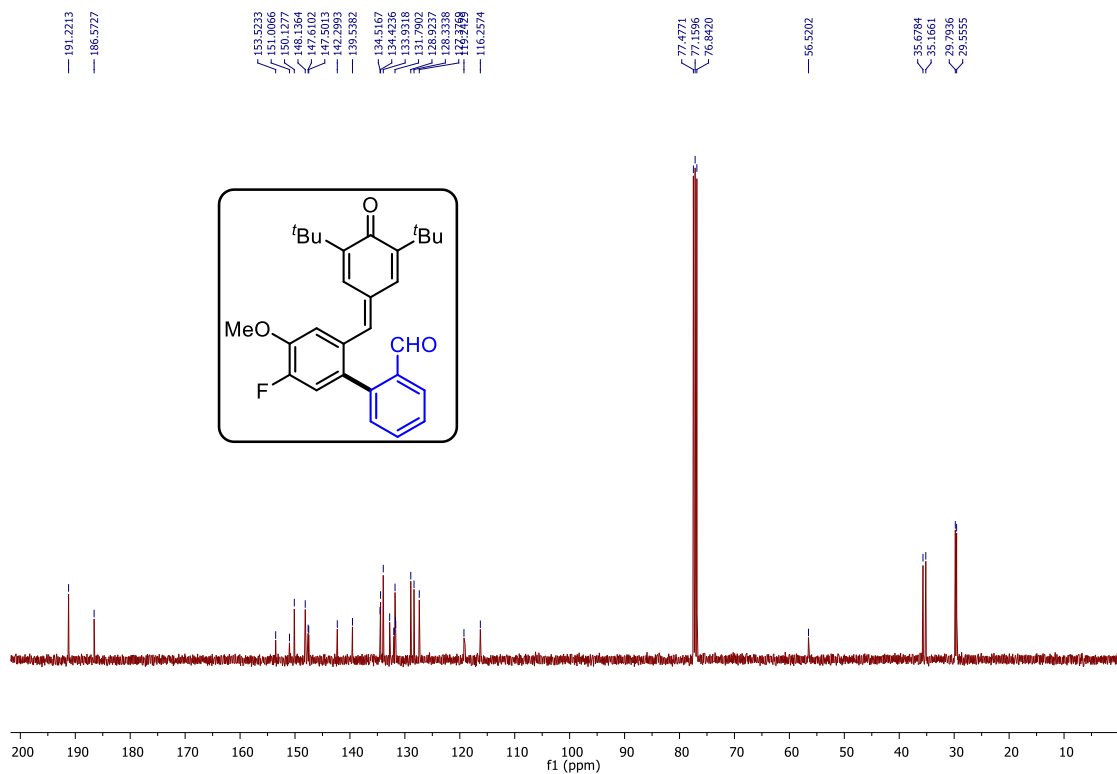


The reaction was performed at 0.089 mmol scale of **33y**; Rf = 0.6 (20% EtOAc in hexane); colourless solid (19.5 mg, 49 % yield); m. p. = 201-203 °C; ^1H NMR (400 MHz, CDCl_3) δ 7.93 – 7.92 (m, 1H), 7.48 (t, J = 6.2 Hz, 1H), 7.35 – 7.31 (m, 3H), 7.13 – 7.06 (m, 2H), 6.89 (d, J = 8.3 Hz, 1H), 6.12 (s, 1H), 5.17 (s, 1H), 3.19 (t, J = 5.9 Hz, 4H), 1.92 – 1.87 (m, 2H), 1.41 (s, 18H); $^{13}\text{C}\{^1\text{H}\}$ NMR (100 MHz, CDCl_3) δ 203.2, 157.8, 157.1, 152.3, 133.8, 133.1, 131.4, 129.8, 129.6, 128.1, 127.4, 127.3, 127.0, 125.1, 124.4, 123.7, 122.5, 102.5, 102.4, 58.6, 34.5, 30.5, 21.8; ; FT-IR (neat): 3637, 3074, 2956, 1706, 1597, 1434, 1390, 1233, 1152, 746 cm^{-1} ; HRMS (ESI): m/z calcd for $\text{C}_{31}\text{H}_{36}\text{O}_4$ $[\text{M}+\text{H}]^+$: 476.2686; found: 476.2686

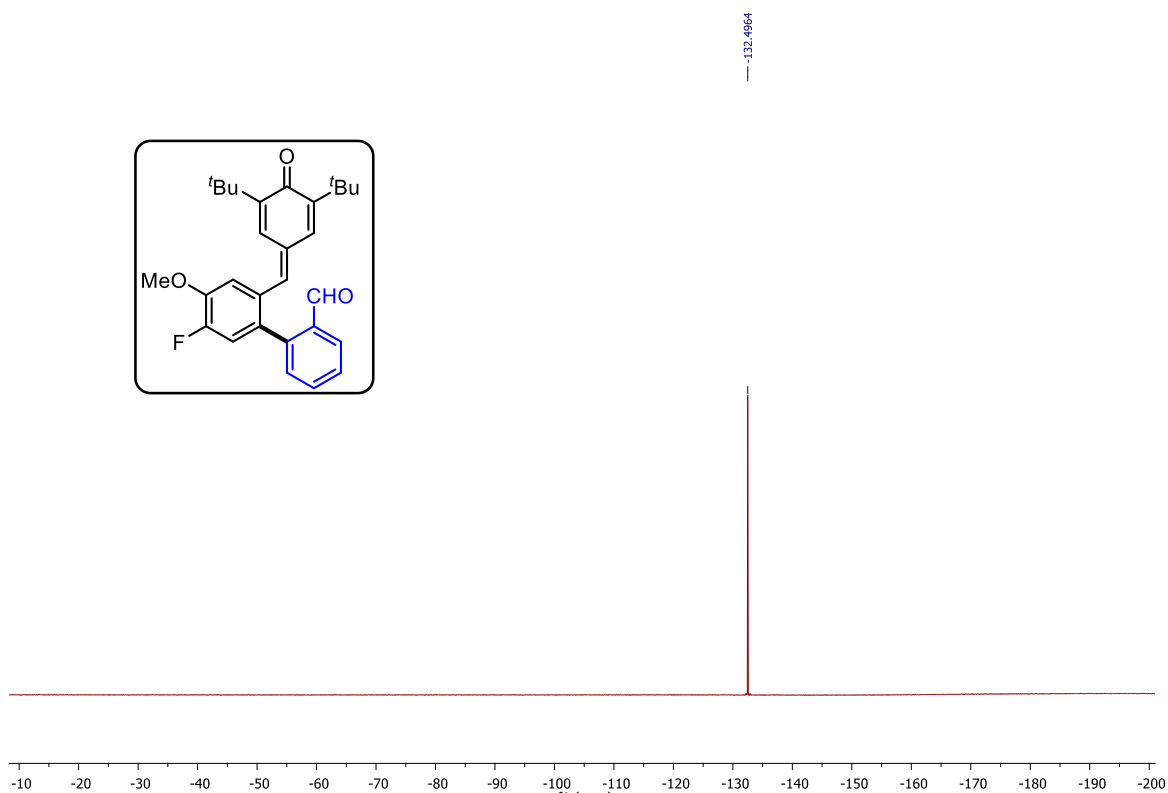
¹H NMR spectrum of **33i**



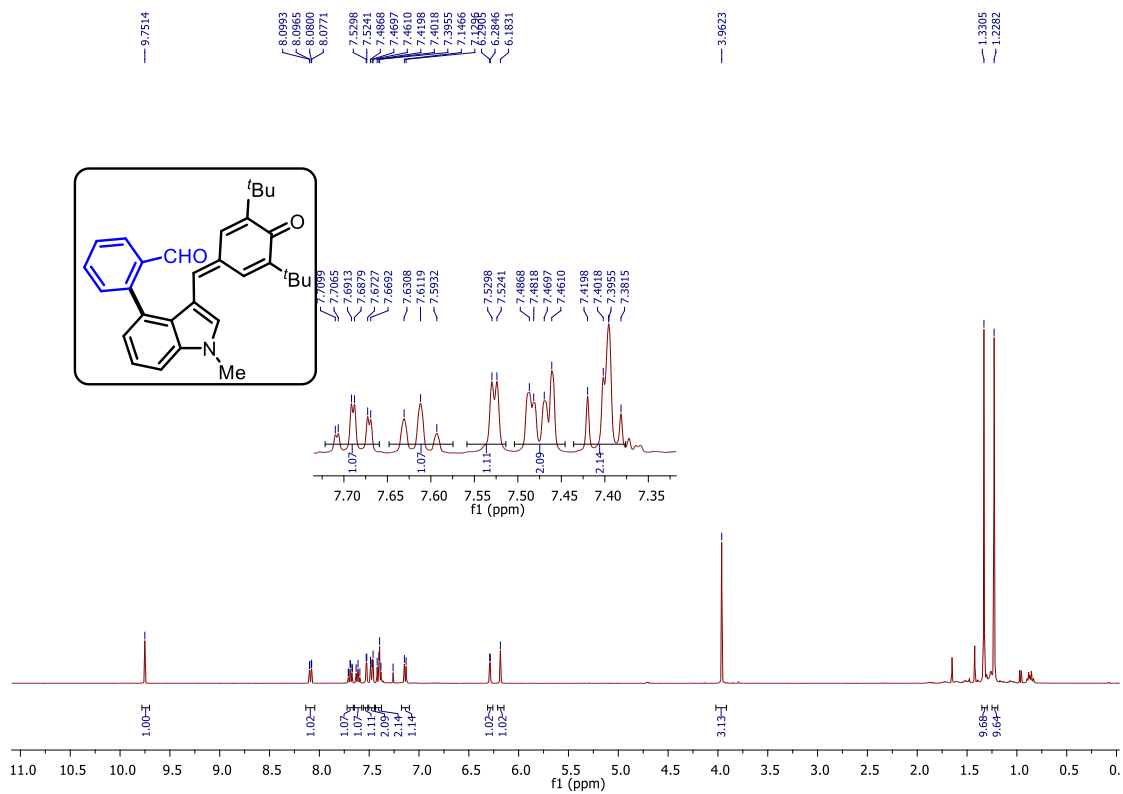
¹³C NMR spectrum of **33i**



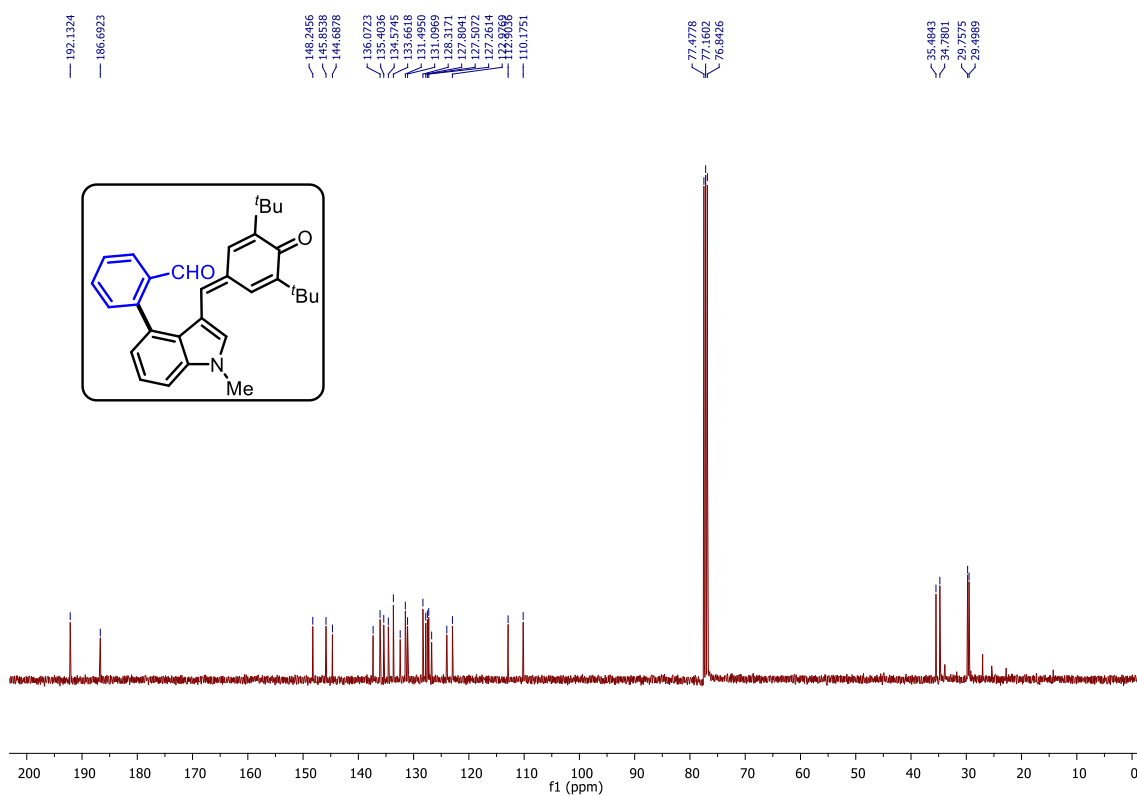
^{19}F NMR spectrum of **33i**



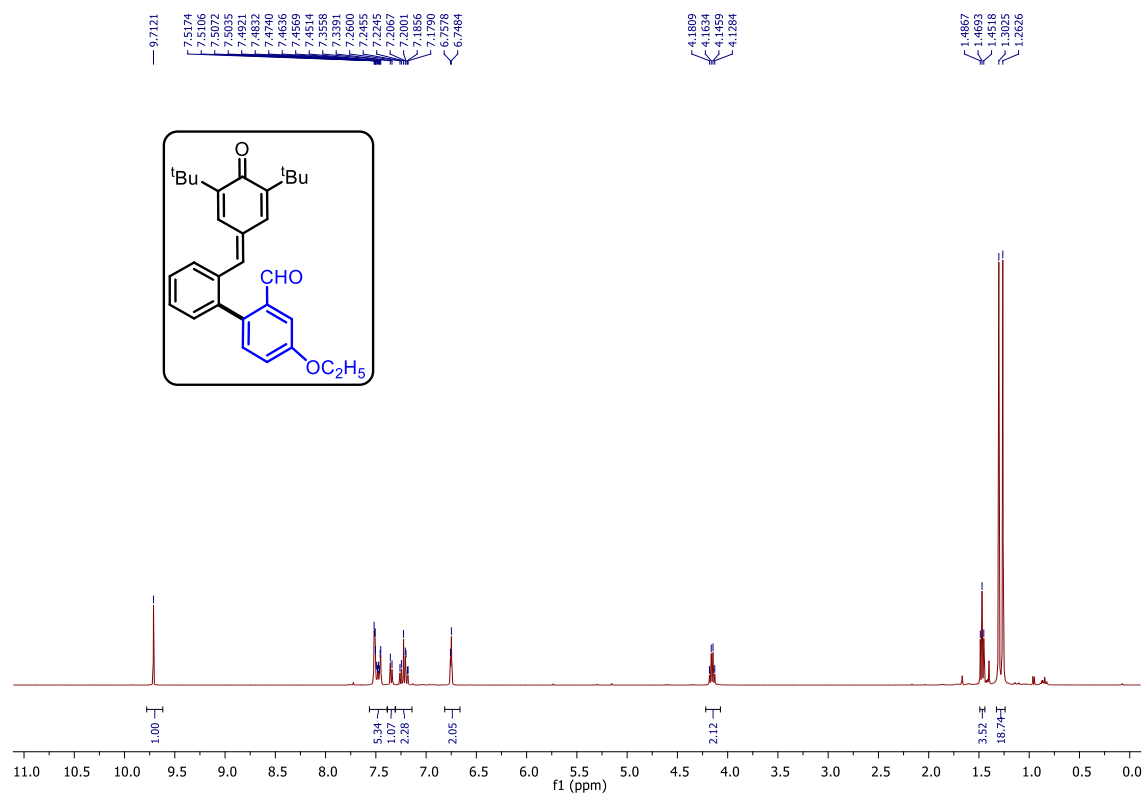
^1H NMR spectrum of **33n**



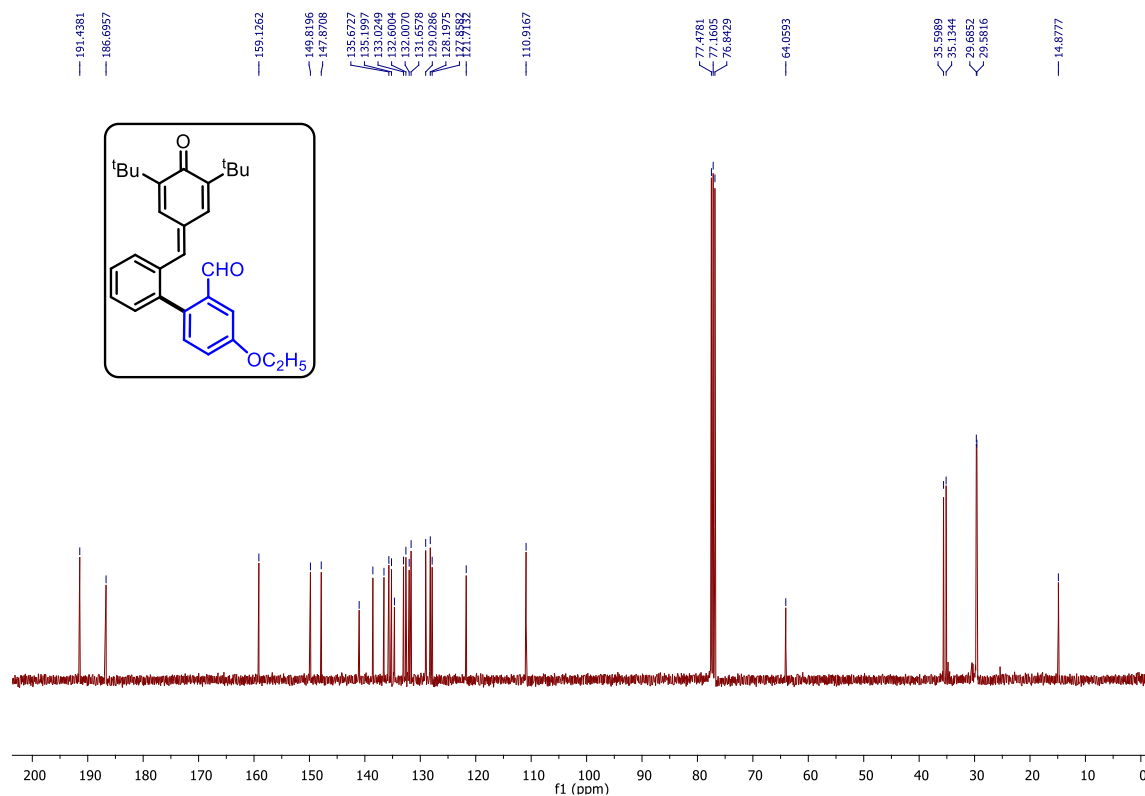
¹³C NMR spectrum of **33n**



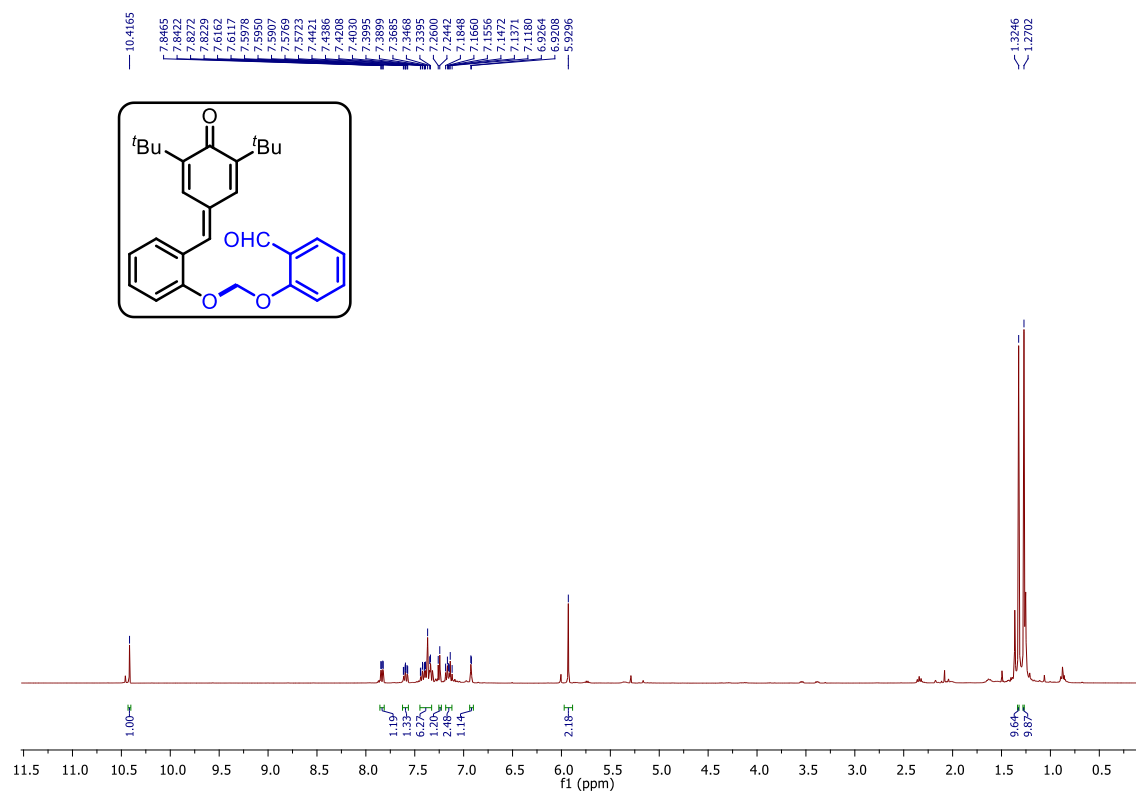
¹³C NMR spectrum of **33q**



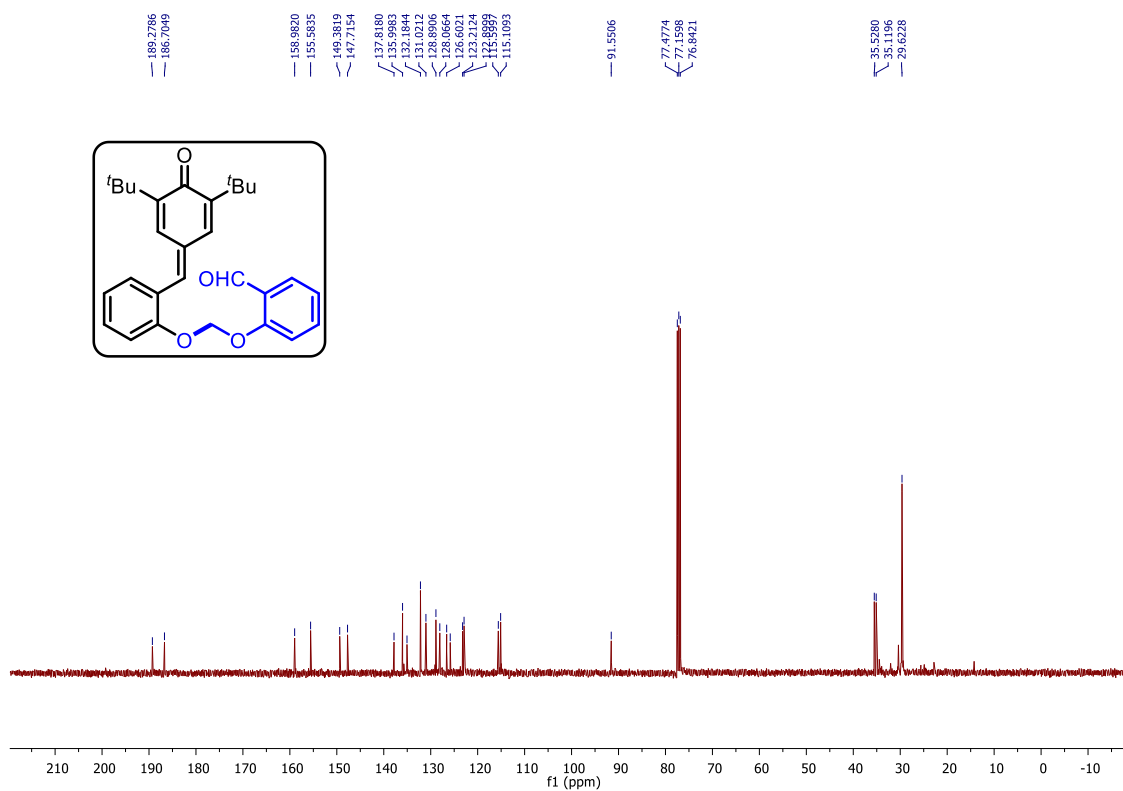
^{13}C NMR spectrum of **33q**



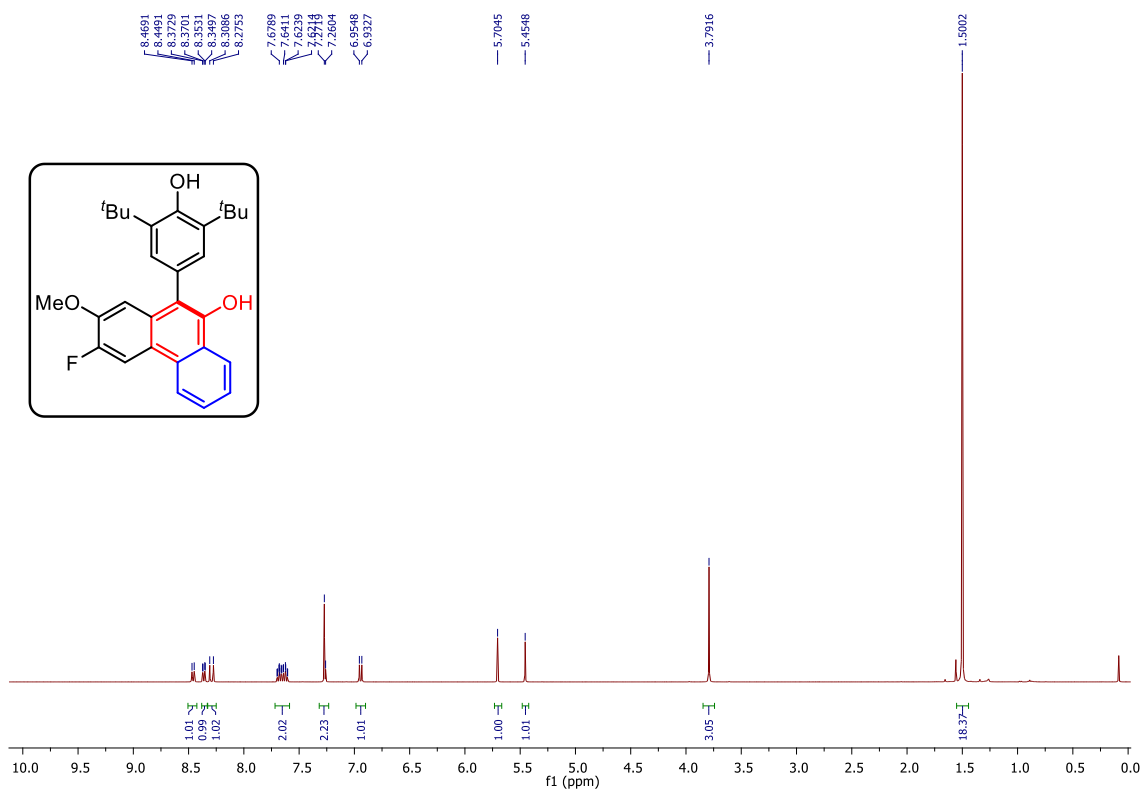
^1H NMR spectrum of **33w**



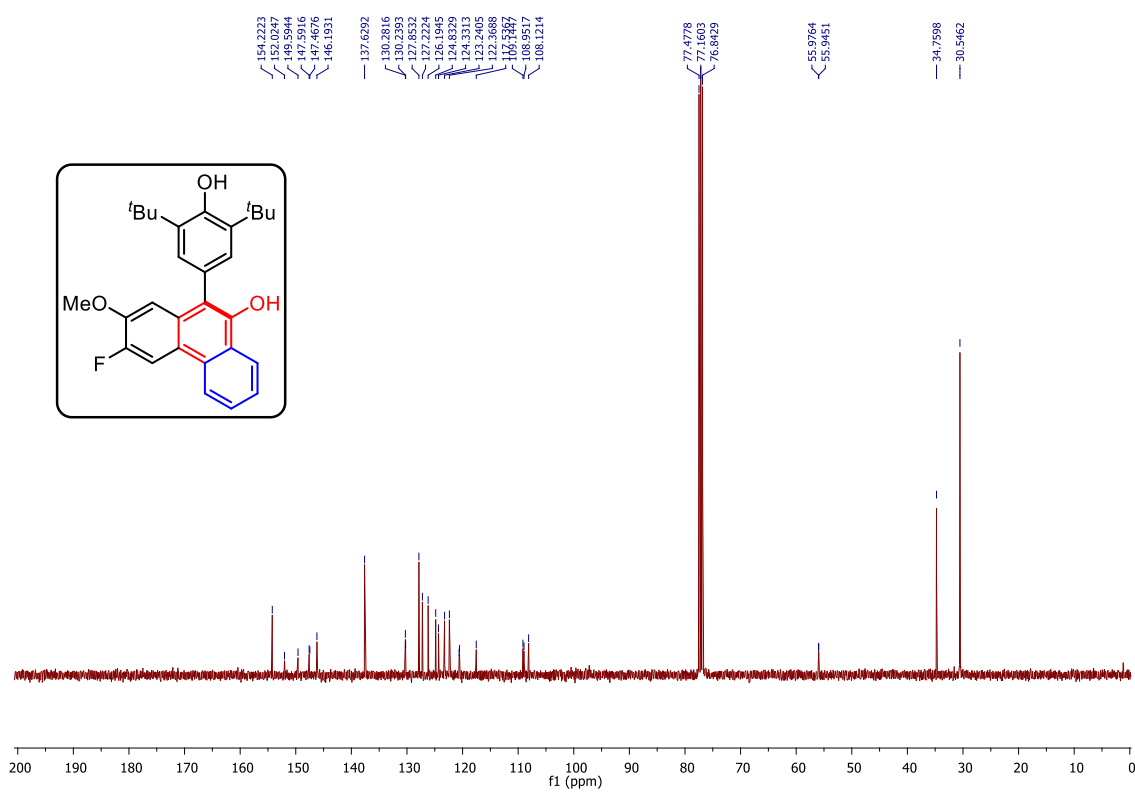
^{13}C NMR spectrum of **33w**



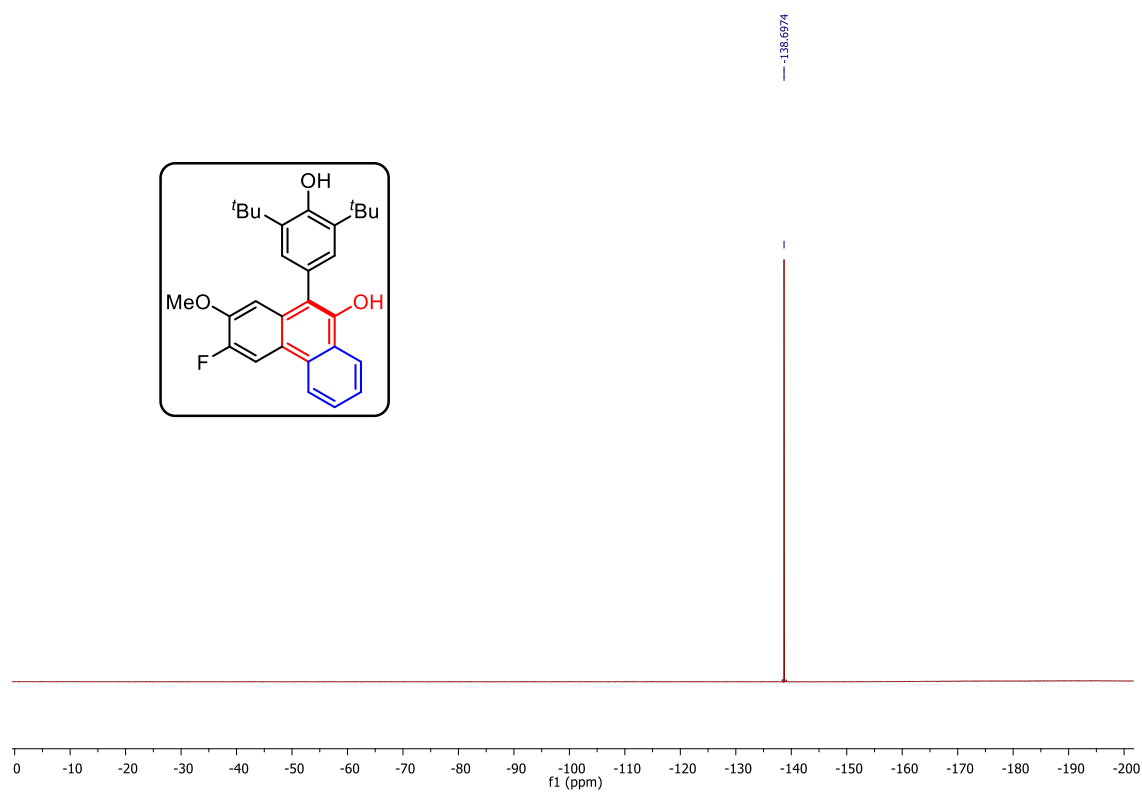
^1H NMR spectrum of **33i**



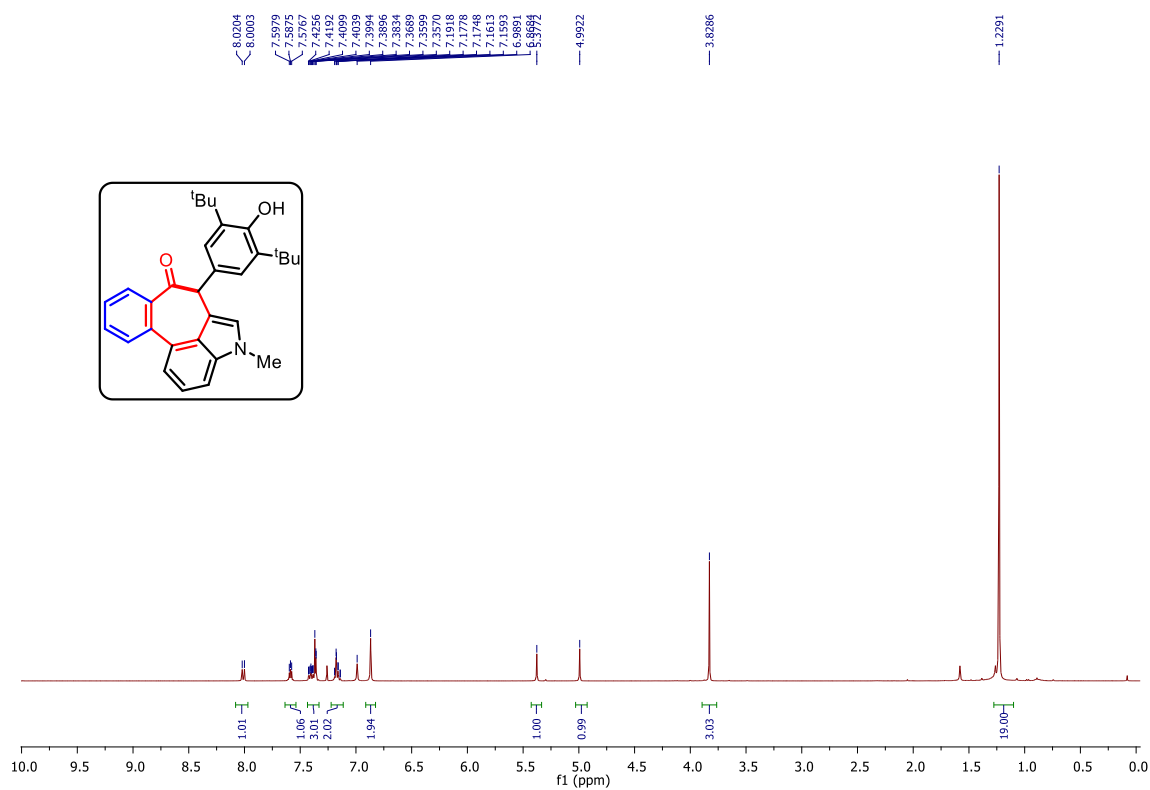
^{13}C NMR spectrum of **33i**



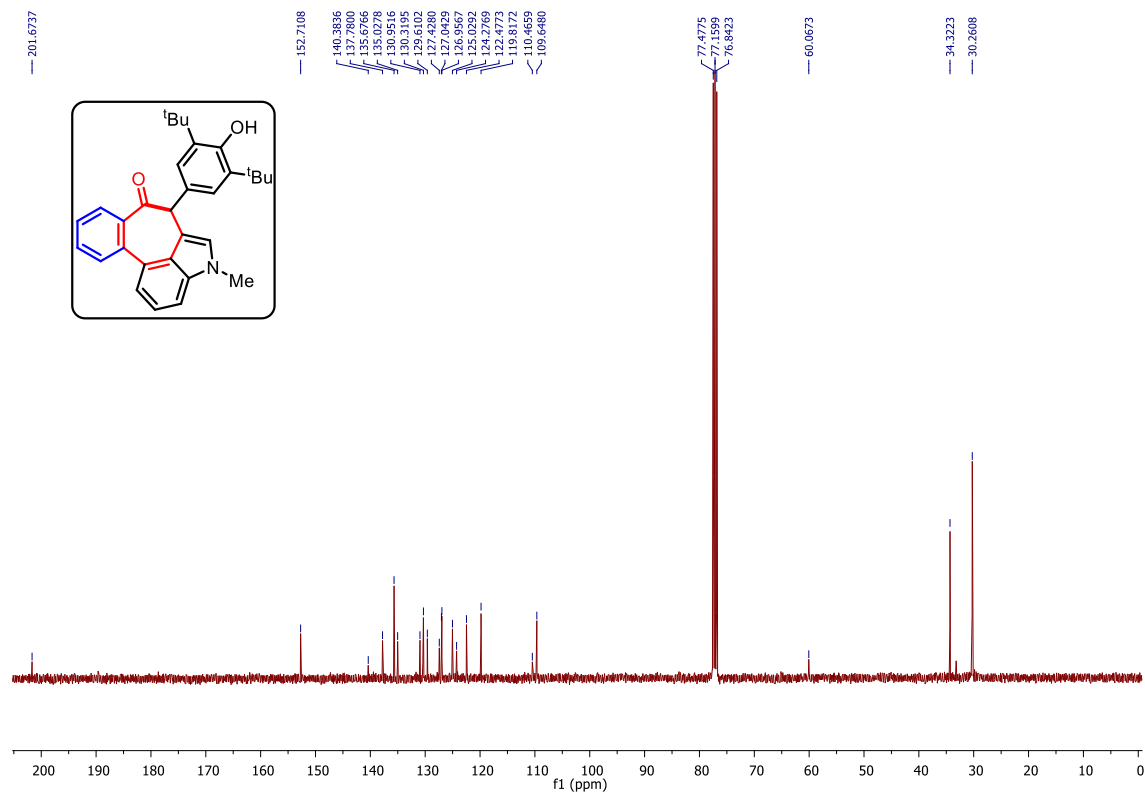
^{19}F NMR spectrum of **33i**



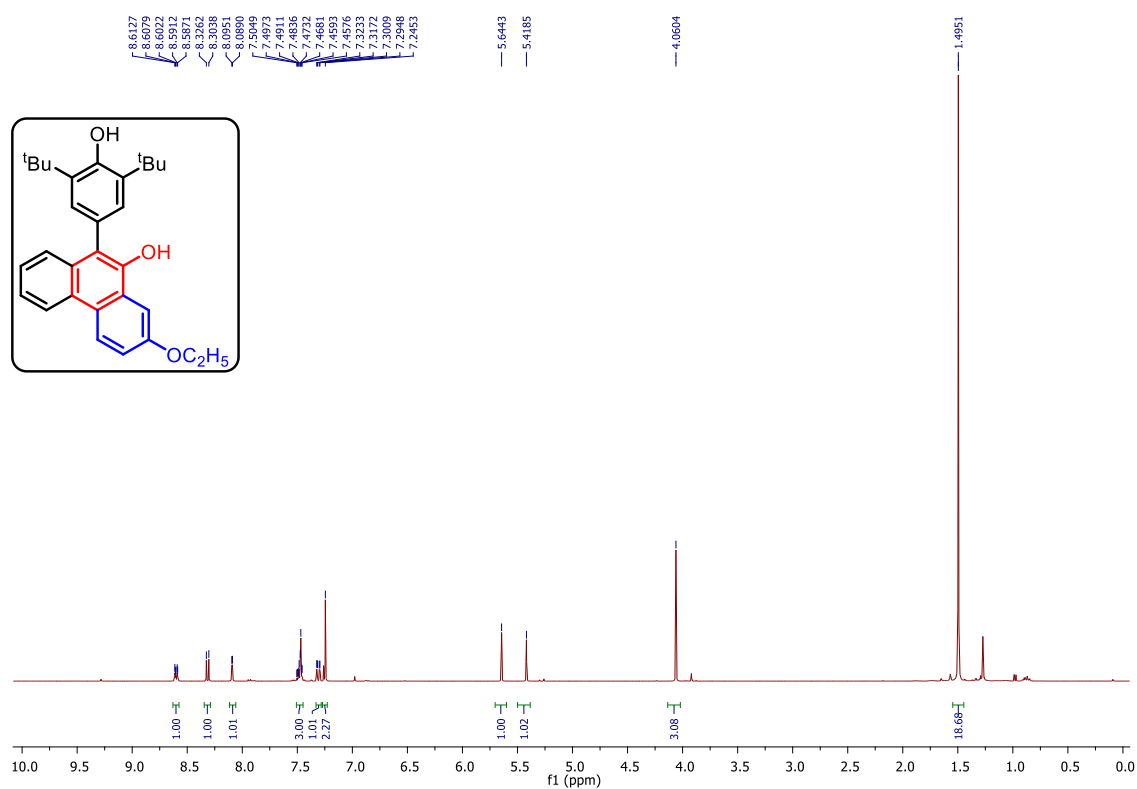
¹H NMR spectrum of **33n**



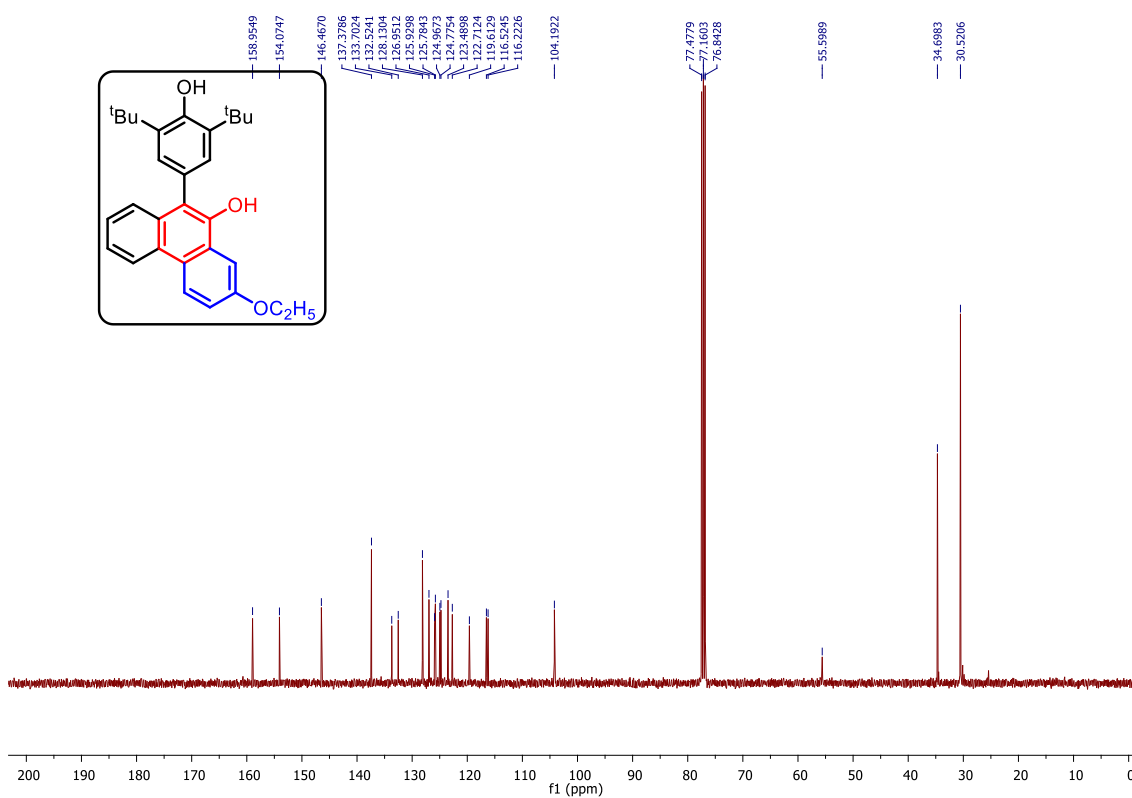
¹³C NMR spectrum of **33n**



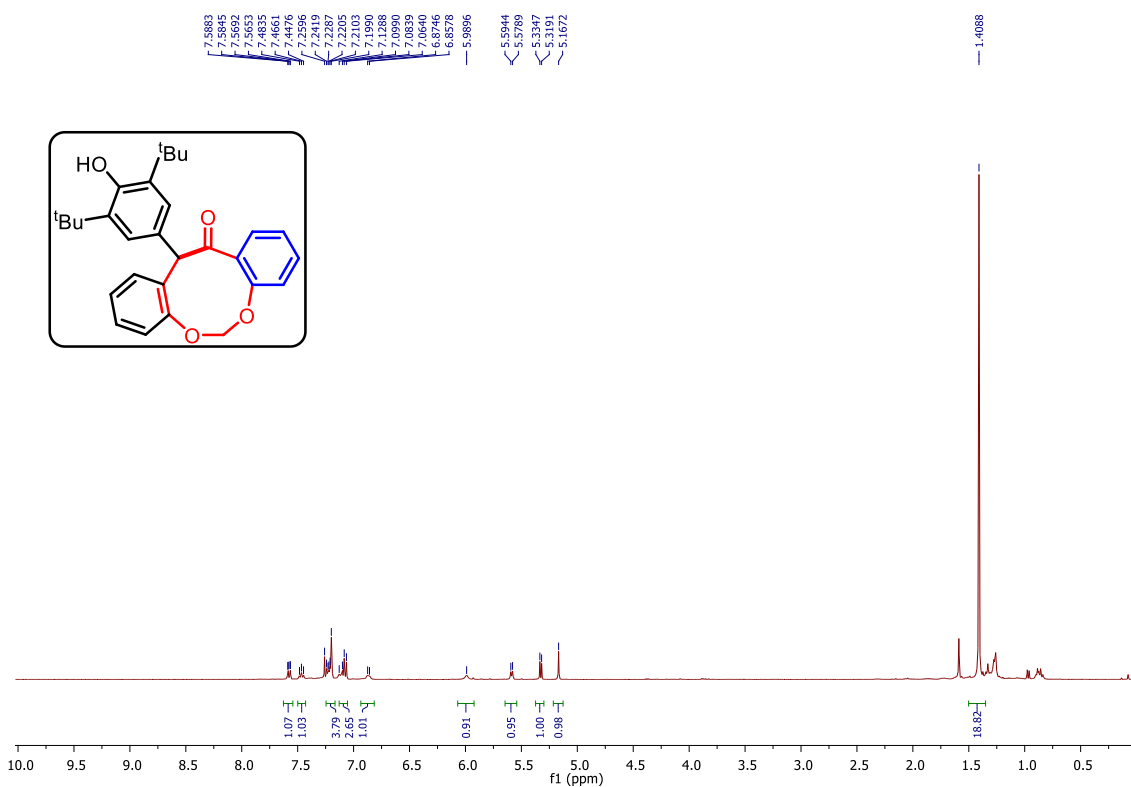
¹H NMR spectrum of **33q**



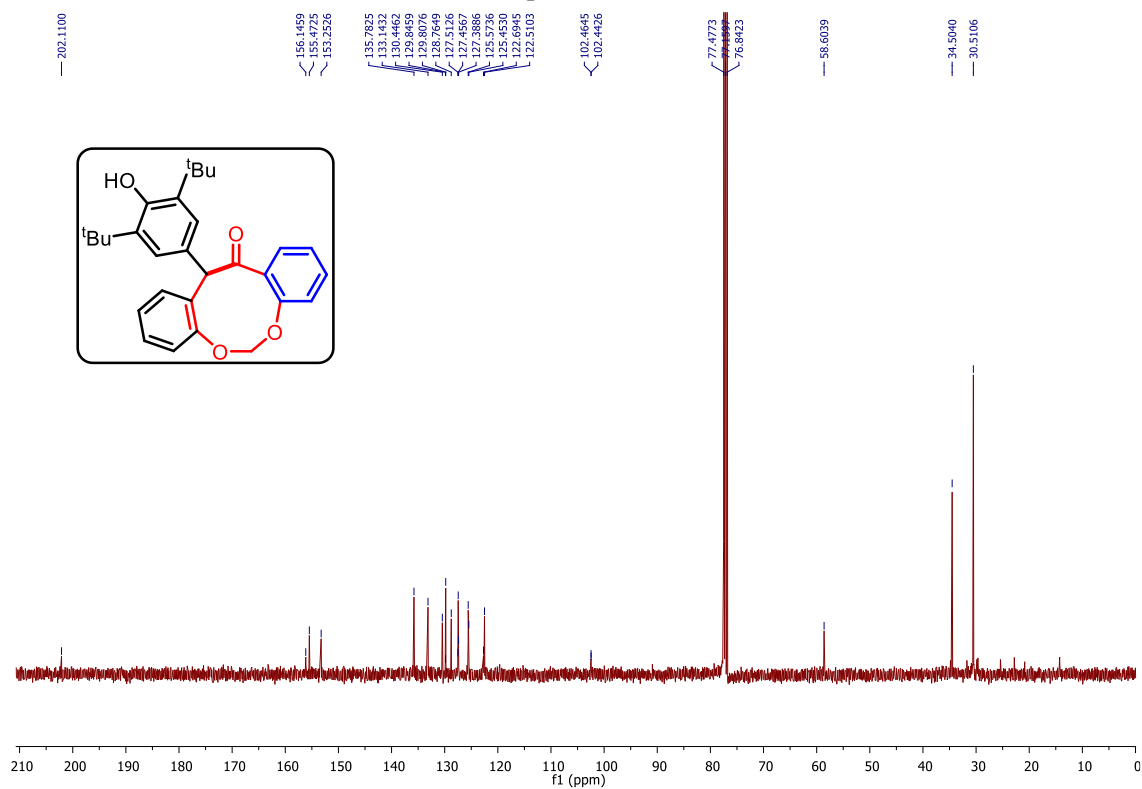
¹³C NMR spectrum of **33q**



¹H NMR spectrum of **33w**

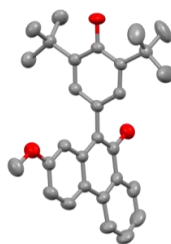
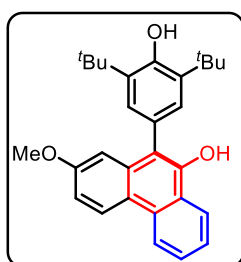


¹³C NMR spectrum of **33w**



Crystal Structure of compound 34b

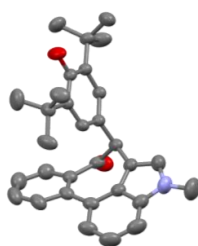
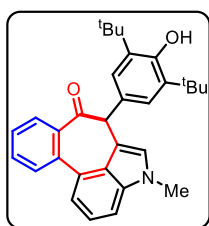
Identification code	34b
Empirical formula	C ₂₉ H ₃₂ O ₃
Formula weight	428.55
Temperature/K	298.0
Crystal system	monoclinic
Space group	C2/c
a/Å	32.7513(12)
b/Å	5.7432(2)
c/Å	26.9363(11)
$\alpha/^\circ$	90.00
$\beta/^\circ$	111.567(4)
$\gamma/^\circ$	90.00
Volume/Å ³	4711.9(3)
Z	8
$\rho_{\text{calc}}/\text{cm}^3$	1.208
μ/mm^{-1}	0.077
F(000)	1840.0
Crystal size/mm ³	0.2 × 0.2 × 0.2
Radiation	Mo K α (λ = 0.71073)
2 θ range for data collection/ $^\circ$	5.34 to 65.5
Index ranges	-48 ≤ h ≤ 49, -8 ≤ k ≤ 8, -40 ≤ l ≤ 40
Reflections collected	64908
Independent reflections	8628 [R _{int} = 0.0397, R _{sigma} = 0.0257]
Data/restraints/parameters	8628/0/301
Goodness-of-fit on F ²	1.044
Final R indexes [I ≥ 2 σ (I)]	R ₁ = 0.0736, wR ₂ = 0.2104
Final R indexes [all data]	R ₁ = 0.1133, wR ₂ = 0.2557
Largest diff. peak/hole / e Å ⁻³	0.49/-0.23



CCDC NO. 2280137

Crystal Structure of compound 34n

Identification code	34n
Empirical formula	C ₃₁ H ₃₃ NO ₂
Formula weight	451.2551
Temperature/K	298.0
Crystal system	Monoclinic
Space group	C2/c
a/Å	32.7513(12)
b/Å	5.7432(2)
c/Å	26.9363(11)
$\alpha/^\circ$	90.00
$\beta/^\circ$	111.567(4)
$\gamma/^\circ$	90.00
Volume/Å ³	4711.9(3)
Z	8
$\rho_{\text{calc}}/\text{cm}^3$	1.208
μ/mm^{-1}	0.077
F(000)	1840.0
Crystal size/mm ³	0.2 × 0.2 × 0.2
Radiation	Mo K α (λ = 0.71073)
2 θ range for data collection/ $^\circ$	5.34 to 65.5
Index ranges	-48 ≤ h ≤ 49, -8 ≤ k ≤ 8, -40 ≤ l ≤ 40
Reflections collected	64908
Independent reflections	8628 [R _{int} = 0.0397, R _{sigma} = 0.0257]
Data/restraints/parameters	8628/0/301
Goodness-of-fit on F ²	1.044
Final R indexes [I ≥ 2 σ (I)]	R1 = 0.0736, wR2 = 0.2104
Final R indexes [all data]	R1 = 0.1133, wR2 = 0.2557
Largest diff. peak/hole / e Å ⁻³	0.49/-0.23



CCDC NO. 2278464

2.1.7 References

- 1) For recent reviews on NHC carbene, see: (a) Enders, D.; Niemeier, O.; Henseler, A. *Chem. Rev.* **2007**, *107*, 5606. (b) Moore, J. L.; Rovis, T. *Top. Curr. Chem.* **2010**, *291*, 77. (c) Biju, A. T.; Kuhl, N.; Glorius, F. *Acc. Chem. Res.* **2011**, *44*, 1182. (d) Nair, V.; Menon, R. S.; Biju, A. T.; Sinu, C. R.; Paul, R. R.; Jose, A.; Sreekumar, V. *Chem. Soc. Rev.* **2011**, *40*, 5336. (e) Bugaut, X.; Glorius, F. *Chem. Soc. Rev.* **2012**, *41*, 3511. (f) Izquierdo, J.; Hutson, G. E.; Cohen, D. T.; Scheidt, K. A. *Angew. Chem. Int. Ed.* **2012**, *51*, 11686. (m) Hopkinson, M. N.; Richter, C.; Schedler, M.; Glorius, F. *Nature* **2014**, *510*, 485. (n) Flanagan, D. M.; Romanov-Michailidis, F.; White, N. A.; Rovis, T. *Chem. Rev.* **2015**, *115*, 9307.
- 2) (a) Arduengo, A. J., III; Dias, H. V. R.; Harlow, R. L.; Kline, M. *J. Am. Chem. Soc.* **1992**, *114*, 5530. (b) Heinemann, C.; Müller, T.; Apeloig, Y.; Schwarz, H. *J. Am. Chem. Soc.* **1996**, *118*, 2023. (c) Arduengo, A. J., III *Acc. Chem. Res.* **1999**, *32*, 913. (d) Bourissou, D.; Guerret, O.; Gabbai, F. P.; Bertrand, G. *Chem. Rev.* **2000**, *100*, 39. (e) Crudden, C. M.; Allen, D. P. *Coord. Chem. Rev.* **2004**, *248*, 2247.
- 3) (a) Canac, Y.; Soleilhavoup, M.; Conejero, S.; Bertrand, G. *J. Organomet. Chem.* **2004**, *689*, 3857. (b) Vignolle, J.; Cattoën, X.; Bourissou, D. *Chem. Rev.* **2009**, *109*, 3333.
- 4) (a) Johnson, L. E.; DuPré, D. B. *J. Phys. Chem. A* **2007**, *111*, 11066. (b) Johnson, L. E.; DuPré, D. B. *J. Phys. Chem. A* **2008**, *112*, 7448.
- 5) (a) Yoshida, Z.; Konishi, H.; Sawada, S.; Ogoshi, H. *J. Chem. Soc., Chem. Commun.* **1977**, 850. (b) Weiss, R.; Priesner, C.; Wolf, H. *Angew. Chem. Int. Ed. Engl.* **1978**, *17*, 446. (c) Konishi, H.; Matsumoto, S.; Kamitori, Y.; Ogoshi, H.; Yoshida, Z. *Chem. Lett.* **1978**, 241. (d) Weiss, R.; Hertel, M.; Wolf, H. *Angew. Chem., Int. Ed. Engl.* **1979**, *18*, 473. (e) Yoshida, Z. *Pure Appl. Chem.* **1982**, *54*, 1059.
- 6) (a) Komatsu, K.; Kitagawa, T. *Chem. Rev.* **2003**, *103*, 1371. (b) Herrmann, W. A.; Öfele, K.; Taubmann, C.; Herdtweck, E.; Hoffmann, S. D. *J. Organomet. Chem.* **2007**, *692*, 3846. (c) Kuchenbeiser, G.; Donnadiou, B.; Bertrand, G. *J. Organomet. Chem.* **2008**, *693*, 899. (d) Kuchenbeiser, G.; Soleilhavoup, M.; Donnadiou, B.; Bertrand, G. *Chem. Asian. J.* **2009**, *4*, 1745. (e) Öfele, K.; Tosh, E.; Taubmann, C.; Herrmann, W. A. *Chem. Rev.* **2009**, *109*, 3408. (f) Melaimi, M.; Soleilhavoup, M.; Bertrand, G. *Angew. Chem., Int. Ed.* **2010**, *49*, 8810. (g) Malik, H. A.; Sormunen, G. J.; Montgomery, J. *J. Am. Chem. Soc.* **2010**, *132*, 6304. (h) Rodrigo, S. K.; Guan, H. *J. Org. Chem.* **2012**, *77*, 8303.

- 7) Lavallo, V.; Canac, Y.; Donnadiou, B.; Schoeller, W. W.; Bertrand, G. *Science* **2006**, 312, 722.
- 8) Lavallo, V.; Ishida, Y.; Donnadiou, B.; Bertrand, G. *Angew. Chem. Int. Ed.* **2006**, 45, 6652.
- 9) Holschumacher, D.; Hrib, C. G.; Jones, P. G.; Tamm, M. *Chem. Commun.* **2007**, 3661.
- 10) Wilde, M. M. D.; Gravel, M. *Angew. Chem., Int. Ed.* **2013**, 52, 12654.
- 11) Rezazadeh Khalkhali, M.; Wilde, M. M. D.; Gravel, M. *Org. Lett.* **2021**, 23, 159.
- 12) Wilde, M. M. D.; Gravel, M. *Org. Lett.* **2014**, 16, 5311.
- 13) a) Ramanjaneyulu, B. T.; Mahesh, S.; Anand, R. V. *Org. Lett.* **2015**, 17, 6. b) Arde, P; Anand, R. V. *Org. Biomol. Chem.* **2016**, 14, 5550. c) Arde, P.; Anand, R. V. *RSC Adv.* **2016**, 6, 77111.
- 14) Ramanjaneyulu, B. T.; Mahesh, S.; Anand, R. V. *Org. Lett.* **2015**, 17, 3952.
- 15) Goswami, P.; Sharma, S.; Singh, G.; Vijaya Anand, R. *J. Org. Chem.* **2018**, 83, 4220.
- 16) Singh, G.; Goswami, P.; Vijaya Anand, R. *Org. Biomol. Chem.* **2018**, 16, 388.
- 17) (a) De Koning, C. B.; Michael, J. P.; Rousseau, A. L. *Tetrahedron Lett.* **1998**, 39, 8725. (b) Kumar, V.; Poonam; Prasad, A. K.; Parmar, V. S. *Nat. Prod. Rep.* **2003**, 20, 565.
- 18) (a) Li, Z.; Jin, Z.; Huang, R. *Synthesis* **2001**, 2001, 2365. (b) Komatsu, H.; Watanabe, M.; Ohyama, M.; Enya, T.; Koyama, K.; Kanazawa, T.; Kawahara, N.; Sugimura, T.; Wakabayashi, K. *J. Med. Chem.* **2001**, 44, 1833. (c) Kim, S.; Lee, Y. M.; Lee, J.; Lee, T.; Fu, Y.; Song, Y.; Cho, J.; Kim, D. *J. Org. Chem.* **2007**, 72, 4886. (d) Michael, J. P. *Nat. Prod. Rep.* **2008**, 25, 139.
- 19) Wang, K.-L.; Hu, Y.-N.; Liu, Y.-X.; Mi, N.; Fan, Z.-J.; Liu, Y.; Wang, Q.-M. *J. Agric. Food Chem.* **2010**, 58, 12337.
- 20) (a) Ciszek, J. W.; Tour, J. M. *Tetrahedron Lett.* **2004**, 45, 2801. (b) Sienkowska, M. J.; Farrar, J. M.; Zhang, F.; Kusuma, S.; Heiney, P. A.; Kaszynski, P. J. *Mater. Chem.* **2007**, 17, 1399.
- 21) Bernert, J. T.; Pirkle, J. L.; Xia, Y.; Jain, R. B.; Ashley, D. L.; Sampson, E. *J. Cancer Epidemiol. Biomarkers Prev.* **2010**, 19, 2977.
- 22) Jiang, Y. T.; Yu, Z. Z.; Zhang, Y. K.; Wang, B. *Organic letters*, **2018**, 20, 3731.
- 23) (b) Almeida, J. F.; Castedo, L.; Fernández, D.; Neo, A. G.; Romero, V.; Tojo, G. *Org. Lett.* **2003**, 5, 4939. (c) Mallory, F. B.; Rudolph, M. J.; Oh, S. M. *J. Org. Chem.* **1989**, 54, 4619.

- 24) (a) Jin, R.; Chen, Y.; Liu, W.; Xu, D.; Li, Y.; Ding, A.; Guo, H. *Chem. Commun.* **2016**, 52, 9909. (b) Jin, R.; Chen, J.; Chen, Y.; Liu, W.; Xu, D.; Li, Y.; Ding, A.; Guo, H. *J. Org. Chem.* **2016**, 81, 12553.
- 25) (a) Mandal, T.; Das, S.; De Sarkar, S. *Adv. Synth. Catal.* **2019**, 361, 3200. (b) Chatterjee, T.; Lee, D. S.; Cho, E. J. *J. Org. Chem.* **2017**, 82, 4369.
- 26) (a) Kurata, Y.; Otsuka, S.; Fukui, N.; Nogi, K.; Yorimitsu, H.; Osuka, A. *Org. Lett.* **2017**, 19, 1274. (b) Daigle, M.; Picard-Lafond, A.; Soligo, E.; Morin, J.-F. *Angew. Chem., Int. Ed.* **2016**, 55, 2042.
- 27) (a) Winter, D. K.; Endoma-Arias, M. A.; Hudlicky, T.; Beutler, J. A.; Porco, J. A. *J. Org. Chem.* **2013**, 78, 7617. (b) Li, H.; He, K.-H.; Liu, J.; Wang, B.-Q.; Zhao, K.-Q.; Hu, P.; Shi, Z.-J. *Chem. Commun.* **2012**, 48, 7028.
- 28) (a) Zhao, X.; Song, C.; Rainier, J. D. *J. Org. Chem.* **2020**, 85, 5449. (b) Okamoto, H.; Yamaji, M.; Gohda, S.; Kubozono, Y.; Komura, N.; Sato, K.; Sugino, H.; Satake, K. *Org. Lett.* **2011**, 13, 2758.
- 29) (a) Qin, Y.; Zhu, L.; Luo, S. *Chem. Rev.* **2017**, 117, 9433. (b) Gutekunst, W. R.; Baran, P. S. *Chem. Soc. Rev.* **2011**, 40, 1976.
- 30) Pankhade, Y. A.; Pandey, R.; Fatma, S.; Ahmad, F.; Anand, R. V. *J. Org. Chem.* **2022**, 87, 3377.
- 31) Rezazadeh Khalkhali, M.; Wilde, M. M. D.; Gravel, M. *Org. Lett.* **2020**, 23, 159.
- 32) Bidal, Y. D.; Lesieur, M.; Melaimi, M.; Cordes, D. B.; Slawin, A. M. Z.; Bertrand, G.; Cazin, C. S. J. *Chem. Commun.* **2015**, 51, 4781.
- 33) Shao, T. M.; Zheng, C. J.; Li, X. B.; Chen, G. Y.; Song, X. P.; Han, C. R. *Nat. Prod. Res.*, **2018**, 32, 2273.
- 34) Hellal, M.; Singh, S.; Cuny, G. D. *J. Org. Chem.* **2012**, 77, 4130.
- 35) Ansari, M. I.; Hussain, M. K.; Arun, A.; Chakravarti, B.; Konwar, R.; Hajela, K. *Eur. J. Med. Chem.* **2015**, 99, 124.
- 36) Keylor, M. H., Matsuura, B. S., & Stephenson, C. R. *Chem. Rev.* **2015**, 115, 9027.
- 37) Enders, D.; Breuer, K.; Kallfass, U.; Balensiefer, T. *Synthesis* **2003**, 2003, 1295.

Chapter 2

Part B

Formal Syntheses of (±)-Shoreaphenol and (±)-Malibatol A Through a BAC-Catalyzed Intramolecular Cyclization Reactions of 2-(Formylaryl)-aryl-substituted *p*-Quinone Methides.

2.2.1 Introduction

Resveratrol is a substance with wide applications that may be useful in promoting health and preventing or treating chronic diseases.¹ Resveratrol has been associated with a diverse range of biological functions, including antioxidant,² anticancer,³ anti-diabetic,⁴ cardioprotective,⁵ and even anti-aging⁶ characteristics. Like many secondary metabolites, resveratrol oligomers are found in plants as dimers, trimers, tetramers, and higher-order oligomers and serve primarily as biological chemicals.

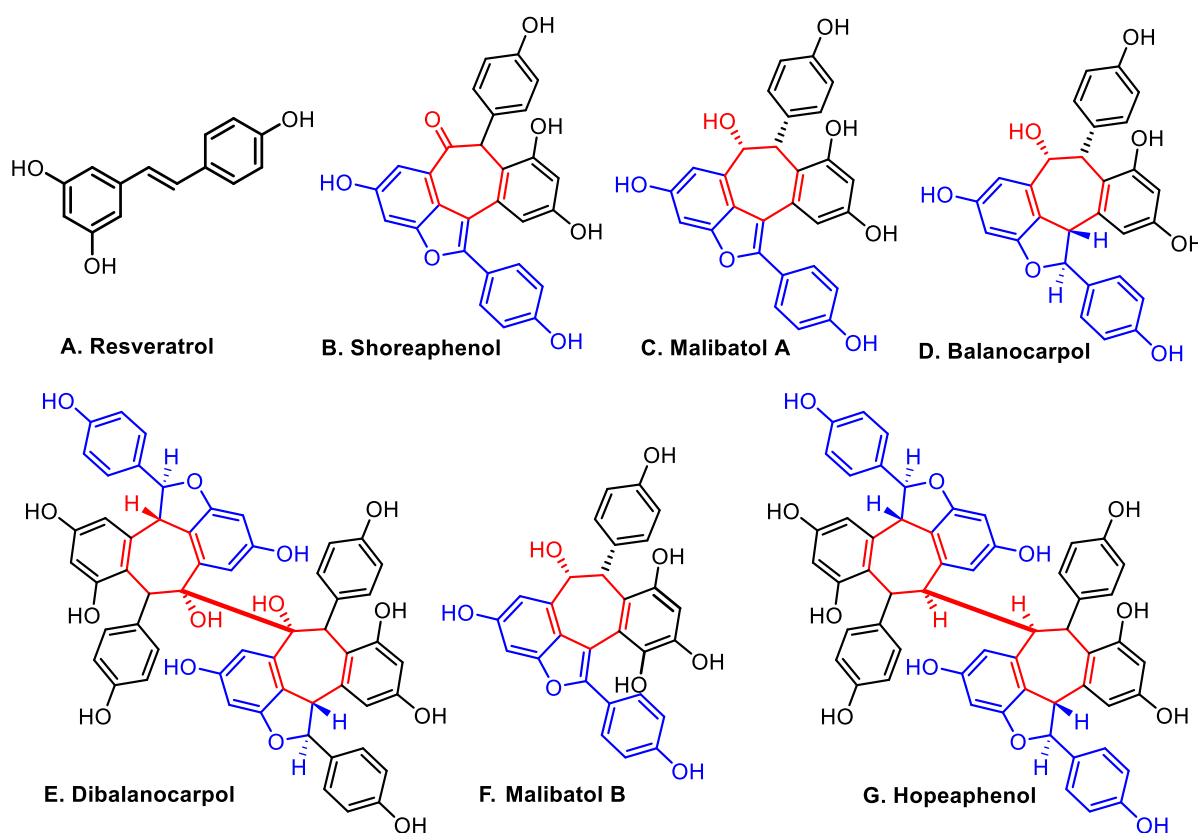
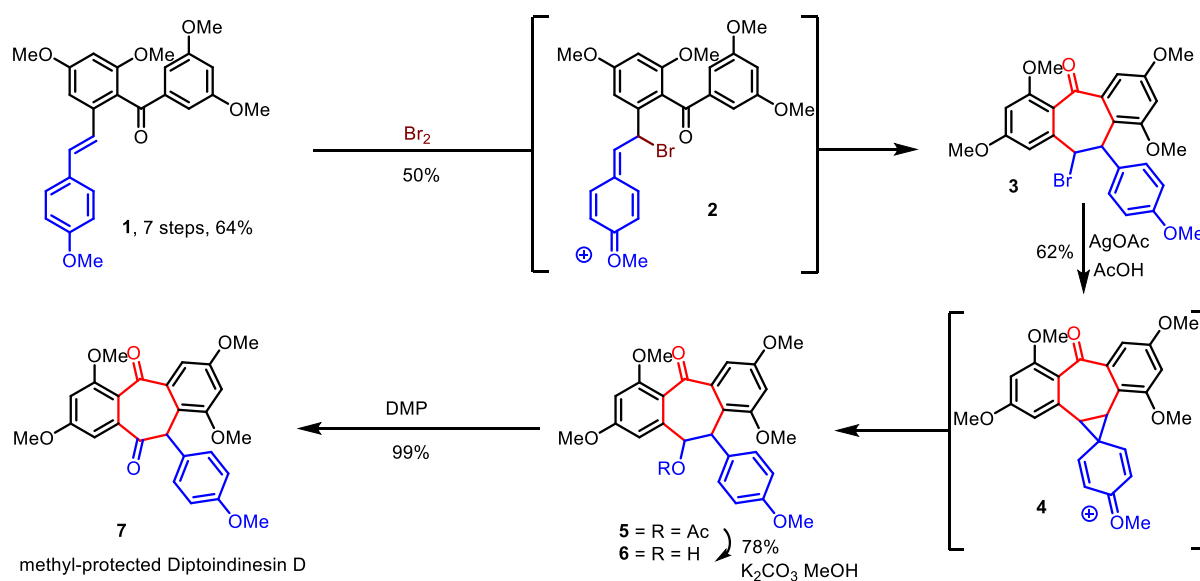


Figure 1. Structure of resveratrol analogues, sharing common core structure: cycloheptenone.

Hopeaphenol (**F**), a resveratrol-based tetramer, was identified and characterized using single-crystal X-ray diffraction (XRD) analysis by Coggon et al.,⁷ was the very first extracted resveratrol oligomer (Figure 1). Numerous natural stilbenoids, including resveratrol, share a similar metabolic route that generates cinnamic acids and flavonoids through the phenylpropanoid pathway.⁸ Intriguingly, the bark of *Shorea robusta* and the stem wood of *Hopea* utilized were found to contain an oxidized counterpart of malibatol A known as shoreaphenol (**A**) or hopeafuran (**F**). For the very first time, in 1998, Boyd and co-workers successfully isolated four important oligostilbenes, Malibatol A (**B**), & B (**E**), Balanocarpol (**C**), and Dibalancarpol (**D**) [Figure 1] from the organic extract of the leaf of *Hopea Malibato*.⁹ Only a few synthetic approaches toward these types of compounds have been reported, despite their intriguing biological activities and distinctive carbon framework. Some of them are discussed below.

2.2.2 Literature reports on the formal synthesis of diptoindonesin D and parviflorol

A variety of resveratrol-based oligomers contain dibenzocycloheptene core; therefore Snyder's research group was interested in synthesizing them.¹⁰ In their strategy, a well-explored stilbene containing benzophenone derivative **1** was employed, and under electrophilic activation using bromine, the cycloheptanone derivative **3** was obtained via the cationic *para*-quinone methide intermediate **2** (Scheme 1). Later a mixture of AgOAc and AcOH was employed to get the targeted natural product **5**; it was proposed by the authors that the reaction



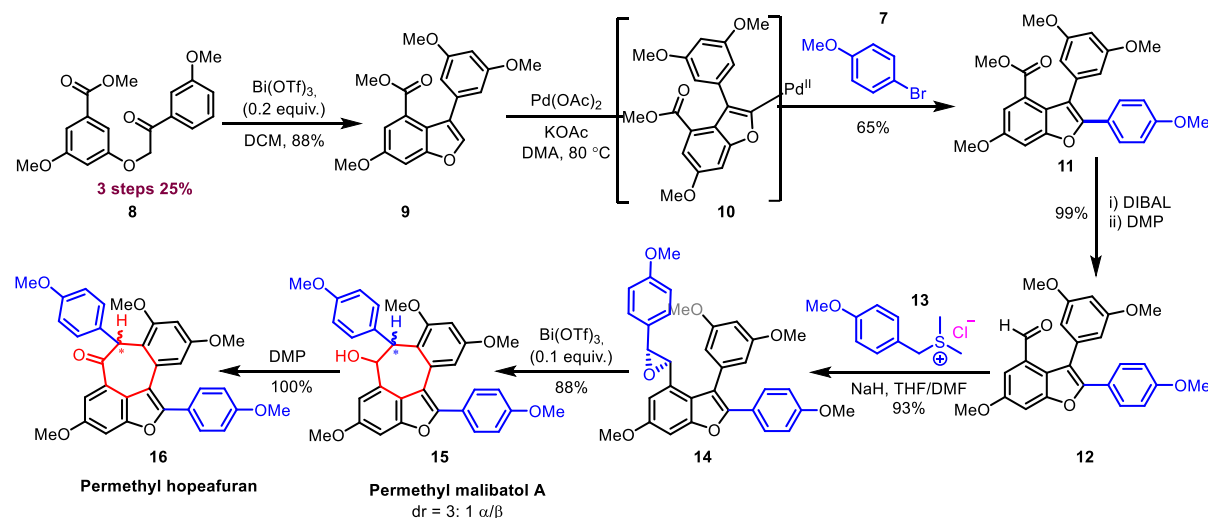
Scheme 1. Preliminary efforts towards dibenzocycloheptanones by Snyder and co-workers

underwent a rare aryl migration (via a dearomatized phenonium **4**). Then demethylation of **5**

was done in the presence of a mild base K_2CO_3 to achieve the parviflorol **6**, which upon oxidation produced diptoindonesin D **7** in an overall yield of 15% (Scheme 1).

2.2.3 Literature reports on total and formal syntheses of malibatol A and shoreaphenol/hopeafuran

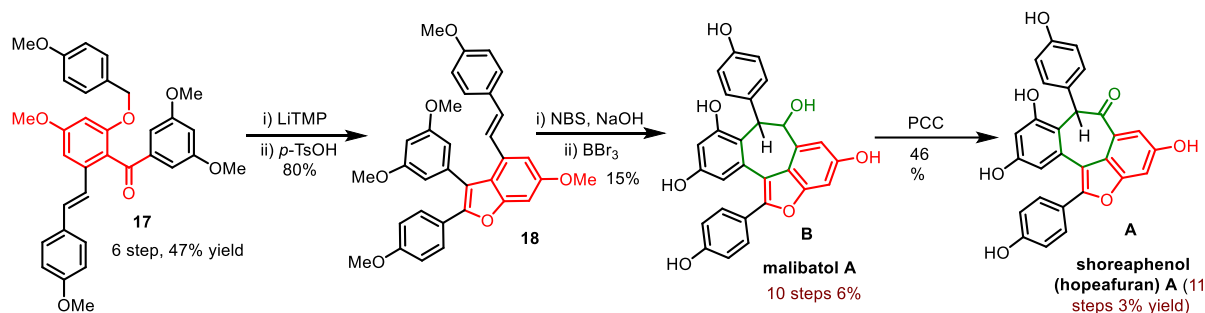
In 2009, Kim and co-workers successfully developed the synthesis of permethyl hopeafuran and permethyl Malibatol A. They approached the synthesis of benzofuran **9** through a well-established $Bi(OTf)_3$ promoted cyclodehydration of α -aryloxyketone **8** (Scheme 2).¹¹ Then, Pd-mediated Heck cross-coupling was accomplished to get the arylation at C-2 of the benzofuran moiety (**11**). Aldehyde **12** was then produced by the reduction of ester **11**, and this compound served as the base for the formation of each of the three natural product analogues including Shoreaphenol/hopeafuran, Malibatol A & B (**A** & **E** in Figure 1). Epoxidation of **12** *via* a Johnson–Corey–Chaykovsky method using sulfur ylide **13**, afforded racemic **14**. Upon exposure of **14** under acidic conditions at cryogenic temperatures produced malibatol A analog **15** and its epimer in a diastereomeric ratio of 3:1. Shoreaphenol/hopeafuran analogue **16** was synthesized *via* subsequent oxidation in an overall yield of 11.6%.



Scheme 2. Kim's approach for the synthesis of Malibatol A and Shoreaphenol/hopeafuran

Later, in 2010, Chen and co-workers developed a strategy for the synthesis of malibatol A (**B**) and shoreaphenol/hopeafuran (**A**), both are benzofuran-containing resveratrol dimers (Figure 1). Conceptually, Chen's method is similar to Kim's approach to these natural products (Scheme 2).¹² Chen's method involved benzofuran synthesis followed by the construction of a 7-membered ring that was facilitated by an electrophilic intermediate. Here, in this case, benzofuran **18** synthesis was attained by deprotonation of the benzyloxy ether **17**

by lithium tetramethylpiperidide (LiTMP) and attack of the resultant alkyl lithium onto the ketone, followed by acid-promoted dehydration. Malibatol A (**B**), which was produced in 6% overall yield by epoxidation and a one-pot cyclization/demethylation method. Later, Shoreaphenol (hopeafuran)[**A**] was produced by further oxidation of **A** with a 3% overall yield.



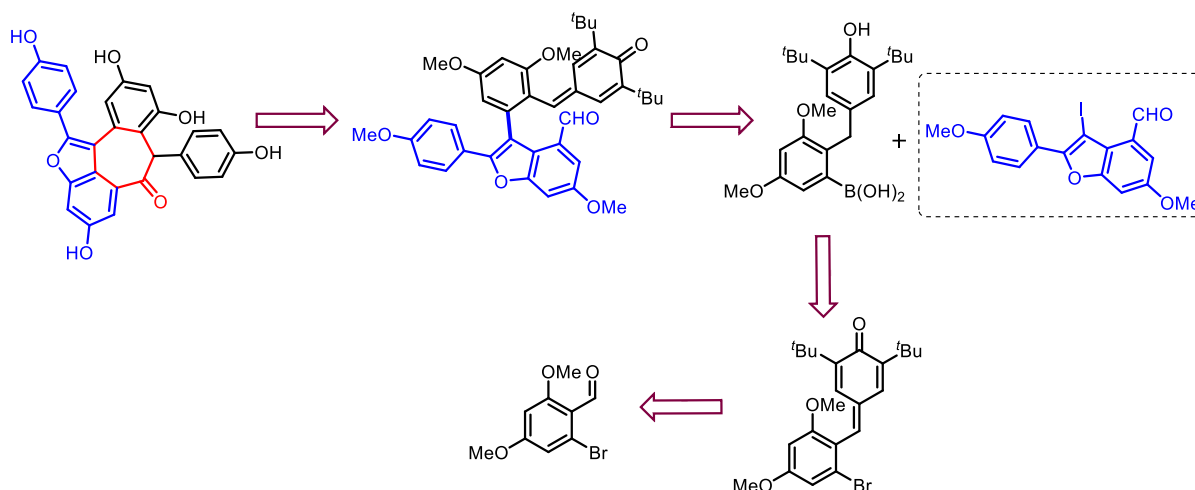
Scheme 3. Chen's Synthesis of Malibatol A and Shoreaphenol

2.2.4 Background

During the course of 9-phenanthrol synthesis using BACs catalyzed intramolecular 1,6 conjugate addition/cyclization sequence from structurally modified *p*-quinone methides (Chapter 2, Part A), we assume that this methodology could be utilized to construct fused cycloheptenone moiety and eventually, to the synthesis of some of the resveratrol based natural products.

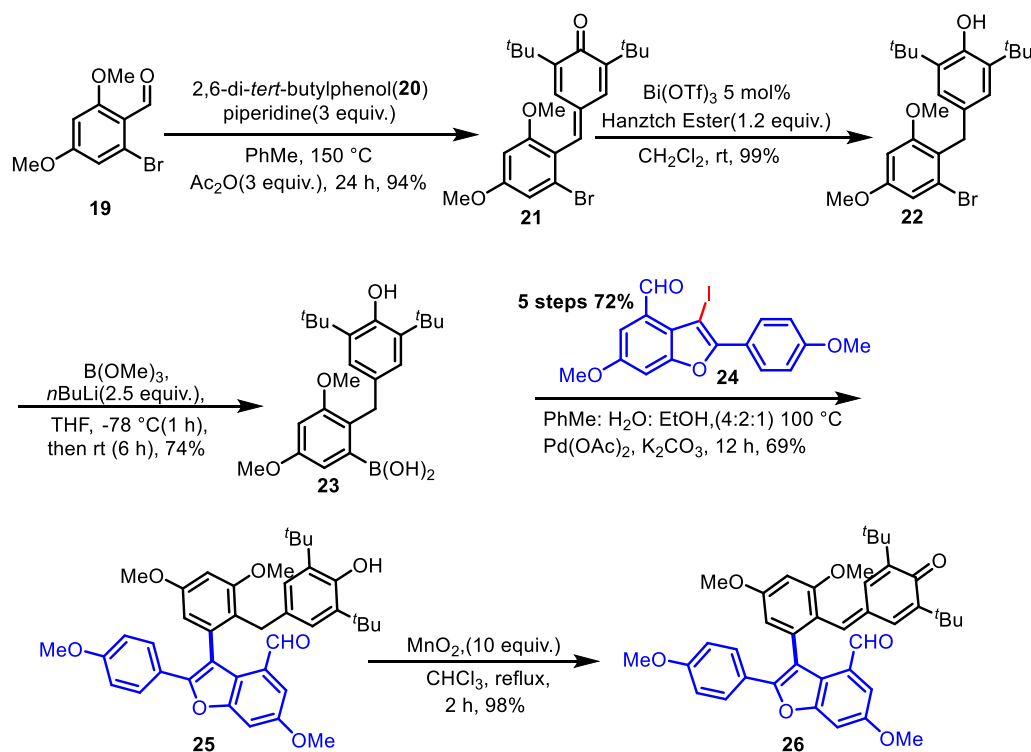
2.2.5 Our approach

A general retrosynthetic analysis of malibatol A/shoreaphenol is presented in Scheme 4. It is evident that these natural products and their related analogue could be synthesized from the respective and easily available derivatives of 2-bromobenzaldehydes. Thus, we began the synthesis by employing 2-bromo-4,6-dimethoxybenzaldehyde **19** (Scheme 5). The aldehyde **19** was treated with 2,6-di-*tert*-butylphenol **20** in the presence of piperidine and acetic anhydride to produce 2-phenyl aryl-substituted *p*-QM **21** in 94% isolated yield. Subsequently, Bi(OTf)₃



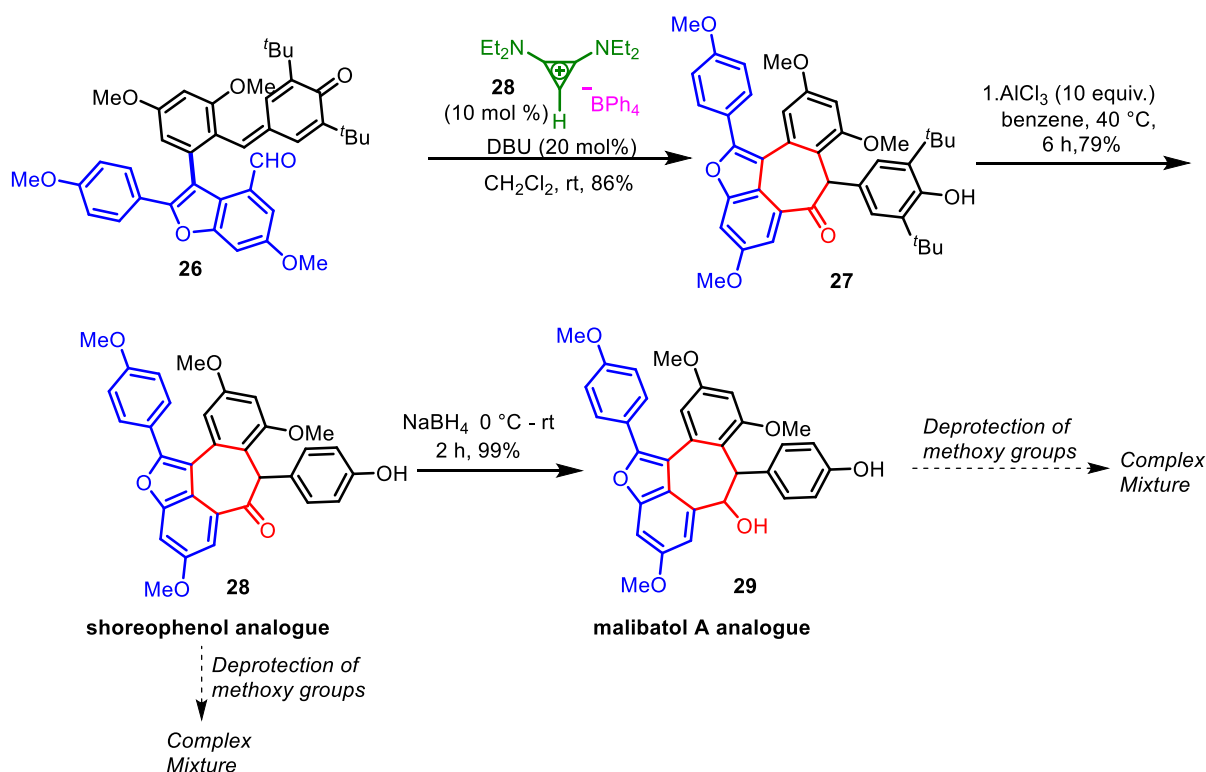
Scheme 4. Retrosynthetic analysis of malibatol A and shoreaphenol

catalyzed reduction of *para*-quinone methide **21** using Hantzsch ester as a reducing source¹³ gave the corresponding diarylmethane **22** with almost a quantitative yield of 99%. The compound **22** was then treated with *n*-BuLi and B(OMe)₃¹⁴ followed by hydrolysis to get the corresponding boronic acid derivative **23** in 74% yield. Then, the Suzuki cross-coupling reaction between 3-iodobenzofuran carboxaldehyde **24**¹⁵ and **23**, under the reaction conditions described before,¹⁶ proceeded well and furnished **25** in 69% yield. MnO₂ mediated oxidation of **25** in CHCl₃ under reflux condition led to the intermediate **26** in 98% yield (Scheme 5).



Scheme 5. Synthesis of intermediate **26**

The intermediate **26** was then subjected to a BAC-catalyzed intramolecular 1,6-conjugate addition/cyclization sequence to produce the desired product **27** in 86% yield (Scheme 6). Subsequently, the de-*tert*-butylation¹⁷ of **27** was achieved using an excess of AlCl₃ (10 equiv.) to get the tetramethylated shoreaphenol derivative **28** in 79% yield. The reduction of **28** with NaBH₄ provided the tetramethylated malibatol A derivative **29** in 99% yield (Scheme 6). However, unfortunately, the deprotection of either **28** or **29** with an excess of BBr₃ ended in the formation of complex mixtures. Further investigation is under progress using other deprotection methods.



Scheme 6. Synthesis of tetramethylated malibatol A and shoreaphenol **28** and **29**

2.2.6 Conclusion

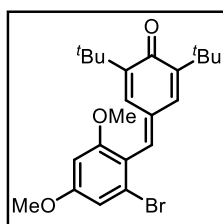
In summary, we have effectively employed our previously developed organocatalytic method (Chapter 2, Part A) to synthesize tetramethylated malibatol A and shoreaphenol derivatives. However, unfortunately, our efforts in the deprotection of methoxy groups in both the tetramethylated shoreaphenol and tetramethylated malibatol A were unsuccessful. Further investigation for the deprotection of methoxy groups with other deprotecting agents is currently in progress.

2.2.7 Experimental section:

General Information. All reactions were carried out under an argon atmosphere employing flame-dried glassware. Most of the reagents and starting materials were purchased from commercial sources and used as such. Intermediate 24 was prepared by following the literature¹⁵ Melting points were recorded on the SMP20 melting point apparatus and were uncorrected. ¹H, ¹³C, and ¹⁹F spectra were recorded in CDCl₃, and DMSO-*d*₆ (400, 100, and 376 MHz, respectively) on Bruker FT-NMR spectrometer. Chemical shift (δ) values are reported in parts per million (ppm) relative to TMS, and the coupling constants (*J*) are reported in Hz. High-resolution mass spectra were recorded on Waters Q-TOF Premier-HAB213 spectrometer. FT-IR spectra were recorded on a Perkin–Elmer FT-IR spectrometer. Thin layer chromatography was performed on Merck silica gel 60 F₂₅₄ TLC plates. Column chromatography was carried out through a silica gel (100-200 mesh) column using a mixture of EtOAc/hexane as eluent.

Synthesis procedure and characterization 21 to 31

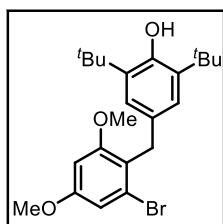
4-(2-bromo-4,6-dimethoxybenzylidene)-2,6-di-*tert*-butylcyclohexa-2,5-dien-1-one (21)¹⁷



In a Dean-Stark apparatus, a mixture of 2-bromo-4,6-dimethoxybenzaldehyde **19** (4.1 mmol, 1 equiv.) and 2,6-di-*tert*-butylphenol **20** (4.5 mmol, 1.1 equiv.) in toluene (30 mL) was heated at 100 °C for 30 min. Piperidine (12.34 mmol, 3 equiv.) was then added to this reaction mixture at 100 °C in a drop-wise manner, and the resultant mixture was stirred at 150 °C for 24 h. The reaction mixture was then cooled to 100 °C, acetic anhydride (3 equiv.) was added, and the resulting solution was stirred for an additional 1 h at the same temperature. The reaction mixture was then cooled to room temperature, poured into ice-cold water (50 mL), and extracted with dichloromethane (50 mL \times 3). The combined organic layer was dried over anhydrous sodium sulfate, filtered, and concentrated under reduced pressure. The residue was purified by neutral alumina column chromatography using a mixture of ethyl acetate/hexane (2/98) to obtain pure 2-bromo 4,6-dimethoxy phenyl *p*-quinone methides **21** *R*_f = 0.4 (10% EtOAc in hexane); yellow solid (1.66 mg, 94% yield); m.p = 94–96 °C; ¹H NMR (400 MHz, CDCl₃) δ 7.04 (d, *J* = 2.4 Hz, 1H), 6.92 (d, *J* = 2.3 Hz, 1H), 6.88 (s, 1H), 6.83 (d, *J* = 2.2 Hz, 1H), 6.47 (d, *J* = 2.2 Hz, 2H), 3.85, (s, 3H), 3.78, (s, 3H), 1.33 (s, 9H), 1.23 (s, 9H); ¹³C NMR (100 MHz, CDCl₃) δ 187.0, 161.5, 159.0, 147.6, 147.2, 137.3, 134.5, 133.3, 130.0, 125.8, 118.2, 109.6, 98.3, 55.8, 35.3, 35.1, 29.7, 29.6; FT-IR (thin film, neat): 2957, 2867, 1615, 1600,

1456, 1360, 1205, 1155 cm⁻¹; HRMS (ESI): *m/z* calcd for C₂₈H₃₁BrO₃ [M+H]⁺: 433.2273; found: 433.2278

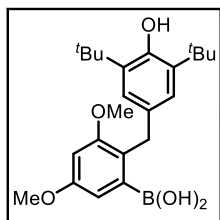
4-(2-bromo-4,6-dimethoxybenzyl)-2,6-di-tert-butylphenol (**22**)



p-Quinone methide (2.3 mmol) was dissolved in a mixture of Bi(OTf)₃ (0.05 mmol) and Hantzsch ester (3.45 mmol) in 15 mL of CH₂Cl₂, and the resulting mixture was stirred at room temperature (27–30 °C) until the *p*-quinone methide was completely consumed (by TLC). The solvent was removed under reduced pressure and the crude reaction mixture was

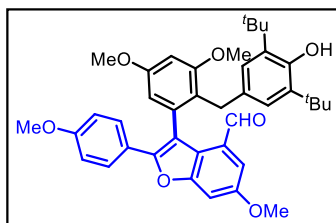
directly loaded on a silica gel column and purified using a hexane/EtOAc mixture as an eluent to obtain pure diarylmethane, *R*_f = 0.3 (5% EtOAc in hexane); colourless gummy solid (991 mg, 99% yield); m. p. = 151–153 °C; ¹H NMR (400 MHz, CDCl₃) δ 7.02 (d, *J* = 2.5 Hz, 1H), 6.99 (s, 2H), 6.73 (d, *J* = 2.5 Hz, 1H), 5.03 (s, 1H), 4.30 (s, 2H), 3.86 (s, 3H), 3.85 (s, 3H), 1.38 (s, 18H); ¹³C{¹H} NMR (100 MHz, CDCl₃) δ 159.2, 159.1, 152.0, 135.8, 135.3, 131.6, 126.7, 124.9, 105.0, 102.6, 56.0, 55.6, 34.4, 30.5, 28.6; IR (neat): 3636, 2958, 1583, 1488, 1455, 1275, 1153, 630 cm⁻¹; HRMS (ESI): *m/z* calcd for C₂₈H₃₁BrO₃ [M+H]⁺: 435.1519; found: 435.1521.

2-(3,5-di-tert-butyl-4-hydroxybenzyl)-3,5-dimethoxyphenylboronic acid (**23**)



A 50 mL round-bottomed flask equipped with a temperature probe, a magnetic stirrer, and a septum was THF (10 mL) and put under a nitrogen atmosphere. The flask was charged with **22** (1.14 mmol). The solution was cooled to -78 °C then *n*-Butyllithium (2.5 M in hexanes, 1.38 mL, 3.45 mmol) was added dropwise via a syringe pump for over 15 min. After the mixture was stirred for an additional 1 h, trimethyl borate (382 μL, 3.45 mmol) was added dropwise, later the reaction mixture was allowed to warm to -20 °C and was further stirred for 5 h, and then 2 N HCl solution (10 mL) was added. When the mixture reached room temperature, it was transferred to a 100 mL separatory funnel and the organic layer was separated layers were separated. Now the aqueous layer is extracted with ethyl acetate (20 ml x2). The combined organic layer was dried over anhydrous sodium sulphate, filtered, and concentrated under reduced pressure. The residue was purified by recrystallization/precipitated in chloroform, a pale-yellow solid residue (371 mg) which was directly utilized in the next step.

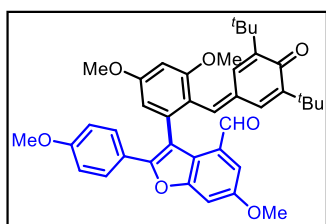
3-(2-(3,5-di-tert-butyl-4-hydroxybenzyl)-3,5-dimethoxyphenyl)-6-methoxy-2-(4-methoxyphenyl)benzofuran-4-carbaldehyde (**25**)



Nitrogen gas was purged through a mixture of aqueous solution of potassium carbonate and toluene (6 mL) for 15 min and then, boronic acid (**23**) [294 mg, 0.73 mmol], Pd(PPh₃)₄ [56.6 mg, 0.049 mmol] and 3-iodo-6-methoxy-2-(4-methoxyphenyl)benzofuran-4-carbaldehyde¹³ (**24**) [200 mg, 0.490 mmol] were added to this

mixture successively. The reaction mixture was refluxed at 100 °C for overnight. After completion of the reaction (monitored by TLC), the reaction mixture was diluted with ethyl acetate (30 mL) and water (10 mL). The organic layer was separated, and the aqueous layer was extracted with ethyl acetate (30 mL × 2). The combined organic layer was dried over anhydrous sodium sulphate, filtered, and concentrated under reduced pressure. The residue was purified through silica gel column chromatography using hexane/EtOAc to obtain pure compound **25** as white solid (138 mg, 69% yield); *R_f* = 0.2 (5% EtOAc in hexane); m. p. = 152-154 °C; ¹H NMR (400 MHz, CDCl₃) δ 9.19 (s, 1H), 7.36 (d, *J* = 9.00 Hz, 2H), 7.31 (d, *J* = 2.32 Hz, 1H), 7.26 (d, *J* = 2.36 Hz, 1H), 6.76 (d, *J* = 9.00 Hz, 1H), 6.66 (d, *J* = 2.28 Hz, 1H), 6.57 (s, 2H), 6.41 (d, *J* = 2.44 Hz, 1H), 4.76 (s, 1H), 3.99 (s, 3H), 3.88 (s, 3H), 3.77 (s, 3H), 3.37 (s, 3H), 1.17 (s, 18H) ¹³C{¹H} NMR (100 MHz, CDCl₃) δ 189.1, 159.9, 159.8, 159.2, 157.3, 155.3, 151.8, 151.5, 135.8, 135.2, 131.2, 129.4, 127.6, 126.9, 125.0, 123.5, 122.9, 114.1, 113.9, 106.9, 105.7, 103.1, 99.4, 56.1, 55.7, 55.5, 55.3, 33.9, 34.0, 30.0; IR (neat): 2924, 1735, 1512, 1273, 1254, 1038, 832 cm⁻¹; HRMS (ESI): *m/z* calcd for C₂₃H₁₉O₄ [M+H]⁺: 637.3160; found : 637.3163.

3-(2-((3,5-di-tert-butyl-4-oxocyclohexa-2,5-dien-1-ylidene)methyl)-3,5-dimethoxyphenyl)-6-methoxy-2-(4-methoxyphenyl)benzofuran-4-carbaldehyde **26**

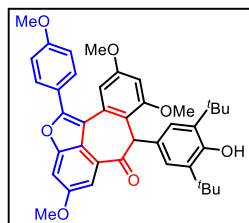


A suspension of benzofuran derivative **25** (2.5 mmol) and MnO₂ (3 mmol) in ethanol-free chloroform (15 ml, filtered through activated basic alumina) was refluxed for 3 hr under nitrogen. The reaction mixture was filtered off and washed with chloroform, and the

solvent was evaporated in vacuo from the combined filtrates to give a yellow-coloured residue which was purified through silica gel column chromatography using hexane/EtOAc to obtain pure compound **26** as a white solid (138 mg, 69% yield); *R_f* = 0.2 (5% EtOAc in hexane); m. p. = 152-154 °C; ¹H NMR (400 MHz, CDCl₃) δ 9.82 (s, 1H), 7.44 (d, *J* = 2.3 Hz, 1H), 7.39 (d, *J* = 8.96 Hz, 1H), 7.33 (d, *J* = 2.3 Hz, 1H), 6.76-6.77 (m, 3H), 6.67 (d, *J* = 2.3 Hz, 1H), 6.65 (d, *J* = 2.3 Hz, 1H), 6.57 (d, *J* = 1.8 Hz, 1H), 6.49 (s, 1H), 3.90 (s, 3H), 3.84 (s, 3H), 3.83 (s, 3H), 3.76 (s, 3H), 1.77 (s, 9H), 1.16 (s, 9H) ¹³C{¹H} NMR (100 MHz, CDCl₃) δ 189.2, 186.8, 162.2, 160.1, 158.7, 157.7, 155.7, 153.1, 147.1, 146.5, 136.9, 134.5, 133.3, 129.7, 129.5, 127.9,

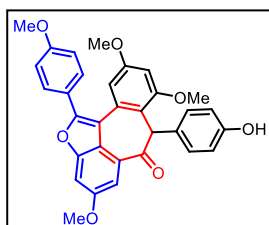
125.6, 122.6, 117.9, 114.2, 112.9, 108.2, 107.0, 103.5, 99.3, 56.3, 55.7, 55.3, 35.1, 34.9, 31.7, 29.6, 22.8, 14.3 ; IR (neat): 2924, 1740, 1681, 1519, 1273, 1254, 1038, 832 cm^{-1} ; HRMS (ESI): m/z calcd for $\text{C}_{23}\text{H}_{19}\text{O}_4$ $[\text{M}+\text{H}]^+$: 637.3160; found : 637.3163.

11-(3,5-di-tert-butyl-4-hydroxyphenyl)-1,3,8-trimethoxy-5-(4-methoxyphenyl)benzo[6,7]cyclohepta[1,2,3-cd]benzofuran-10(11H)-one (27)



An oven-dried Schlenk tube with a magnet stir bar was applied full Schlenk conditions and charged with BACs precursor **28** (0.02 mmol) and benzofuran-substituted *p*-quinone methides **26** (*p*-QMs) [0.1mmol]. The tube underwent deaeration cycles three times. followed by the addition of DBU (0.02 mmol) and CH_2Cl_2 (1 ml) under argon. The mixture was sealed and stirred at room temperature. The reaction was monitored by TLC, and the reaction mixture was concentrated under reduced pressure and directly loaded onto a silica-gel column and was purified using EtOAc in hexane as an eluent to provide pure cyclic compound **27** pale yellow solid (54.6 mg, 86% yield); R_f = 0.2 (10% EtOAc in hexane); m. p. = 252-254 $^\circ\text{C}$; ^1H NMR (400 MHz, CDCl_3) δ 7.68 (d, J = 8.9 Hz, 2H), 7.44 (d, J = 2.2 Hz, 1H), 7.08 (d, J = 2.2 Hz, 1H), 6.93 (d, J = 8.8 Hz, 1H), 6.78 (d, J = 2.4 Hz, 1H), 6.68 (d, J = 6.8 Hz, 1H), 6.76-6.77 (m, 3H), 6.67 (d, J = 2.3 Hz, 1H), 6.65 (d, J = 2.3 Hz, 1H), 6.57 (d, J = 1.8 Hz, 2H), 6.51 (d, J = 2.4 Hz, 1H), 6.19 (s, 1H), 4.84 (s, 1H), 3.89 (s, 3H), 3.88 (s, 3H), 3.87 (s, 3H), 3.85 (s, 3H), 1.73 (s, 18H); $^{13}\text{C}\{^1\text{H}\}$ NMR (100 MHz, CDCl_3) δ 189.2, 186.8, 162.2, 160.1, 158.7, 157.7, 155.7, 153.1, 147.1, 146.5, 136.9, 134.5, 133.3, 129.7, 129.5, 127.9, 125.6, 122.6, 117.9, 114.2, 112.9, 108.2, 107.0, 103.5, 99.3, 56.3, 55.7, 55.3, 35.1, 34.9, 31.7, 29.6, 22.8, 14.3 ; IR (neat): 2924, 1778, 1505, 1273, 1254, 1038, 832 cm^{-1} ; HRMS (ESI): m/z calcd for $\text{C}_{33}\text{H}_{28}\text{O}_7$ $[\text{M}-\text{H}]^-$: 533.2858, found 533.2858.

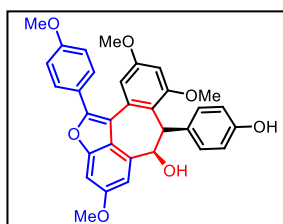
11-(4-hydroxyphenyl)-1,3,8-trimethoxy-5-(4-methoxyphenyl)benzo[6,7]cyclohepta[1,2,3-cd]benzofuran-10(11H)-one (29)



AlCl_3 (66.6 mg, 0.5 mmol) was added to a solution of compound **27** (40 mg, 0.063 mmol) in 3 mL of toluene, and the resultant mixture was stirred at 50 $^\circ\text{C}$ for 6 h. It was then transferred to a separatory funnel containing 1:1 ice/1 N HCl solution and extracted with ethyl acetate (3 \times 10 mL). The combined organic layer was washed with sat. aq. NaHCO_3 and brine solution successively dried over anhydrous Na_2SO_4 and concentrated under a vacuum. The crude material obtained was then purified through column chromatography (40% acetone in hexane) to get pure permethyl Shoreaphenol (**29**) as pale-yellow gummy solid (27.7 mg, 55% yield). R_f = 0.3 (70% EtOAc in hexane); ^1H NMR (400 MHz, $\text{DMSO}-d_6$) δ 9.16

(s, 1H), 7.72 (d, $J = 8.8$, Hz, 2H), 7.39 (d, $J = 2.2$ Hz, 1H), 7.27 (d, $J = 2.2$ Hz, 1H), 7.13 (d, $J = 8.8$ Hz, 2H), 6.68-6.63 (m, 4H), 6.67 (d, $J = 8.6$ Hz, 2H), 5.96 (s, 1H), 3.86 (s, 3H), 3.85 (s, 3H), 3.84 (s, 3H), 3.53 (s, 3H); $^{13}\text{C}\{^1\text{H}\}$ NMR (100 MHz, CDCl_3) δ 195.0, 160.6, 159.2, 158.8, 157.4, 155.6, 153.4, 152.5, 133.3, 130.0, 129.3, 127.9, 127.2, 122.1, 115.2, 115.0, 114.9, 114.7, 110.2, 106.0, 100.9, 98.4, 56.3, 56.0, 55.4, 54.8, 54.5; IR (neat): 2924, 1780, 1682, 1505, 1273, 1254, 1038, 832 cm^{-1} ; HRMS (ESI): m/z calcd for HRMS (ESI): m/z calcd for $\text{C}_{33}\text{H}_{28}\text{O}_7$ $[\text{M}+\text{H}]^+$: 536.1835, found 536.1833.

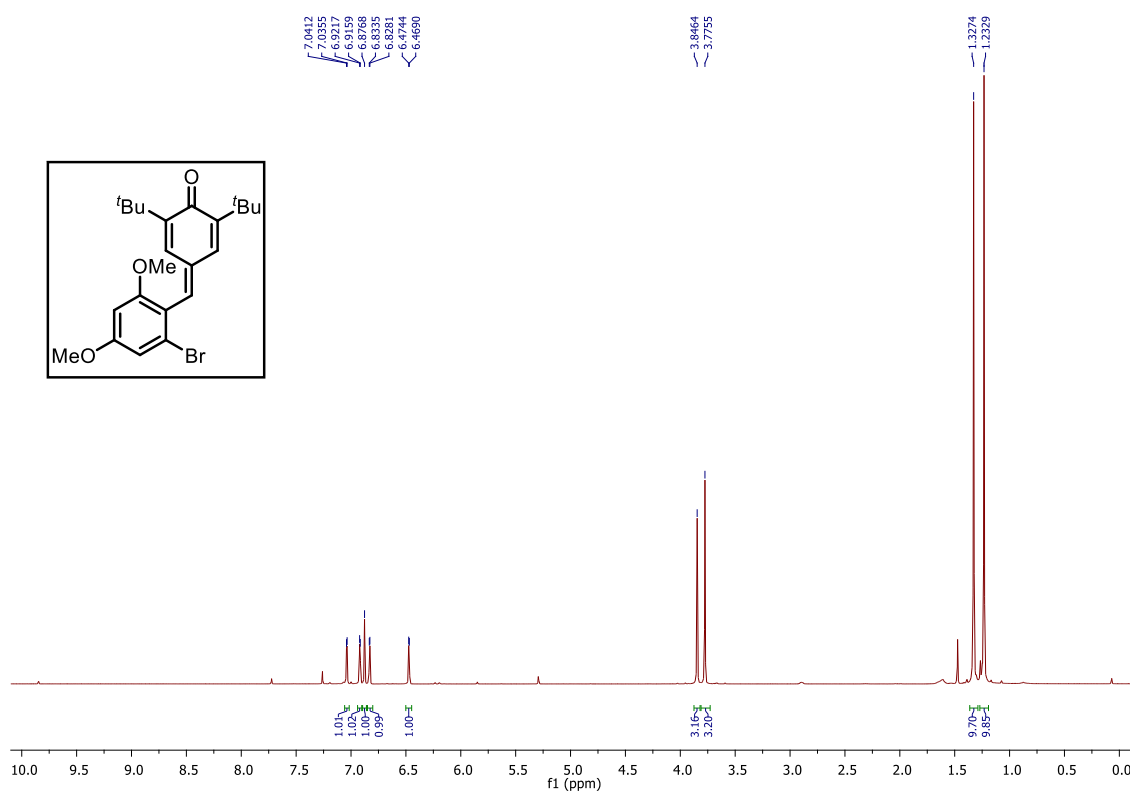
11-(4-hydroxyphenyl)-1,3,8-trimethoxy-5-(4-methoxyphenyl)benzo[6,7]cyclohepta[1,2,3-cd]benzofuran-10(11H)-one (30)



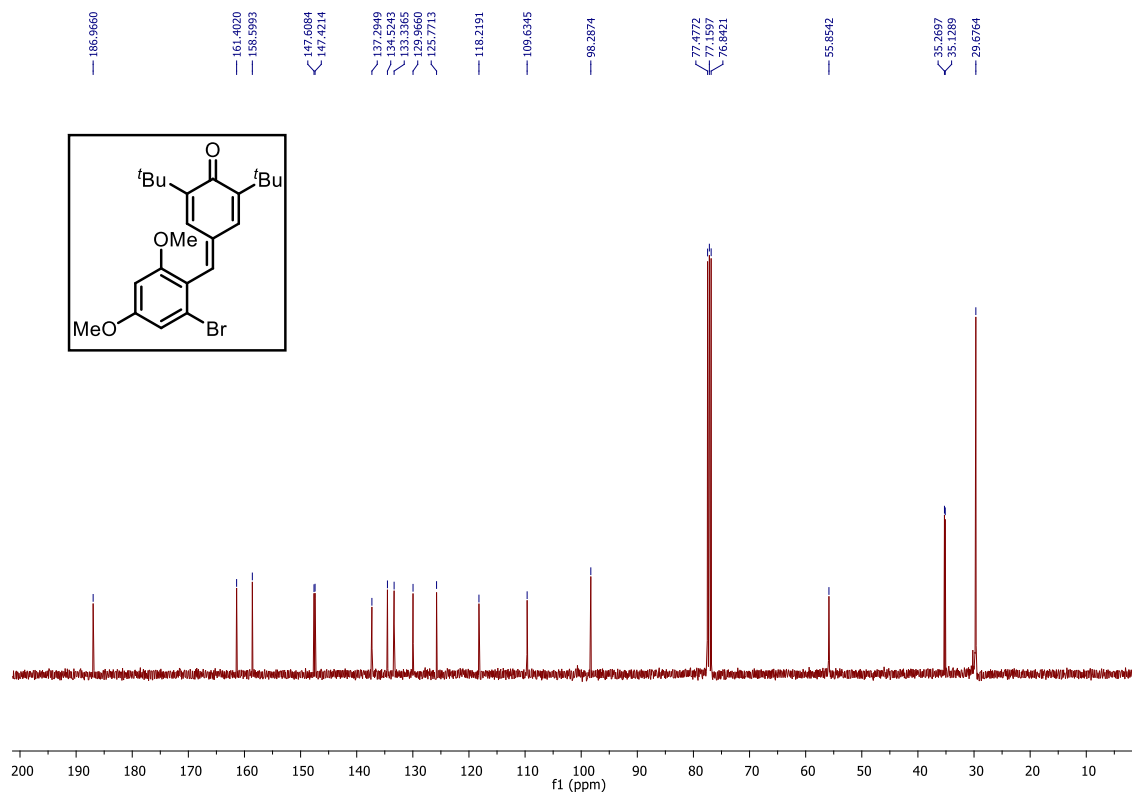
To a solution of **29** (15 mg, 0.028 mmol) in 3 mL of MeOH/THF (1/1) was added NaBH_4 (2.6 mg, 2.5 equiv) at 0 °C. After 30 min, the mixture was quenched with saturated NH_4Cl at 0 °C. After the mixture was concentrated in vacuo, the residue was diluted with ethyl acetate and washed with brine. The organic layer was dried over MgSO_4 ,

filtered, and evaporated in vacuo to give the crude permethyl MalibatolA (**30**) as pale-yellow gummy solid (27.7 mg, 55% yield). $R_f = 0.3$ (70% EtOAc in hexane); ^1H NMR (400 MHz, $\text{DMSO}-d_6$) δ 9.16 (s, 1H), 7.72 (d, $J = 8.8$, Hz, 2H), 7.39 (d, $J = 2.2$ Hz, 1H), 7.27 (d, $J = 2.2$ Hz, 1H), 7.13 (d, $J = 8.8$ Hz, 2H), 6.68-6.63 (m, 4H), 6.67 (d, $J = 8.6$ Hz, 2H), 5.96 (s, 1H), 3.86 (s, 3H), 3.85 (s, 3H), 3.84 (s, 3H), 3.53 (s, 3H); $^{13}\text{C}\{^1\text{H}\}$ NMR (100 MHz, CDCl_3) δ 161.6, 159.2, 158.8, 156.4, 155.7, 153.4, 152.5, 136.3, 133.0, 129.3, 128.9, 127.2, 123.1, 118.2, 115.0, 114.9, 114.7, 111.2, 106.0, 100.9, 98.4, 56.3, 56.0, 55.4, 54.8, 54.5; IR (neat): 3400, 2924, 1682, 1505, 1273, 1254, 1038, 832 cm^{-1} ; HRMS (ESI): m/z calcd for $\text{C}_{33}\text{H}_{30}\text{O}_7$ $[\text{M}+\text{H}]^+$: 538.1992, found 538.1995.

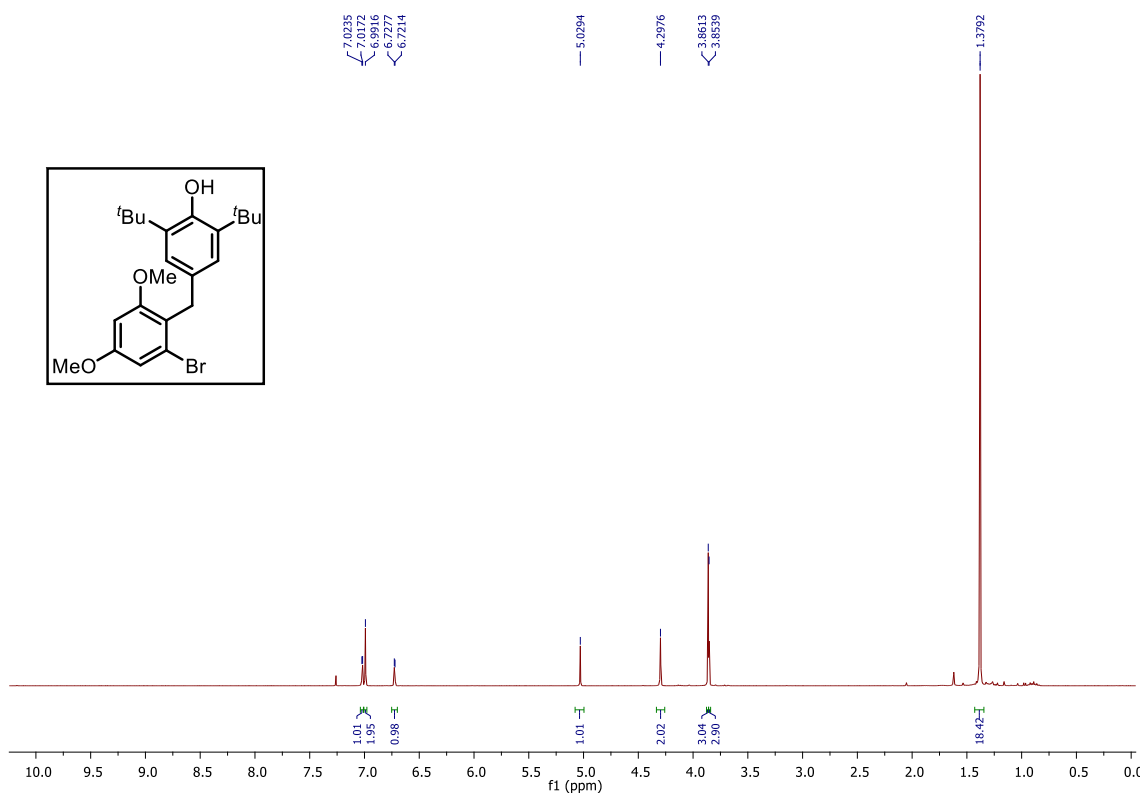
¹H NMR (400 MHz, CDCl₃) spectrum of compound **21**



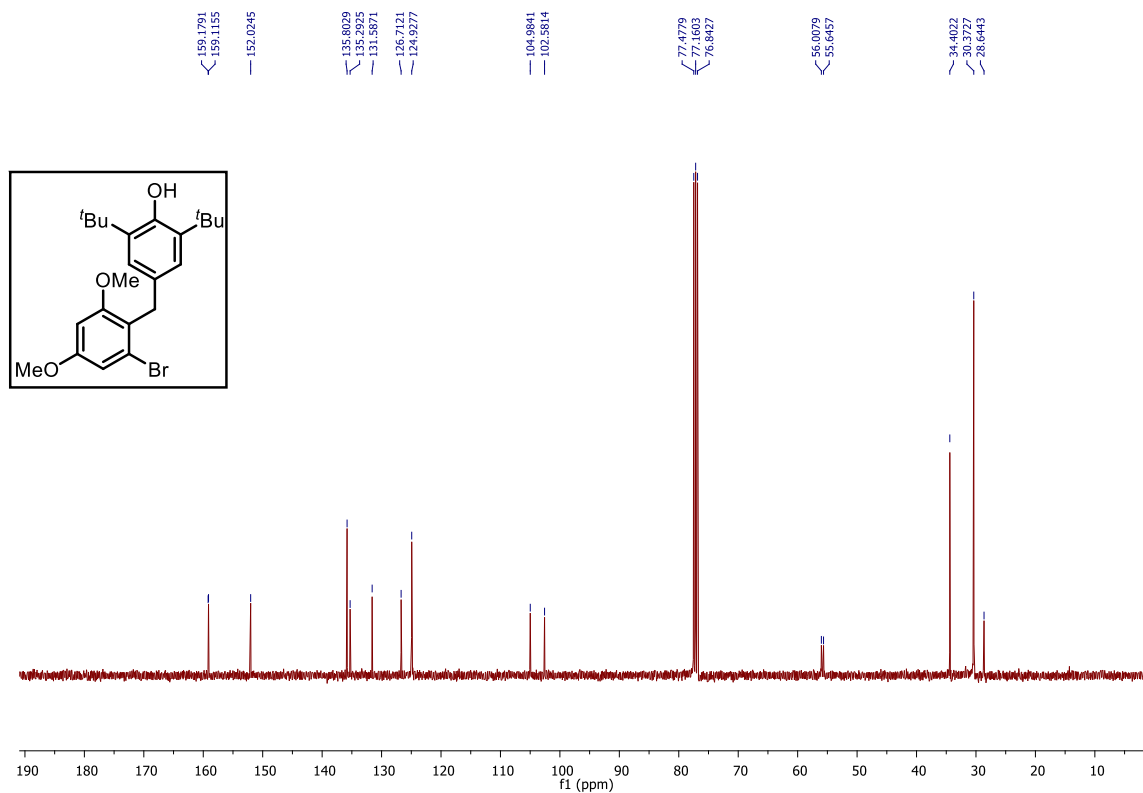
¹³C NMR (100 MHz, CDCl₃) spectrum of compound **21**



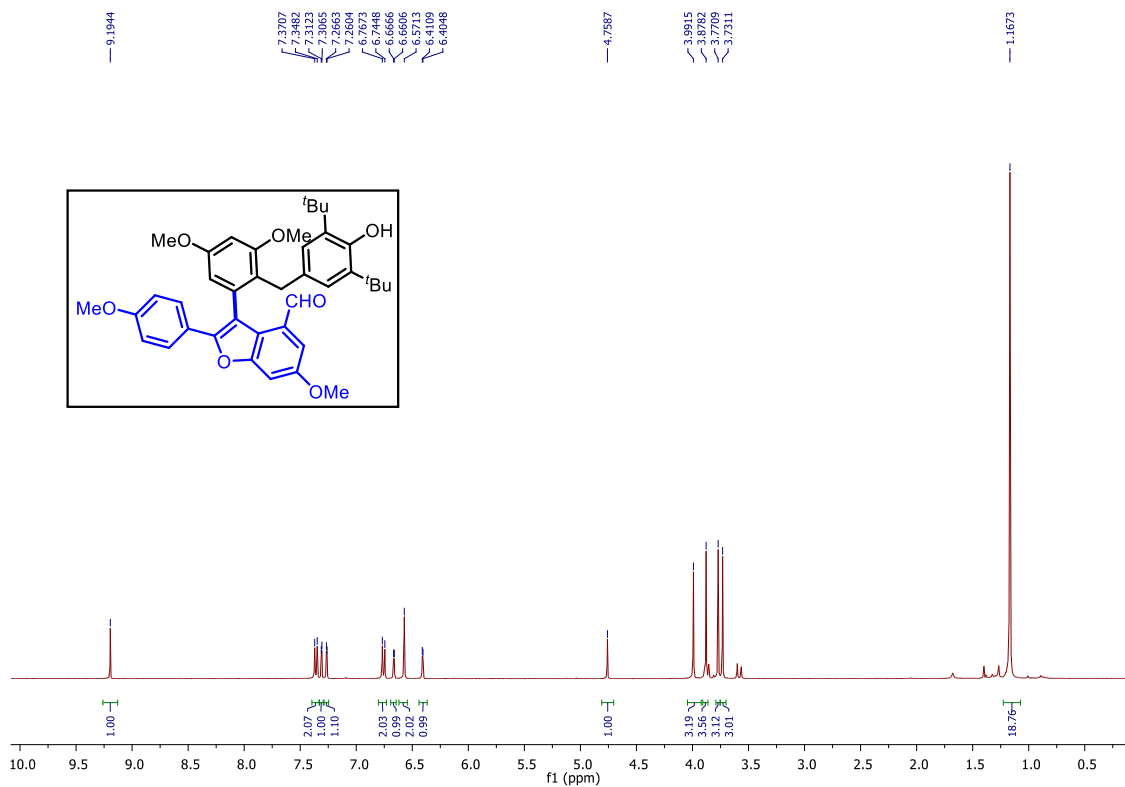
^1H NMR (400 MHz, CDCl_3) spectrum of compound **22**



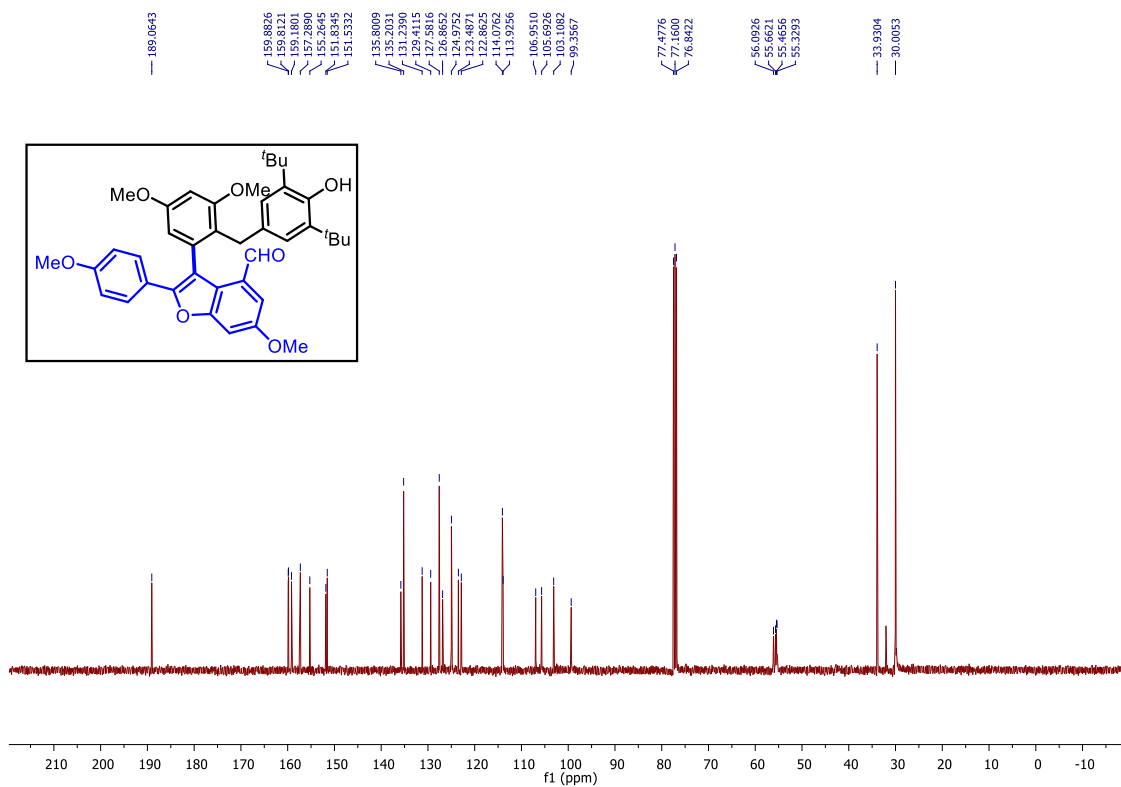
^{13}C NMR (100 MHz, CDCl_3) spectrum of compound **22**



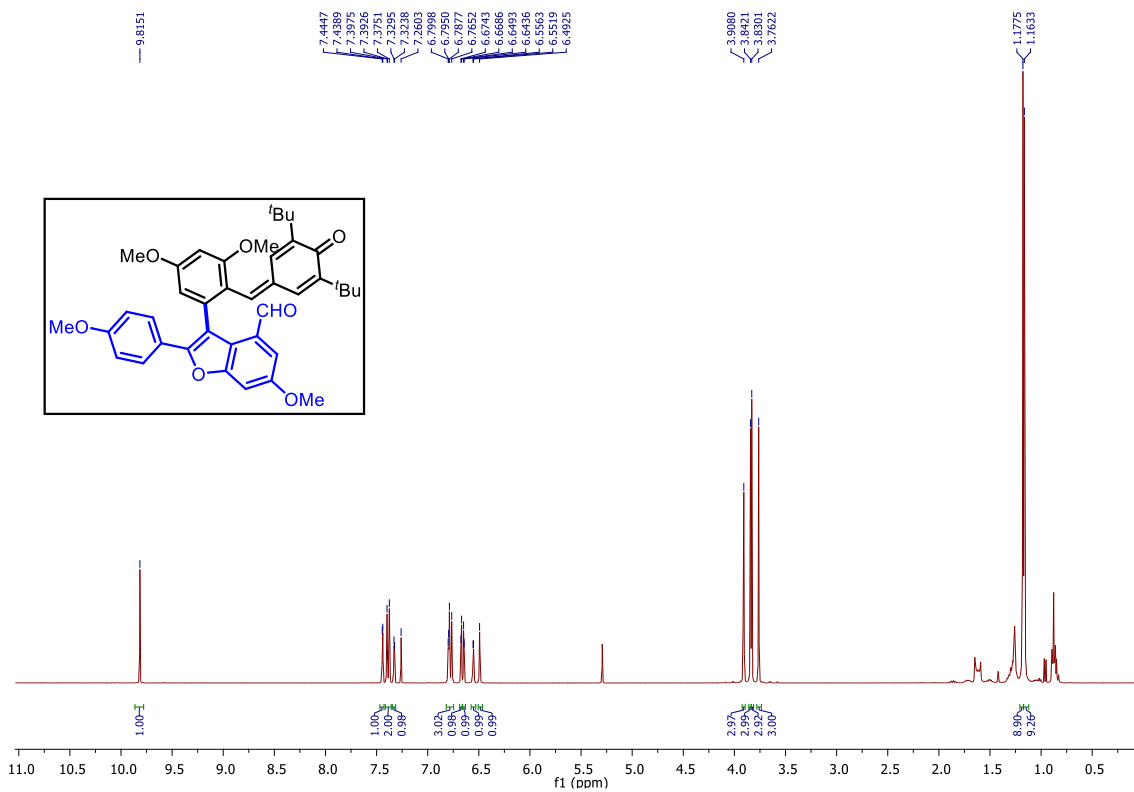
¹H NMR (400 MHz, CDCl₃) spectrum of compound **25**



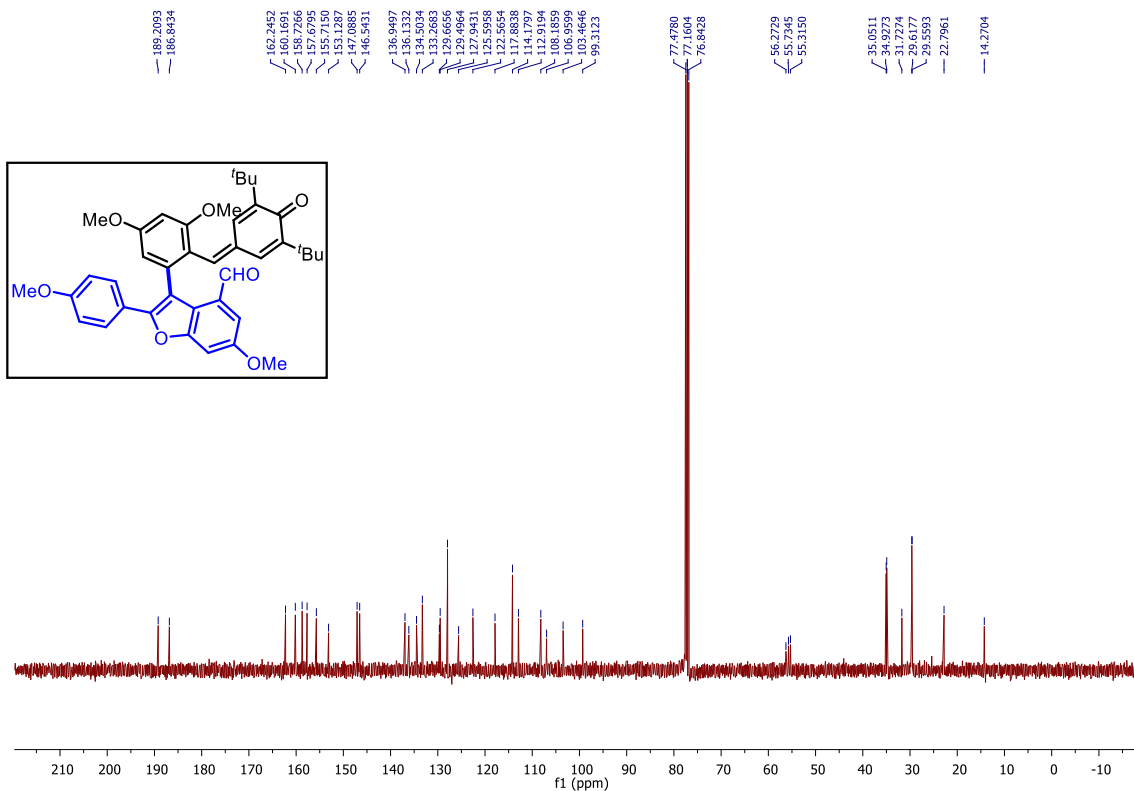
¹³C NMR (100 MHz, CDCl₃) spectrum of compound **25**



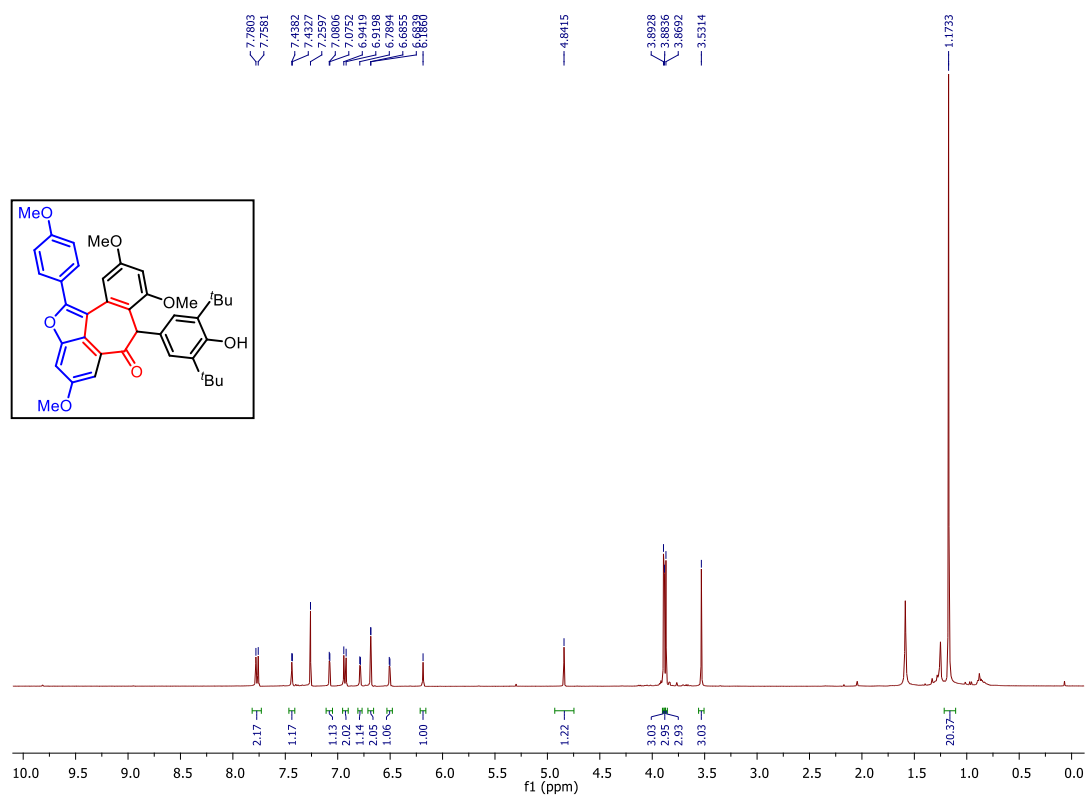
¹H NMR (400 MHz, CDCl₃) spectrum of compound **26**



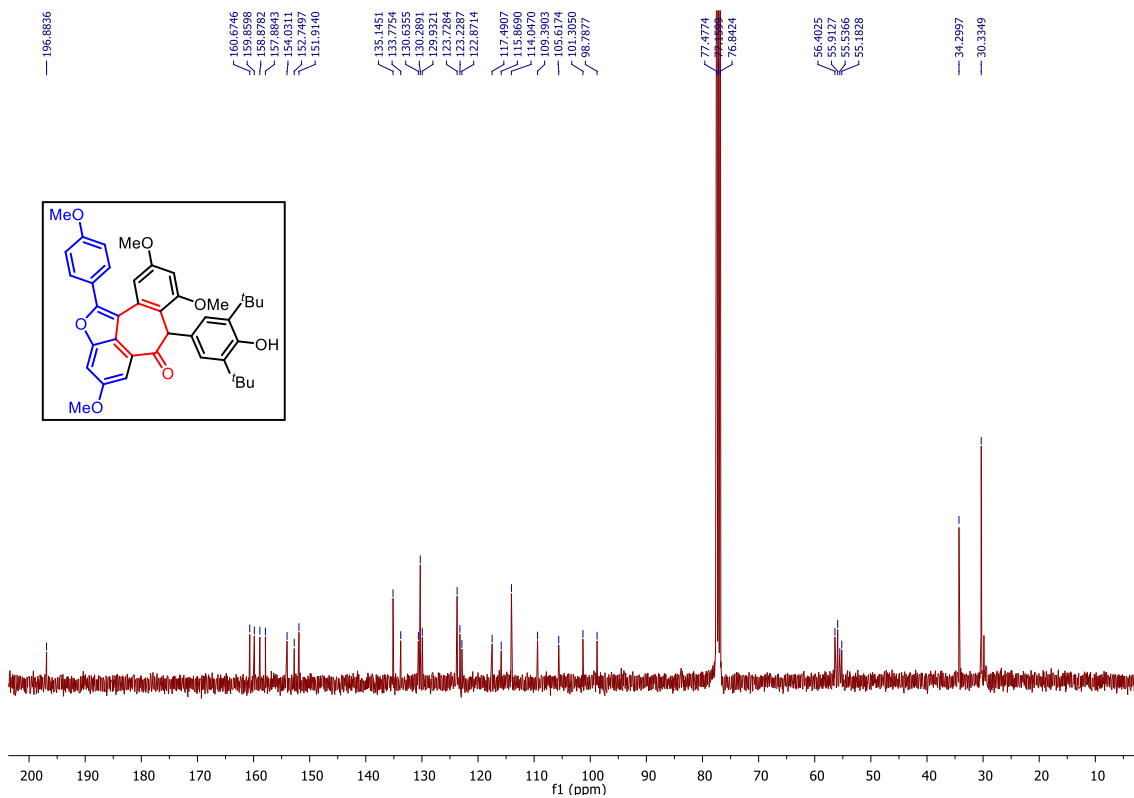
¹³C NMR (100 MHz, CDCl₃) spectrum of compound **26**



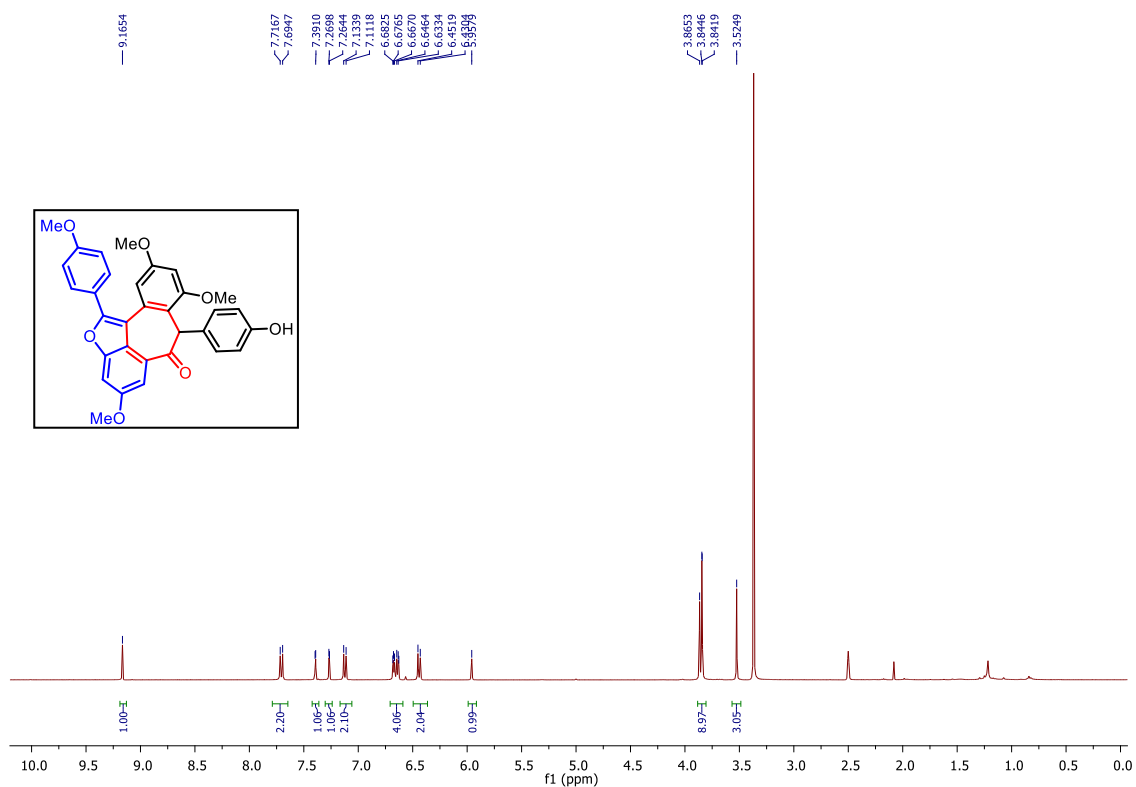
¹H NMR (400 MHz, CDCl₃) spectrum of compound **28**



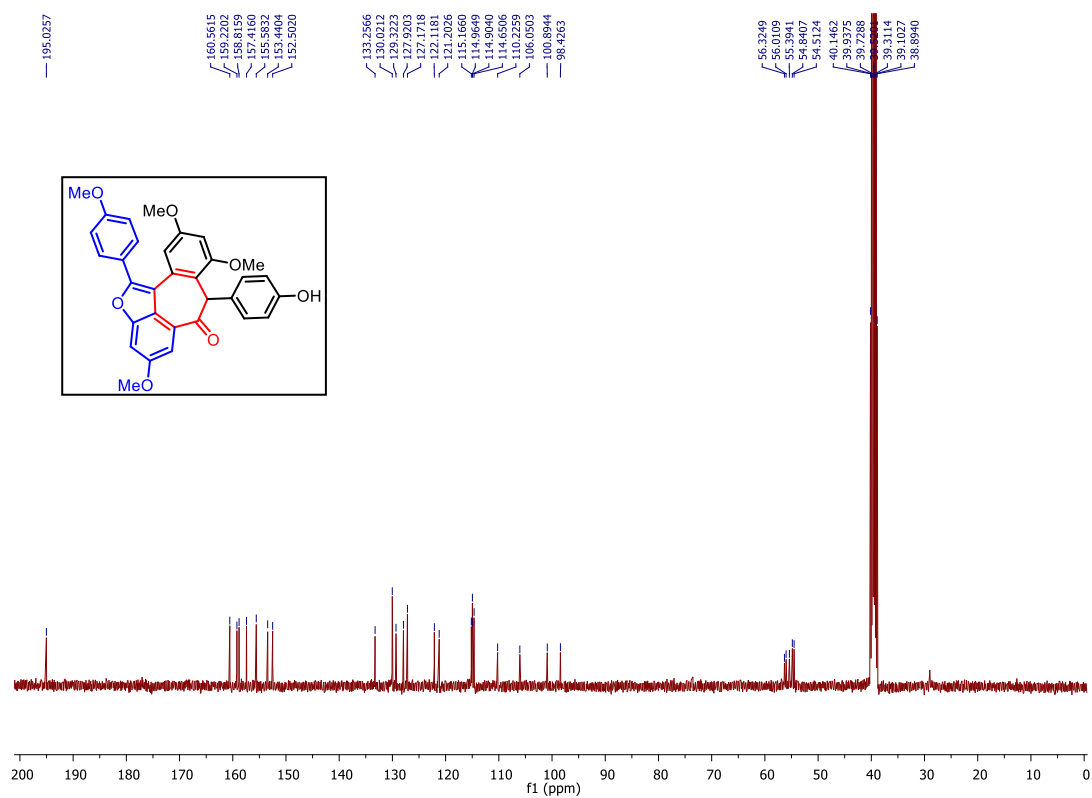
¹³C NMR (100 MHz, CDCl₃) spectrum of compound **28**



¹H NMR (400 MHz, CDCl₃) spectrum of compound **29**



¹³C NMR (100 MHz, CDCl₃) spectrum of compound **29**



2.2.8 References: -

- 1) Frankel, E. N.; German, J. B.; Kinsella, J. E.; Parks, E.; Kanner, J. *Lancet* **1993**, *341*, 454.
- 2) He, S.; Yan, X. *Curr. Med. Chem.* **2013**, *20*, 1005.
- 3) Jang, M.; Cai, L.; Udeani, G. O.; Slowing, K. V.; Thomas, C. F.; Beecher, C.W. W.; Fong, H. H. S.; Farnsworth, N. R.; Kinghorn, A. D.; Mehta, R. G.; Moon, R. C.; Pezzuto, J. M. *Science* **1997**, *275*, 218.
- 4) a) Banks, A. S.; Kon, N.; Knight, C.; Matsumoto, M.; Gutiérrez-Juárez, R.; Rossetti, L.; Gu, W.; Accili, D. *Cell Metab.* **2008**, *8*, 333. b) Milne, J. C.; Lambert, P. D.; Schenk, S.; Carney, D. P.; Smith, J. J.; Gagne, D. J.; Jin, L.; Boss, O.; Perni, R. B.; Vu, C. B.; Bemis, J. E.; Xie, R.; Disch, J. S.; Ng, P. Y.; Nunes, J. J.; Lynch, A. V.; Yang, H.; Galonek, H.; Israelian, K.; Choy, W.; Iffland, A.; Lavu, S.; Medvedik, O.; Sinclair, D. A.; Olefsky, J. M.; Jirousek, M. R.; Elliott, P. J.; Westphal, C. H. *Nature* **2007**, *450*, 712.
- 5) Frankel, E. N.; Waterhouse, A. L.; Kinsella, J. E. *Lancet* **1993**, *341*, 1103.
- 6) Baur, J. A.; Pearson, K. J.; Price, N. L.; Jamieson, H. A.; Lerin, C.; Kalra, A.; Prabhu, V. V.; Allard, J. S.; Lopez-Lluch, G.; Lewis, K.; Pistell, P. J.; Poosala, S.; Becker, K. G.; Boss, O.; Gwinn, D.; Wang, M.; Ramaswamy, S.; Fishbein, K. W.; Spencer, R. G.; Lakatta, E. G.; Le Couteur, D.; Shaw, R. J.; Navas, P.; Puigserver, P.; Ingram, D. K.; de Cabo, R.; Sinclair, D. A. *Nature* **2006**, *444*, 337.
- 7) Coggon, P.; King, T. J.; Wallwork, S. C. *Chem. Commun.* **1966**, 439. b) Coggon, P.; McPhail, A. T.; Wallwork, S. C. *J. Chem. Soc. B* **1970**, 884. c) Coggon, P.; Janes, N. F.; King, F. E.; King, T. J.; Molyneux, R. J.; Morgan, J. W. W.; Sellars, K. *J. Chem. Soc.* **1965**, 406.
- 8) Vogt, T. *Mol. Plant* **2010**, *3*, 2.
- 9) Dai, J.-R.; Hallock, Y. F.; Cardellina, J. H.; Boyd, M. R. *J. Nat. Prod.* **1998**, *61*, 351.
- 10) Snyder, S. A.; Zografos, A. L.; Lin, Y. *Angew. Chem., Int. Ed.* **2007**, *46*, 8186.
- 11) Kim, I.; Choi, J. *Org. Biomol. Chem.* **2009**, *7*, 2788.
- 12) Chen, D. Y.-K.; Kang, Q.; Wu, T. R. *Molecules* **2010**, *15*, 5909.
- 13) Mahesh, S.; Anand, R. V. *Org. Biomol. Chem.* **2017**, *15*, 8393.
- 14) Li, W.; Nelson, D. P.; Jensen, M. S.; Hoerrner, R. S.; Cai, D.; Larsen, R. D.; Reide, P. J. *J. Org. Chem.* **2002**, *67*, 5394.
- 15) Jung, Y.; Singh, D. K.; Kim, I. *Beilstein J. Org. Chem.* **2016**, *12*, 2689.
- 16) Jung, Y.; Kim, I. *Asian J. Org. Chem.* **2016**, *5*, 147.

- 17) a) Ramanjaneyulu, B. T.; Mahesh, S.; Anand, R. V. *Org. Lett.* **2015**, *17*, 3952. b) Reddy, V.; Anand, R. V. *Org. Lett.* **2015**, *17*, 3390. c) Arde, P; Anand, R. V. *Org. Biomol. Chem.* **2016**, *14*, 5550.

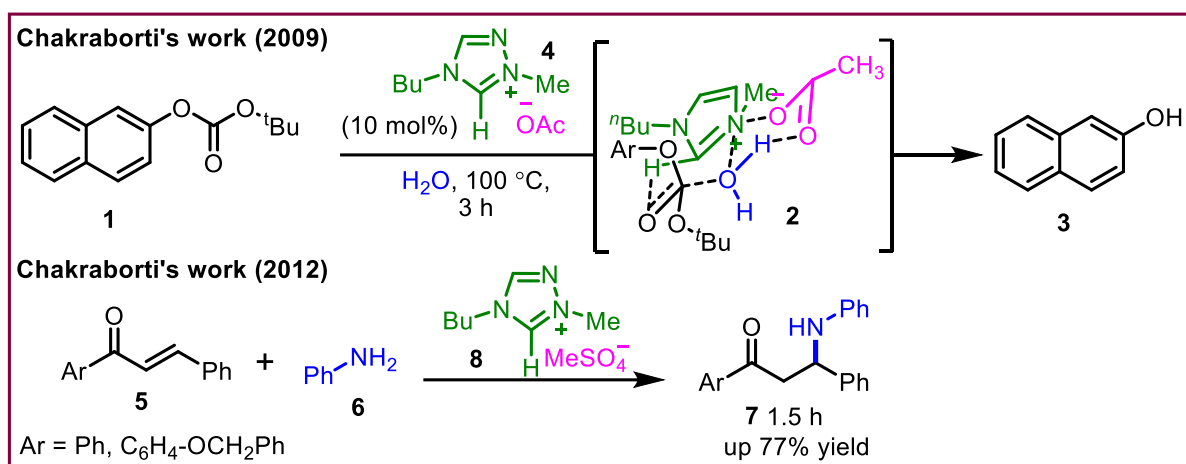
Bis(amino)cyclopropenium Ion as a Hydrogen-bond Donor Catalyst for 1,6-Conjugate Addition Reactions

3.1 Introduction

The concept of hydrogen bonding has been well-acknowledged in the fields of chemistry, biology, and crystal engineering.¹ One of the major breakthroughs, and relatively recent evolution, in this area, is ‘*hydrogen-bond donor catalysis*’,² which basically relies on the activation of organic molecules and/or stabilization of the key transition state(s) by the catalyst through hydrogen bonding interactions and, subsequently, enhance the rate of the reaction. As a major part of ‘*non-covalent organocatalysis*’, this particular advancement has been appreciated in many organic transformations,³ including asymmetric synthesis.⁴ In recent years, another sub-area in organocatalysis, called ‘*ionic liquid catalysis*’ has emerged. Although the concepts of ‘catalysis in ionic liquid medium’⁵ and ‘catalysis by ionic liquids’⁶ have been well established, the catalytic activation of organic molecules by ionic liquids through non-covalent hydrogen bonding interactions is relatively a new concept and still up-and-coming. It is noteworthy to mention that most of the ionic liquids, utilized in hydrogen bond donor catalysis, are based on imidazolium salts. In fact, the modes of hydrogen bonding interactions of the C-2 hydrogen of the imidazolium salts in catalytic activation have been extensively studied through experimental as well as computational methods.⁷ Some of the imidazolium salts have been utilized as hydrogen bond donor catalysts in fundamental organic transformations.

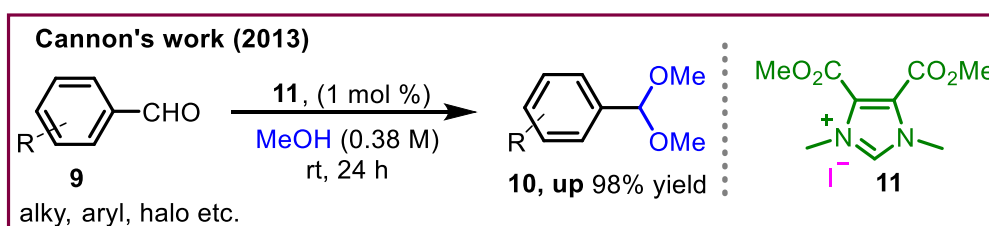
3.2 Literature reports on the imidazolium-based H-bond donor catalysts

In 2009, Chakraborti and co-workers reported the deprotection of the Boc group from the carbonate **1** to get 2-naphthol **3** in 98% yield in the presence of a triazolium salt **4** (10 mol %). The reaction is believed to proceed via complex **2** (Scheme 1).^{8a} Later in 2012, the same research group employed triazolium salt **8** for the Friedel-Crafts type reaction of benzyl amine **6** and enones **5** to access alkylated benzylamines **7** (Scheme 1).^{8b}



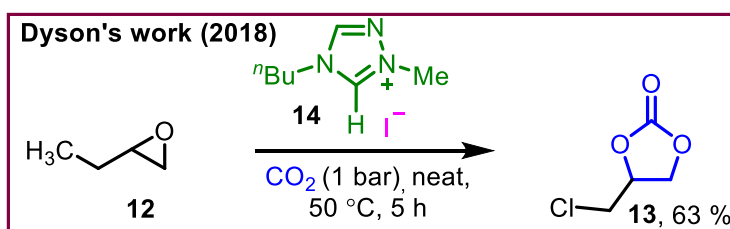
Scheme 1. Triazolium salt catalyzed *O*-*t*-Boc deprotection and aza-Michael reaction.

In 2013, Cannon and co-workers established an imidazolium salt **11** catalyzed acetylation of aryl aldehydes (**9**) in the presence of methanol. The author has suggested that the reaction worked well irrespective of the electronic nature of aldehyde and the respective acetals (**10**) were obtained in excellent yields within 24 h (Scheme 2).⁹



Scheme 2. Imidazolium salt catalyzed acetylation reaction.

Recently, in 2018, Dyson and co-workers described the synthesis of a cyclic carbonate **13** through a formal [3+2]-annulation of the epoxide **12** with CO₂ using an imidazolium salt **14**. DFT-based calculations have shown that the reaction proceeds through a hydrogen bonding interaction between epoxide **12** and catalyst **14** (Scheme 3).¹⁰



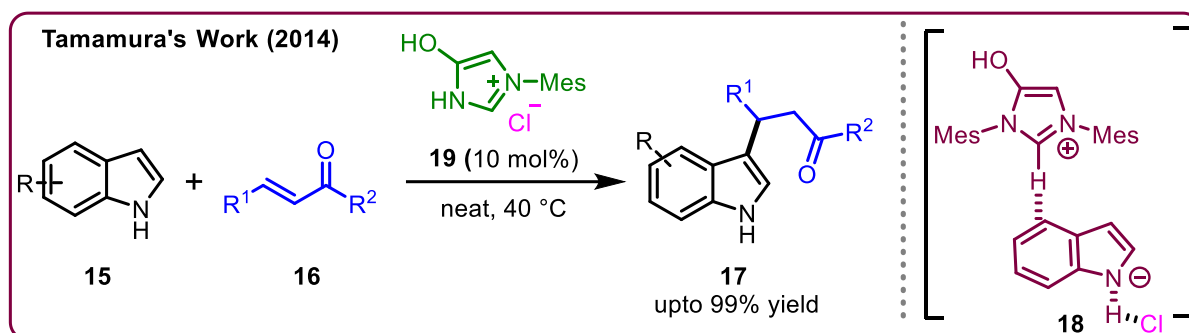
Scheme 3. Imidazolium salt-catalyzed cycloaddition of CO₂ into epoxides

3.2.1 Imidazolium/triazolium catalyzed conjugate addition reactions

A few reports are available for the imidazolium salt-catalyzed conjugate addition reactions of enones and dienones with C-nucleophiles; some examples are listed below.

3.2.2 1,4 Conjugate addition reactions

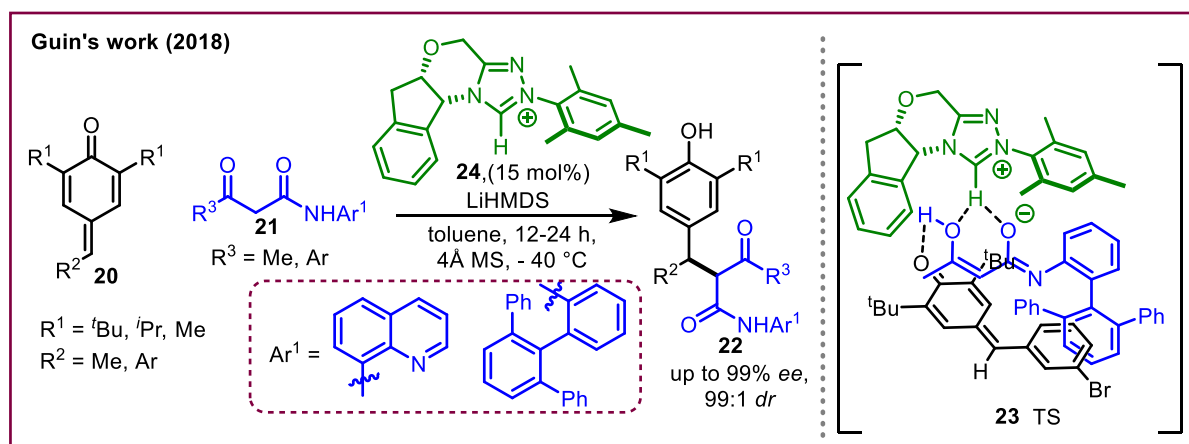
Tamamura and co-workers reported an imidazolium salt-catalyzed Friedel-Crafts-type reaction of indoles (**15**) with enones (**16**) to access 3-alkylated indoles (**17**) [Scheme 4].¹¹ Based on control experiments and computational methods, the authors proposed that the indole is activated by the imidazolium salt through cation- π interaction (**TS 18**) and, at the same time, the counter anion (Cl^- in their case) acts as a Lewis base to abstract the indole NH proton.¹¹



Scheme 4: Friedel-Crafts-type conjugate addition of indole (**15**) to chalcone using an imidazolium salt catalyst.

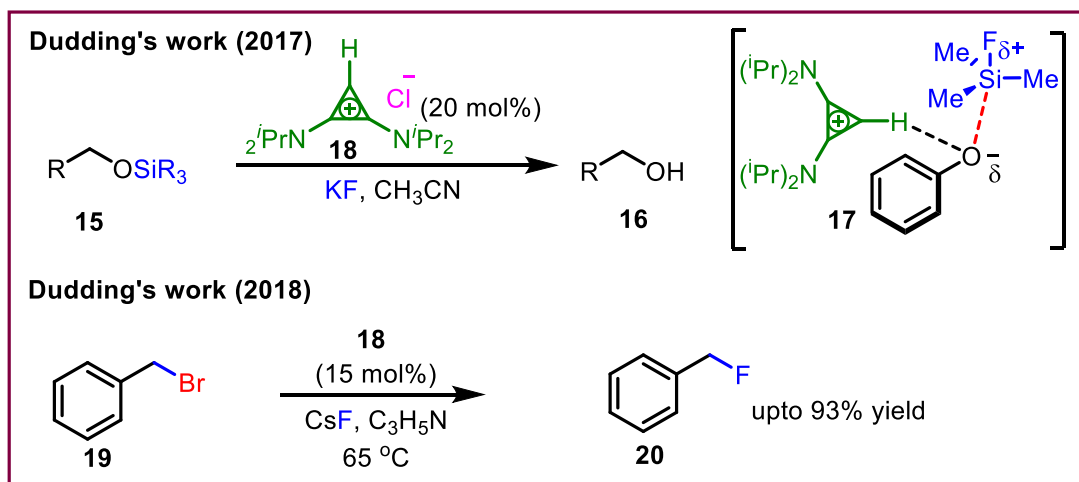
3.2.3 1,6-Conjugate addition reactions

Recently, Guin's group demonstrated a chiral NHC (**24**) catalyzed enantioselective addition of 1,3-diketodimides (**21**) to *p*-quinone methides (**20**) [Scheme 5]. The reaction is thought to proceed through an ion-pair intermediate **23**. This approach tolerated a wide range of *p*-QMs and 1,3-ketoamides and the products (**22**) with moderate to good yields and high enantio- and diastereoselectivity (70-99% *ee*, *dr* 54:46-99:1) [Scheme 5].¹²



Scheme 5: Chiral NHC catalyzed 1,6-conjugate addition of 1,3-ketodimides to *p*-quinone methides.

Though the cyclopropenium salts have been known for the past several decades,^{13a} their potential as organocatalysts in synthetic transformations has been uncovered only recently.^{13b} Otherwise, the cyclopropenium salts, especially aminocyclopropenium salts, have been majorly utilized as ionic liquids,¹⁴ polyelectrolytes,¹⁵ ligands in transition metal or main group chemistry¹⁶ and as activators/promoters in nucleophilic substitution reactions.¹⁷ While considering the catalytic applications in organic transformations, the tris(dialkylamino)cyclopropenium (TDAC) salts, have been found to serve as effective phase-transfer catalysts in many fundamental organic transformations.¹⁸ Moreover, some of the cyclopropenium-based compounds such as bis(dialkylamino)cyclopropeneimines¹⁹ and bis(dialkylamino)cyclopropenylidenes (BACs)²⁰ [both derived from cyclopropenium salts] have found applications as organocatalysts in organic transformations, including enantioselective reactions.



Scheme 6. *O*-Silyl ether deprotection and benzylic fluorination reactions

In 2017, Dudding and co-workers reported the deprotection of silyl group from silyl ethers (**15**) using a cyclopropenium salt **18** as a phase-transfer catalyst (Scheme 6).²¹ Si–O bond cleavage, accompanied by hydrogen bond stabilization of the developing phenoxy anion, occurs through the transition state **17**.²¹ A year later, the same group reported the use of cyclopropenium cation **18** as a phase-transfer catalyst for the benzylic fluorination of **19** (Scheme 6).²²

3.3 Background

The role of H-bonding interactions of the N–H proton ($N-H\cdots X$) in tris(dialkylamino)cyclopropenium (TDAC) salts catalyzed organic transformations has been investigated thoroughly (**I**, Fig. 1).²³ Nevertheless, the catalytic mode of activation through the

H-bonding interaction by the C–H proton ($\text{C–H}\cdots\text{X}$) of the cyclopropene ring in bis(dialkylamino)cyclopropenium salts²² in organic reactions is rather limited. However, although a report is available for the activation of the carbonyl group by the C–H proton of the cyclopropene ring ($\text{C–H}\cdots\text{O=C}$) in bis(dialkylamino)cyclopropenium salts (**III**, Fig. 1),²⁴ surprisingly, this concept has not been utilized yet in organocatalytic transformations. This prompted us to investigate the catalytic applications of bis(dialkylamino)cyclopropenium salts in conjugate addition reactions, especially in 1,6-conjugate addition reactions of *p*-quinone methides²⁵ as our current research interest is inclined towards this research area.^{26,27}

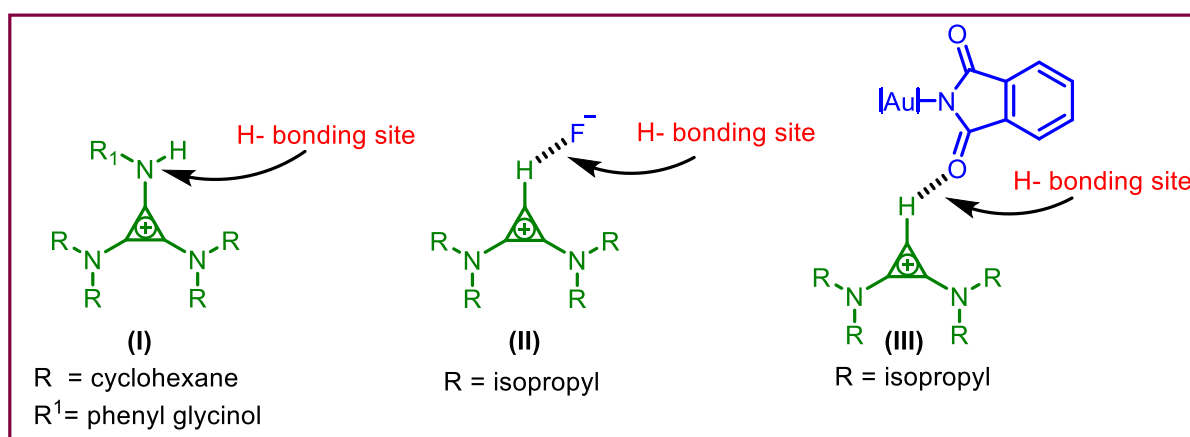
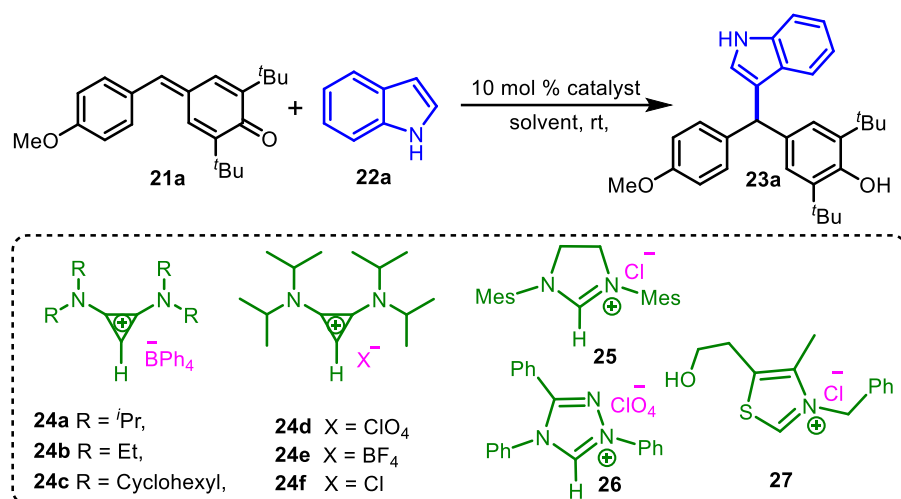


Figure 1. Various activation modes of cyclopropenium salts through H-bonding

3.4 Results and discussion

The optimization experiments were carried out using 4-methoxy-substituted *p*-QM (**21a**) and indole (**22a**) using a wide range of H-bond donor catalysts under different conditions and, the results are summarized in Table 1. Initially, when the reaction between **21a** and **22a** was carried out using bis(diisopropylamino)cyclopropenium salt **24a** as a catalyst in diethyl ether, the expected triarylmethane derivative **23a** was obtained in 26% yield (entry 1). Changing the reaction medium from diethyl ether to THF improved the yield of **23a** considerably (entry 2). However, the polar aprotic solvents such as DMF or 1,4-dioxane were found to be unsuitable for this transformation as **23a** was not observed in both cases (entries 3 & 4). Acetonitrile was found to be effective for this transformation and product **23a** was obtained in 75% isolated yield (entry 5). Interestingly, when the reaction was performed in chlorinated solvents such as CH_2Cl_2 and CHCl_3 , **23a** was isolated in 96 and 90% yields, respectively (entries 6 & 7). As expected, other *N,N*-dialkylated cyclopropenium salts such as **24b** and **24c** were also found to promote the reaction effectively, but with a bit lower yields of **23a** when compared to the reaction with **24a** (entries 8 & 9). To compare the catalytic activity of bis(amino)cyclopropenium salts (**24a-c**) with the conventional heterocycle-based salts towards this transformation, a few reactions were performed by using dihydroimidazolium (**25**), triazolium (**26**) and

thiazolium (**27**) salts (entries 10-12). Notably, the triazolium salt **26** drove the reaction to completion and, the product **23a** was obtained in 90% yield with a relatively lower reaction rate (24 h) [entry 11]. Surprisingly, the other two salts **25** & **27** failed to catalyze this transformation (entries 10 & 12). To understand the role of counter anion in this reaction, a few experiments were conducted with a few other bis(amino)cyclopropenium salts (**24d-f**) having different counter anions (ClO_4^- , BF_4^- and Cl^-) [entries 13-15]. Interestingly, the reaction time and the yield of **23a** in all those three experiments were almost the same when compared to the reaction using **24a** as a catalyst (entry 6). This observation clearly indicates that the counter ion does not play any role in the entire course of the reaction. This finding was further supported by a couple of experiments, in which NaBPh_4 and Bu_4NBPh_4 were used as a catalyst, and, in those case, only traces of **23a** was observed even after 24 h (entries 16 & 17). When the reaction was carried out without a catalyst, **23a** was not observed, which clearly indicates that a catalyst is required for this transformation (entry 19). Another possibility, although less likely, is that the counter anion in the catalyst might deprotonate the N–H proton of indole and produce the corresponding strong conjugate acid (HBPh_4 , HBF_4 , HClO_4 , etc.), which might be actually catalyzing the reaction. In line with this, an experiment was carried out with 5 mol % of HBPh_4 as a catalyst (entry 18). Intriguingly, in this case, the reaction reached completion within 5 min and product **23a** was obtained in 97% yield. However, when this result is compared with the actual optimized condition with **24a** (entry 6), one can easily realize that the reaction catalyzed by **24a** was too slow and took at least 16 h to reach completion. This observation indicates that HBPh_4 was probably not formed during the reaction catalyzed by **24a** (entry 6). To further confirm this, a mixture of equimolar quantities of **24a** and indole (**22a**) in CDCl_3 was stirred for a few hours and monitored by ^1H NMR spectroscopy. However, the N–H proton was intact even after 12 hours and, no additional peak that corresponds to the formation of HBPh_4 was observed. Based on the above-mentioned experiments, one can convincingly exclude the possibility of the formation of HBPh_4 under the optimized reaction conditions catalyzed by **24a** (entry 6).

Table 1. Optimization Study^a

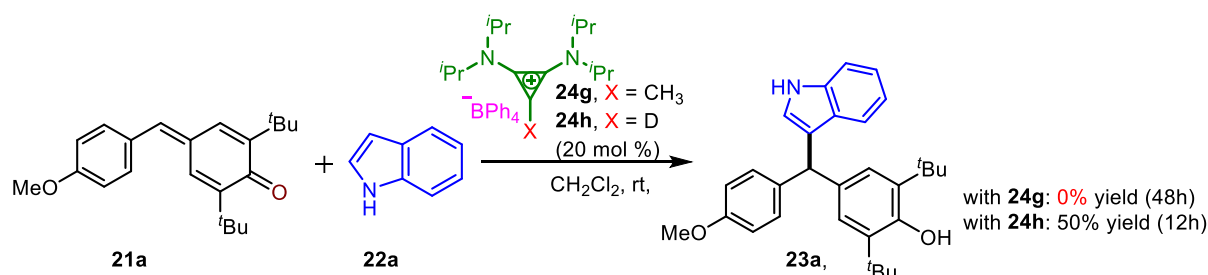
entry	catalyst	solvent	time	isolated yield [%] ^b
1	24a	Et ₂ O	24 h	26
2	24a	THF	24 h	87
3	24a	DMF	24 h	0
4	24a	1,4-dioxane	24 h	0
5	24a	CH ₃ CN	24 h	75
6 ^c	24a	CH ₂ Cl ₂	16 h	96
7	24a	CHCl ₃	24 h	90
8	24b	CH ₂ Cl ₂	16 h	91
9	24c	CH ₂ Cl ₂	24 h	92
10	25	CH ₂ Cl ₂	24 h	trace
11	26	CH ₂ Cl ₂	24 h	90
12	27	CH ₂ Cl ₂	24 h	trace
13	24d	CH ₂ Cl ₂	16 h	92
14	24e	CH ₂ Cl ₂	16 h	96
15	24f	CH ₂ Cl ₂	16 h	92
16	NaBPh ₄	CH ₂ Cl ₂	24 h	trace
17	Bu ₄ NBPh ₄	CH ₂ Cl ₂	24 h	trace
18 ^d	HBPh ₄	CH ₂ Cl ₂	<5 min	97
19	--	CH ₂ Cl ₂	48 h	0

^aAll reactions were carried out with **21a** (0.123 mmol), **22a** (0.148 mmol), and 10 mol % of catalyst in 1 mL of solvent at room temperature. ^bIsolated yields. ^cOptimal condition. ^d5 mol % of catalyst was used.

At this point, based on the optimization studies (Table 1), we were partially convinced that the cyclopropenium ion is acting as a catalyst and drives this transformation. We envisaged that the hydrogen atom, which is attached to the carbocation of the cyclopropene ring in **24a**, could be acidic enough to act as a H-bond donor catalyst to activate the carbonyl-group of the *p*-QM (**24a**). To further confirm this concept, a couple of experiments were carried out, in which, two other bis(amino)cyclopropenium salts **24g** & **24h** (where the hydrogen atom in the cyclopropene ring was replaced with a methyl group and deuterium, respectively) were employed (Scheme 7). When **24g** (20 mol %) was used as a catalyst, the product **23a** was not formed even after 2 days. In the case of reaction using 20 mol % of **24h** (99.99 % D), as

expected, the reaction was found to be relatively slow (when compared to the reaction catalyzed by 20 mol % of **24a**; more details are given in the experimental section) and gave the product **23a** in ~ 50% yield (by ^1H NMR) in 12 h (Scheme 7). These findings clearly confirm that the hydrogen atom (C–H) that is present in the cyclopropene ring is indeed solely responsible for catalyzing this transformation.

Scheme 7. Control Experiments with Catalysts **24g** & **24h**



The reactions were carried out in 40 mg scale of **21a**. Yields reported are isolated yields.

In order to get some insight on the mode(s) of activation of **21a** and/or **22a** by the catalyst **24a**, a few ^1H & ^{13}C NMR based control experiments have been performed. In this regard, initially, the ^1H NMR spectra for the mixture of **21a** and **24a** in CDCl₃ at various stoichiometric ratios between **21a** or **24a** were recorded and stacked as shown in Figure 2. It was observed that the chemical shift of the C–H proton (actual value $\delta = 4.9434$ ppm), which is attached to the carbocation in the cyclopropene ring, was gradually shifted to the downfield region with the increasing concentration of **24a** ($\delta = 5.0605$ ppm with 10 equiv. of **24a** with respect to **21a**) [(a), Figure 2]. Similarly, in ^{13}C NMR, it was observed that the chemical shift of carbonyl carbon of **21a** (actual value $\delta = 186.6205$ ppm) was gradually shifted to the up-field region with the increasing concentration of the catalyst **24a** ($\delta = 186.4350$ ppm with 15 equiv. of **24a** with respect to **21a**) [(b), Fig. 2; for full ^{13}C NMR spectra, experimental section]. In fact, similar changes were observed in ^1H as well as ^{13}C spectra, when the NMR titration experiments were performed between **21a** and **24b** or **21a** and **24c** in CDCl₃ (experimental section).

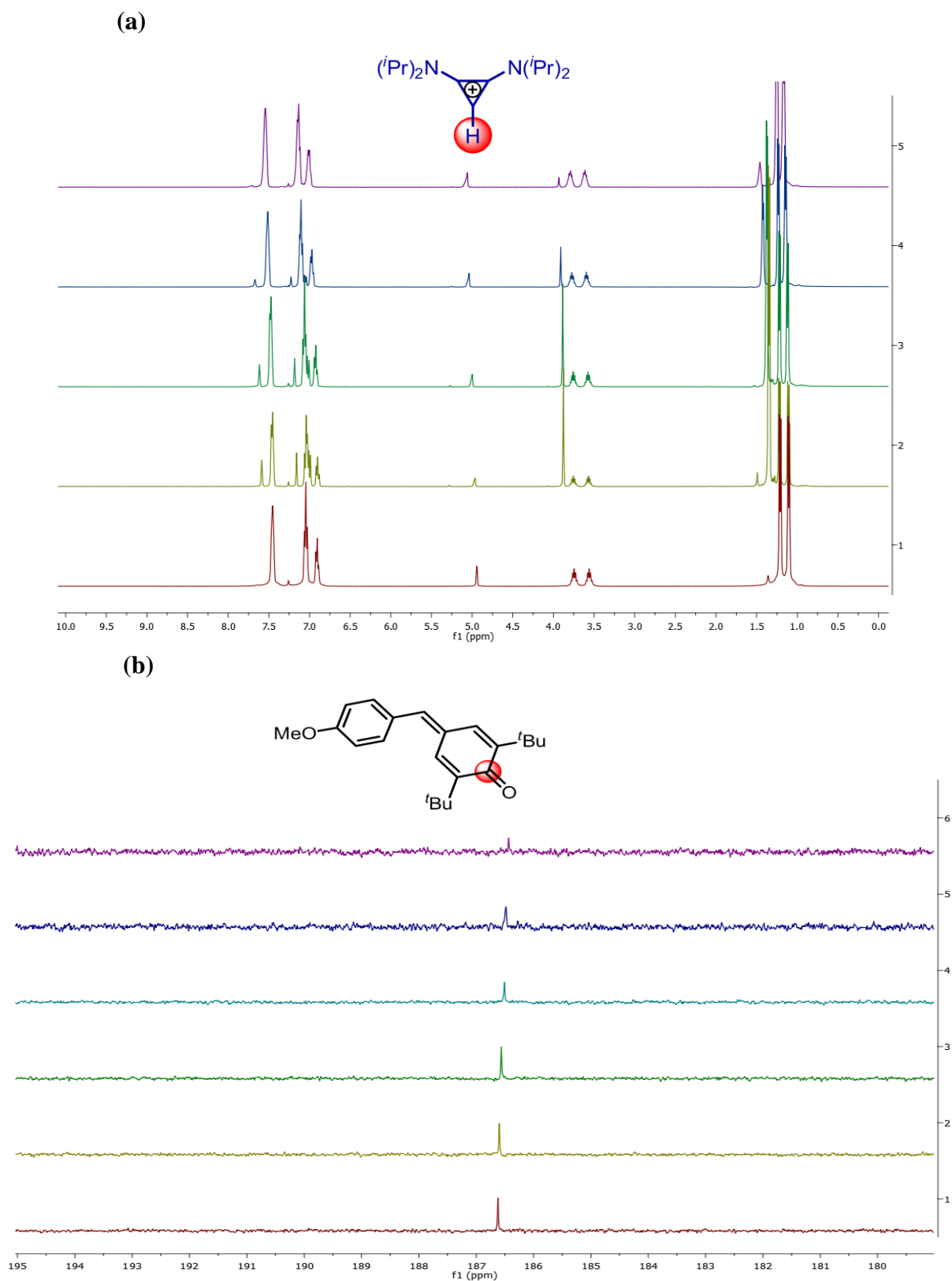


Figure 2. ^1H & ^{13}C NMR Titration Experiments with **21a** & **24a** in CDCl_3 (The stoichiometric ratios between **21a** & **24a**, the chemical shifts of C–H proton of **24a** in ^1H NMR (a), and C=O signal of **21a** in ^{13}C NMR (b) are indicated. The shifts are relative to residual CHCl_3).

Based on the magnitude as well as the mode of the shifts [downfield shifts in C-H proton signal (**a**, Fig. 2) and upfield shifts in carbonyl carbon signal (**b**, Fig. 2) upon complexation, it is evident that the carbonyl-group of **21a** and the hydrogen atom (C-H) of cyclopropene ring in **24a** exhibits non-covalent type interactions. Furthermore, this observation strongly supports that the C-H hydrogen does not get removed/abstracted from the cyclopropene ring by **21a** during the course of the reaction.

Furthermore, the association constant between **21a** and **24a** has been estimated using BindFit program.²⁸ To enumerate the complexation process, *p*-QM (**21a**) was titrated against the catalyst **24a**, and the changes in the absorption feature of **21a** (at 380 nm) were followed using UV-vis spectroscopy (**a**, Figure 3). We observed an isosbestic point along with the decrease in the absorption feature of **21a**, which clearly indicates the complexation between **21a** and the catalyst **24a**. Based on the fit, the association constant was found to be $1.01 \times 10^6 \pm 0.38 \times 10^5 \text{ M}^{-1}$. Likewise, another titration was performed between **21a** and the deuterated catalyst **24h** (99.99% D), and similar changes were observed (**b**, Figure 3). However, in this case, saturation has been reached with relatively fewer changes in the absorption feature of **21a**. In fact, the association constant was found to be $2.28 \times 10^5 \pm 0.21 \times 10^5 \text{ M}^{-1}$ (refer to the experimental section for more details).

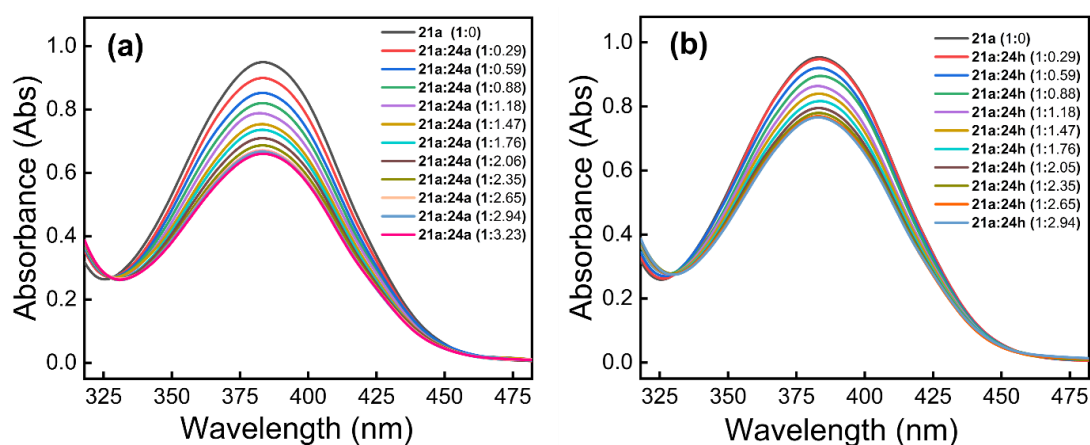


Figure 3. UV-vis-spectroscopic determination of association constants in CHCl_3 for (a) **21a** vs **24a** (b) **21a** vs **24h** [Concentration of stock solution of **21a**: $6.817 \times 10^2 \text{ } \mu\text{M}$ and the stock solutions of **24a/24h**: 20 mM] For both the experiments, **24a/24h** was added in the order 10, 20, 30,110 μL to a solution of **21a** (990, 980, 970,890 μL , respectively), and the total volume of the solution was made up to 1 mL.

The difference of approximately one order of magnitude decrease in the association constant in the case of **24h** related to **24a** is very well corroborating with the isolated yields as indicated in Scheme 7. These experiments further confirm the existence of non-covalent interactions between **21a** and **24a**, and also the role of C–H hydrogen of **24a** in the activation of the carbonyl group of **21a**.

Later, to understand whether or not the indole **22a** is getting activated by the catalyst **24a** during the reaction, we decided to perform a few more ^1H NMR-based experiments. In this context, the ^1H NMR of a mixture of **22a** and **24a** in CDCl_3 at various concentrations of **22a** or **24a** have been recorded (Figure 4). In all those cases, no perceptible changes were observed in the chemical shift of the cyclopropene C–H proton, which clearly indicates that the cyclopropene C–H proton is not involved in the activation of indole either through covalent bond formation or through H-bonding interactions. However, interestingly, the chemical shifts of C–H as well as CH_3 protons of the isopropyl group in the amine part have been shifted noticeably to the shielding region with increasing concentration of indole (Figure 4). We believe that the shielding is probably due to ‘diamagnetic anisotropic effect’ in the presence of excess indole in the solution.

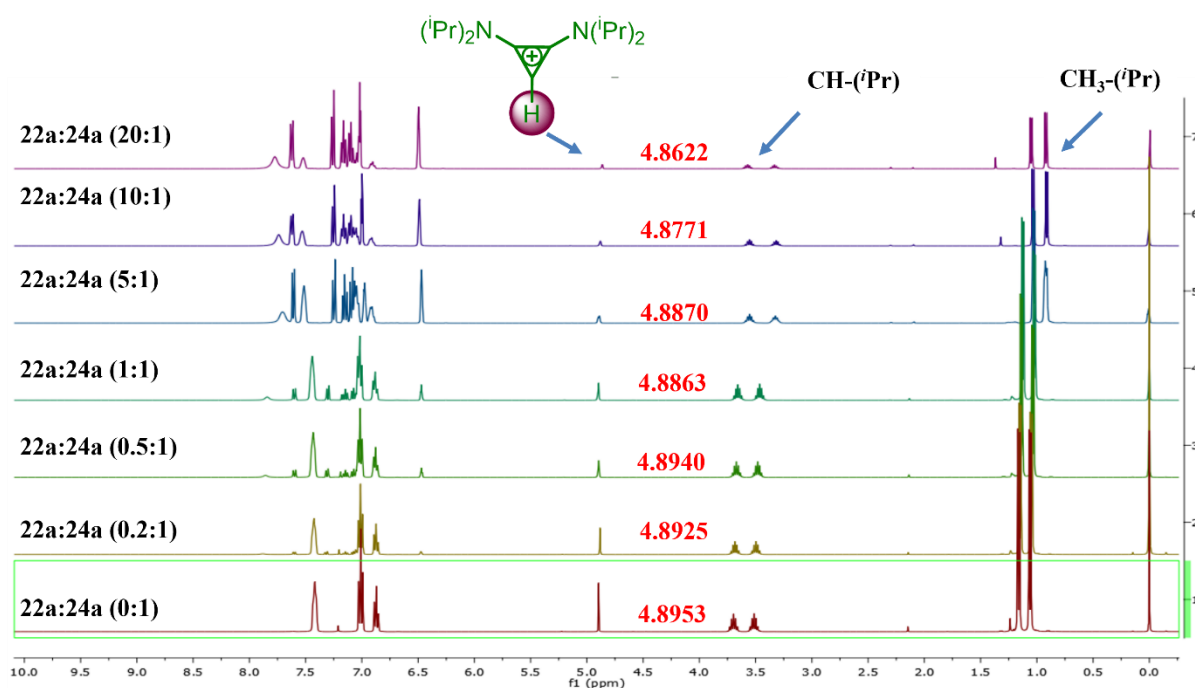
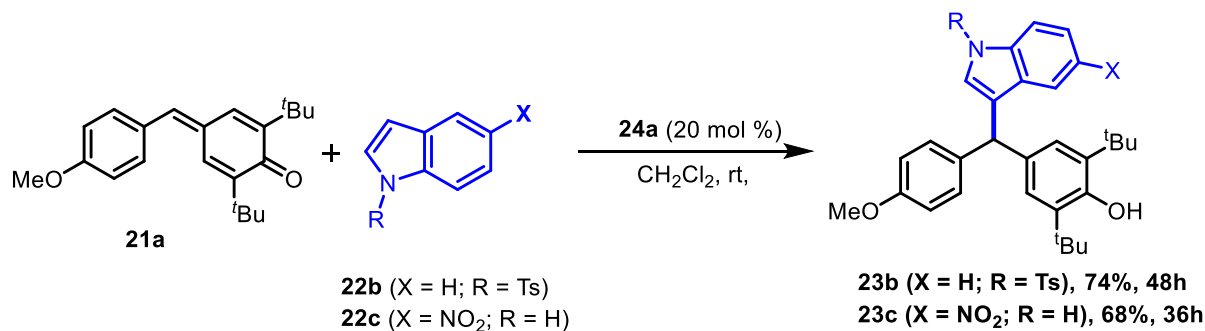


Figure 4. ^1H NMR Titration Experiments with **22a** & **24a** in CDCl_3 (The stoichiometric ratios between **22a** & **24a**, and the chemical shifts of C–H proton of **24a** in ^1H NMR are indicated. The shifts are relative to TMS).

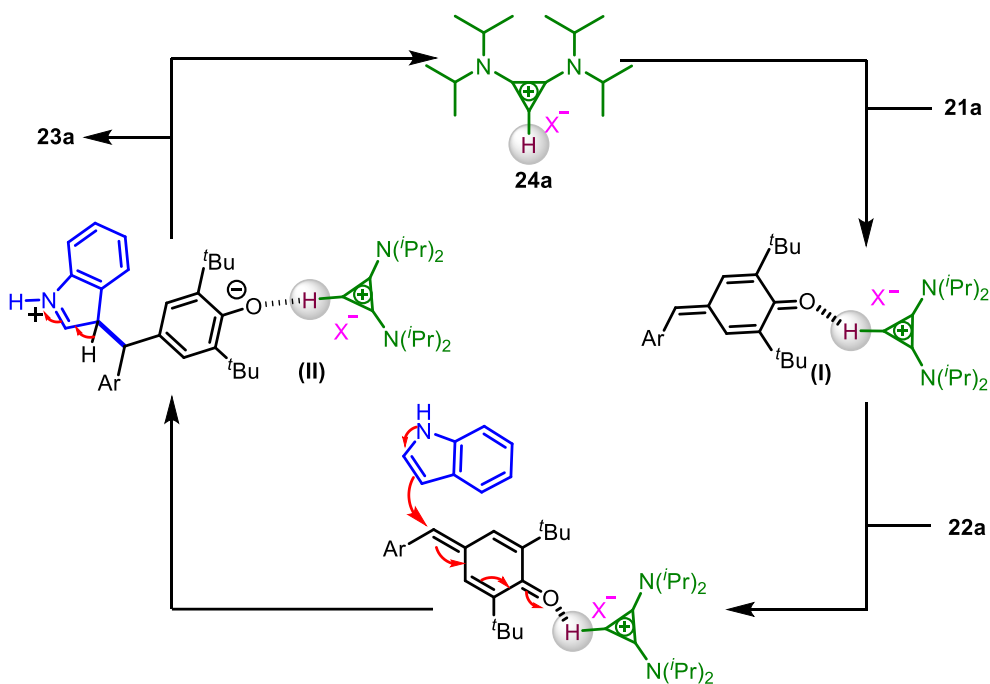
An important point to be noted at this juncture is that the above-mentioned observations are in sharp contrast to the previous results reported by Tamamura and co-workers for the imidazolium salt catalyzed 1,4-addition of indoles to enones.¹¹ Of course, the catalyst used by them was an imidazolium salt and, in our case, it is a cyclopropenium salt. Tamamura's group observed a significant up-field shift of the C–H proton of the imidazolium ring with the increasing concentration of indole and, based on this observation as well as computational calculations, they concluded that there was a cation- π type interaction between the imidazolium salt and the 'electron-rich' indole. The comparison between Tamamura's results and our observations evidently signifies that the cation- π interaction between the catalyst **24a** and indole **22a** is absent in our case since there were no noticeable changes observed in the chemical shift of C–H proton of the cyclopropene even in the presence of excess amounts of indole. Moreover, in our case, **24a** was also found to be effective for the reaction between **21a** and 'electron-deficient' indoles such as 5-nitro indole **22b** and *N*-tosyl indole **22c**, although both the reactions took relatively longer period due to the deactivation of the indole ring by the electron-withdrawing group present in the aryl ring and on nitrogen, respectively (Scheme 8). Therefore, based on the aforementioned control experiments and NMR studies, one can persuasively conclude that the catalyst **24a** is not involved in the activation of indole **22a** either by cation- π interaction or through H-bonding. Besides, as indicated in the optimization studies (entries 13-15, Table 1), the counter anion is not involved in the activation of indole **22a** as no substantial change was observed either in the rate of the reaction or the yield of the product **23a**, by using the cyclopropenium salt with different counter anions (ClO_4^- , BF_4^- and Cl^-), when compared with the optimal condition (entry 6, Table 1). As observed through the control experiments (Scheme 8) as well as NMR (Figure 2) and UV-vis (Figure 3) studies, we strongly believe that the catalyst **24a** is activating the *p*-QM (**21a**) through hydrogen bonding.

Scheme 8. Reactions with Electron-deficient Indoles (**22b** & **22c**)



^aReaction conditions: All reactions were carried out in 40 mg scale of **21a**. Yields reported are isolated yields.

Therefore, based on this, a plausible mechanism for this transformation has been proposed (Scheme 9). Initially, the catalyst **24a** activates the *p*-QM **21a** through H-bonding and forms the complex **I**. At this point, indole **22a** adds to complex **I** in a 1,6 fashion, which leads to the formation of complex **II**. This complex (**II**) then undergoes rearomatization through the elimination of proton to form the product **23a** and, during this process, the catalyst **24a** gets detached from the complex **II** (Scheme 9).

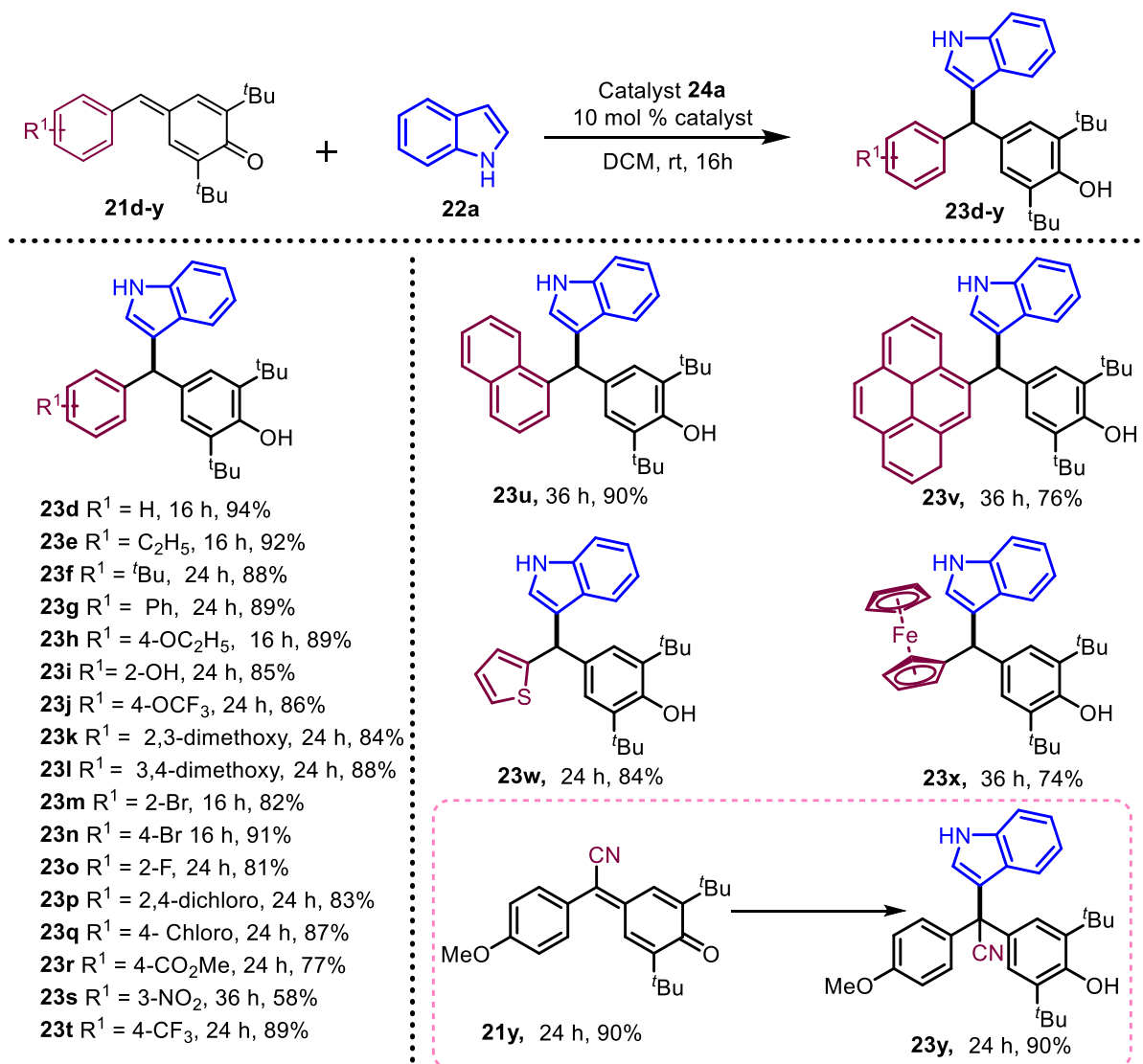


Scheme 9. Plausible Mechanism

While evaluating the substrate scope (Chart 1), we observed that most of the *p*-quinone methides reacted with indole (**22a**) smoothly and provided the corresponding indolyl diarylmethane derivatives in good to excellent yields under the optimized conditions (entry 6, Table 1). For example, *p*-QMs, derived from benzaldehyde and alkyl/aryl-substituted benzaldehydes, gave the desired products (**23d-g**) in the range of 88-94% yields. Under optimized conditions, other *p*-QMs, substituted with alkoxy- or halo substituents in the arene part, reacted with **22a** and gave the corresponding indolyl diarylmethanes (**23h-q**) in excellent yields (82-91% yields). However, in the cases of *p*-QMs, having electron-deficient groups in the arene part, the desired products **23r** & **23s** were obtained in relatively lesser yields (77 and 58% yields, respectively). In the case of trifluoromethyl-arene substituted *p*-QM, the corresponding product **23t** was obtained in 89% isolated yield. This protocol was also found to be effective for the *p*-QMs, substituted with other aromatic hydrocarbons and heteroarenes,

and, in all those cases, the respective indolyl diarylmethanes (**23u-x**) were obtained in the range of 74-90% yields. In the case of 6-cyano-*p*-QM^{21a} (**21w**), the corresponding product **23y** was isolated in 90% yield.

Chart 1. Substrate Scope with Different *p*-QMs^a

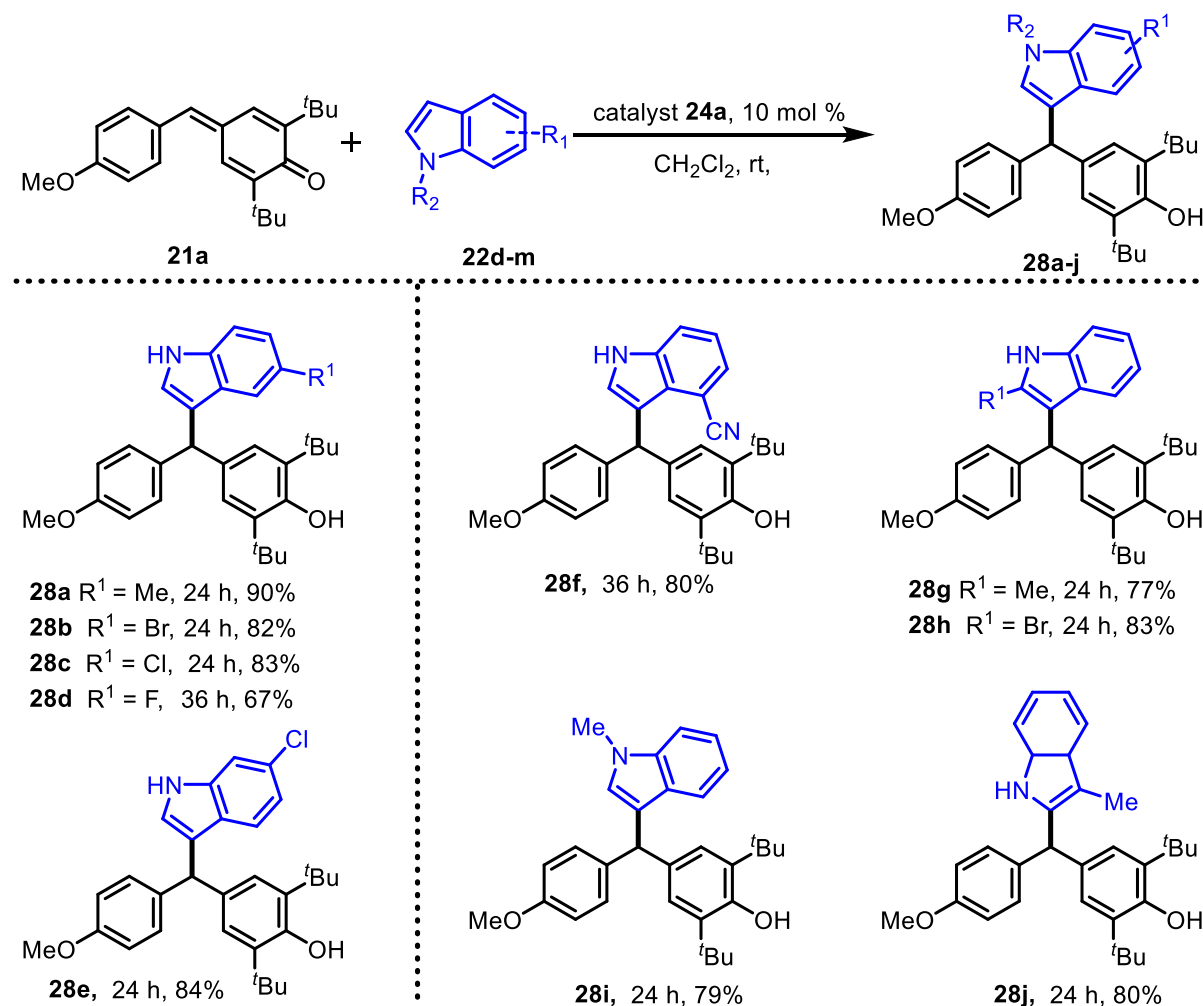


^aReaction conditions: All reactions were carried out in 40 mg scale of **21b-w**. Yields reported are isolated yields.

The optimized condition was also found to be very effective for the reaction between **21a** and a wide range of substituted indoles (**22d-m**) and, in most of the cases, the expected products were formed in good yields (Chart 2). Alkyl- and halo-substituted indoles reacted with **21a** and provided the indolyl diarylmethane derivatives **28a-e** in good yields (67-90%). In the case of 4-cyano-indole, **28f** was obtained in an 80% isolated yield. 2-Substituted indoles such as 2-methyl indole and 2-phenyl indole underwent reaction with **21a** and gave the corresponding products **28g** & **28h** in 77% and 83% yields, respectively. 1-Methyl indole

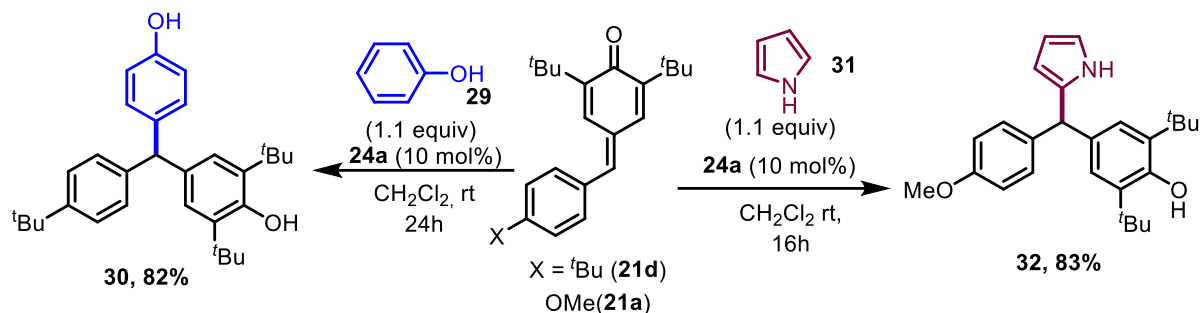
produced **28i** in 79% yield. Interestingly, in the case of 3-methyl indole, the substitution took place at the 2-position of indole and led to the product **28j** in 80% yield.

Chart 2. Substrate Scope with Different Indoles^a



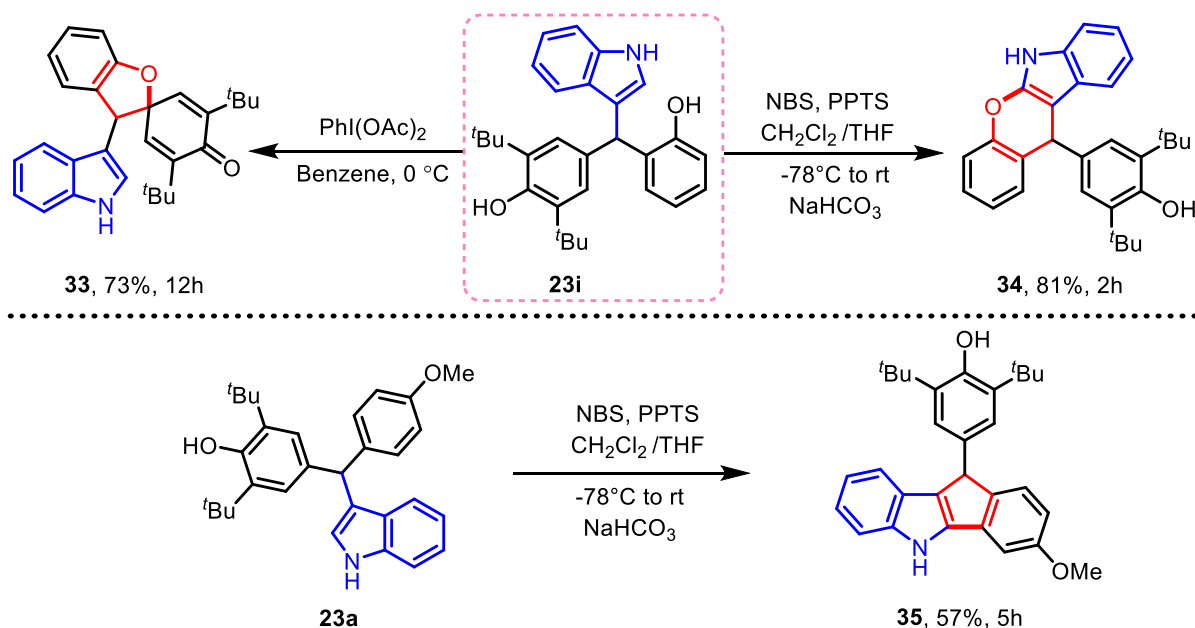
^aReaction conditions: All reactions were carried out in 40 mg scale of **21a**. Yields reported are isolated yields.

To further show the catalytic application of **24a** some other nucleophiles have also been tried, Interestingly, the catalyst **24a** was found to be very effective for the 1,6-conjugate addition of other nucleophiles to *p*-quinone methides. For example, **24a** effectively catalyzed the reaction between phenol **29** and *p*-QM **21d**, and, in this case, the corresponding unsymmetrical triarylmethane^{29a,b} **30** was obtained 82% isolated yields. Similarly, pyrrole **31** also underwent a 1,6-addition reaction with *p*-QM **21a** and gave the corresponding 2-diarylmethane-substituted pyrrole **32**^{29c} in excellent yield (83%) [Scheme 10].

Scheme 10. 1,6-conjugate addition of phenol and pyrrole to *p*-QMs catalyzed by **24a**

^aReaction conditions: Both reactions were carried out in 20 mg scale of *p*-QMs. Yields reported are isolated yields.

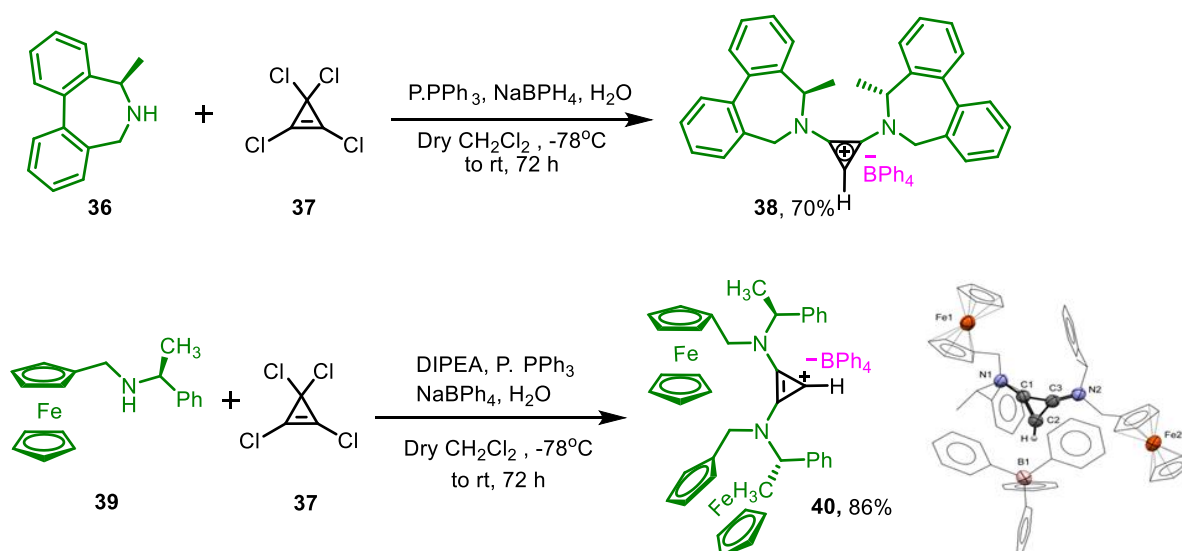
To show synthetic applications of this protocol, some of the indolyl diarylmethanes have been subsequently converted to other useful compounds (Scheme 11). For example, **23i** was oxidized with (diacetoxyiodo)benzene to access a spiro-cyclic compound³⁰ **33** in a 73% yield. In another experiment, **23i** was treated with NBS and PPTS followed by sodium bicarbonate to get dihydrochromeno[2,3-*b*]indole³¹ **34** in 64% yield. When **23a** was treated with NBS and PPTS followed by sodium bicarbonate, indene-fused indole **35** was obtained in 57% yield (Scheme 11).

Scheme 11. Synthetic Elaborations

^aReaction conditions: All reactions were carried out in 40 mg scale. Yields reported are isolated yields.

At this point, to explore an enantioselective version of this transformation, we have synthesized a couple of chiral cyclopropenium salts **38** & **40** using easily accessible chiral secondary amines and commercially available tetrachlorocyclopropene **37** (Scheme 12). The chiral cyclopropenium salt **38** was prepared by treating (*R,S*)-6,7-dihydro-5-methyl-5H-dibenz[*c,e*]azepine (+)-**36**³² with **37** in the presence of polymer-bound triphenylphosphine (P.PPh₃), sodium tetraphenyl borate and H₂O. In this case, the chiral cyclopropenium salt **38** was obtained in 70% yield (Scheme 12). A similar and slightly modified procedure was followed for the synthesis of ferrocene-based chiral cyclopropenium salt **40** through the reaction between ferrocene-based amine **39**³³ and **34** (Scheme 12). In this case, the expected chiral salt **40** was obtained with 86% yield. The structure of **40** was further confirmed by X-ray crystallography.

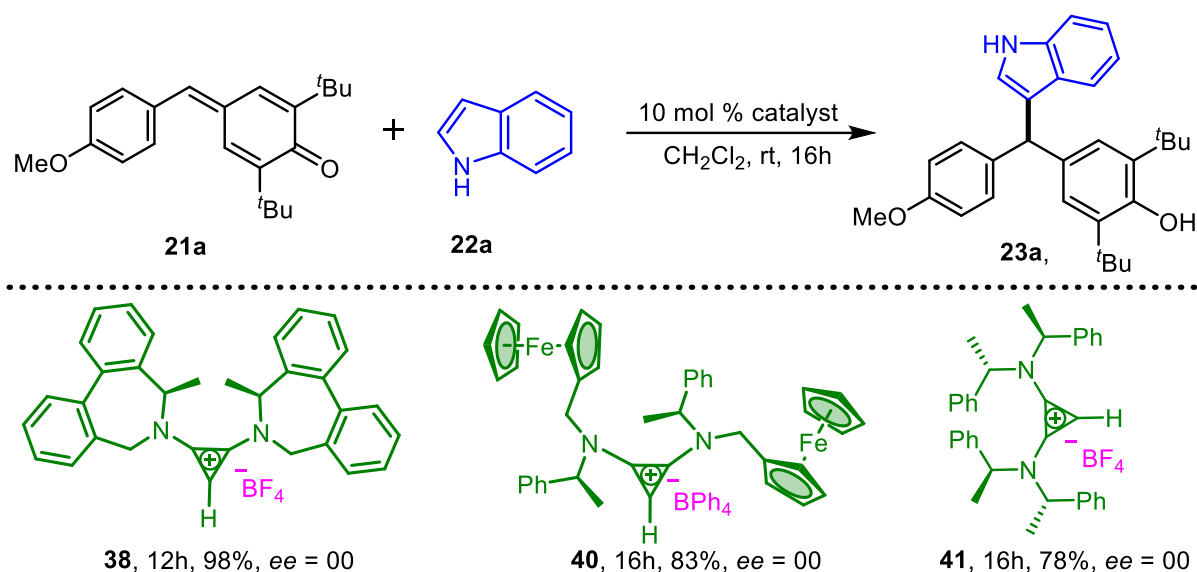
Scheme 12. Synthesis of chiral cyclopropenium salts



^aReaction conditions: All reactions were carried out in 250 mg scale of **37**. Yields reported are isolated yields.

After preparing the chiral cyclopropenium salts **38** & **40**, we attempted a few enantioselective reactions of **21a** with **22a** at different conditions (Scheme 13). A known chiral cyclopropenium salt **41**³⁵ was also examined for this reaction. Although the reaction was proceeding with all three catalysts employed, unfortunately, those catalysts failed to induce enantioselectivity in the product **23a**. In all the cases, **23a** was obtained as a racemic mixture (Scheme 13).

Scheme 13. Attempted Enantioselective Version



All reactions were carried out in 40 mg scale of **21a**. Yields reported are isolated yields.

3.5 Conclusion

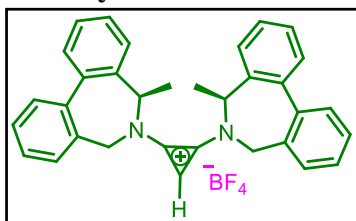
In conclusion, we have uncovered the unprecedented catalytic application of bis(amino)cyclopropenium ion in 1,6-conjugate addition reactions of *p*-quinone methides with various nucleophiles. Detailed mechanistic investigations through NMR/UV-vis spectroscopic studies and control experiments revealed that the hydrogen (C–H), which is present in the cyclopropene ring is responsible for catalyzing this transformation. It is evident from the mechanistic investigations that the C–H hydrogen activates the carbonyl group of the *p*-QM through H-bonding. A variety of nucleophiles such as indoles, phenol, and pyrrole reacted with *p*-QMs under optimized conditions and provided the corresponding triaryl- and diarylmethanes in good to excellent yields. Although the enantioselective version of this transformation is not successful at this point in time, further attempts to make it successful using other chiral bis(amino)cyclopropenium salts are currently under progress.

3.6 Experimental section

General Information: All reactions were carried out under an argon atmosphere in an oven-dried round bottom flask. All the solvents were distilled before use and stored under an argon atmosphere. Most of the reagents, starting materials, and NHC precursors **6** and **7** were purchased from commercial sources and used as such. All *p*-quinone methides have been prepared by following a literature procedure.^{35,36} The bis(amino)cyclopropenium salts **4a-4e**,³⁷ **4f**³⁸ and the NHC precursor **5**³⁹ were prepared according to the literature procedure. Other

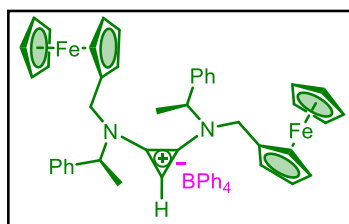
bis(amino)cyclopropenium salts **4g**⁴⁰ and **4h**⁴¹ were prepared by following literature procedures. Melting points were recorded on the SMP20 melting point apparatus and were uncorrected. ¹H, ¹³C, and ¹⁹F spectra were recorded in CDCl₃ (400, 100, and 376 MHz respectively) on Bruker FT-NMR spectrometer. Chemical shift (δ) values are reported in parts per million relatives to TMS and the coupling constants (*J*) are reported in Hz. High-resolution mass spectra were recorded on Waters Q-TOF Premier-HAB213 spectrometer. FT-IR spectra were recorded on a Perkin-Elmer FTIR spectrometer. Thin layer chromatography was performed on Merck silica gel 60 F₂₅₄ TLC pellets and visualized by UV irradiation and/or KMnO₄ stain. Column chromatography was carried out through silica gel (100–200 mesh) using an EtOAc/hexane mixture as an eluent. The UV-vis absorption spectra were recorded using a Cary 5000 UV-Vis-NIR spectrophotometer or Cary 60 UV-Vis spectrophotometer.

3.6.1. Synthesis and characterization of **38**



A solution of chiral secondary amine (7.03 mmol) in dry CH₂Cl₂ (2 mL, pre-cooled to -78 °C) was slowly added to a solution of tetrachlorocyclopropene (1.41 mmol) in dry CH₂Cl₂ (3.0 mL) under nitrogen at -78 °C. The reaction mixture was then warmed up to room temperature over 3 hours. It was then cooled back down to -40 °C, and polystyrene-bound triphenylphosphine (6.0 mmol/g) was added as a portion. The nitrogen atmosphere was restored, and the mixture was warmed to room temperature over 2 hours. Distilled water (10 mL) and sodium tetraphenylborate (0.56 mmol) were then added and the mixture was stirred vigorously for two days. The resulting mixture was filtered through sintered glass and transferred to a separatory funnel with CH₂Cl₂. The aqueous layer was decanted, and the organic layer was washed with 0.5 M HCl, saturated with aqueous NaHCO₃, and H₂O, then dried over Na₂SO₄ and concentrated *in vacuo*. The crude product was first recrystallized from MeOH/water to give a yellow solid. This yellow solid was then dissolved in hot EtOAc and allowed to cool and stand for 2 days. The liquid was decanted and crystals that adhered to the glass were washed with hexanes and collected to give a beige powder 70% yield, melting point = 193-195, ; ¹H NMR (400 MHz, CDCl₃) δ 7.63 – 7.54 (m, 10H), 7.40 – 7.37 (m, 12H), 7.27 – 7.25 (m, 2H), 7.21 (d, *J* = 7.56 2H), 6.97 (t, *J* = 7.32 Hz, 7H), 6.81 (t, *J* = 7.12 Hz, 3H), 4.87 (q, *J* = 14.0 2H), 4.50(d, *J* = 12.52 2H), 4.36 (d, *J* = 12.64 2H), 3.48 (s, 1H), 1.25 (2, *J* = 7.0 Hz, 6H); ¹³C NMR (100 MHz, CDCl₃) δ 140.54, 138.15, 136.37, 135.11, 131.53, 130.54, 130.47, 130.18, 129.41, 129.19, 129.13, 128.74, 125.55, 125.53, 125.50, 125.47, 121.52, 114.64, 64.58, 54.54, 22.86; HRMS (ESI): *m/z* calcd for C₃₃H₂₉N₂⁺ [M+H]⁺: 453.2331; found: 453.2331.

3.6.1. Synthesis and characterization of 40



A solution of chiral secondary amine (3.1 mmol) in dry CH_2Cl_2 (2 mL, pre-cooled to -78°C) was slowly added to a solution of tetrachlorocyclopropene (1.41 mmol) in dry CH_2Cl_2 (3.0 mL) under nitrogen at -78°C followed by dropwise addition of DIPEA (3.1 mmol). The reaction mixture was then warmed up to room temperature over 3 hours. It was then cooled back down to -40°C , and polystyrene-bound triphenylphosphine (6.0 mmol/g) was added as a portion. The nitrogen atmosphere was restored, and the mixture was warmed to room temperature over 2 hours. Distilled water (10 mL) and sodium tetraphenylborate (0.56 mmol) were then added and the mixture was stirred vigorously for two days. The resulting mixture was filtered through sintered glass and transferred to a separatory funnel with CH_2Cl_2 . The aqueous layer was decanted, and the organic layer was washed with 0.5 M HCl, saturated with aqueous NaHCO_3 , and H_2O , then dried over Na_2SO_4 and concentrated *in vacuo*. The crude product was first recrystallized from MeOH/water to give a yellow solid. This yellow solid was then dissolved in hot EtOAc and allowed to cool and stand for 2 days. The liquid was decanted and crystals which adhered to the glass were washed with hexanes and collected to give a beige powder 83% yield, melting point = $227\text{--}229^\circ\text{C}$, ^1H NMR (400 MHz, CDCl_3) δ 6.62 (d, $J = 7.32$ Hz, 2H), 7.54 (s, 6H), 7.48 – 7.34 (m, 8H), 7.19 (s, 2H), 7.08 (t, $J = 7.36$ Hz, 8H), 6.92 (t, $J = 7.16$ Hz, 4H), 4.72 (s, 2H), 4.18 – 4.15 (m, 2H), 4.12 – 4.09 (m, 8H), 4.07 (s, 6H), 3.93 (s, 2H), 1.74 (d, $J = 6.6$ Hz, 3H), 1.34 (d, $J = 6.8$ Hz, 3H); ^{13}C NMR (100 MHz, CDCl_3) δ 136.8, 136.4, 136.2, 129.3, 129.2, 129.1, 129.0, 128.8, 128.0, 127.2, 126.6, 126.5, 126.4, 125.9, 121.9, 79.3, 79.2, 75.5, 71.2, 69.5, 69.0, 68.8, 44.4, 21.3, HRMS (ESI): m/z calcd for $\text{C}_{41}\text{H}_{44}\text{Fe}_2\text{N}_2$ $[\text{M}+\text{H}]^+$: 675.2199; found: 675.2197. $[\alpha]_D^{20^\circ\text{C}} = 0^\circ$ (0.3 g/100 mL in CHCl_3)

3.6.1. Synthesis and characterization of 41⁹

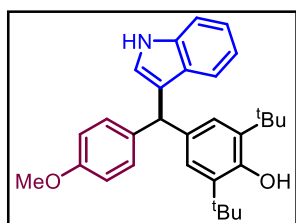
The procedure is analogous to the preparation of **40**: (+)-Bis[(R)-1-phenylethyl]amine (4.4 mmol,) tetrachlorocyclopropene (1 mmol,) tetrafluoroboric acid solution (50 wt. % in water, 0.137 mL) triphenylphosphine (1.15 mmol,). The resulting product was a white solid of (**41**) BF_4 . Yield: 0.52 g, 90%. ^1H NMR (400 MHz, CDCl_3): δ = 7.51 (s, 1H); 7.22–7.33 (m, 12H), 7.00 (m, 4H), 6.83 (m, 4H), 4.84 (dq, $J = 7.1$ Hz, 4H), 1.88 (d, $J = 7.1$ Hz, 6H), 1.82 (d, $J = 7.1$ Hz, 6H).

General procedure for the 1,6-conjugate addition of indole to *p*-quinone methides:

Anhydrous CH_2Cl_2 (1.0 mL) was added to the mixture of *p*-quinone methide (0.123 mmol),

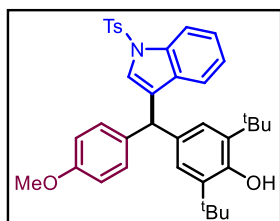
indole (0.148 mmol), and catalyst **24a** (0.0123 mmol) under argon atmosphere and the resulting solution was stirred at room temperature. After the reaction was complete (based on TLC analysis), the reaction mixture was concentrated under reduced pressure. The residue was then purified through a silica gel column, using an EtOAc/Hexane mixture as an eluent, to get the pure product.

4-((1H-indol-3-yl)(4-methoxyphenyl)methyl)-2,6-di-tert-butylphenol (23a):



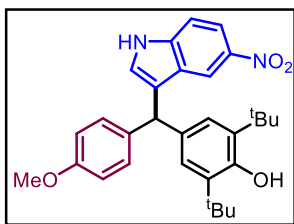
The reaction was performed at 0.123 mmol scale of **21a**; $R_f = 0.2$ (5% EtOAc in hexane); White solid (51.9 mg, 96% yield); m.p. = 170 – 171 °C; ^1H NMR (400 MHz, CDCl_3) δ 7.92 (brs, 1H), 7.34 (d, $J = 8.1$ Hz, 1H), 7.25 (d, $J = 8.7$ Hz, 1H), 7.18 – 7.14 (m, 3H), 7.05 (s, 2H), 7.01 – 6.97 (m, 1H), 6.82 (d, $J = 7.8$ Hz, 2H), 6.60 (s, 1H), 5.53 (s, 1H), 5.07 (s, 1H), 3.79 (s, 3H), 1.38 (s, 18H); $^{13}\text{C}\{^1\text{H}\}$ NMR (100 MHz, CDCl_3) δ 157.8, 152.1, 137.0, 136.8, 135.4, 134.9, 130.0, 127.2, 125.6, 123.9, 122.0, 121.3, 120.2, 119.3, 113.6, 111.0, 55.3, 48.1, 34.5, 30.5; FT-IR (thin film, neat): 3637, 3417, 2957, 1610, 1456, 1154, 1121 cm^{-1} ; HRMS (ESI-TOF) m/z : $[\text{M}-\text{H}]^-$ calcd for $\text{C}_{30}\text{H}_{34}\text{NO}_2$ 440.2590 found: 440.2609.

2,6-di-tert-butyl-4-((4-methoxyphenyl)(1-tosyl-1H-indol-3-yl)methyl)phenol (23b):



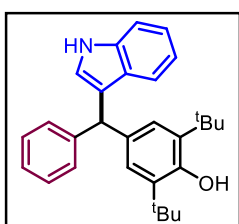
The reaction was performed at 0.123 mmol scale of **21a**; $R_f = 0.3$ (5% EtOAc in hexane); White solid (54.2 mg, 74% yield); m.p. = 163 – 165 °C; ^1H NMR (400 MHz, CDCl_3) δ 8.0 (d, $J = 8.4$ Hz, 1H), 7.7 (d, $J = 8.4$ Hz, 2H), 7.29 – 7.25 (m, 1H), 7.21 (d, $J = 8.1$ Hz, 2H), 7.12 – 7.09 (m, 2H), 7.05 (d, $J = 8.7$ Hz, 2H), 6.92 – 6.90 (m, 3H), 6.82 (d, $J = 8.7$ Hz, 2H), 5.39 (s, 1H), 5.12 (s, 1H), 3.80 (s, 3H), 2.37 (s, 3H), 1.36 (s, 18H); $^{13}\text{C}\{^1\text{H}\}$ NMR (100 MHz, CDCl_3) δ 158.2, 152.4, 144.8, 136.0, 135.6, 135.3, 134.8, 133.0, 130.8, 129.9 (2C), 128.5, 126.8, 125.5, 125.4, 124.7, 123.2, 120.8, 113.9, 113.8, 55.3, 47.6, 34.4, 30.4, 21.7; FT-IR (thin film, neat): 3632, 2957, 1610, 1510, 1434, 1174, 1127 cm^{-1} ; HRMS (ESI-TOF) m/z : $[\text{M}+\text{Na}]^+$ calcd for $\text{C}_{37}\text{H}_{41}\text{NO}_4\text{SNa}$ 618.2654 found: 618.2645.

2,6-di-tert-butyl-4-((4-methoxyphenyl)(5-nitro-1H-indol-3-yl)methyl)phenol (23c):



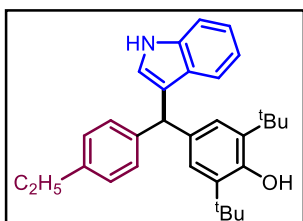
The reaction was performed at 0.123 mmol scale of **21a**; $R_f = 0.1$ (5% EtOAc in hexane); Yellow solid (40.6 mg, 68% yield); m. p. = 196 – 197°C; ^1H NMR (400 MHz, CDCl_3), δ 8.33 (brs, 1H), 8.18 (s, 1H), 8.06 (d, $J = 9.0$ Hz, 1H), 7.36 (d, $J = 8.9$ Hz, 1H), 7.13 (d, $J = 7.6$ Hz, 1H), 7.01 (s, 2H), 6.83 (d, $J = 7.6$ Hz, 2H), 6.79 (s, 1H), 5.54 (s, 1H), 5.09 (s, 1H), 3.79 (s, 3H), 1.36 (s, 18H); $^{13}\text{C}\{^1\text{H}\}$ NMR (100 MHz, CDCl_3) δ 158.2, 152.4, 141.6, 139.8, 136.0, 135.8, 133.9, 129.8 (2C), 126.7, 125.4, 124.0, 117.9, 117.6, 113.9, 111.1, 55.4, 47.7, 34.5, 30.5; FT-IR (thin film, neat): 3628, 3400, 2955, 1610, 1468, 1434 cm^{-1} ; HRMS (ESI-TOF) m/z : $[\text{M}+\text{H}]^+$ calcd for $\text{C}_{30}\text{H}_{35}\text{N}_2\text{O}_4$ 487.2597; found: 487.2581.

4-((1H-indol-3-yl)(phenyl)methyl)-2,6-di-tert-butylphenol (23d):



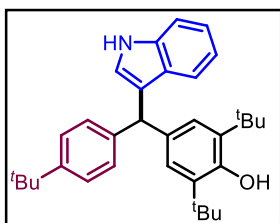
The reaction was performed at 0.1360 mmol scale of **21b**; $R_f = 0.4$ (5% EtOAc in hexane); White solid (52.6 mg, 94% yield); m.p. = 148 – 149 °C; ^1H NMR (400 MHz, CDCl_3) δ 7.90 (brs, 1H), 7.35 (d, $J = 8.1$ Hz, 1H), 7.28 – 7.25 (m, 5H), 7.22 – 7.15 (m, 2H), 7.07 (s, 2H), 6.99 (t, $J = 7.4$ Hz, 1H), 6.61 (d, $J = 0.96$ Hz, 1H), 5.59 (s, 1H), 5.08 (s, 1H), 1.38 (s, 18H); $^{13}\text{C}\{^1\text{H}\}$ NMR (100 MHz, CDCl_3) δ 152.1, 144.7, 136.8, 135.5, 134.6, 129.1, 128.2, 127.3, 126.1, 125.7, 124.0, 122.0, 121.0, 120.2, 119.3, 111.1, 48.9, 34.5, 30.5; FT-IR (thin film, neat): 3641, 3421, 2958, 1601, 1456, cm^{-1} ; HRMS (ESI-TOF) m/z : $[\text{M}+\text{H}]^+$ calcd for $\text{C}_{29}\text{H}_{32}\text{NO}$ 410.2484; found: 410.2477.

2,6-di-tert-butyl-4-((4-ethylphenyl)(1H-indol-3-yl)methyl)phenol (23e):



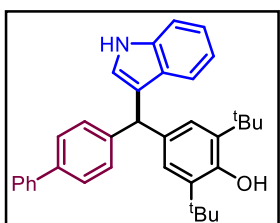
The reaction was performed at 0.124 mmol scale of **21c**; $R_f = 0.5$ (5% EtOAc in hexane); white solid (50.0 mg, 92% yield); m.p = 161 – 162 °C; ^1H NMR (400 MHz, CDCl_3) δ 7.86 (brs, 1H), 7.33 (d, $J = 8.1$ Hz, 1H), 7.27 (d, $J = 7.9$ Hz, 1H), 7.17 (t, $J = 7.5$ Hz, 3H), 7.14 – 7.10 (m, 2H), 7.08 (s, 2H), 7.0 (t, $J = 7.4$ Hz, 1H), 6.62 (s, 1H), 5.55 (s, 1H), 5.07 (s, 1H), 2.64 (q, $J = 7.5$ Hz, 2H), 1.39 (s, 18H), 1.24 (t, $J = 7.6$ Hz, 3H); $^{13}\text{C}\{^1\text{H}\}$ NMR (100 MHz, CDCl_3) δ 152.1, 142.0, 141.8, 136.8, 135.4, 134.8, 128.9, 127.7, 127.3, 125.6, 123.8, 122.0, 121.2, 120.3, 119.3, 111.0, 48.6, 34.5, 30.5, 28.6, 15.7; FT-IR (thin film, neat): 3636, 3418, 2961, 1510, 1456, 1154, 764 cm^{-1} ; HRMS (ESI-TOF) m/z : $[\text{M}+\text{H}]^+$ calcd for $\text{C}_{31}\text{H}_{38}\text{NO}$: 440.2953; found: 440.2968.

2,6-di-tert-butyl-4-((4-(tert-butyl)phenyl)(1H-indol-3-yl)methyl)phenol (23f):



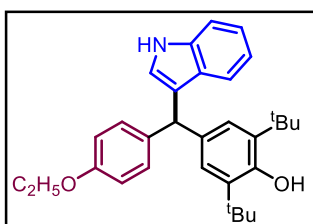
The reaction was performed at 0.1141 mmol scale of **21d**; $R_f = 0.5$ (5% EtOAc in hexane); White solid (47.0 mg, 88% yield); m.p. = 172 – 173°C; ^1H NMR (400 MHz, CDCl_3) δ 7.90 (brs, 1H), 7.33 (d, $J = 8.1$ Hz, 1H), 7.28 – 7.24 (m, 3H), 7.17 – 7.12 (m, 3H), 7.05 (s, 2H), 6.97 (t, $J = 7.6$ Hz, 1H), 6.64 (s, 1H), 5.52 (s, 1H), 5.04 (s, 1H), 1.36 (s, 18H), 1.29 (s, 9H); $^{13}\text{C}\{^1\text{H}\}$ NMR (100 MHz, CDCl_3) δ 152.1, 148.7, 141.7, 136.8, 135.4, 134.8, 128.5, 127.4, 125.7, 125.1, 123.8, 122.0, 121.2, 120.3, 119.2, 111.0, 48.5, 34.5 (2C), 31.6, 30.5; FT-IR (thin film, neat): 3641, 3419, 2959, 1456, 1434, 764.37 cm^{-1} ; HRMS (ESI-TOF) m/z : $[\text{M}-\text{H}]^-$ calcd for $\text{C}_{33}\text{H}_{40}\text{NO}$ 466.3110; found: 466.3130.

4-([1,1'-biphenyl]-4-yl)(1H-indol-3-yl)methyl)-2,6-di-tert-butylphenol (23g):



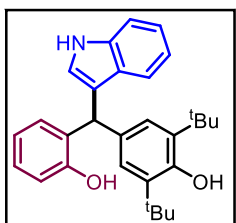
The reaction was performed at 0.108mmol scale of **21e**; $R_f = 0.2$ (5% EtOAc in hexane); White solid (46.8 mg, 89% yield); m.p. = 116 – 118 °C; ^1H NMR (400 MHz, CDCl_3) δ 7.94 (brs, 1H), 7.63 (d, $J = 7.7$ Hz, 2H), 7.55 (d, $J = 7.6$ Hz, 2H), 7.45 (t, $J = 7.2$ Hz, 2H), 7.37 – 7.35 (m, 3H), 7.33 (d, $J = 7.7$ Hz, 2H), 7.19 (t, $J = 7.4$ Hz, 1H), 7.13 (s, 2H), 7.03 (t, $J = 7.6$ Hz, 1H), 6.67 (s, 1H), 5.65 (s, 1H), 5.12 (s, 1H), 1.41 (s, 18H); $^{13}\text{C}\{^1\text{H}\}$ NMR (100 MHz, CDCl_3) δ 152.2, 144.0, 141.2, 138.7, 136.8, 135.5, 134.5, 129.4, 128.8, 127.2, 127.1 (2C), 126.9, 125.7, 124.0, 122.1, 120.8, 120.2, 119.4, 111.1, 48.6, 34.5, 30.5; FT-IR (thin film, neat): 3628, 3417, 2956, 1632, 1486, 1154, 1091, 760 cm^{-1} ; HRMS (ESI-TOF) m/z : $[\text{M}+\text{H}]^+$ calcd for $\text{C}_{35}\text{H}_{38}\text{NO}$ 488.2953; found: 488.2931.

2,6-di-tert-butyl-4-((4-ethoxyphenyl)(1H-indol-3-yl)methyl)phenol (23h):



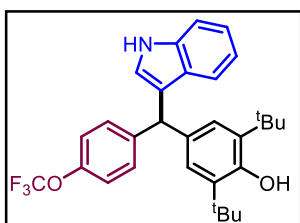
The reaction was performed at 0.118 mmol scale of **21f**; $R_f = 0.2$ (5% EtOAc in hexane); Brown solid (47.9 mg, 89% yield); m.p. = 160 – 162 °C; ^1H NMR (400 MHz, CDCl_3) δ 7.91 (brs, 1H), 7.34 (d, $J = 8.1$ Hz, 1H), 7.24 (d, $J = 8.0$ Hz, 1H), 7.14 (d, $J = 7.96$ Hz, 3H), 7.04 (s, 2H), 6.98 (t, $J = 7.4$ Hz, 1H), 6.80 (d, $J = 8.2$ Hz, 2H), 6.59 (s, 1H), 5.51 (s, 1H), 5.05 (s, 1H), 4.0 (q, $J = 6.7$ Hz, 2H), 1.44 – 1.40 (m, 3H), 1.37 (s, 18H); $^{13}\text{C}\{^1\text{H}\}$ NMR (100 MHz, CDCl_3) δ 157.3, 152.1, 136.9, 136.8, 135.5, 135.0, 130.0, 127.3, 125.6, 123.9, 122.0, 121.3, 120.3, 119.3, 114.2, 111.02, 63.5, 48.1, 34.5, 30.5, 15.1; FT-IR (thin film, neat): 3634, 3415, 2957, 1610, 1456, 1117 cm^{-1} ; HRMS (ESI-TOF): m/z : $[\text{M}+\text{H}]^+$ calcd for $\text{C}_{31}\text{H}_{38}\text{NO}_2$ 456.2903; found: 456.2921.

2,6-di-tert-butyl-4-((2-hydroxyphenyl)(1H-indol-3-yl)methyl)phenol (23i):



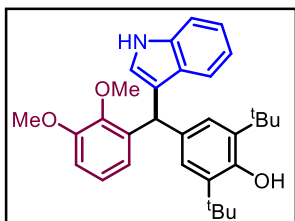
The reaction was performed at 0.129 mmol scale of **21g**; $R_f = 0.1$ (5% EtOAc in hexane); Brown solid (46.4 mg, 85% yield); m.p = 147 – 148 °C; ^1H NMR (400 MHz, CDCl_3) δ 8.0 (brs, 1H), 7.35 (d, $J = 8.2$ Hz, 1H), 7.32 (d, $J = 8.2$ Hz, 1H), 7.22 – 7.15 (m, 2H), 7.12 (s, 2H), 7.05 – 7.01 (m, 2H), 6.89 – 6.84 (m, 2H), 6.69 (s, 1H), 5.71 (s, 1H), 5.19 (s, 1H), 5.15 (s, 1H), 1.38 (s, 18H); $^{13}\text{C}\{^1\text{H}\}$ NMR (100 MHz, CDCl_3) δ 154.3, 152.6, 137.0, 136.0, 132.3, 130.2, 130.1, 128.0, 127.0, 125.5, 123.9, 122.5, 120.8, 120.04, 119.7, 118.6, 116.5, 111.3, 44.0, 34.5, 30.4; FT-IR (thin film, neat): 3634, 3413, 2958, 1456, 1154, 1091 cm^{-1} ; HRMS (ESI-TOF): m/z : $[\text{M}-\text{H}]^-$ calcd for $\text{C}_{29}\text{H}_{32}\text{NO}_2$ 426.2433; found: 426.2449.

4-((1H-indol-3-yl)(4-(trifluoromethoxy)phenyl)methyl)-2,6-di-tert-butylphenol (23j):



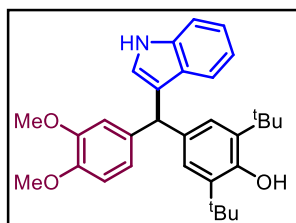
The reaction was performed at 0.106 mmol scale of **21h**; $R_f = 0.2$ (5% EtOAc in hexane); White solid (45.1 mg, 86% yield); m.p. = 164 – 165 °C; ^1H NMR (400 MHz, CDCl_3) δ 7.96 (brs, 1H), 7.37 (d, $J = 8.1$ Hz, 1H), 7.27 (d, $J = 7.5$ Hz, 2H), 7.23 (d, $J = 8.04$ Hz, 1H), 7.18 (t, $J = 7.4$ Hz, 1H), 7.12 (d, $J = 8.04$ Hz, 2H), 7.02 – 6.99 (m, 3H), 6.61 (s, 1H), 5.59 (s, 1H), 5.11 (s, 1H), 1.38 (s, 18H); $^{13}\text{C}\{^1\text{H}\}$ NMR (100 MHz, CDCl_3) δ 152.3, 147.6 (q, $^3J_{\text{C-F}} = 1.7$ Hz), 143.5, 136.8, 135.7, 134.03, 130.3, 127.0, 125.6, 124.0, 121.1 (q, $^1J_{\text{C-F}} = 221.0$ Hz), 120.7, 120.4, 119.5, 111.2, 48.2, 34.5, 30.5; $^{19}\text{F}\{^1\text{H}\}$ NMR (376 MHz, CDCl_3) δ -57.82; FT-IR (thin film, neat): 3641, 3414, 2960, 1434, 1222, 1162, 764, 749 cm^{-1} ; HRMS (ESI-TOF): m/z : $[\text{M}-\text{H}]^-$ calcd for $\text{C}_{30}\text{H}_{31}\text{F}_3\text{NO}_2$ 494.2307; found: 494.2322.

2,6-di-tert-butyl-4-((2,3-dimethoxyphenyl)(1H-indol-3-yl)methyl)phenol (23k):



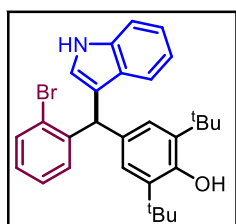
The reaction was performed at 0.1128 mmol scale of **21i**; $R_f = 0.1$ (5% EtOAc in hexane); Colourless gummy solid (44.3 mg, 84% yield); ^1H NMR (400 MHz, CDCl_3) δ 7.92 (brs, 1H), 7.32 (d, $J = 8.1$ Hz, 1H), 7.27 (d, $J = 8.5$ Hz, 1H), 7.14 (t, $J = 7.3$ Hz, 1H), 7.09 (s, 1H), 6.97 (t, $J = 7.3$ Hz, 1H), 6.91 (t, $J = 7.96$ Hz, 1H), 6.78 (d, $J = 8.0$, 1H), 6.70 (d, $J = 7.7$ Hz, 1H), 6.64 (s, 1H), 6.0 (s, 1H), 5.03 (s, 1H), 3.87 (s, 3H), 3.58 (s, 3H), 1.37 (s, 18H); $^{13}\text{C}\{^1\text{H}\}$ NMR (100 MHz, CDCl_3) δ 152.7, 152.0, 146.8, 139.0, 136.8, 135.4, 134.5, 127.3, 125.7, 124.1, 123.5, 122.0, 121.9, 120.7, 120.2, 119.2, 111.0, 110.3, 60.5, 55.8, 41.7, 34.5, 30.5; FT-IR (thin film, neat): 3634, 3415, 2959, 1476, 1275, 1155, 1072 cm^{-1} ; HRMS (ESI-TOF) m/z : $[\text{M}+\text{H}]^+$ calcd for $\text{C}_{31}\text{H}_{38}\text{NO}_3$ 472.2852; found: 472.2838.

2,6-di-tert-butyl-4-((3,4-dimethoxyphenyl)(1H-indol-3-yl)methyl)phenol (**23l**):



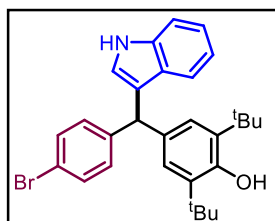
The reaction was performed at 0.113 mmol scale of **21j**; $R_f = 0.1$ (5% EtOAc in hexane); Colourless solid (46.41 mg, 88% yield); m. p. = 200–203 °C; ^1H NMR (400 MHz, CDCl_3) δ 7.95 (brs, 1H), 7.34 (d, $J = 8.1$ Hz, 1H), 7.26 (d, $J = 7.7$ Hz, 1H), 7.15 (t, $J = 7.8$ Hz, 1H), 7.07 (s, 2H), 6.98 (t, $J = 7.6$ Hz, 1H), 6.83 (s, 1H), 6.79 – 6.75 (m, 2H), 6.60 (s, 1H), 5.51 (s, 1H), 5.07 (s, 1H), 3.86 (s, 3H), 3.77 (s, 3H), 1.37 (s, 18H). $^{13}\text{C}\{^1\text{H}\}$ NMR (100 MHz, CDCl_3) δ 152.1, 148.6, 147.2, 137.4, 136.8, 135.4, 134.6, 127.2, 125.5, 123.8, 122.0, 121.3, 121.1, 120.2, 119.3, 112.5, 111.0, 110.9, 55.9, 48.5, 34.5, 30.5; FT-IR (thin film, neat): 3638, 3411, 2956, 1434, 1232, 1138, 1027 cm^{-1} ; HRMS (ESI-TOF) m/z : $[\text{M}+\text{H}]^+$ calcd for $\text{C}_{31}\text{H}_{38}\text{NO}_3$ 472.2852; found: 472.2866.

4-((2-bromophenyl)(1H-indol-3-yl)methyl)-2,6-di-tert-butylphenol (**23m**):

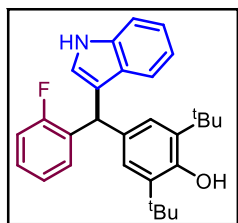


The reaction was performed at 0.107 mmol scale of **21k**; $R_f = 0.2$ (5% EtOAc in hexane); White solid (47.8 mg, 82% yield); m.p = 173 – 174 °C; ^1H NMR (400 MHz, CDCl_3) δ 7.93 (brs, 1H), 7.59 (d, $J = 7.8$ Hz, 1H), 7.34 (d, $J = 8.2$, 1H), 7.20 (d, $J = 7.96$ Hz, 1H), 7.18 – 7.15 (m, 3H), 7.07 – 7.03 (m, 3H), 7.0 (t, $J = 7.2$ Hz, 1H), 6.60 (s, 1H), 6.0 (s, 1H), 5.1 (s, 1H), 1.38 (s, 18H); $^{13}\text{C}\{^1\text{H}\}$ NMR (100 MHz, CDCl_3) δ 152.2, 143.8, 136.8, 135.5, 132.9, 132.5, 130.7, 127.8, 127.3, 127.1, 125.9, 125.2, 124.2, 122.2, 120.2, 120.1, 119.5, 111.1, 47.9, 34.5, 30.5; FT-IR (thin film, neat): 3637, 3419, 2958, 1457, 1234, 805 cm^{-1} ; HRMS (ESI-TOF) m/z : $[\text{M}+\text{H}]^+$ calcd for $\text{C}_{29}\text{H}_{33}\text{BrNO}$ 490.1746; found: 490.1729.

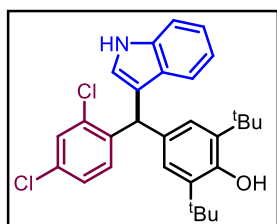
4-((4-bromophenyl)(1H-indol-3-yl)methyl)-2,6-di-tert-butylphenol (**23n**):



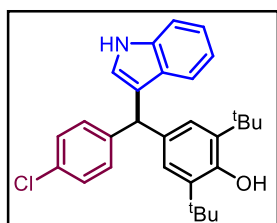
The reaction was performed at 0.122 mmol scale of **21l**; $R_f = 0.3$ (5% EtOAc in hexane); White solid (48.2 mg, 91% yield); m.p = 188 – 189 °C; ^1H NMR (400 MHz, CDCl_3) δ 7.94 (brs, 1H), 7.39 (d, $J = 7.9$ Hz, 2H), 7.35 (d, $J = 8.1$ Hz, 1H), 7.21 (d, $J = 7.96$ Hz, 1H), 7.18 (t, $J = 7.8$ Hz, 1H), 7.13 (d, $J = 8.0$ Hz, 2H), 7.03 (s, 2H), 6.99 (d, $J = 7.4$ Hz, 1H), 6.60 (s, 1H), 5.53 (s, 1H), 5.11 (s, 1H), 1.38 (s, 18H); $^{13}\text{C}\{^1\text{H}\}$ NMR (100 MHz, CDCl_3) δ 152.3, 143.9, 136.8, 135.6, 133.9, 131.3, 130.8, 127.0, 125.5, 124.0, 122.2, 120.3, 120.0, 119.9, 119.5, 111.2, 48.4, 34.5, 30.5; FT-IR (thin film, neat): 3628, 3414, 2957, 1633, 1485, 760 cm^{-1} ; HRMS (ESI-TOF): m/z : $[\text{M}-\text{H}]^-$ calcd for $\text{C}_{29}\text{H}_{31}\text{BrNO}$ 488.1589; found: 488.1573.

2,6-di-tert-butyl-4-((2-fluorophenyl)(1H-indol-3-yl)methyl)phenol (23o):

The reaction was performed at 0.128 mmol scale of **21m**; $R_f = 0.2$ (5% EtOAc in hexane); White solid (44.6 mg, 81% yield); m.p. = 194 – 196 °C; ^1H NMR (400 MHz, CDCl_3) δ 7.93 (brs, 1H), 7.35 (d, $J = 8.1$ Hz, 1H), 7.25 (d, $J = 7.84$ Hz, 1H), 7.21 – 7.15 (m, 2H), 7.13 – 7.09 (m, 1H), 7.09 – 7.07 (m, 3H), 7.02 – 6.98 (m, 2H), 6.63 (s, 1H), 5.90 (s, 1H), 5.09 (s, 1H), 1.38 (s, 18H); $^{13}\text{C}\{^1\text{H}\}$ NMR (100 MHz, CDCl_3) δ 160.8 (d, $^1J_{\text{C-F}} = 244.4$ Hz), 152.3, 136.9, 135.6, 133.1, 131.7 (d, $^2J_{\text{C-F}} = 14.2$ Hz), 130.5 (d, $^4J_{\text{C-F}} = 4.2$ Hz), 127.8 (d, $^3J_{\text{C-F}} = 8.1$ Hz), 127.05, 125.5, 124.1, 123.9 (d, $^5J_{\text{C-F}} = 3.4$ Hz), 122.2, 119.9, 119.7, 119.4, 115.3 (d, $^2J_{\text{C-F}} = 22.2$ Hz), 111.1, 41.1 (d, $^5J_{\text{C-F}} = 3.4$ Hz), 34.5, 30.5; $^{19}\text{F}\{^1\text{H}\}$ NMR (376 MHz, CDCl_3) δ -117.78; FT-IR (thin film, neat): 3634, 3418, 2958, 1455, 763, 749 cm^{-1} ; HRMS (ESI-TOF) m/z : $[\text{M-H}]^-$ calcd for $\text{C}_{29}\text{H}_{31}\text{FNO}$ 428.2490; found: 428.2479.

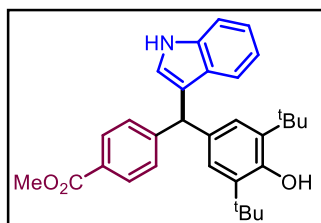
2,6-di-tert-butyl-4-((2,4-dichlorophenyl)(1H-indol-3-yl)methyl)phenol (23p):

The reaction was performed at 0.110 mmol scale of **21n**; $R_f = 0.3$ (5% EtOAc in hexane); White solid (43.9 mg, 83% yield); m.p = 181 – 183 °C; ^1H NMR (400 MHz, CDCl_3) δ 7.96 (brs, 1H), 7.40 (s, 1H), 7.36 (d, $J = 8.3$ Hz, 1H), 7.18 – 7.15 (m, 2H), 7.10 – 7.04 (m, 2H), 7.01 (s, 2H), 6.99 (d, $J = 7.8$ Hz, 1H), 6.59 (s, 1H), 5.93 (s, 1H), 5.09 (s, 1H), 1.37 (s, 18H); $^{13}\text{C}\{^1\text{H}\}$ NMR (100 MHz, CDCl_3) δ 152.4, 141.0, 136.9, 135.7, 134.9, 132.4, 132.1, 131.4, 129.4, 126.9, 126.88, 125.7, 124.3, 122.4, 119.9, 119.6, 119.5, 111.2, 44.9, 34.5, 30.5; FT-IR (thin film, neat): 3634, 3417, 2960, 1588, 1434, 798 cm^{-1} ; HRMS (ESI-TOF) m/z : $[\text{M-H}]^-$ calcd for $\text{C}_{29}\text{H}_{30}\text{Cl}_2\text{NO}$ 478.1704; found: 478.1720.

2,6-di-tert-butyl-4-((4-chlorophenyl)(1H-indol-3-yl)methyl)phenol (23q):

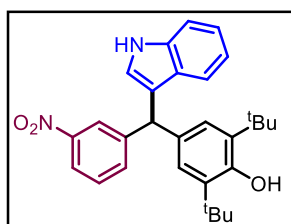
The reaction was performed at 0.122 mmol scale of **21o**; $R_f = 0.3$ (5% EtOAc in hexane); White solid (47.4 mg, 87% yield); m.p = 188 – 189 °C; ^1H NMR (400 MHz, CDCl_3) δ 7.94 (brs, 1H), 7.36 (d, $J = 8.1$ Hz, 1H), 7.26 – 7.16 (m, 6H), 7.03 (s, 2H), 7.0 (d, $J = 7.7$ Hz, 1H), 6.60 (s, 1H), 5.55 (s, 1H), 5.10 (s, 1H), 1.38 (s, 18H); $^{13}\text{C}\{^1\text{H}\}$ NMR (100 MHz, CDCl_3) δ 152.3, 143.3, 136.8, 135.7, 134.06, 131.7, 130.4, 128.4, 127.0, 125.5, 124.0, 122.2, 120.5, 120.07, 119.5, 111.2, 48.3, 34.5, 30.5; FT-IR (thin film, neat): 3636, 3416, 2959, 1488, 1456 cm^{-1} ; HRMS (ESI-TOF) m/z : $[\text{M-H}]^-$ calcd for $\text{C}_{29}\text{H}_{31}\text{ClNO}$ 444.2094; found: 444.2109.

Methyl 4-((3,5-di-tert-butyl-4-hydroxyphenyl)(1H-indol-3-yl)methyl)benzoate (23r):



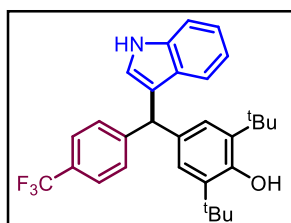
The reaction was performed at 0.123 mmol scale of **21p**; $R_f = 0.2$ (5% EtOAc in hexane); White solid (39.6 mg, 77% yield); m.p. = 170 – 171 °C; ^1H NMR (400 MHz, CDCl_3) δ 8.0 (brs, 1H), 7.95 (d, $J = 8.0$ Hz, 2H), 7.36 (d, $J = 8.1$ Hz, 1H), 7.32 (d, $J = 8.0$ Hz, 2H), 7.19 – 7.14 (m, 2H), 7.01 (s, 2H), 6.98 (t, $J = 7.5$ Hz, 1H), 6.60 (s, 1H), 5.61 (s, 1H), 5.10 (s, 1H), 3.89 (s, 3H), 1.36 (s, 18H); $^{13}\text{C}\{^1\text{H}\}$ NMR (100 MHz, CDCl_3) δ 167.4, 152.3, 150.3, 136.8, 135.7, 133.7, 129.7, 129.1, 128.0, 127.0, 125.6, 124.1, 122.2, 120.1, 120.0, 119.5, 111.2, 52.1, 48.9, 34.5, 30.5; FT-IR (thin film, neat): 3628, 3417, 2953, 1710, 1433, 1281, 1119 cm^{-1} ; HRMS (ESI-TOF) m/z : $[\text{M}-\text{H}]^-$ calcd for $\text{C}_{31}\text{H}_{34}\text{NO}_3$ 468.2539; found: 468.2559.

4-((1H-indol-3-yl)(3-nitrophenyl)methyl)-2,6-di-tert-butylphenol (23s):



The reaction was performed at 0.118 mmol scale of **21q**; $R_f = 0.2$ (5% EtOAc in hexane); Yellow solid (31.2 mg, 58% yield); m.p. = 190 – 192 °C; ^1H NMR (400 MHz, CDCl_3) δ 8.15 (brs, 1H), 8.07 (d, $J = 8.3$ Hz, 1H), 8.04 (s, 1H), 7.58 (d, $J = 7.6$ Hz, 1H), 7.43 (t, $J = 7.9$ Hz, 1H), 7.38 (d, $J = 8.4$ Hz, 1H), 7.20 – 7.17 (m, 2H), 7.02 (s, 2H), 7.0 (d, $J = 7.6$ Hz, 1H), 6.63 (s, 1H), 5.7 (s, 1H), 5.14 (s, 1H), 1.37 (s, 18H); $^{13}\text{C}\{^1\text{H}\}$ NMR (100 MHz, CDCl_3) δ 152.6, 148.5, 147.1, 136.9, 135.9, 135.2, 133.03, 129.2, 126.7, 125.5 (2C), 124.2, 124.0, 122.4, 121.5, 119.7, 119.5, 111.3, 48.6, 34.5, 30.4; FT-IR (thin film, neat): 3631, 3415, 2958, 1528, 1456, 1235, 1094 cm^{-1} ; HRMS (ESI-TOF) m/z : $[\text{M}-\text{H}]^-$ calcd for $\text{C}_{29}\text{H}_{31}\text{N}_2\text{O}_3$ 455.2335; found: 455.2345.

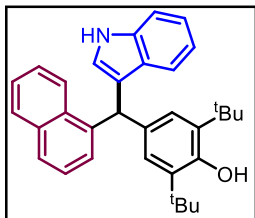
4-((1H-indol-3-yl)(4-(trifluoromethyl)phenyl)methyl)-2,6-di-tert-butylphenol (23t):



The reaction was performed at 0.110 mmol scale of **21r**; $R_f = 0.2$ (5% EtOAc in hexane); White solid (46.9 mg, 89% yield); m.p. = 177 – 179 °C; ^1H NMR (400 MHz, CDCl_3) δ 7.97 (brs, 1H), 7.53 (d, $J = 8.1$ Hz, 2H), 7.37 (d, $J = 8.2$ Hz, 3H), 7.21 – 7.17 (m, 2H), 7.03 (s, 2H), 7.0 (d, $J = 7.4$ Hz, 1H), 6.62 (d, $J = 1.5$ Hz, 1H), 5.63 (s, 1H), 5.12 (s, 1H), 1.38 (s, 18H); $^{13}\text{C}\{^1\text{H}\}$ NMR (100 MHz, CDCl_3) δ 152.4, 149.0, 136.9, 135.8, 133.6, 129.3, 128.4 (q, $^2J_{\text{C-F}} = 30.6$ Hz), 127.0, 125.7 (q, $^1J_{\text{C-F}} = 270.0$ Hz), 125.6, 125.2 (q, $^3J_{\text{C-F}} = 3.4$ Hz), 124.1, 122.3, 120.0 (q, $^3J_{\text{C-F}} = 4.8$ Hz), 119.9, 119.6, 111.2, 48.8, 34.5, 30.5; $^{19}\text{F}\{^1\text{H}\}$ NMR (376 MHz,

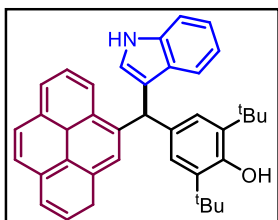
CDCl_3) δ -62.14; FT-IR (thin film, neat): 3638, 3416, 2959, 11617, 1456, 1235, 861, 760 cm^{-1} ; HRMS (ESI-TOF) m/z : $[\text{M}-\text{H}]^-$ calcd for $\text{C}_{30}\text{H}_{31}\text{F}_3\text{NO}$: 478.2358; found: 478.2372.

4-((1H-indol-3-yl)(naphthalen-2-yl)methyl)-2,6-di-tert-butylphenol (23u):



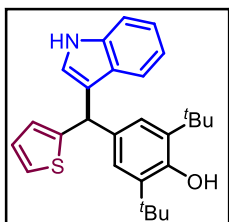
The reaction was performed at 0.116 mmol scale of **21s**; R_f = 0.2 (5% EtOAc in hexane); white solid (48.3 mg, 90% yield); m.p. = 200 – 202 $^\circ\text{C}$; ^1H NMR (400 MHz, CDCl_3) δ 8.20 (d, J = 7.7 Hz, 1H), 7.88 – 7.86 (m, 2H), 7.73 (d, J = 7.9 Hz, 1H), 7.45 – 7.40 (m, 2H), 7.36 – 7.34 (m, 2H), 7.25 (d, J = 8.8 Hz, 1H), 7.18 – 7.15 (m, 2H), 7.08 (s, 2H), 6.98 (t, J = 7.4 Hz, 1H), 6.50 (s, 1H), 6.34 (s, 1H), 5.05 (s, 1H), 1.35 (s, 18H); $^{13}\text{C}\{^1\text{H}\}$ NMR (100 MHz, CDCl_3) δ 152.2, 147.2, 140.6, 136.8, 135.5, 134.0, 133.8, 132.1, 128.7, 127.2, 126.9, 126.7, 125.9 (2C), 125.5, 125.3, 124.6, 124.5, 122.1, 120.9, 120.1, 119.3, 111.1, 44.6, 34.5, 30.5; FT-IR (thin film, neat): 3625, 3420, 2963, 1632, 1433, 1260, 764 cm^{-1} ; HRMS (ESI-TOF) m/z : $[\text{M}+\text{H}]^+$ calcd for $\text{C}_{33}\text{H}_{36}\text{NO}$ 462.2797; found: 462.2785.

4-((1H-indol-3-yl)(pyren-1-yl)methyl)-2,6-di-tert-butylphenol (23v):



The reaction was performed at 0.1161 mmol scale of **21t**; R_f = 0.2 (5% EtOAc in hexane); white solid (40.7 mg, 76% yield); m.p. = 218 – 220 $^\circ\text{C}$; ^1H NMR (400 MHz, CDCl_3) δ 8.50 (d, J = 9.4 Hz, 1H), 8.16 (t, J = 6.8 Hz, 2H), 8.06 (d, J = 8.5 Hz, 2H), 8.03 (s, 2H), 7.98 (t, J = 7.6, 2H), 7.92 (s, 1H), 7.76 (d, J = 8.0 Hz, 1H), 7.36 (d, J = 8.1 Hz, 1H), 7.19 – 7.16 (m, 2H), 7.15 (s, 2H), 6.93 (t, J = 7.2 Hz, 1H), 6.67 (s, 1H), 6.52 (d, J = 1.44 Hz, 1H), 5.08 (s, 1H), 1.34 (s, 18H); $^{13}\text{C}\{^1\text{H}\}$ NMR (100 MHz, CDCl_3) δ 152.2, 138.8, 136.9, 135.6, 134.1, 131.6, 131.0, 130.0, 128.9, 127.8, 127.4, 127.3, 127.2, 126.8, 126.0, 125.9 (2C), 125.3, 125.1, 125.0, 124.88, 124.86, 124.77, 124.0, 122.1, 121.3, 120.2, 119.4, 111.1, 45.0, 34.5, 30.5; FT-IR (thin film, neat): 3625, 3420, 2963, 1632, 1433, 1260, 764 cm^{-1} ; HRMS (ESI-TOF) m/z : $[\text{M}-\text{H}]^-$ calcd for $\text{C}_{39}\text{H}_{36}\text{NO}$ 534.2797; found: 534.2811.

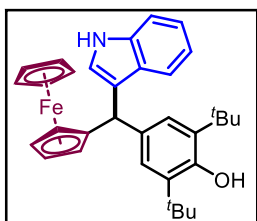
4-((1H-indol-3-yl)(thiophen-2-yl)methyl)-2,6-di-tert-butylphenol (23w):



The reaction was performed at 0.136 mmol scale of **21u**; R_f = 0.3 (5% EtOAc in hexane); White solid (46.9 mg, 84% yield); m.p. = 164–165 $^\circ\text{C}$; ^1H NMR (400 MHz, CDCl_3) δ 7.95 (brs, 1H), 7.36 (t, J = 9.3 Hz, 2H), 7.19 – 7.15 (m, 4H), 7.03 (t, J = 7.5 Hz, 1H), 6.92 (s, 1H), 6.81 (s, 1H), 6.78 (s, 1H), 5.79 (s, 1H), 5.09 (s, 1H), 1.39 (s, 18H); $^{13}\text{C}\{^1\text{H}\}$ NMR (100

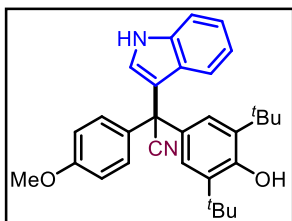
MHz, CDCl₃) δ 152.4, 149.5, 136.6, 135.6, 134.4, 127.0, 126.5, 125.4, 125.2, 123.9, 123.3, 122.1, 120.9, 120.0, 119.5, 111.2, 44.2, 34.5, 30.5; FT-IR (thin film, neat): 3634, 3416, 2956, 1433, 1270, 760, 697 cm⁻¹; HRMS (ESI-TOF) m/z : [M+H]⁺ calcd for C₂₇H₃₂NOS 418.2205; found: 418.2188.

4-((1H-indol-3-yl)(ferrocene-2-yl)methyl)-2,6-di-tert-butylphenol (23x):



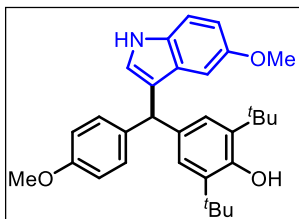
The reaction was performed at 0.136mmol scale of **21v**; R_f = 0.3 (5% EtOAc in hexane); White solid (38.5 mg, 74% yield); m. p. = 134 – 135°C; ¹H NMR (400 MHz, CDCl₃) δ 7.87 (brs, 1H), 7.38 (d, J = 7.9 Hz, 1H), 7.30 (d, J = 8.1 Hz, 1H), 7.19 (s, 2H), 7.12 (t, J = 7.7 Hz, 1H), 7.00 (t, J = 7.3 Hz, 1H), 6.83 (s, 1H), 5.20 (s, 1H), 5.03 (s, 1H), 4.17 (s, 1H), 4.10 (s, 2H), 3.96 (s, 6H), 1.42 (s, 18H); ¹³C{¹H} NMR (100 MHz, CDCl₃) δ 152.0, 136.5, 135.2 (2C), 127.0, 125.3, 122.2, 122.1, 121.8, 120.0, 119.1, 111.0, 94.0, 68.9, 68.7, 68.4, 68.0, 67.3, 67.2, 43.5, 34.5, 30.6; FT-IR (thin film, neat): 3634, 3416, 2956, 1433, 1270, 760, 697 cm⁻¹; HRMS (ESI-TOF) m/z : [M+H]⁺ calcd for C₃₃H₃₈FeNO 520.2303; found: 520.2327.

2-(3,5-di-tert-butyl-4-hydroxyphenyl)-2-(1H-indol-3-yl)-2-(4-methoxyphenyl)acetonitrile (23y):



The reaction was performed at 0.130 mmol scale of **21w**; R_f = 0.2 (5% EtOAc in hexane); white solid (46.1 mg, 90% yield); m.p. = 170 – 171 °C ¹H NMR (400 MHz, CDCl₃) δ 8.23 (brs, 1H), 7.35 (d, J = 6.90 Hz, 1H), 7.33 (t, J = 9.8 Hz, 3H), 7.20 (d, J = 7.4 Hz, 1H), 7.16 (s, 2H), 7.04 (t, J = 7.5 Hz, 1H), 6.86 (d, J = 8.08 Hz, 2H), 6.50 (s, 1H), 5.28 (s, 1H), 3.81 (s, 3H), 1.35 (s, 18H); ¹³C{¹H} NMR (100 MHz, CDCl₃) δ 159.1, 153.4, 137.0, 135.8, 132.5, 130.6, 129.5, 125.5, 125.4, 125.1, 123.2, 122.7, 120.9, 117.4, 113.8, 111.5, 55.4, 50.4, 34.6, 30.3; FT-IR (thin film, neat): 3637, 3417, 2957, 2217, 1610, 1456, 1154, 1121 cm⁻¹; HRMS (ESI-TOF) m/z : [M-H]⁻ calcd for C₃₁H₃₃N₂O₂ 465.2542; found: 465.2534.

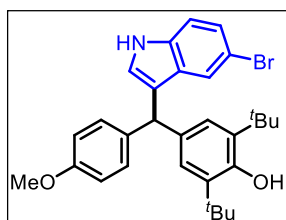
2,6-di-tert-butyl-4-((4-methoxyphenyl)(5-methyl-1H-indol-3-yl)methyl)phenol (28a):



The reaction was performed at 0.123mmol scale of **21a**; R_f = 0.3 (5% EtOAc in hexane); white solid (50.5 mg, 90% yield); m.p. = 184 – 186°C; ¹H NMR (400 MHz, CDCl₃) δ 7.82 (brs, 1H), 7.23 (d, J = 8.2 Hz, 1H), 7.16 (d, J = 8.2 Hz, 2H), 7.05 (s, 3H), 7.05 (d, J = 8.2 Hz, 1H), 6.82 (d, J = 8.1 Hz, 2H), 6.56 (s, 1H), 5.51 (s, 1H), 5.06 (s, 1H), 3.80 (s, 3H), 2.35 (s,

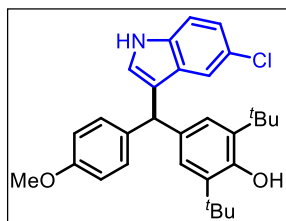
3H), 1.38 (s, 18H); ^{13}C { ^1H } NMR (100 MHz, CDCl_3) δ 157.8, 152.0, 137.1, 135.4, 135.12, 135.07, 129.9, 128.5, 127.5, 125.6, 124.0, 123.6, 120.7, 119.7, 113.5, 110.7, 55.3, 47.9, 34.5, 30.5, 21.6; FT-IR (thin film, neat): 3637, 3415, 2955, 1609, 1433 cm^{-1} ; HRMS (ESI-TOF) m/z : $[\text{M}+\text{H}]^+$ calcd for $\text{C}_{31}\text{H}_{38}\text{NO}_2$ 456.2903; found: 456.2923.

4-((5-bromo-1H-indol-3-yl)(4-methoxyphenyl)methyl)-2,6-di-tert-butylphenol (28b):



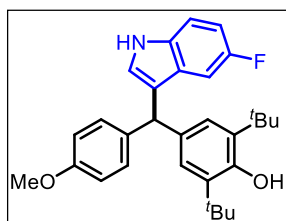
The reaction was performed at 0.123 mmol scale of **21a**; $R_f = 0.3$ (5% EtOAc in hexane); White solid (52.39 mg, 82% yield); m.p. = 192–194 °C; ^1H NMR (400 MHz, CDCl_3), δ 7.96 (brs, 1H), 7.34 (s, 1H), 7.21 (s, 2H), 7.12 (d, $J = 8.1$ Hz, 2H), 7.00 (s, 2H), 6.81 (d, $J = 7.9$ Hz, 2H), 6.61 (s, 1H), 5.45 (s, 1H), 5.07 (s, 1H), 3.79 (s, 3H), 1.36 (s, 18H); ^{13}C { ^1H } NMR (100 MHz, CDCl_3) δ 158.0, 152.2, 136.5, 135.5, 135.4, 134.4, 129.9, 129.0, 125.5, 125.0, 124.9, 122.8, 121.0, 113.7, 112.6, 112.5, 55.4, 47.8, 34.5, 30.5; FT-IR (thin film, neat): 3629, 3421, 2955, 1610, 1460, 1433 cm^{-1} ; HRMS (ESI-TOF) m/z : $[\text{M}+\text{H}]^+$ calcd for $\text{C}_{30}\text{H}_{35}\text{BrNO}_2$ 520.1851; found 520.1829.

2,6-di-tert-butyl-4-((5-chloro-1H-indol-3-yl)(4-methoxyphenyl)methyl)phenol (28c):



The reaction was performed at 0.123mmol scale of **21a**; $R_f = 0.5$ (5% EtOAc in hexane); Pale yellow solid (48.9 mg, 83% yield); m.p. = 115–116 °C; ^1H NMR (400 MHz, CDCl_3), δ 8.28 (brs, 1H), 7.56 (d, $J = 8.2$ Hz, 1H), 7.40 (d, $J = 7.4$ Hz, 1H), 7.18 (t, $J = 7.9$ Hz, 1H), 7.11 (d, $J = 8.4$ Hz, 2H), 7.01 (s, 2H), 6.80 (d, $J = 8.4$ Hz, 2H), 6.78 (s, 1H), 6.08 (s, 1H), 5.06 (s, 1H), 3.77 (s, 3H), 1.36 (s, 18H); ^{13}C { ^1H } NMR (100 MHz, CDCl_3) δ 157.9, 152.1, 136.9, 136.6, 135.5, 134.7, 130.2, 127.0, 126.8., 126.3, 125.8, 125.6, 121.7, 119.3, 116.0, 113.5, 102.8, 55.3, 46.5, 34.5, 30.5; FT-IR (thin film, neat): 3634, 3420, 2955, 1609, 1509, 743 cm^{-1} ; HRMS (ESI-TOF) m/z : $[\text{M}+\text{H}]^+$ calcd for $\text{C}_{30}\text{H}_{35}\text{ClNO}_2$: 476.2356; found: 476.2339.

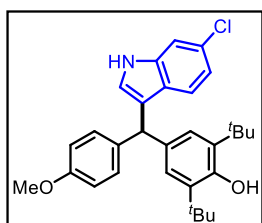
2,6-di-tert-butyl-4-((5-fluoro-1H-indol-3-yl)(4-methoxyphenyl)methyl)phenol (28d):



The reaction was performed at 0.123mmol scale of **21a**; $R_f = 0.5$ (5% EtOAc in hexane); Pale yellow solid (49.0 mg, 67% yield); m.p. = 145 – 146 °C; ^1H NMR (400 MHz, CDCl_3), δ 7.92 (brs, 1H), 7.26 – 7.22 (m, 1H), 7.09 (d, $J = 7.7$ Hz, 2H), 7.03 (s, 2H), 6.91 – 6.81 (m, 4H), 6.64 (s, 1H), 5.44 (s, 1H), 5.08 (s, 1H), 3.80 (s, 3H), 1.37 (s, 18H); ^{13}C { ^1H } NMR (100 MHz, CDCl_3) δ 157.9, 157.5(d, $^1J_{\text{C-F}} = 232.4$ Hz), 152.2, 136.6, 135.5, 134.4, 133.3, 129.9, 127.6 (d,

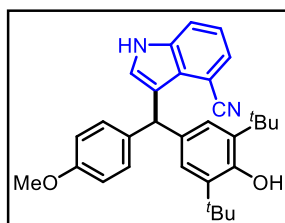
$^3J_{\text{C-F}} = 9.84$ Hz), 125.6, 125.5, 121.5 (d, $^3J_{\text{C-F}} = 4.69$ Hz), 113.7, 111.6, (d, $^3J_{\text{C-F}} = 9.5$ Hz), 110.4 (d, $^2J_{\text{C-F}} = 26.3$ Hz), 105.2 (d, $^2J_{\text{C-F}} = 23.4$ Hz), 55.4, 48.0, 34.5, 30.5; ^{19}F NMR (376 MHz, CDCl_3) δ -124.8; FT-IR (thin film, neat): 3628, 2953, 1600, 1509, 1453, 738 cm^{-1} ; HRMS (ESI-TOF) m/z : $[\text{M}+\text{H}]^+$ calcd for $\text{C}_{30}\text{H}_{35}\text{FNO}_2$ 460.2652; found: 460.2643.

2,6-di-tert-butyl-4-((6-chloro-1H-indol-3-yl)(4-methoxyphenyl)methyl)phenol (28e):



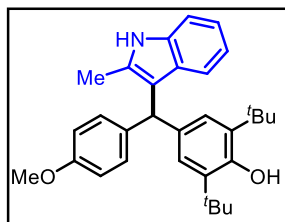
The reaction was performed at 0.123 mmol scale of **21a**; $R_f = 0.5$ (5% EtOAc in hexane); Pale yellow solid (49.21 mg, 84% yield); m. p. = 115–116 °C; ^1H NMR (400 MHz, CDCl_3) δ 7.91 (brs, 1H), 7.32 (s, 1H), 7.12 (d, $J = 8.4$ Hz, 2H), 7.08 (d, $J = 8.5$ Hz, 1H), 7.0 (s, 2H), 6.93 (d, $J = 8.5$ Hz, 1H), 6.81 (d, $J = 8.4$ Hz, 2H), 6.57 (s, 1H), 5.46 (s, 1H), 5.06 (s, 1H), 3.78 (s, 3H), 1.36 (s, 18H); $^{13}\text{C}\{^1\text{H}\}$ NMR (100 MHz, CDCl_3) δ 157.9, 152.2, 137.2, 136.7, 135.5, 134.5, 129.9, 127.9, 125.8, 125.5, 124.5, 121.5, 121.2, 120.0, 113.6, 111.0, 55.3, 48.0, 34.5, 30.5; FT-IR (thin film, neat): 3634, 3413, 2956, 1609, 1453, 805 cm^{-1} ; HRMS (ESI-TOF) m/z : $[\text{M}+\text{H}]^+$ calcd for $\text{C}_{30}\text{H}_{35}\text{ClNO}_2$ 476.2356; found: 476.2339.

3-((3,5-di-tert-butyl-4-hydroxyphenyl)(4-methoxyphenyl)methyl)-1H-indole-4-carbonitrile (28f):



The reaction was performed at 0.123 mmol scale of **21a**; $R_f = 0.2$ (5% EtOAc in hexane); White solid (48.6 mg, 80% yield); m. p. = 182 – 183 °C; ^1H NMR (400 MHz, CDCl_3) δ 8.29 (brs, 1H), 7.56 (d, $J = 8.2$ Hz, 1H), 7.40 (d, $J = 7.4$ Hz, 1H), 7.18 (t, $J = 7.8$ Hz, 1H), 7.11 (d, $J = 8.1$ Hz, 2H), 7.00 (s, 2H), 6.80 (d, $J = 8.1$ Hz, 2H), 6.78 (s, 1H), 6.08 (s, 1H), 5.06 (s, 1H), 3.80 (s, 3H), 1.36 (s, 18); $^{13}\text{C}\{^1\text{H}\}$ NMR (100 MHz, CDCl_3) δ 157.9, 152.1, 136.9, 136.6, 135.5, 134.7, 130.2, 127.1, 126.8, 126.3, 125.8, 121.7, 119.3, 116.0, 113.5, 102.8, 55.3, 46.5, 34.5, 30.5; FT-IR (thin film, neat): 3636, 3402, 2955, 2217, 1600, 1493 cm^{-1} ; HRMS (ESI-TOF) m/z : $[\text{M}+\text{H}]^+$ calcd for $\text{C}_{31}\text{H}_{35}\text{N}_2\text{O}_2$ 467.2699; found: 467.2679.

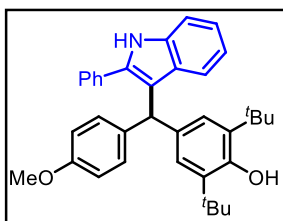
2,6-di-tert-butyl-4-((4-methoxyphenyl)(2-methyl-1H-indol-3-yl)methyl)phenol (28g):



The reaction was performed at 0.123 mmol scale of **21a**; $R_f = 0.3$ (10% EtOAc in hexane); Yellow solid (43.3mg, 77% yield); m. p. = 165–166 °C; ^1H NMR (400 MHz, CDCl_3) δ 7.72 (s, 1H), 7.24 (d, $J = 8.0$ Hz, 1H), 7.11–7.09 (m, 3H), 7.05–7.02 (m, 2H), 6.90 (t, $J = 7.5$ Hz, 1H), 6.79 (d, $J = 7.7$ Hz, 2H), 5.60 (s, 1H), 5.06 (s, 1H), 3.78 (s, 3H),

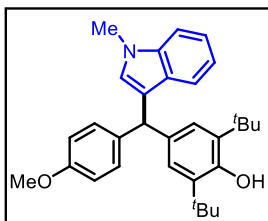
2.16 (s, 3H), 1.35 (s, 18H); $^{13}\text{C}\{^1\text{H}\}$ NMR (100 MHz, CDCl_3) δ 157.7, 152.0, 137.1, 135.4, 135.3, 134.5, 131.7, 130.0, 128.6, 125.9, 120.7, 119.9, 119.0, 115.2, 113.4, 110.0, 55.3, 46.9, 34.4, 30.5, 12.6, FT-IR (thin film, neat): 3636, 3402, 2955, 1609, 1509 cm^{-1} ; HRMS (ESI-TOF) m/z : $[\text{M}+\text{H}]^+$ calcd for $\text{C}_{31}\text{H}_{38}\text{NO}_2$ 456.2903; found: 456.2888.

2,6-di-tert-butyl-4-((4-methoxyphenyl)(2-phenyl-1H-indol-3-yl)methyl)phenol (28h):



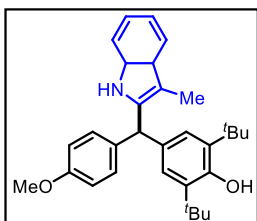
The reaction was performed 0.123mmol scale of **21a**; R_f = 0.4 (5% EtOAc in hexane); Brown gummy solid (49.0 mg, 83% yield); ^1H NMR (400 MHz, CDCl_3) δ 8.05 (brs, 1H), 7.50 (d, J = 7.3 Hz, 2H), 7.41 (t, J = 7.4 Hz, 2H), 7.36 (t, J = 6.4 Hz, 2H), 7.15 (t, J = 8.4 Hz, 1H), 7.07 (d, J = 10.2 Hz, 4H), 6.92 (t, J = 7.7 Hz, 1H), 6.77 (d, J = 7.5 Hz, 2H), 5.69 (s, 1H), 5.03 (s, 1H), 3.77 (s, 3H), 1.32 (s, 18H); $^{13}\text{C}\{^1\text{H}\}$ NMR (100 MHz, CDCl_3) δ 157.6, 151.9, 137.2, 136.3, 135.44, 135.38, 134.7, 133.4, 130.1, 128.9, 128.7, 128.4, 127.9, 126.1, 121.9, 121.87, 119.5, 116.6, 133.4, 110.7, 55.3, 47.0, 34.4, 30.5, FT-IR (thin film, neat): 3641, 3405, 2957, 1599, 1492, 909 cm^{-1} ; HRMS (ESI-TOF) m/z : $[\text{M}+\text{H}]^+$ calcd for $\text{C}_{36}\text{H}_{40}\text{NO}_2$ 518.3059; found: 518.3034.

2,6-di-tert-butyl-4-((4-methoxyphenyl)(1-methyl-1H-indol-3-yl)methyl)phenol (28i):



The reaction was performed at 0.123mmol scale of **21a**; R_f = 0.3 (5% EtOAc in hexane); Orange solid (44.2 mg, 79% yield); m. p. = 177–179 $^{\circ}\text{C}$; ^1H NMR (400 MHz, CDCl_3) δ 7.29 (d, J = 8.2, 1H), 7.23 (d, J = 7.9 1H), 7.21 – 7.16 (m, 3H) 7.06 (s, 2H), 6.98 (t, J = 7.8 Hz, 1H), 6.82 (d, J = 8.7 2H), 6.46 (s, 1H), 5.53 (s, 1H), 5.07 (s, 1H), 3.80 (s, 3H), 3.72 (s, 3H), 1.39 (s, 18H); $^{13}\text{C}\{^1\text{H}\}$ NMR (100 MHz, CDCl_3) δ 157.8, 152.0, 137.5, 137.2, 135.4, 135.0, 129.9, 128.5, 127.6, 125.6, 121.5, 120.3, 119.6, 118.7, 113.5, 109.1, 55.3, 48.1, 34.5, 32.8, 30.5; FT-IR (thin film, neat): 3639, 2954, 1609, 1509 cm^{-1} ; HRMS (ESI-TOF) m/z : $[\text{M}-\text{H}]^-$ calcd for $\text{C}_{31}\text{H}_{36}\text{NO}_2$ 454.2746; found: 454.2728.

2,6-di-tert-butyl-4-((4-methoxyphenyl)(3-methyl-1H-indol-2-yl)methyl)phenol (28j):



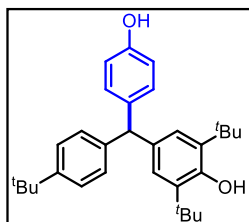
The reaction was performed at 0.123mmol scale of **21a**; R_f = 0.3 (5% EtOAc in hexane); Colourless liquid (44.87 mg, 80% yield); ^1H NMR (400 MHz, CDCl_3) δ 7.56 (d, J = 7.56 Hz, 1H), 7.52 (s, 1H), 7.25 (d, J = 7.2 Hz, 1H), 7.15 – 7.11 (m, 2H), 7.09 (d, J = 8.0 Hz, 2H), 7.00 (s, 2H), 6.85 (d, J = 7.96 Hz, 2H), 5.64 (s, 1H), 5.18 (s, 1H), 3.81 (s, 3H), 2.18 (s, 3H), 1.40 (s, 18H);

$^{13}\text{C}\{^1\text{H}\}$ NMR (100 MHz, CDCl_3) δ 158.2, 152.6, 136.6, 136.0, 135.1, 135.0, 132.7, 129.9, 129.8, 125.7, 121.1, 119.1, 118.4, 113.8, 110.6, 107.8, 55.4, 47.9, 34.4, 30.4; 8.8; FT-IR (thin film, neat): 3629, 3463, 2955, 1609, 1460 cm^{-1} ; HRMS (ESI-TOF): m/z : $[\text{M}+\text{H}]^+$ calcd for $\text{C}_{31}\text{H}_{38}\text{NO}_2$ 456.2903; found: 456.2893.

Gram-scale synthesis of **23a**:

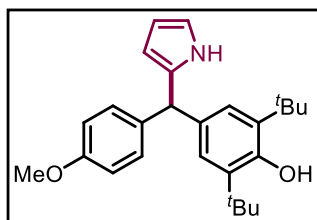
Anhydrous CH_2Cl_2 (15 mL) was added to the mixture of *p*-quinone methide **21a** (1.0 g, 3.08 mmol), indole **22a** (397.3 mg, 3.39 mmol), and catalyst **24a** (39.7 mg, 0.308 mmol) under argon atmosphere and the resulting solution was stirred at room temperature. After the reaction was complete (24 h based on TLC analysis), the reaction mixture was concentrated under reduced pressure. The residue was then purified through a silica gel column, using EtOAc/Hexane mixture as an eluent, to get the pure product **23a** in 84% yield (1.14 g).

2,6-di-*tert*-butyl-4-((4-(*tert*-butyl)phenyl)(4-hydroxyphenyl)methyl)phenol (**30**):



Anhydrous CH_2Cl_2 (2.0 mL) was added to the mixture of **21d** (0.114 mmol), phenol **29** (0.125 mmol), and catalyst **24a** (0.012 mmol) under argon atmosphere, and the resulting suspension was stirred at room temperature. After the reaction was complete (based on TLC analysis), the reaction mixture was concentrated under reduced pressure. The residue was then purified through a silica gel column using an EtOAc/Hexane mixture as an eluent to get the pure product. (41.63 mg, 82% yield); R_f = 0.2 (5% EtOAc in hexane); m.p = 175 – 176 $^\circ\text{C}$; ^1H NMR (400 MHz, CDCl_3) δ 7.28 (d, J = 8.36 Hz, 2H), 7.03 (d, J = 8.20 Hz, 2H), 6.99 (d, J = 8.44 Hz, 2H), 6.91 (s, 2H), 6.73 (d, J = 8.56 Hz, 2H), 5.34 (s, 1H), 5.07 (s, 1H), 4.67 (s, 1H), 1.37 (s, 18H), 1.30 (s, 9H); $^{13}\text{C}\{^1\text{H}\}$ NMR (100 MHz, CDCl_3) δ 153.7, 152.1, 148.8, 142.1, 137.7, 135.5, 134.7, 130.6, 129.0, 126.1, 125.1, 115.0, 55.7, 34.48, 34.46, 31.5, 30.5; FT-IR (thin film, neat): 3634, 3369, 2960, 1519, 1421, 1243 cm^{-1} ; HRMS (ESI-TOF) m/z : $[\text{M}+\text{H}]^+$ calcd for $\text{C}_{31}\text{H}_{41}\text{O}_2$ 445.3107; found: 445.3118.

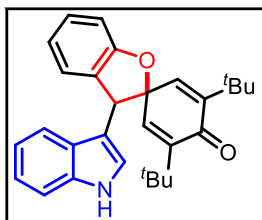
2,6-di-*tert*-butyl-4-((4-methoxyphenyl)(1H-pyrrol-2-yl)methyl)phenol (**32**):



Anhydrous CH_2Cl_2 (2.0 mL) was added to the mixture of **21a** (0.123 mmol), pyrrole **31** (0.135 mmol), and catalyst **24a** (0.012 mmol) under argon atmosphere and the resulting suspension was stirred at room temperature. After the reaction was complete (based on TLC analysis), the reaction mixture was concentrated under

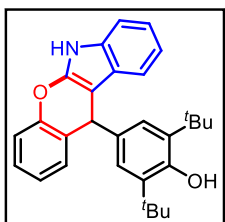
reduced pressure. The residue was then purified through a silica gel column using an EtOAc/Hexane mixture as an eluent to get the pure product (39.70 mg, 83% yield).; R_f = 0.2 (10% EtOAc in hexane); light brown gummy solid; ^1H NMR (400 MHz, CDCl_3) δ 7.79 (brs, 1H), 7.12 (d, J = 8.64 Hz, 2H), 6.98 (s, 1H), 6.83 (d, J = 8.68 Hz, 2H), 6.69 (q, J = 1.56 Hz, 1H), 6.14 (q, J = 3.04 Hz, 1H), 5.77 (brs, 1H), 5.30 (brs, 1H), 5.10 (brs, 1H), 3.80 (s, 3H), 1.38 (s, 18H); $^{13}\text{C}\{^1\text{H}\}$ NMR (100 MHz, CDCl_3) δ 158.2, 152.5, 136.2, 135.8, 135.1, 133.8, 129.9, 125.5, 116.8, 113.8, 108.2, 107.6, 55.4, 49.9, 34.5, 30.5; FT-IR (thin film, neat): 3634, 3461, 3385, 2958, 2925, 1510, 1464, 1248, 1035 cm^{-1} ; HRMS (ESI-TOF) m/z : $[\text{M}+\text{H}]^+$ calcd for $\text{C}_{26}\text{H}_{34}\text{NO}_2$ 392.2590; found: 392.2598

3',5'-di-tert-butyl-3-(1H-indol-3-yl)-3H-spiro[benzofuran-2,1'-cyclohexa[2,5]dien]-4'-one (33):



To a solution of **23i** (50mg, 0.117mmol, 1.0 equiv.) in benzene (1mL) was added iodobenzene diacetate (45.2 mg, 0.140mmol, 1.2 equiv.) at 0°C. Then reaction mixture was stirred at rt overnight. Upon completion, the solvent was removed under reduced pressure and the residue was then purified by silica gel column chromatography to afford pure **33** as a pale yellow solid (36.19 mg, 73% yield).; R_f = 0.1 (5% EtOAc in hexane); m.p = 189 – 191 °C; ^1H NMR (400 MHz, CDCl_3) δ 8.13 (brs, 1H), 7.32 – 7.30 (m, 2H), 7.22 – 7.01 (m, 2H), 7.35 (d, J = 8.2 Hz, 1H), 7.32 (d, J = 8.2 Hz, 1H), 7.22 – 7.20 (m, 1H), 7.14 (t, J = 7.64 Hz, 2H), 7.00 – 6.98 (m, 3H), 6.90 (s, 1H), 6.85 (s, 1H), 6.37 (brs, 1H), 5.09 (brs, 1H), 1.30 (s, 9H), 0.60 (s, 9H); $^{13}\text{C}\{^1\text{H}\}$ NMR (100 MHz, CDCl_3) δ 186.1, 158.6, 147.14, 147.11, 147.0, 146.2, 146.1, 139.1, 137.4, 136.74, 136.70, 129.2, 128.9, 126.8, 126.2, 122.5, 121.2, 119.9, 111.4, 110.8, 35.0, 34.3, 29.6, 28.6, 27.0; FT-IR (thin film, neat): 3634, 3413, 2958, 1456, 1154, 1091 cm^{-1} ; HRMS (ESI-TOF) m/z : $[\text{M}+\text{H}]^+$ calcd for $\text{C}_{29}\text{H}_{32}\text{NO}_2$ 426.2433; found: 426.2448.

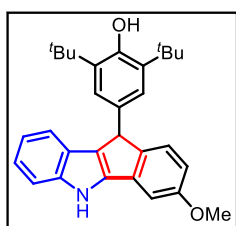
2,6-di-tert-butyl-4-(6,11-dihydrochromeno[2,3-b]indol-11-yl)phenol (34):



Pyridine *p*-toluenesulfonate (32.34 mg, 0.129mmol) was added to a solution of **23i** (50mg, 0.117mmol) in anhydrous CH_2Cl_2 (2.0 mL) and the reaction mixture was cooled to -78 °C. At this temperature *N*-bromosuccinimide (22.9 mg, 0.129mmol) in 2mL of dry THF was dropwise added to the reaction mixture. The reaction mixture was allowed to stir at -78 °C for 45 min and then quenched with a saturated solution of NaHCO_3 . The reaction mixture was extracted with CH_2Cl_2 (5 mL x 2) and dried over anhydrous Na_2SO_4 . The organic layer was

concentrated under reduced pressure and the crude was purified through column chromatography to get pure product **34**. Pale yellow solid (31.93 mg, 64% yield); R_f = 0.1 (5% EtOAc in hexane); m.p = 231 – 233 °C; ^1H NMR (400 MHz, CDCl_3) δ 7.82 (s, 1H), 7.27 – 7.24 (m, 1H), 7.22 – 7.20 (m, 2H), 7.15 – 7.10 (m, 2H), 7.09 – 7.04 (m, 4H), 7.02 – 6.97 (m, 1H), 5.38 (s, 1H), 5.02 (s, 1H), 1.36 (s, 18H); $^{13}\text{C}\{^1\text{H}\}$ NMR (100 MHz, CDCl_3) δ 152.4, 150.9, 144.6, 136.5, 135.6, 131.4, 131.1, 127.5, 126.5, 125.7, 125.2, 124.1, 120.4, 120.1, 118.4, 116.8, 91.1, 41.1, 34.4, 30.5; FT-IR (thin film, neat): 3634, 3413, 2958, 1456, 1154, 1091 cm^{-1} ; HRMS (ESI-TOF): m/z : $[\text{M}+\text{H}]^+$ calcd for $\text{C}_{29}\text{H}_{32}\text{NO}_2$ 426.2433; found: 426.2422.

2,6-di-tert-butyl-4-(3-methoxy-5,10-dihydroindeno[1,2-b]indol-10-yl)phenol (**35**):



Pyridine *p*-toluenesulfonate (28.47 mg, 0.124mmol) was added to a solution of **23a** (50 mg, 0.113 mmol) in anhydrous CH_2Cl_2 (2.0 mL) and the reaction mixture was cooled to -78 °C. At this temperature, *N*-bromosuccinimide (22.18 mg, 0.124mmol) in 2mL of dry THF was dropwise added to the reaction mixture. The reaction mixture was allowed to stir at -78 °C for 45 min and then quenched with a saturated solution of NaHCO_3 . The reaction mixture was extracted with CH_2Cl_2 (5 mL x 2) and dried over anhydrous Na_2SO_4 . The organic layer was concentrated under reduced pressure and the crude was purified through column chromatography to get pure product **35**. White solid (29.3 mg, 57% yield); R_f = 0.2 (5% EtOAc in hexane); m.p = 170 – 171 °C; ^1H NMR (400 MHz, CDCl_3) δ 8.03 (s, 1H), 7.26 – 7.24 (m, 1H), 7.13 – 7.11 (m, 5H), 6.92 (t, J = 7.48 Hz, 1H), 6.79 (d, J = 7.68 Hz, 2H), 5.60 (s, 1H), 5.07 (s, 1H), 3.78 (s, 3H), 1.34 (s, 18H); $^{13}\text{C}\{^1\text{H}\}$ NMR (100 MHz, CDCl_3) δ 157.8, 152.2, 136.5, 135.8, 135.5, 133.3, 130.0, 127.1, 126.0, 122.1, 120.4, 119.8, 118.6, 113.5, 110.4, 109.1, 55.3, 47.6, 34.4, 30.5; FT-IR (thin film, neat): 3637, 3417, 2957, 1610, 1456, 1154, 1121 cm^{-1} ; HRMS (ESI-TOF): m/z : $[\text{M}+\text{H}]^+$ calcd for $\text{C}_{30}\text{H}_{34}\text{NO}_2$ 440.2590; found 440.2574.

1 Comparison of rate of the reactions catalyzed by **24a** and **24h**

Two independent experiments have been performed in a 100 mg (0.308 mmol) scale of the **21a** and **22a** (0.339 mmol) in 3 mL of CH_2Cl_2 . In the first experiment, 20 mol% of **24a** (0.061 mmol) was used and in another experiment, 20 mol% of **24h** (D = 99.99%) [0.061 mmol] was used as a catalyst. During the progress of the reactions, 0.3 mL of the reaction mixture was withdrawn from each the reaction mixture at an interval of 0.5 h, 1 h, 2 h, 3 h, 4 h....12 h and passed through the silica gel column and then analyzed by ^1H NMR spectroscopy. Figure 5. shows the comparison between the rate of the reactions catalyzed by **24a** and **24h**. It is evident

from Figure 5 that the rate of the reaction as well as the conversion is much less in the case of the reaction catalyzed by **24h** when compared to the reaction catalyzed by **24a**. The reaction catalyzed by **24a** reached completion within 12 h. However, only 50% conversion was observed in the case of reaction using **24h** as a catalyst after 12 h. This observation clearly confirms the involvement of the C-H hydrogen of the cyclopropene ring of **24a** in catalyzing the reaction (Scheme 14).

Scheme 14. Reaction kinetics of **24a** and **24h**

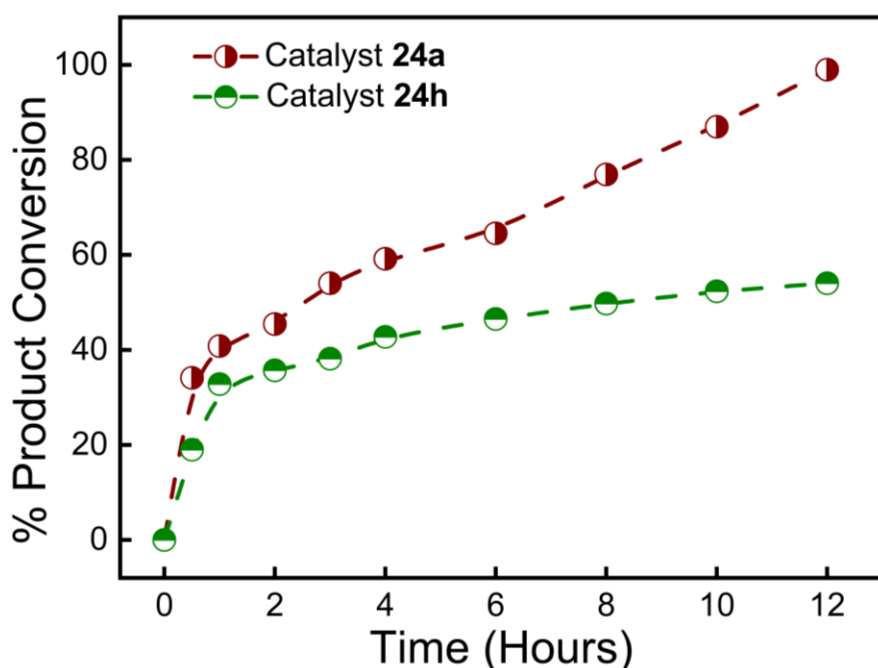
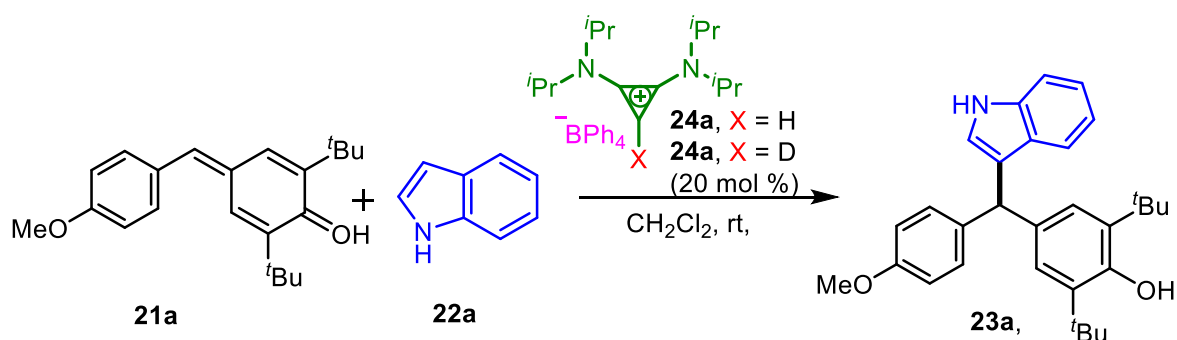


Figure 5. ^1H NMR experimental determination of the rate of reaction catalyzed by **24a** and **24h**.

2. ^{13}C NMR stacking experiments using various concentrations of **21a** and **24a**

The ^{13}C NMR-based experiments have been carried out using stock solutions of **21a** (0.05 M), and **24a** (0.05M) in CDCl_3 . In these experiments, solutions of various molar ratios of **21a** and **24a** have been prepared by mixing the stock solutions of **21a** and **24a** and allowed to mix for

30 min. These mixtures were then analyzed by ^{13}C NMR spectroscopy. It is evident from Fig. S2 that the chemical shift of the carbonyl group of *p*-QM (**21a**) has been gradually shifted to the upfield region with the increasing concentration of **24a**. This observation clearly confirms that the C=O group of **21a** is getting activated by the catalyst **24a** through non-covalent interactions.

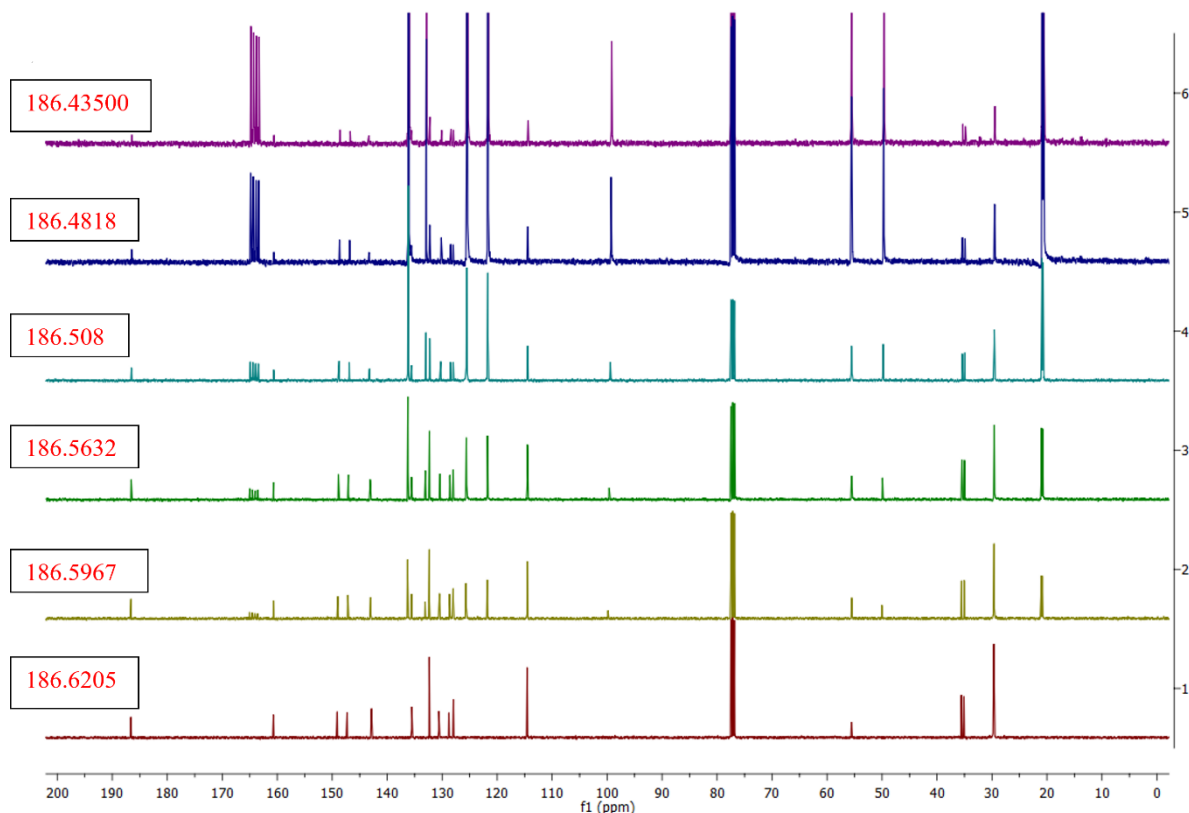


Figure 6. ^{13}C -NMR experiment depicting the shifts in the substrate **21a** upon titration with **24a** with molar stoichiometric ratios (**21a:24a**) as follows: (bottom to top, **21a:24a**): 1:0; 1:0.5; 1:1; 1:2; 1:10 1:15; (concentration of **21a** 0.062 mM in CDCl_3)

3. ^1H & ^{13}C NMR stacking for **21a and **24b** (using various conc. of **24b** in CDCl_3)**

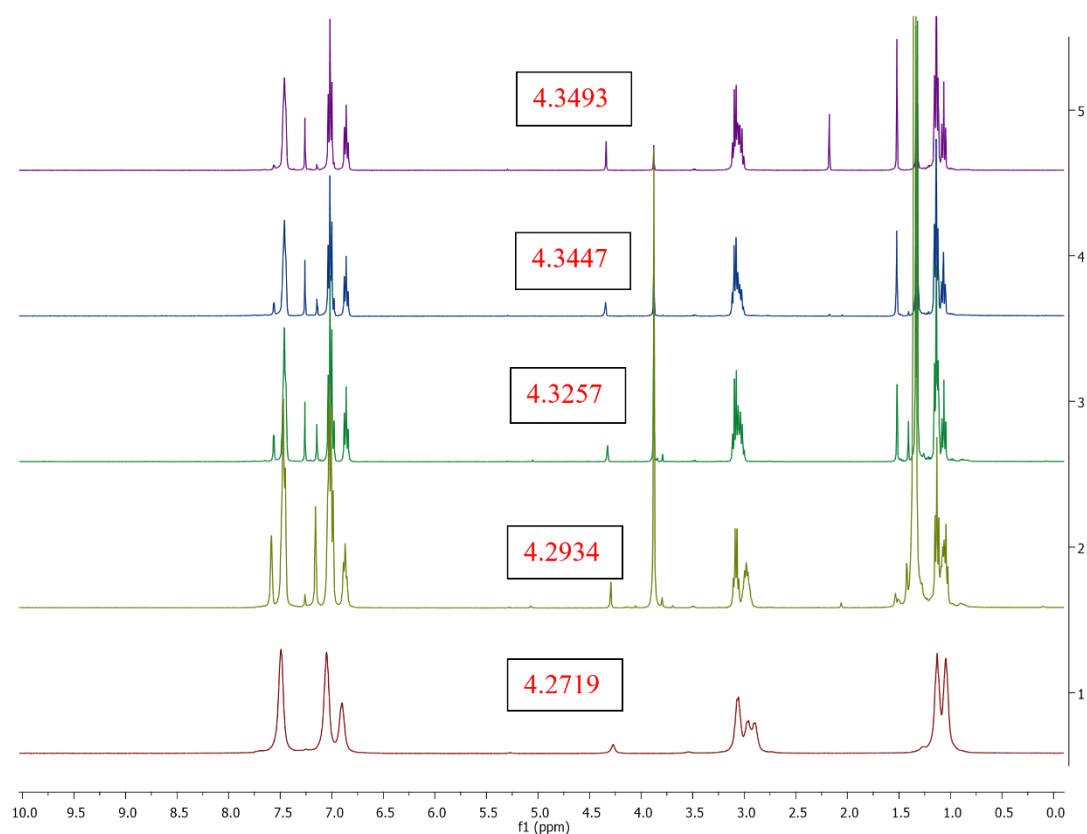


Figure 7. ^1H -NMR experiment depicting the shifts in the substrate **21a** upon titration with **24b** with molar stoichiometric ratios (**21a**:**24b**) as follows: (bottom to top, **21a**:**24b**): 1:0; 1:0.5; 1:1; 1:2; 1:10 1:15; (concentration of **21a** 0.062 mM in CDCl_3)

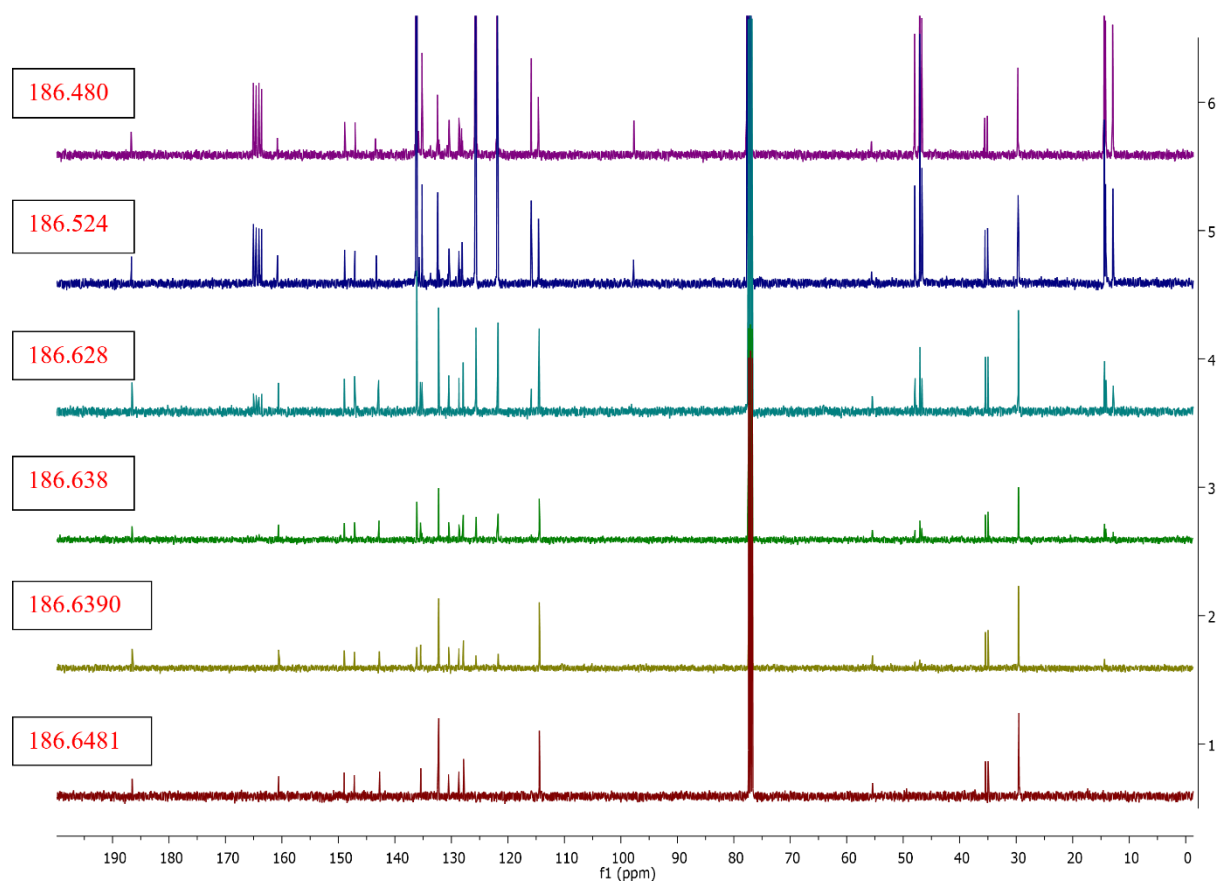


Figure 8. ^{13}C -NMR experiment depicting the shifts in the substrate **21a** upon titration with **24b** with molar stoichiometric ratios (**21a:24b**) as follows: (bottom to top, **21a:24b**): 1:0; 1:0.5; 1:1; 1:2; 1:10 1:15; (concentration of **21a** 0.062 mM in CDCl_3)

4. ^1H & ^{13}C NMR stacking for **21a and **24c** (using various conc. of **24c** in CDCl_3)**

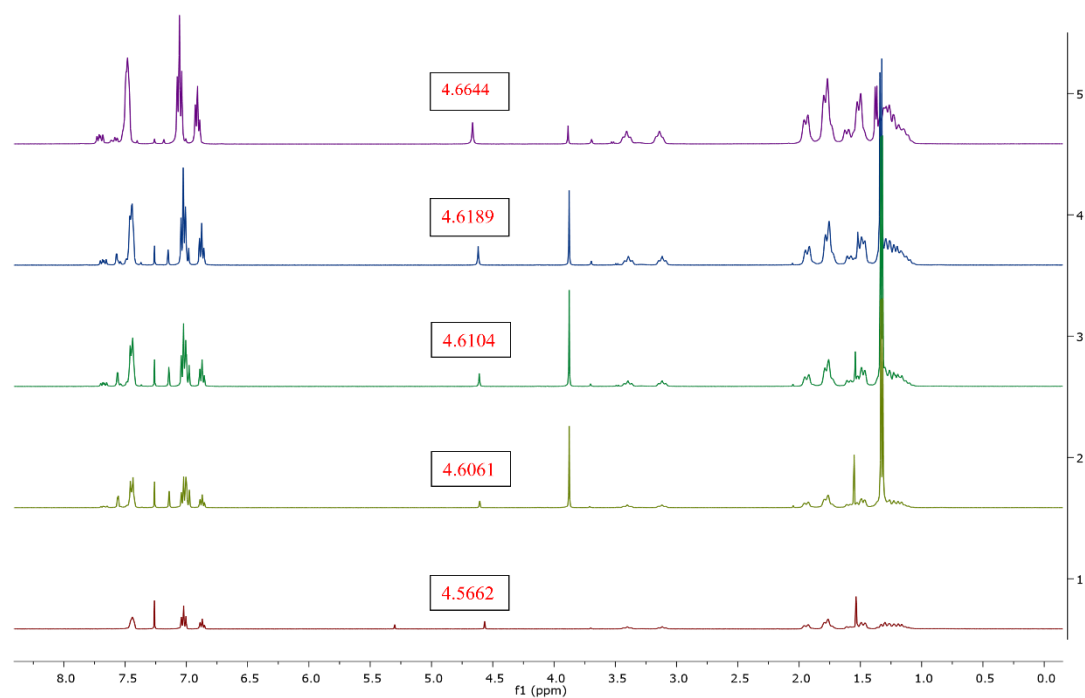


Figure 9. ^1H -NMR experiment depicting the shifts in the substrate **21a** upon titration with **24c** with molar stoichiometric ratios (**21a:24c**) as follows: (bottom to top, **21a:24c**): 1:0; 1:0.5; 1:1; 1:2; 1:10 1:15; (concentration of **21a** 0.062 mM in CDCl_3)

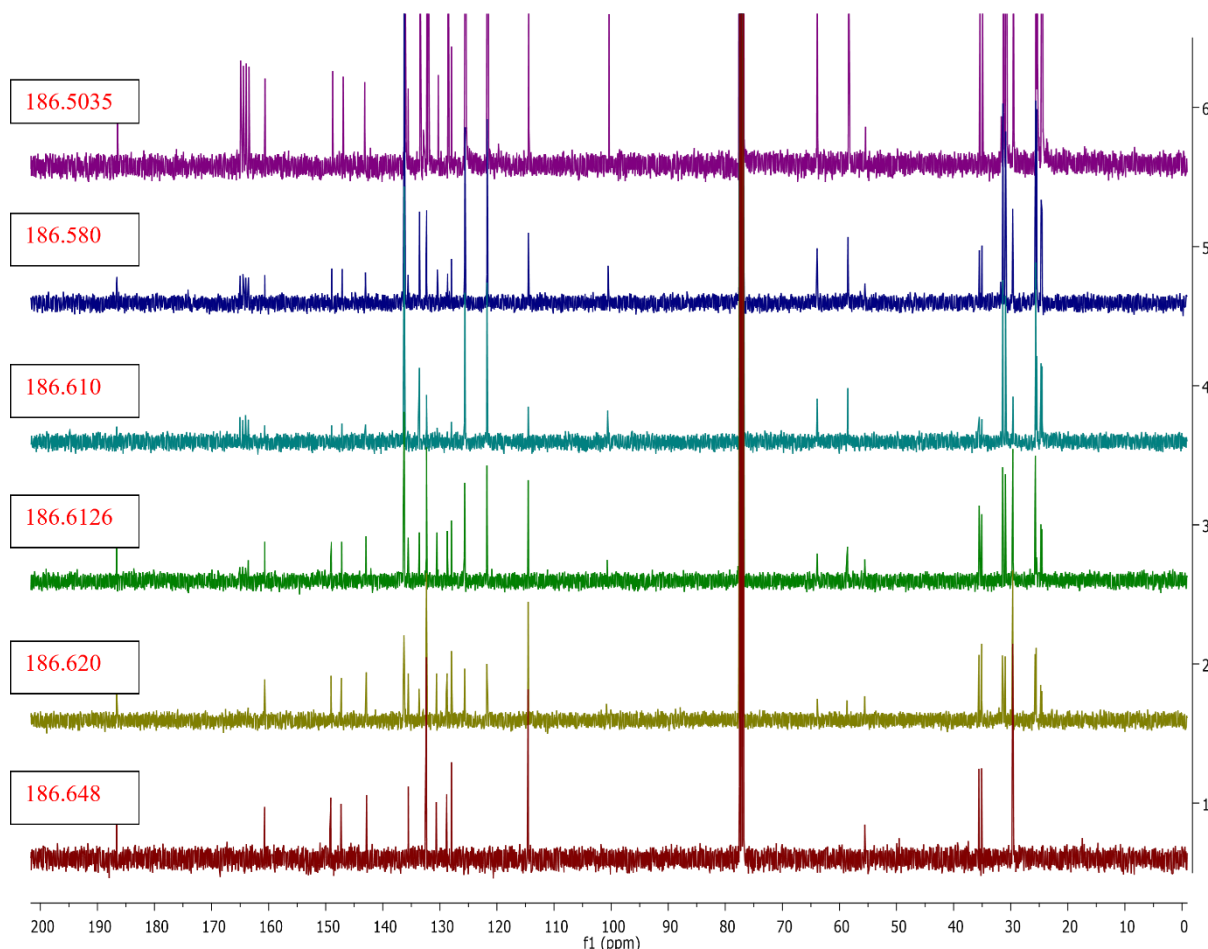


Figure 10. ^{13}C -NMR experiment depicting the shifts in the substrate **21a** upon titration with **24c** with molar stoichiometric ratios (**21a**:**24c**) as follows: (bottom to top, **21a**:**24c**): 1:0; 1:0.5; 1:1; 1:2; 1:10 1:15; (concentration of **21a** 0.062 mM in CDCl_3)

5. Estimation of association/binding constant between **21a** and **24a**

The association constant between **21a** and **24a** has been estimated by fitting the UV-vis spectroscopic data in BindFit program.¹ The experimental procedure for the UV-vis spectroscopy is given below.

Procedure: Stock solutions of **21a** ($6.81 \times 10^2 \mu\text{M}$) and **24a** ($2 \times 10^4 \mu\text{M}$) have been prepared in CHCl_3 . A stock solution of **24a** was added gradually in the order 10, 20, 30,110 μL to a solution of **21a** (990, 980, 970,890 μL , respectively), and the total volume of the solution was made up to 1 mL. The UV-vis spectra for each sample have been recorded. For each sample, the wavelength (λ_{max}) was found to be 384 nm, and absorbance values at this wavelength were used for further calculations. For obtaining the association constants, concentration of **21a**, **24a** and their corresponding absorbance based on the UV-vis titration

data have been considered. The results are tabulated in Table 2

Table 2. Determination of association/binding constant between **24a** and **21a**

21a (Host concentration / M)	24a: (Guest concentration / M)	Absorbance S 384.00104	BindFit data
6.80E-06	0	0.95145	$K_a = 100656.84 \text{ M}^{-1}$ Error = $\pm 3.7678 \%$ SSR = $2.1747\text{e-}4$ Method = Nelder-Mead Fitter = UV1to1 Link: http://app.supramolecular.org/bindfit/view/6be099b2-8e92-4d9f-805d-888ac089a1da
6.80E-06	1.98E-06	0.90111	
6.80E-06	3.96E-06	0.85395	
6.80E-06	5.94E-06	0.82165	
6.80E-06	0.00000792	0.7877	
6.80E-06	0.0000099	0.75462	
6.80E-06	0.00001188	0.73696	
6.80E-06	0.00001386	0.71069	
6.80E-06	0.00001584	0.68782	
6.80E-06	0.00001782	0.67132	
6.80E-06	0.0000198	0.66707	
6.80E-06	0.00002178	0.66092	

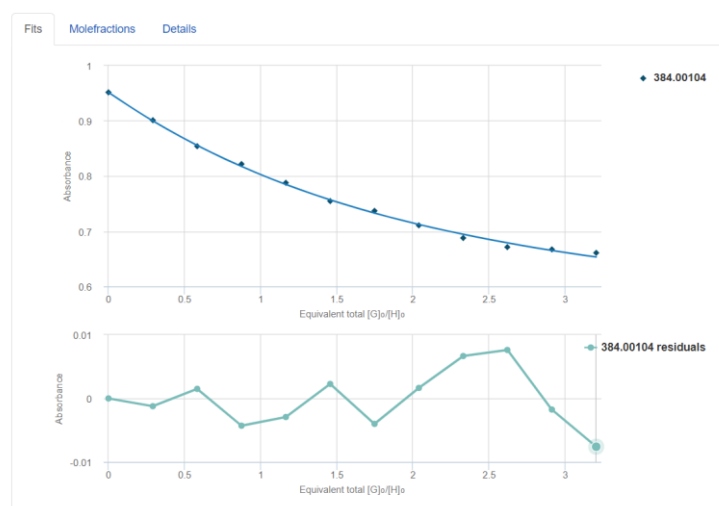


Figure 11. Determination of association constant between **24a** and **21a** using a UV-vis spectroscopy titration experiment. The association constant has been estimated using the web based BindFit program.¹

6. Estimation of association/binding constant between **21a** and **24h**

The association constant between **21a** and **24h** has been estimated using the same protocol that we have followed for **21a** & **24a**. In this case, a stock solution of **24h** was added gradually in the order 10, 20, 30,110 μL to a solution of **21a** (990, 980, 970,890 μL , respectively), and the total volume of the solution was made up to 1 mL. The UV-vis spectra for each sample have been recorded. For obtaining the association constants, concentration of **21a**, **24h** and their corresponding absorbance based on the UV-vis titration data have been considered. The results are tabulated in Table 3.

Table 3. Determination of association/binding constant between **24h** and **21a**

21a (Host concentration / M)	24h : (Guest concentration / M)	Absorbance 384	BindFit data
6.80E-06	0	0.95586	$K_a = 22812.26 \text{ M}^{-1}$ Error = $\pm 9.1869 \%$ SSR = $1.5005\text{e-}3$ Method = Nelder-Mead Fitter = UV1to1 Link: http://app.supramolecular.org/bindfit/view/cdb0121c-17e1-4e0a-ac40-106b8d87a297
6.80E-06	1.98E-06	0.95002	
6.80E-06	3.96E-06	0.92197	
6.80E-06	5.94E-06	0.8997	
6.80E-06	0.00000792	0.86488	
6.80E-06	0.0000099	0.84159	
6.80E-06	0.00001188	0.8183	
6.80E-06	0.00001386	0.79671	
6.80E-06	0.00001584	0.78135	
6.80E-06	0.00001782	0.77099	
6.80E-06	0.0000198	0.76738	
6.80E-06	0.00002178	0.76538	

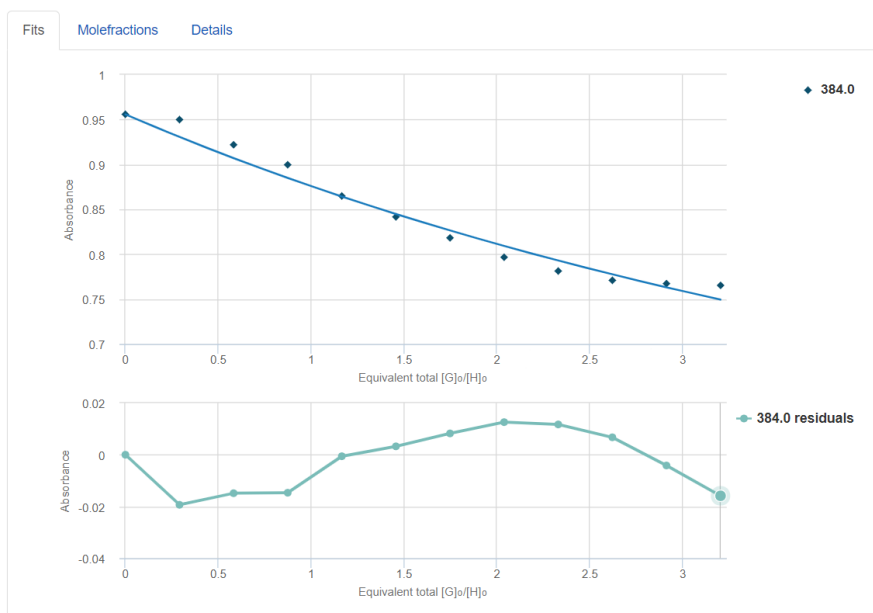


Figure 12. Determination of association constant between **24h** and **21a** using a UV-vis spectroscopy titration experiment. The association constant has been estimated using the web based BindFit program

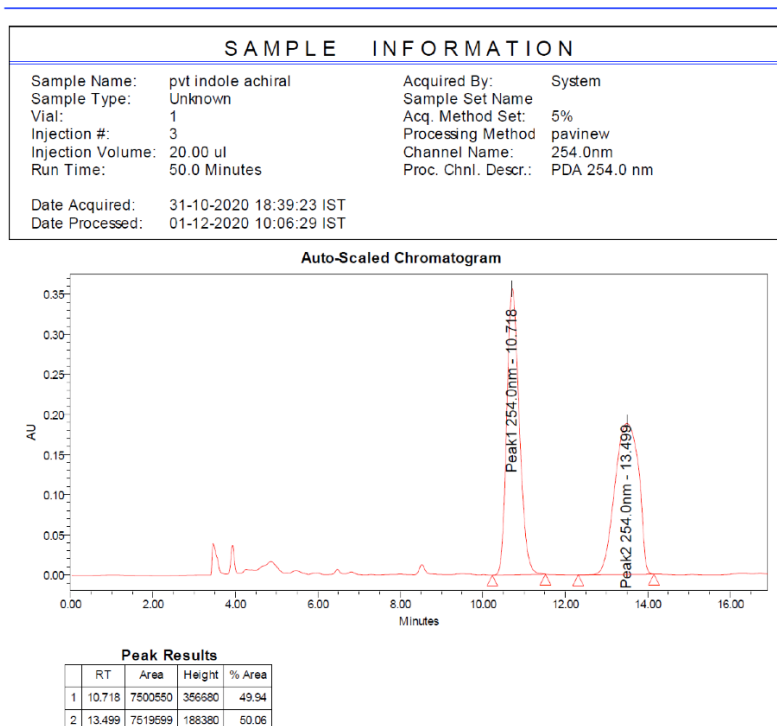
7. Attempted enantioselective version using **24i** as a chiral catalyst:

Anhydrous CH_2Cl_2 (1.5 mL) was added to the mixture of *p*-quinone methide **21a** (20 mg, 0.062 mmol), indole **22a** (8.5 mg, 0.074 mmol), and catalyst (0.012 mmol) under argon atmosphere

and the resulting solution was stirred at room temperature. After the reaction was complete the reaction mixture was concentrated under reduced pressure. The residue was then purified through a silica gel column, using EtOAc/Hexane mixture as an eluent, to get the pure product **23a** in a 78% (20.8 mg) isolated yield. Unfortunately, only traces of **23a** were obtained when the reaction was carried out at 0 °C.

HPLC data:

For the racemic mixture:

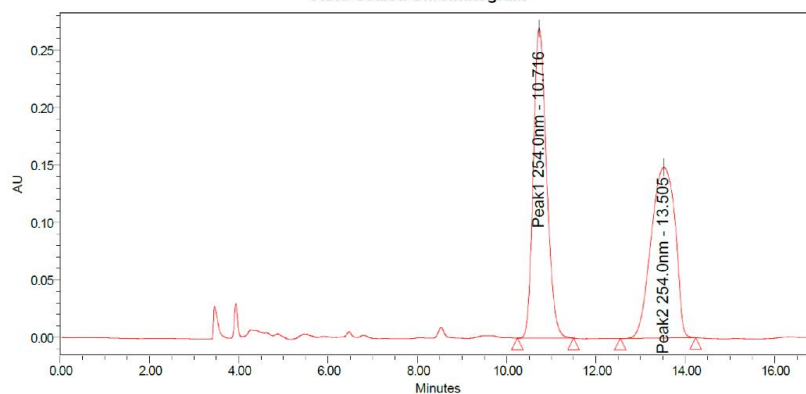


For the product isolated in the attempted enantioselective reaction:

SAMPLE INFORMATION

Sample Name:	pvt indole chiral	Acquired By:	System
Sample Type:	Unknown	Sample Set Name:	
Vial:	1	Acq. Method Set:	5%
Injection #:	2	Processing Method:	pavichiral
Injection Volume:	20.00 ul	Channel Name:	254.0nm
Run Time:	50.0 Minutes	Proc. Chnl. Descr.:	PDA 254.0 nm
Date Acquired:	31-10-2020 18:21:33	IST	
Date Processed:	01-12-2020 10:09:53	IST	

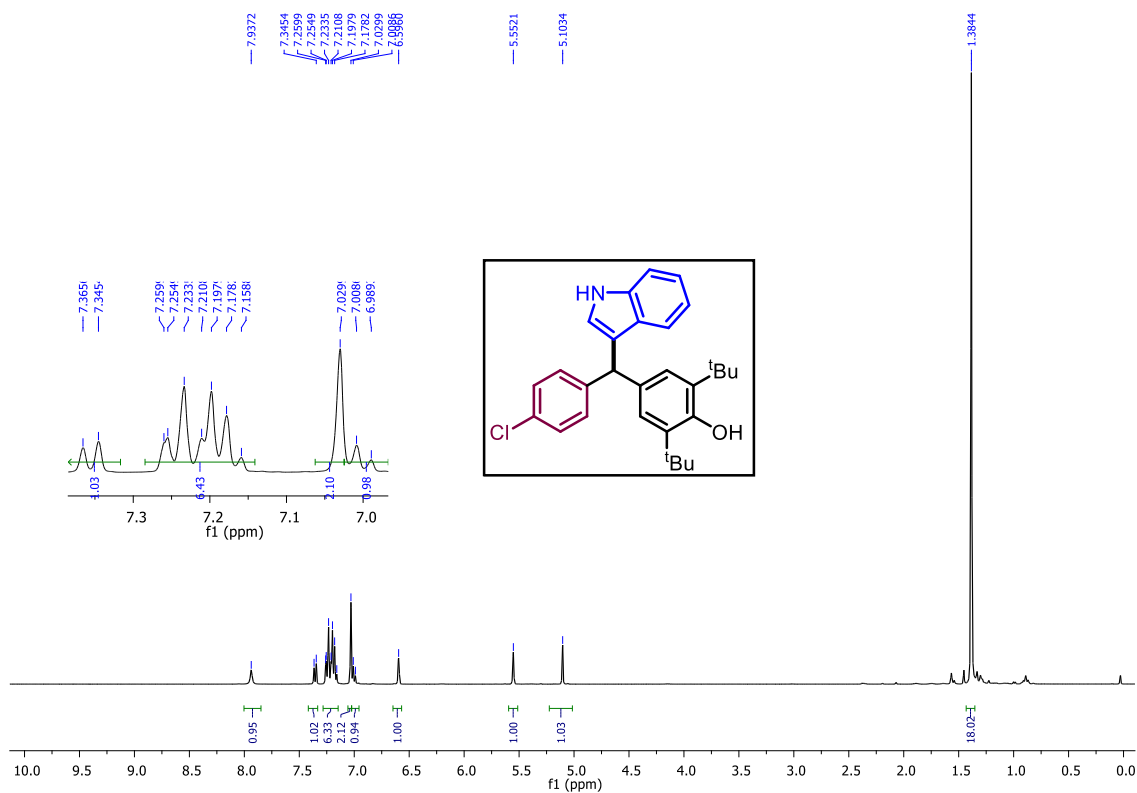
Auto-Scaled Chromatogram



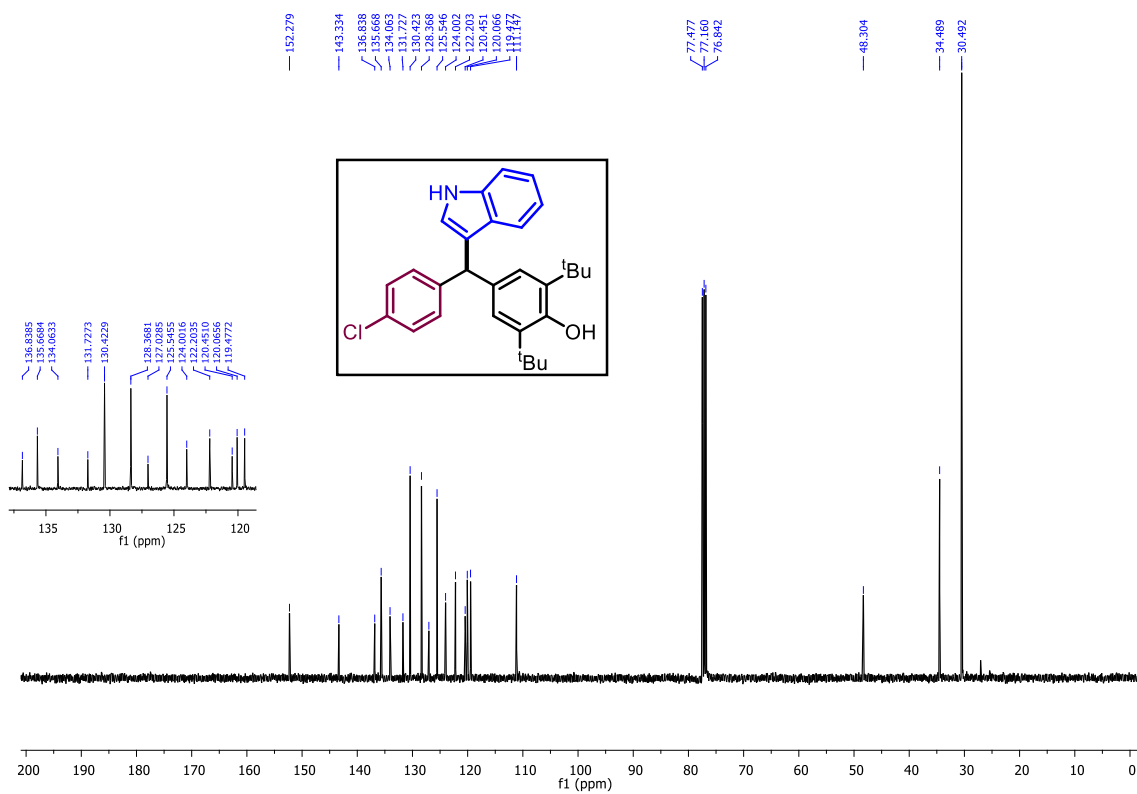
Peak Results

	RT	Area	Height	% Area
1	10.716	5540554	269749	49.96
2	13.505	5549608	148580	50.04

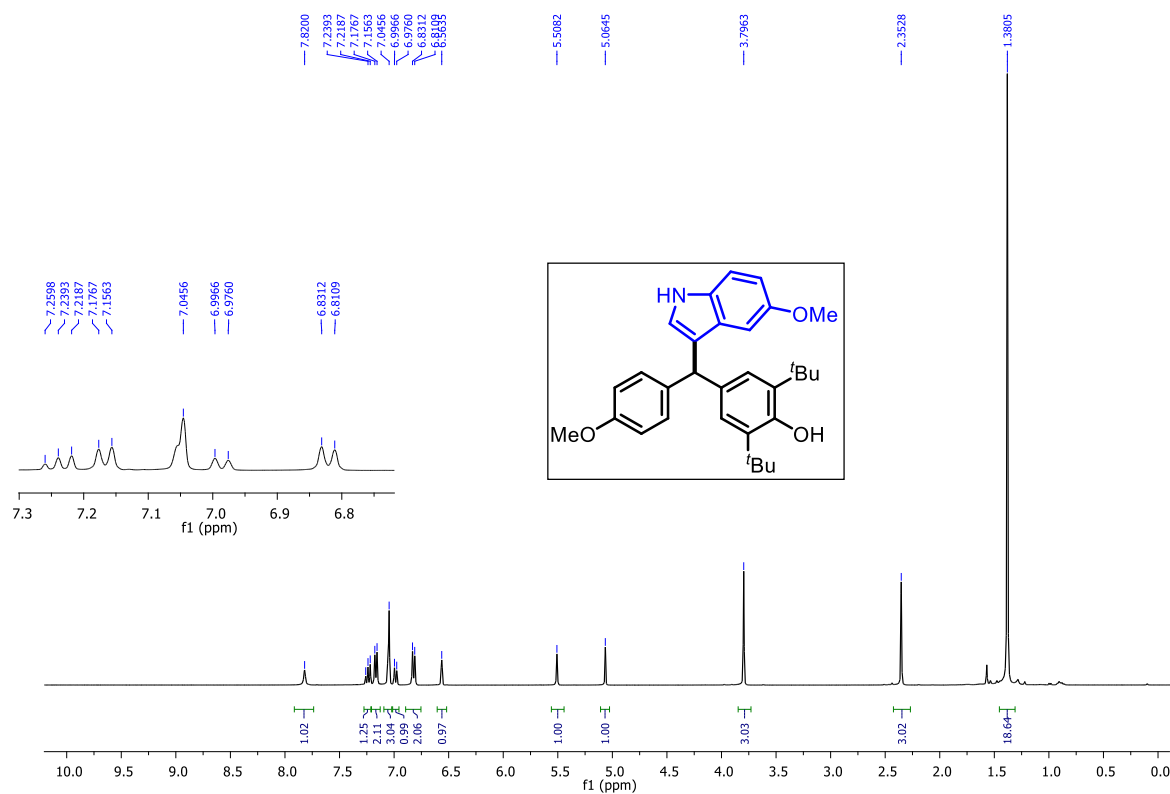
¹H NMR spectrum of **23q** (400 MHz, CDCl₃)



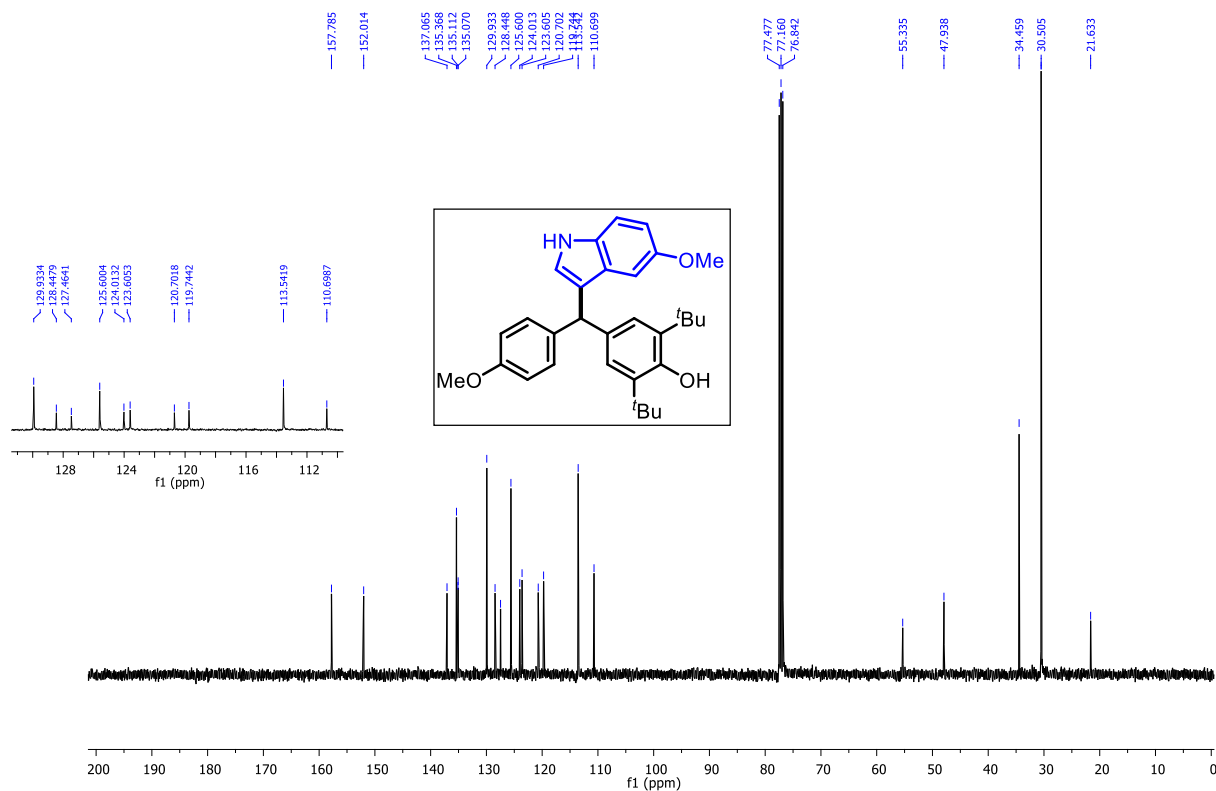
¹³C{¹H} NMR spectrum of **23q** (100 MHz, CDCl₃)



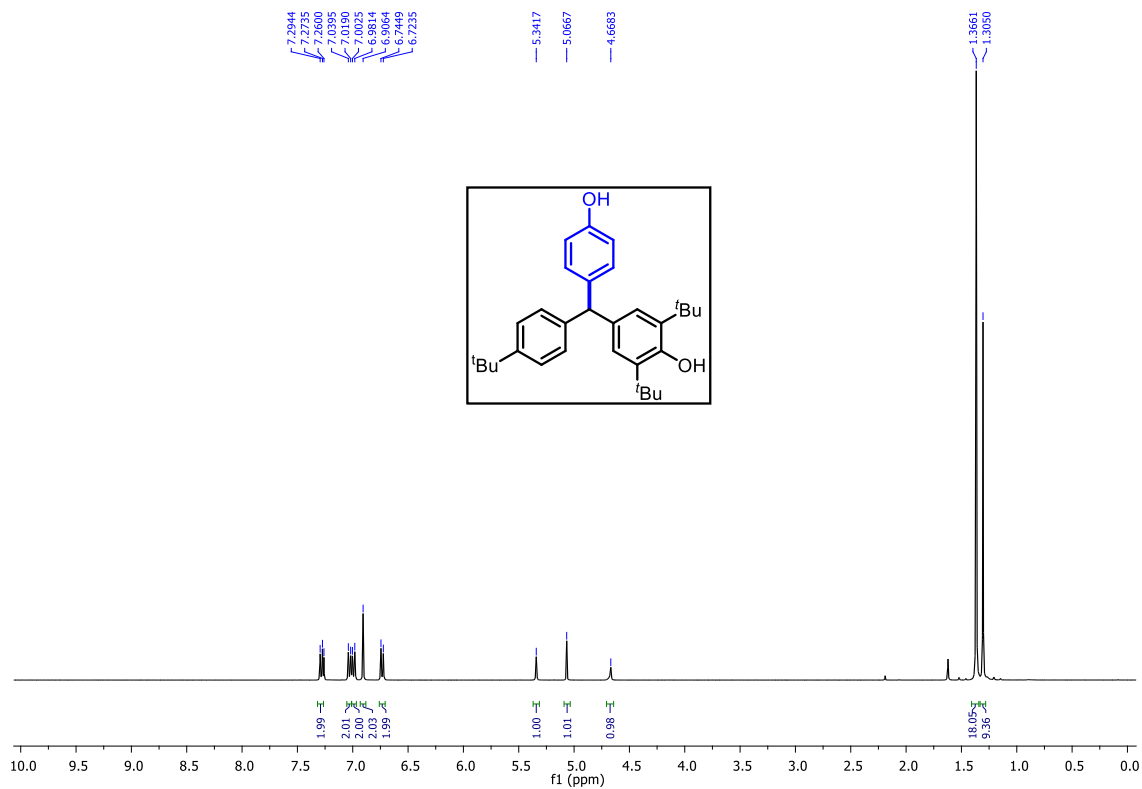
^1H NMR spectrum of 28a (400 MHz, CDCl_3)



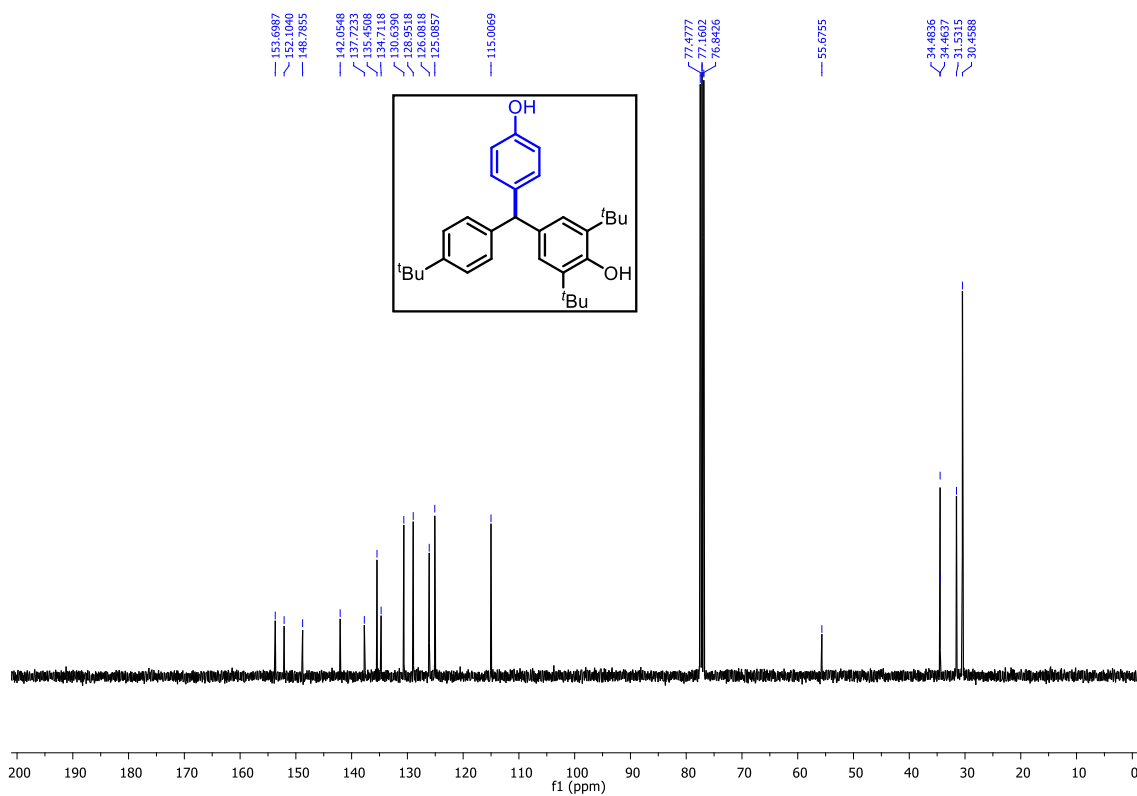
$^{13}\text{C}\{^1\text{H}\}$ NMR spectrum of 28a (100 MHz, CDCl_3)



^1H NMR spectrum of 30 (400 MHz, CDCl_3)



$^{13}\text{C}\{^1\text{H}\}$ NMR spectrum of 30 (100 MHz, CDCl_3)



3.7 References:

- 1) (a) Jeffrey, G. A. *An Introduction to Hydrogen Bonding*. Oxford University Press: New York, 1997. (b) Desiraju, G. R.; Steiner, T. *The Weak Hydrogen Bond in Structural Chemistry and Biology*; OUP: Oxford, 1999; pp 108-113. (c) G. A. Jeffrey, G. A.; Saenger, W. *Hydrogen Bonding in Biological Structures*. Springer-Verlag Berlin Heidelberg, 1991. (d) Aakeroy, C. B.; Seddon, K. R. *Chem. Soc. Rev.* **1993**, 397 – 407. (e) Desiraju, G. R. *J. Am. Chem. Soc.* **2013**, 135, 27, 9952 – 9967.
- 2) Schreiner, P. R. *Chem. Soc. Rev.* **2003**, 32, 289 – 296.
- 3) For selected examples: (a) Pihko, P. M. *Hydrogen Bonding in Organic Synthesis*. WILEY-VCH Verlag GmbH & Co. KGaA: Weinheim, 2009. (b) Lelais, G.; MacMillan, D. W. C. *History and Perspective of Chiral Organic Catalysts*. In *New Frontiers in Asymmetric Catalysis*, John Wiley & Sons Inc., 2006, pp 313 – 358. (c) Etzenbach-Effers K., Berkessel A. *Topics in Current Chemistry*, vol 291, Springer, Berlin, Heidelberg, 2010, pp 38 – 69.
- 4) For selected examples: (a) Taylor, M. S.; Jacobsen, E. N. *Angew. Chem. Int. Ed.* **2006**, 45, 1520 – 1543. (b) Pihko, P. M. *Angew. Chem. Int. Ed.* **2004**, 43, 2062-2064. (c) Doyle, A. G.; Jacobsen, E. N. *Chem. Rev.* **2007**, 107, 5713-5743. (d) Yu, X.; Wang, W. *Chem. Asian J.* **2008**, 3, 516 – 532. (e) Knowles, R. R.; Jacobson, E. N. *Proc. Natl. Acad. Sci. U.S.A.* **2010**, 107, 20678 – 20685.
- 5) For selected reviews: (a) Parvulescu, V. I.; Hardacre, C. *Chem. Rev.* **2007**, 107, 2615–2665. (b) Welton, T. *Biophy. Rev.* **2018**, 10, 691 – 706. (c) Karimi, B.; Tavakolian, M.; Akbari, M.; Mansouri, F. *ChemCatChem* **2018**, 10, 3173 – 3205. (d) Steinrück, H. -P.; Wasserscheid, P. *Catal. Lett.* **2015**, 145, 380 – 397.
- 6) For selected reviews: (a) Zhang, Q.; Zhang, S.; Deng, Y. *Green Chem.* **2011**, 13, 2619–2637. (b) Vekariya, R. L. *J. Mol. Liquids* **2017**, 227, 44 – 60.
- 7) For reviews: (b) Hunt, P. A.; Ashworth, C. R.; Mathew, R. P. *Chem. Soc. Rev.* **2015**, 44, 1257 – 1288. (b) Dong, K.; Zhang, S.; Wang, J. *Chem. Commun.* **2016**, 52, 6744 – 6764.
- 8) Chakraborty, A. K.; Roy, S. R. *J. Am. Chem. Soc.* **2009**, 131, 6902 – 6903. (b) Chakraborty, A. K.; Roy, S. R. *Org. Lett.* **2010**, 12, 3866–3869.

- 9) Myles, L.; Gore, R. G.; Gathergood, N.; Connon, S. J. *Green Chem.* **2013**, *15*, 2740 – 2746.
- 10) Bobbink, F. D.; Vasilyev, D.; Hulla, M.; Chamam, S.; Menoud, F.; Laurenczy, G.; Katsyuba, S.; Dyson, P. J. *ACS Catal.* **2018**, *8*, 2589 – 2594.
- 11) Narumi, T.; Tsuzuki, S.; Tamamura, H. *Asian J. Org. Chem.* **2014**, *3*, 497 – 503.
- 12) (a) Santra, S.; Porey, A.; Jana, B.; Guin, J. *Chem. Sci.* **2018**, *9*, 6446 – 6450. (b) Santra, S.; Maji, U.; Guin, J. *Org. Lett.* **2020**, *22*, 468 – 473.
- 13) For reviews: (a) Komatsu, K.; Kitagawa, T. *Chem. Rev.* **2003**, *103*, 1371 – 1427. (b) Bandar, J. S.; Lambert, T. H. **2013**, *45*, 2485 – 2498.
- 14) For selected examples: (a) Curnow, O. J.; MacFarlane, D. R.; Walst, K. J. *Chem. Commun.* **2011**, *47*, 10248 – 10250. (b) Curnow, O. J.; Holmes, M. T.; Ratten, L. C.; Walst, K. J.; Yunis, R. *RSC Adv.* **2012**, *2*, 10794 – 10797. (c) Wallace, A. J.; Jayasinghe, C. D.; Polson, M. I. J.; Curnow, O. J.; Crittenden, D. L. *J. Am. Chem. Soc.* **2015**, *137*, 15528 – 15532. (d) Freyer, J. L.; Brucks, S. D.; Gobieski, G. S.; Russell, S. T.; Yozwiak, C. E.; Sun, M.; Chen, Z.; Jiang, Y.; Bandar, J. S.; Stockwell, B. R.; Lambert, T. H.; Campos, L. M. *Angew. Chem. Int. Ed.* **2016**, *9*, 79 – 87. (e) Curnow, O. J.; Polson, M. I. J.; Walst, K. J.; Yunis, R. *RSC Adv.* **2018**, *8*, 28313 – 28322.
- 15) For selected examples: (a) Jiang, Y.; Freyer, J. L.; Cotanda, P.; Brucks, S. D.; Killops, K. L.; Bandar, J. S.; Torsitano, C.; Balsara, N. P.; Lambert, T. H.; Campos, L. M. *Nature Comm.* **2015**, *6*, 5950. (b) Brucks, S. D.; Freyer, J. L.; Lambert, T. H.; Campos, L. M. *Polymers* **2017**, *9*, 79 – 87. (c) Griffin, P. J.; Freyer, J. L.; Han, N.; Yin, X.; Gheewala, C.; Lambert, T. H.; Campos, L. M.; Winey, K. I. *Macromolecules* **2018**, *51*, 1681 – 1687.
- 16) For selected examples: (a) Kuchenbeiser, G.; Donnadieu, B.; Bertrand, G. *J. Organomet. Chem.* **2008**, *693*, 899 – 904. (b) Bruns, H.; Patil, M.; Carreras, J.; Vázquez, A.; Thiel, W.; Goddard, R.; Alcarazo, M. *Angew. Chem. Int. Ed.* **2010**, *49*, 3680 – 3683. (c) Petuskova, J.; Patil, M.; Holle, S.; Lehmann, C. W.; Thiel, W.; Alcarazo, M. *J. Am. Chem. Soc.* **2011**, *133*, 20758 – 20760. (d) Carreras, J.; Patil, M.; Thiel, W.; Alcarazo, M. J.: *J. Am. Chem. Soc.* **2012**, *134*, 16753 – 16758. (e) Mir, R.; Dudding, T. *J. Org. Chem.* **2018**, *83*, 4384 – 4388. (f) Mir, R.; Rowshanpour, R.; Dempsey, K.; Pilkington, M.; Dudding, T. *J. Org. Chem.* **2019**, *84*, 5726 – 5731.

- 17) (a) For a recent review: An, J.; Denton, R. M.; Lambert, T. H.; Nacsa, E. *Org. Biomol. Chem.* **2014**, *12*, 2993 – 3003. (b) Kelly, B. D.; Lambert, T. H. *J. Am. Chem. Soc.* **2009**, *131*, 13930 – 13931. (c) Hardee, D. J.; Kovalchuke, L.; Lambert, T. H. *J. Am. Chem. Soc.* **2010**, *132*, 5002 – 5003. (d) Vanos, C. M.; Lambert, T. H. *Chem. Sci.* **2010**, *1*, 705 – 708. (e) Kelly, B. D.; Lambert, T. H. *Org. Lett.* **2011**, *13*, 740 – 743. (f) Vanos, C. M.; Lambert, T. H. *Angew. Chem. Int. Ed.* **2011**, *50*, 12222 – 12226.
- 18) For selected examples: (a) Mirabdolbaghi, R.; Dudding, T.; Stamatatos, T. *Org. Lett.* **2014**, *16*, 2790 – 2793. (b) Bandar, J. S.; Tanaset, A.; Lambert, T. H. *Chem. Eur. J.* **2015**, *21*, 7365 – 7368. (c) Belding, L.; Stoyanov, P.; Dudding, T. *J. Org. Chem.* **2016**, *81*, 553 – 558.
- 19) (a) Bandar, J. S.; Lambert, T. H. *J. Am. Chem. Soc.* **2012**, *134*, 5552 – 5555. (b) Bandar, J. S.; Lambert, T. H. *J. Am. Chem. Soc.* **2013**, *135*, 11799 – 11802. (c) Bandar, J. S.; Sauer, G. S.; Wulff, W. D.; Lambert, T. H.; Veticatt, M. J. *J. Am. Chem. Soc.* **2014**, *136*, 10700 – 10707. (d) Bandar, J. S.; Barthelme, A. P.; Mazori, A. Y.; Lambert, T. H. *Chem. Sci.* **2015**, *6*, 1537 – 1547. (e) Nacsa, E. D.; Lambert, T. H. *J. Am. Chem. Soc.* **2015**, *137*, 10246 – 10253.
- 20) (a) Holschumacher, D.; Hrib, C. G.; Jones, P. G.; Tamm, M. *Chem. Commun.* **2007**, 3661 – 3663. (b) Wilde, M. M. D.; Gravel, M. *Angew. Chem. Int. Ed.* **2013**, *52*, 12651 – 12654. (c) Wilde, M. M. D.; Gravel, M. *Org. Lett.* **2014**, *16*, 20, 5308 – 5311. (d) Ramanjaneyulu, B. T.; Mahesh, S.; Anand, R. V. *Org. Lett.* **2015**, *17*, 3952 – 3955. (e) Haghshenas, P.; Langdon, S. M.; Gravel, M. *Synlett* **2017**, *28*, 542 – 559. (f) Goswami, P.; Sharma, S.; Singh, G.; Anand, R. V. *J. Org. Chem.* **2018**, *83*, 4213 – 4220. (g) Singh, G.; Goswami, P.; Anand, R. V. *Org. Biomol. Chem.* **2018**, *16*, 384 – 388.
- 21) Mir, R.; Dudding, T. *J. Org. Chem.* **2017**, *82*, 709–714.
- 22) Dempsey, K.; Mir, R.; Smajlagic, I.; Dudding, T. *Tetrahedron* **2018**, *74*, 3507 – 3511.
- 23) Belding, L.; Stoyanov, P.; Dudding, T. *J. Org. Chem.* **2016**, *81*, 6–13. (b) Mirabdolbaghi, R.; Dudding, T. *Org. Lett.* **2015**, *17*, 1930–1933. (c) Smajlagic, I.; Durán, R.; Pilkington, M.; Dudding, T. *J. Org. Chem.* **2018**, *83*, 13973–13980. (d) Le Sueur, R.; Guest, M.; Belding, L.; Pilkington, M.; Dudding, T. *Tetrahedron Lett.* **2019**, *60*, 150928. (e) Smajlagic, I.; Guest, M.; Durán, R.; Herrera, B.; Dudding, T. *Organocatalysis. J. Org. Chem.* **2020**, *85*, 585 – 593.

- 24) Mir, R.; Dudding, T. A Au(I)-Precatalyst with a Cyclopropenium Counterion: An Unusual Ion Pair. *J. Org. Chem.* **2016**, *81*, 2675–2679.
- 25) For recent reviews: (a) Lima, C. G. S.; Pauli, F. P.; Costa, D. C. S.; de Souza, A. S.; Forezi, L. S. M.; Ferreira, V. F.; da Silva, F. C. *Eur. J. Org. Chem.* **2020**, 2650 – 2692. (b) Wang, J. -Y.; Hao, W. -J.; Tu, S. -J.; Jiang, B. *Org. Chem. Front.* **2020**, *7*, 1743 – 1778 and references cited therein.
- 26) For selected recent examples: (a) Goswami, P.; Singh, G.; Anand, R. V. *Org. Lett.* **2017**, *19*, 1982 – 1985. (b) Singh, G.; Goswami, P.; Sharma, S.; Anand, R. V. *J. Org. Chem.* **2018**, *83*, 10546 – 10554. (c) Singh, G.; Kumar, S.; Chowdhury, A.; Anand, R. V. *J. Org. Chem.* **2019**, *84*, 15978 – 15989.
- 27) (a) Holschumacher, D.; Hrib, C. G.; Jones, P. G.; Tamm, M. *Chem. Commun.* **2007**, 3661 – 3663. (b) Wilde, M. M. D.; Gravel, M. *Angew. Chem. Int. Ed.* **2013**, *52*, 12651 – 12654. (c) Wilde, M. M. D.; Gravel, M. *Org. Lett.* **2014**, *16*, 20, 5308 – 5311. (d) Ramanjaneyulu, B. T.; Mahesh, S.; Anand, R. V. *Org. Lett.* **2015**, *17*, 3952 – 3955. (e) Haghshenas, P.; Langdon, S. M.; Gravel, M. *Synlett* **2017**, *28*, 542 – 559. (f) Goswami, P.; Sharma, S.; Singh, G.; Anand, R. V. *J. Org. Chem.* **2018**, *83*, 4213 – 4220. (g) Singh, G.; Goswami, P.; Anand, R. V. *Org. Biomol. Chem.* **2018**, *16*, 384 – 388.
- 28) Please refer to the website: <http://supramolecular.org> (b) Thordarson, P. *Chem. Soc. Rev.* **2011**, *40*, 1305 – 1323.
- 29) (a) Arde, P.; Anand, R. V. *RSC Adv.* **2016**, *6*, 77111 – 77115. (b) Cheng, Y.; Fang, Z.; Jia, Y.; Lu, Z.; Li, W.; Li, P. *RSC Adv.*, **2019**, *9*, 24212 – 24217. (c) Jadhav, A. S.; Anand, R. V. *Eur. J. Org. Chem.* **2017**, 3716 – 3721.
- 30) Wong, Y. F.; Wang, Z.; Sun, J. *Org. Biomol. Chem.* **2016**, *14*, 5751 – 5754.
- 31) Saha, S.; Alamsetti, S. K.; Schneider, C. *Chem. Commun.* **2015**, *51*, 1461 – 1464.
- 32) Cheetham, C. A.; Massey, R. S.; Pira, S. L.; Pritchard, R. G.; Wallace, T. W. *Org. Biomol. Chem.* **2011**, *9*, 1831.
- 33) David, D.M.; Kane-Maguire, L.A.; Pyne, S.G. *Chem. Commun.* **1990**, 888-889.

- 34) Holschumacher, D.; Hrib, C. G.; Jones, P. G.; Tamm, M. A. *Chem. Commun.* **2007**, 3661–3663.
- 35) For the reports on transition-metal or Lewis acid catalyzed 1,6-conjugate addition of indoles to *p*-quinone methides from our research group, please see: (a) Reddy, V.; Anand, R. V. *Org. Lett.* **2015**, *17*, 3390 – 3393. (b) Jadhav, A. S.; Pankhade, Y. A.; Anand, R. V. *J. Org. Chem.* **2018**, *83*, 8615 – 8626. (c) Goswami, P.; Anand, R. V. *Chemistry Select* **2016**, *1*, 2556 – 2559. (d) For a catalyst-free 1,6-conjugate addition of indole to *p*-quinone methides at elevated temperatures, see: Kumaran, S.; Prabhakaran, M.; Mariyammal, N.; Parthasarathy, K. *Org. Biomol. Chem.* **2020**, *18*, 7837. (e) Wang, J.-R.; Jiang, X.-L.; Hang, Q.-Q.; Zhang, S.; Mei, G. -J.; Shi, F. *J. Org. Chem.* **2019**, *84*, 7829–7839.
- 36) Chu, W. D.; Zhang, L. F.; Bao, X.; Zhao, X. H.; Zeng, C.; Du, J. Y.; Zhang, G. B.; Wang, F. X.; Ma, X. Y.; and Fan, C. A. *Angew. Chem., Int. Ed.*, **2013**, *52*, 9229 – 9233.
- 37) Lavallo, V.; Canac, Y.; Donnadieu, B.; Schoeller, W. W.; and Bertrand, G. *Science* **2006**, *312*, 722 – 724.
- 38) Bidal, Y. D.; Lesieur, M.; Melaimi, M.; Cordes, D. B.; Slawin, A. M. Z.; Bertrand G. and Cazin., C. S. J. *Chem. Commun.* **2015**, *51*, 4778 – 4781.
- 39) Enders, D.; Breuer, K.; Kallfass, U. and Balensiefer, T. *Synthesis* **2003**, *8*, 1292 – 1295.
- 40) Yoshida, Z.-I.; Konishi, H.; Miura, Y.; Ogoshi, H. *Tetrahedron Lett.* **1977**, *18*, 4319 – 4322
- 41) Weiss, V. R.; Priesner, C. *Angew. Chem. Int. Ed.* **2006**, *45*, 6652 – 6655.

Tris-arylcyclopropenium carbocation as an organic Lewis acid catalyst in Nazarov cyclization and conjugate addition reactions.

4.1 Introduction

Carbocations are generally described as non-isolable and inherently unstable intermediates in fundamental transformations such as E1, S_N1, and rearrangement reactions.¹ However, this is not completely true, because some delocalized carbocations have been found to exist in a stable form in aqueous media even without inert conditions.² For example, tropylium carbocation was the first stable carbocation to be identified in 1891.³ Since then, the stability, reactivity, and other characteristics of several forms of other carbocations have been thoroughly investigated.² Carbocations have been recognized for more than 130 years, thus it is somewhat unexpected that their applications in organic synthesis have recently been investigated. Nowadays, carbocations like tropylium and trityl cation are frequently utilized as Lewis acids to activate electrophiles by decreasing their LUMO,⁴ and as Bronsted acids to activate nucleophiles like alcohols. Additionally, carbocations have also been employed as photocatalysts and electrophotocatalysts for radical-mediated transformations (Figure 1).^{5–8}

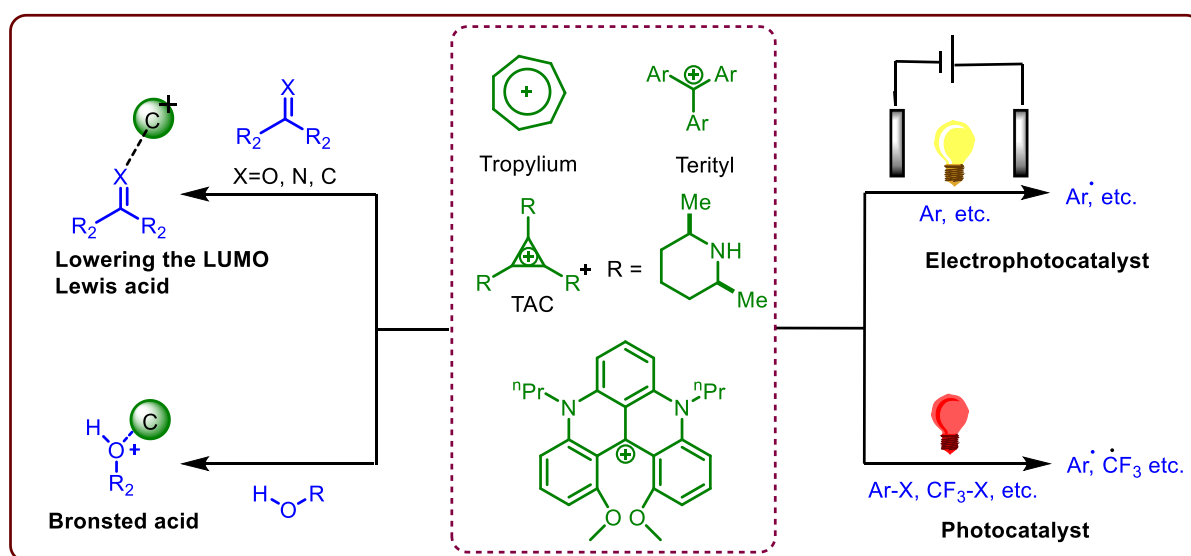


Figure 1. The activation pattern of carbocations

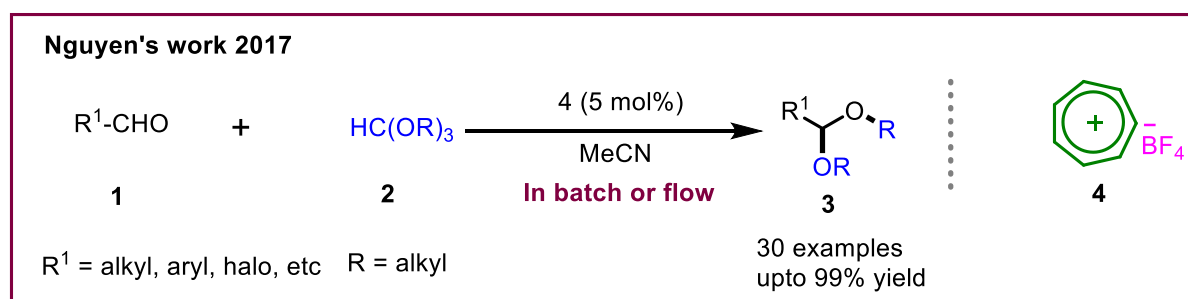
This chapter describes the recent advancement in carbocation-promoted organic reactions over the past decade.

4.2 Literature reports on carbocation-catalyzed organic transformations

In the last few years, carbocations have been used for the activation of various functional groups, and some of the recent reports are listed below.

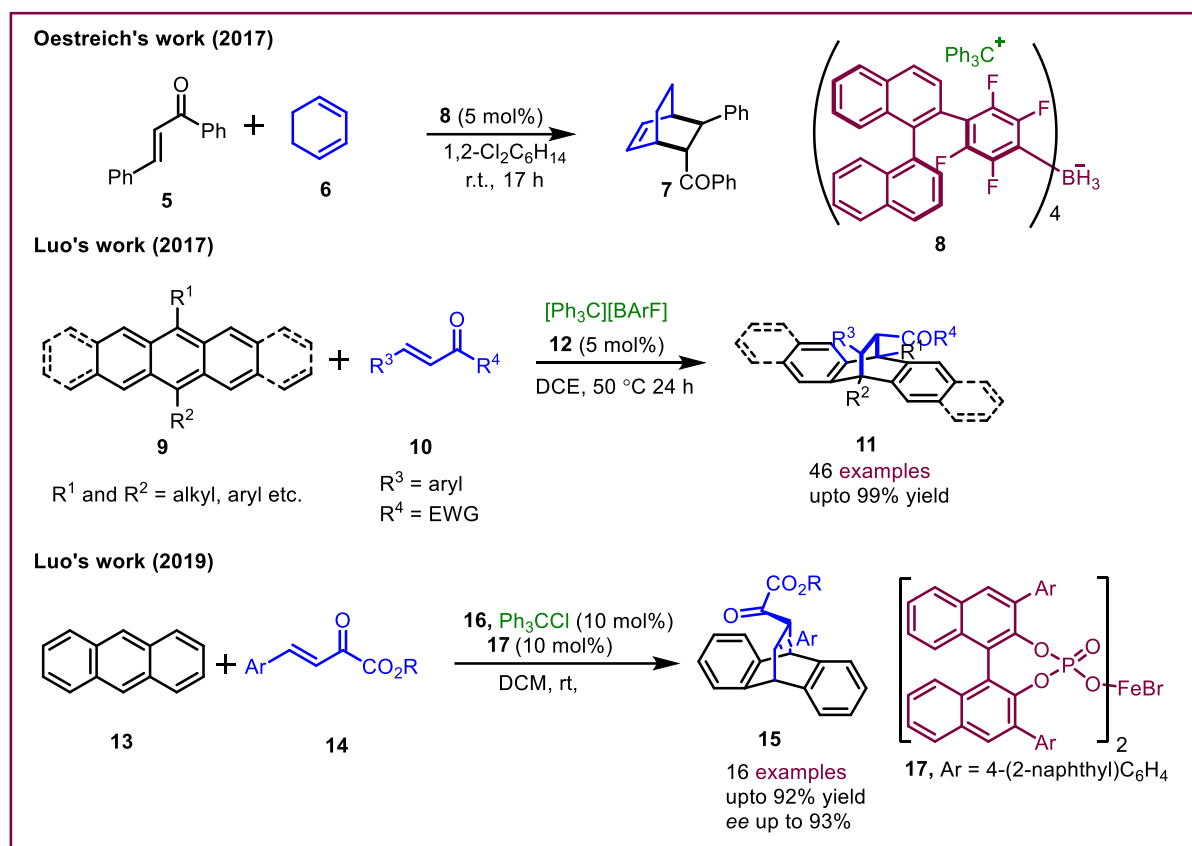
4.2.1 Activation of carbonyl group by carbocation

Due to their diverse and common chemical nature in organic transformations, carbonyl compounds belong to the most synthetically significant classes of organic substances. The acetalization reaction is the most widely used masking strategy for aldehydes and ketones.⁹ In 2017, Nguyen and co-workers established a tropylium cation **4** catalyzed acetalization reaction using a variety of aldehydes (**1**) and trialkyl orthoformate (**2**) under both batch and flow setups to produce the corresponding diacetyl derivatives (**3**) in good yields (Scheme 1).¹⁰



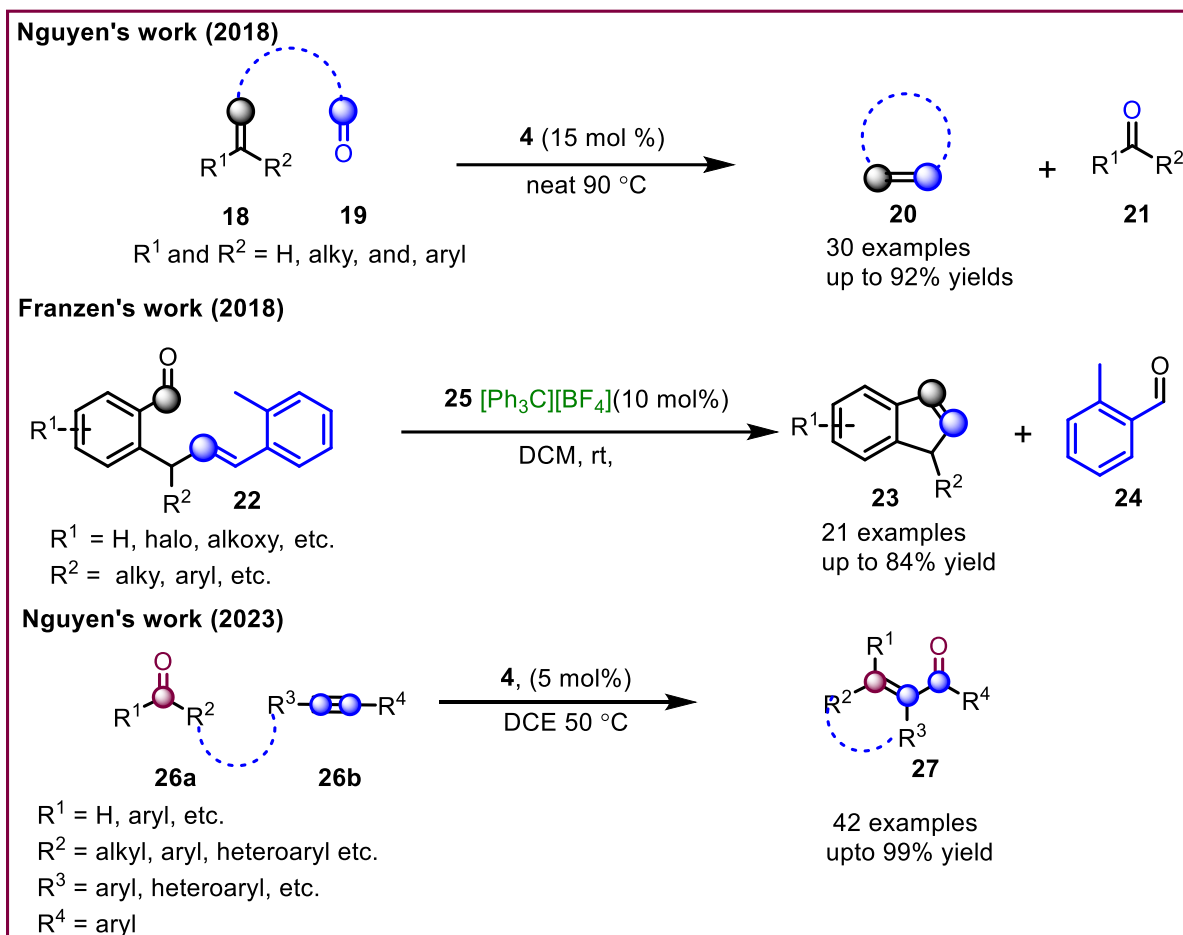
Scheme 1. Tropylium cation catalyzed acetalization reactions.

In 2017, Oestreich and co-workers developed a Mukaiyama aldol addition through a directed Diels-Alder reaction using **8** (a chiral derivative of $[\text{B}(\text{C}_6\text{F}_5)_4]^-$ where the trityl carbocation was the counter ion). However, the dienophile **5** and diene **6** could generate only racemic product **7** (Scheme 2).¹¹ Later in 2017, Luo and co-workers reported a Diels Alder reaction with anthracene derivatives (**9**) and α,β -unsaturated carbonyl compounds (**10**) through activation of LUMO of dienophile (carbonyl compounds) to prepare the corresponding cyclic products (**11**) in excellent yields.¹² In continuation of this work, the same research group has established the design and synthesis of a chiral complex **17** and the precursor of trityl carbocation **16**. They have employed this chiral catalyst **17** for the Diels–Alder reaction of anthracene **13** with activated dienophiles (**14**) to get the desired products (**15**) in good to excellent yield with very high chiral induction of up to 93% *ee* (Scheme 2).¹³



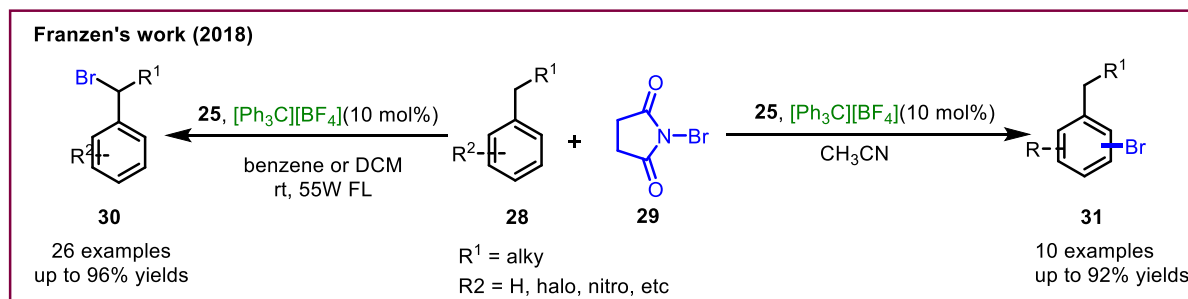
Scheme 2. Tropylium cation catalyzed Diels-Alder reactions.

Carbonyl and olefin metathesis reactions using metal-based Lewis acids have been explored by Schindler's group^{14–17} and Li's group.¹⁸ However, in 2018, Nguyen and co-workers developed an organocatalytic carbonyl-olefin metathesis using tropylium salt as an organic Lewis acid. They suggested that tropylium activates the aldehyde by lowering its LUMO and enables the nucleophilic attack by olefin followed by the sequential intramolecular cyclization and retro [2+2] cycloaddition reaction to furnish the corresponding products (**20**) [Scheme 3].¹⁹ In the same year, Franzen's research group reported an intramolecular ring-closing carbonyl-olefin metathesis reaction of enals (**22**) by employing tropylium cation **25** as an organocatalyst to generate the indenenes (**23**) in moderate to good yields.²⁰ Very recently, the Nguyen group has developed an inter- and intramolecular carbonyl-alkyne metathesis (CAM) reaction. Compounds **26a/26b** were subjected to optimized conditions to generate the 2-H chromene and phenanthrene products (**27**). The author suggested that the CAM reactions begin with a [2+2]-cycloaddition of the carbonyl and the alkyne, followed by a [2+2]-cyclo-reversion of a four-membered oxetane to produce the 2-H chromene and phenanthrene products **27** (Scheme 3).²¹



Scheme 3. Tropylium and trityl carbocation catalyzed inter- and intramolecular metathesis reactions

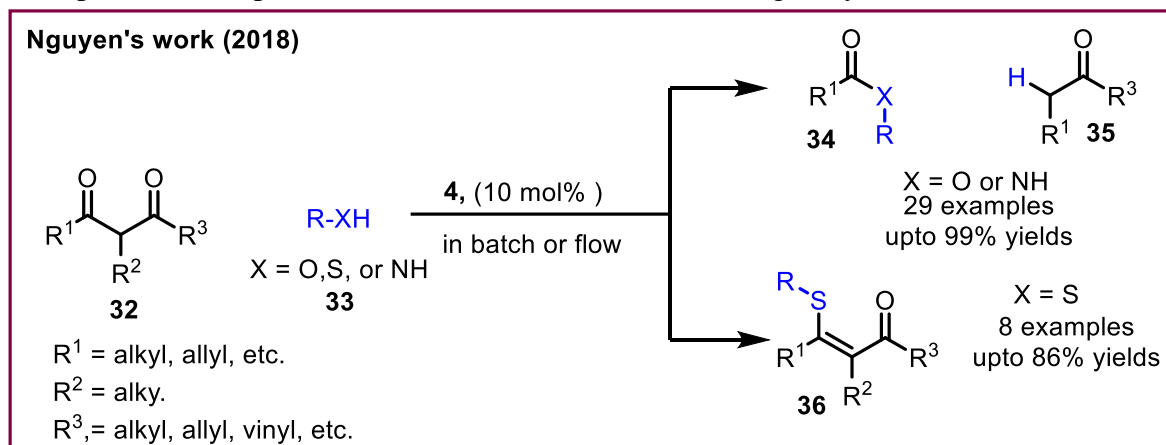
Franzen and co-workers, in 2018 established a highly chemoselective bromination of alkyl arenes (**28**) using trityl carbocation **25** as an organic Lewis acid catalyst; here, *N*-bromosuccinimide **29** was employed as a bromination source. It was proposed that under light-mediated reaction conditions, trityl cation helps in producing bromine from NBS and facilitating nucleophilic addition of bromide ion to generate benzyl bromide product **30**.



Scheme 4. Trityl carbocation catalyzed chemoselective bromination reactions.

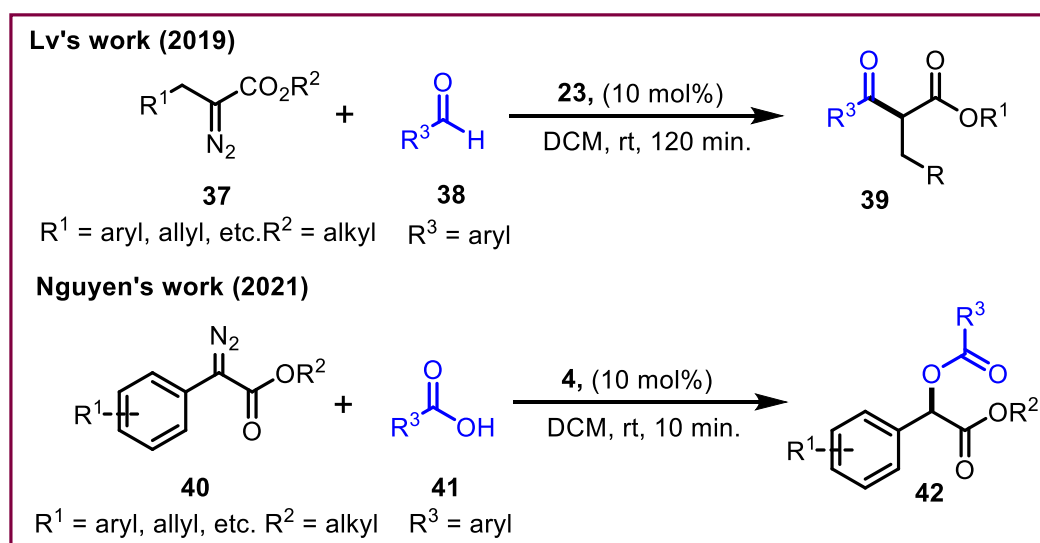
On the other hand, in acetonitrile solvent and the absence of light, aryl-bromides (**31**) were obtained as a major product (Scheme 4).²²

In 2018, Nguyen and co-workers demonstrated tropylium salt **4** catalyzed Retro-Claisen rearrangement type reaction, where C-C bond cleavage of diketones (**32**) produced the corresponding amines (**34**) and esters (**35**). Additionally, by employing thiols as the nucleophiles, the respective thioethers (**36**) were obtained in good yields (Scheme 5).²³



Scheme 5. Tropylium carbocation mediated retro-Claisen rearrangement.

Lv and co-workers, in 2019, reported the Roskamp reaction between α -alkyl diazoacetates (**37**) and aldehydes (**38**) by utilizing the trityl carbocation as a catalyst to access a wide range of α -branched β -ketocarboxyls (**39**) in moderate yields (Scheme 6).²⁴

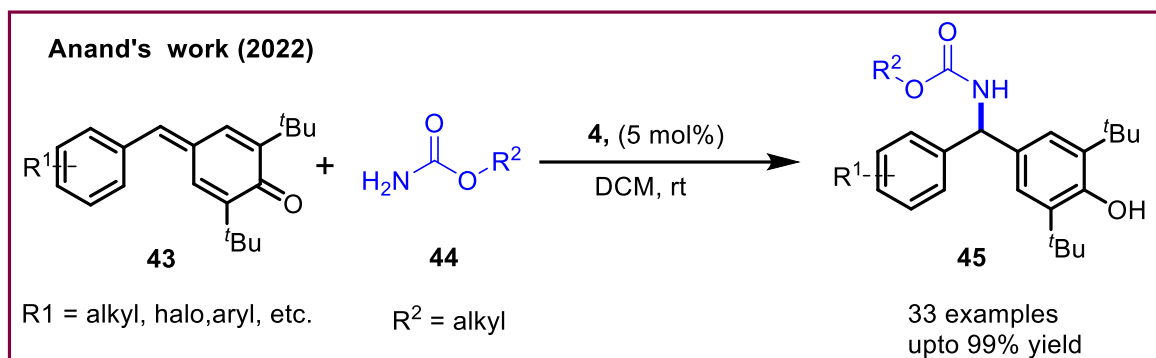


Scheme 6. Roskamp reaction of aldehydes and α -alkyldiazoacetates.

Later, in 2021, Nguyen's research group developed an analogous methodology for the synthesis of α -functionalized esters (**42**) through tropylium-catalyzed O-H insertion reaction of diazoalkanes (**40**) with carboxylic acids (**41**). This reaction tolerated various functional groups and produced the functionalized esters in moderate to good yields (Scheme 6).³³

A vinylogous aza-Michael addition of carbamates (**44**) to *p*-quinone methides (**43**) was demonstrated by Anand and co-workers. Several different, α,α' -diarylmethyl carbamates (**45**)

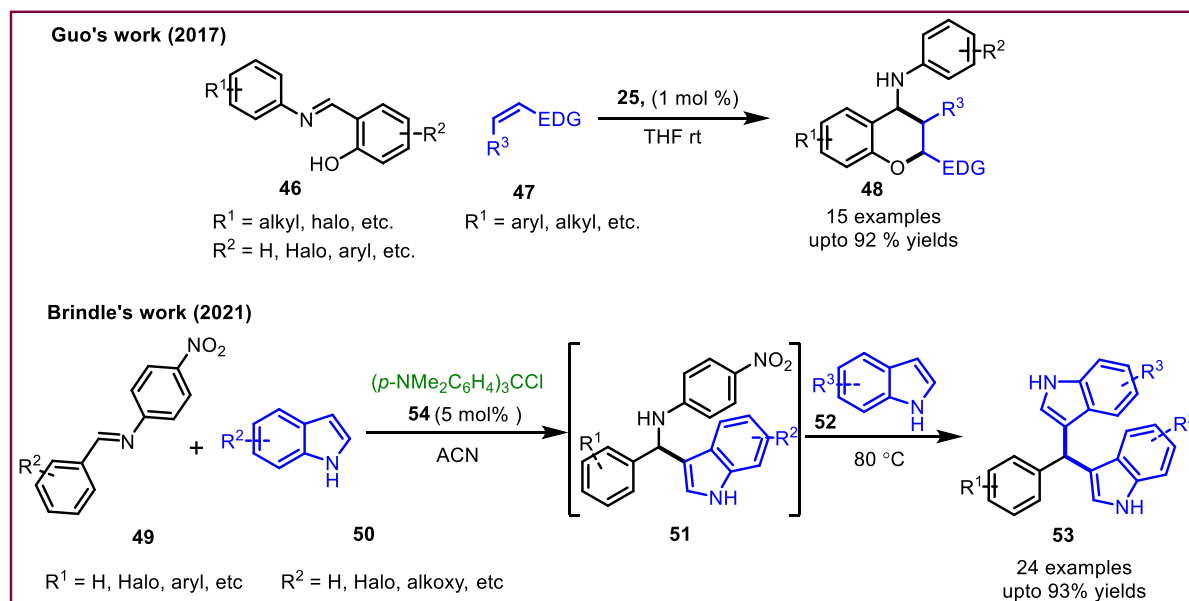
were isolated in good to exceptional yields. The author proposed two different plausible mechanisms, including hidden Bronsted acid activation *via in-situ* generation of HBF₄ and Lewis acid activation through tropylium carbocation coordination to *p*-QMs (Scheme 7).²⁵



Scheme 7. Vinylogous aza-Michael addition of carbamates to *para*-quinone methides.

4.2.2. Activation of imines by carbocation

Guo and co-workers reported the synthesis of *cis*-4-aminobenzodihydropyrans (**48**) from salicylaldimines (**46**) and enones (**47**) under trityl cation **25** promoted interrupted Povarov reaction (Scheme 8).²⁶ Recently, Brindle's group reported the synthesis of enantiomerically-

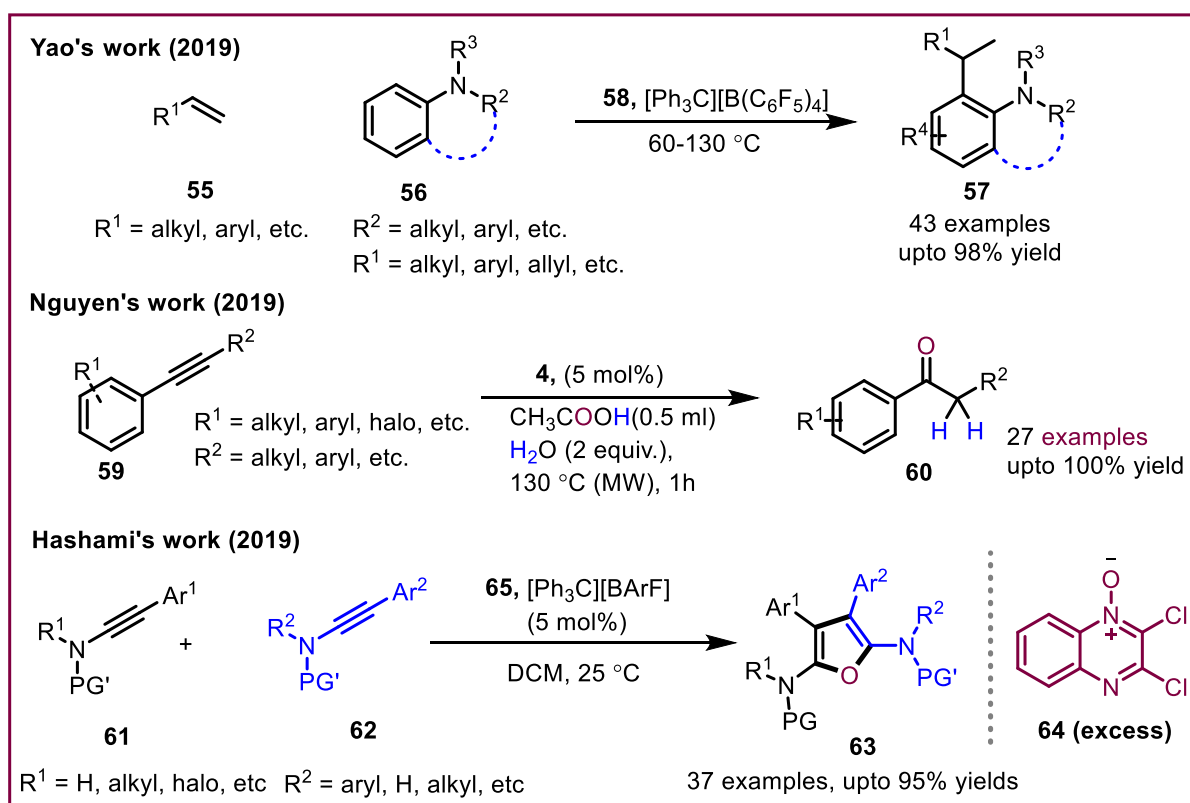


Scheme 8. Vinylogous aza-Michael addition of carbamates to *para*-quinone methides.

pure bisindolylmethanes (**51**) through the reaction between *N*-arylimines **49** and two different indoles **50** & **52** and using stable carbocation **54** (Scheme 8).²⁷

4.2.3 Activation of alkenes and alkynes by carbocation

The carbocations have also been utilized as alkenophylic and alkynophylic organic Lewis acid catalysts in organic transformations. In 2018, Yao and co-workers demonstrated a hydroarylation reaction between alkenes (**55**) and aromatic amines (**56**) by employing trityl carbocation **58** as a Lewis acid to produce the respective alkylated arenes (**57**) in excellent yield (Scheme 9).²⁸ In the same year, Nguyen and co-workers developed a tropylium-catalyzed hydration reaction of alkynes (**59**) in the presence of acetic acid or water to produce the corresponding ketones (**60**) in good to excellent yields. According to the proposed mechanism, the tropylium cation not only interacts with alkyne via π - π stacking but also with acetic acid or water to form an intermediate, which upon proton transfer yields the desired product (Scheme 9).²⁹ Similarly, in 2019, the Hashami research group established the synthesis of furan derivatives (**63**) by employing a trityl carbocation **65**, which promoted the oxidative [2+2+1] cycloaddition of two different molecules of ynamides **61** and **62** with 2,3-dichloroquinoxaline-*N*-oxide **64** (Scheme 9).³⁰

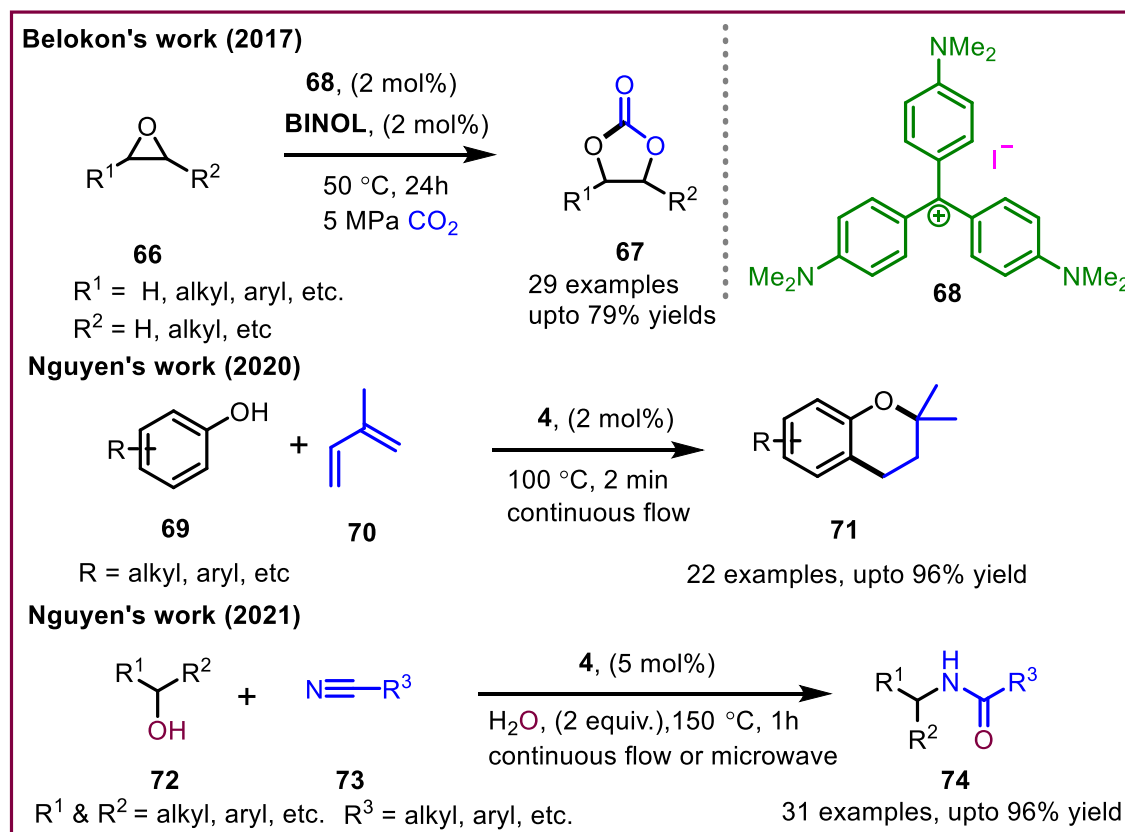


Scheme 9. Alkenophylic and alkynophylic activation utilizing different carbocations.

4.2.4 Activation of epoxides and alcohols by carbocation

In 2017, Belokon and co-workers established a methodology to produce cyclic carbonates (**67**) from epoxides (**66**) and carbon dioxide, catalyzed by carbocation **68** and

BINOL (Scheme 10).³¹ Later in 2020, Nguyen and co-workers reported a tropylium-catalyzed inexpensive method to synthesize 2,2-dimethylchromans (**71**) through prenylation reactions of phenols (**69**) with dienes (**70**) [Scheme 10].³² In 2021, the same group described a Ritter-type reaction between alcohols (**72**) and the nitriles (**73**) to generate the corresponding amides (**74**) in good to excellent yields (Scheme 10).³³

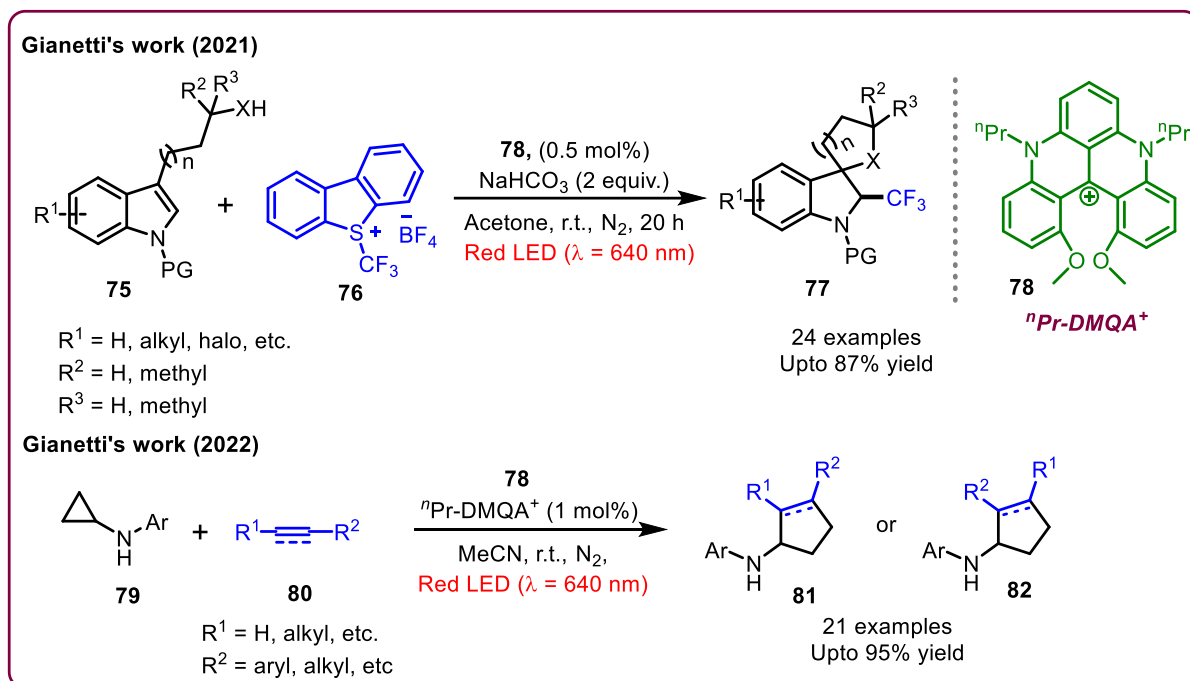


Scheme 10. Activation of epoxide and alcohols by carbocations

4.2.5 Photoredox catalysis by carbocation

In pursuit of promoting the SET process in organic reactions, photoredox catalysis has evolved into an efficient and environmentally beneficial synthetic tool. In 2021, Gianetti and co-workers established that the helical carbonium ion **78** could promote useful organic photoredox transformations under visible-light. The author developed *n*Pr-DMQA⁺ (**78**) catalyzed trifluoromethylation/dearomatization cascade reaction, utilizing *N*-protected indole-3-propionic acids (**75**) and Umemoto's reagent **76** (as a CF_3 source) to synthesize differently functionalized CF_3 -containing 3,3'-spirocyclic indoles (**77**) [Scheme 11].³⁴ Similarly, in 2022, the same research group discovered the [3+2]-cycloaddition of alkynes and alkenes (**80**) with cyclopropylamines (**79**) under mild conditions to access a wide range of

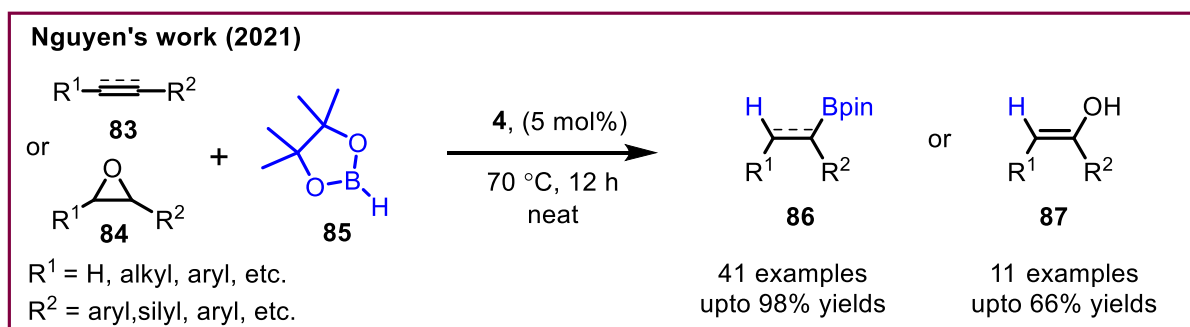
cyclopentane/cyclopentene derivatives (**81** and/or **82**) in moderate to good yields.³⁵



Scheme 11. Photoredox catalysis using carbocations

4.2.6 Miscellaneous reports on carbocation-catalyzed organic transformations

One of the most commonly used reactions in organic synthesis is the hydroboration reaction. Typically, a main group element or transition metal would catalyze the hydroboration reaction. However, in 2021, Nguyen and co-workers established a tropylium-catalyzed hydroboration



Scheme 12. Tropylium-catalyzed hydroborylation reaction of Alkynes, Alkenes, and Epoxides the reaction of alkynes, alkenes (**83**), and epoxides (**84**) to produce the corresponding products (**86** or **87**) in good to excellent yield (Scheme 12).³⁶

4.3 Background

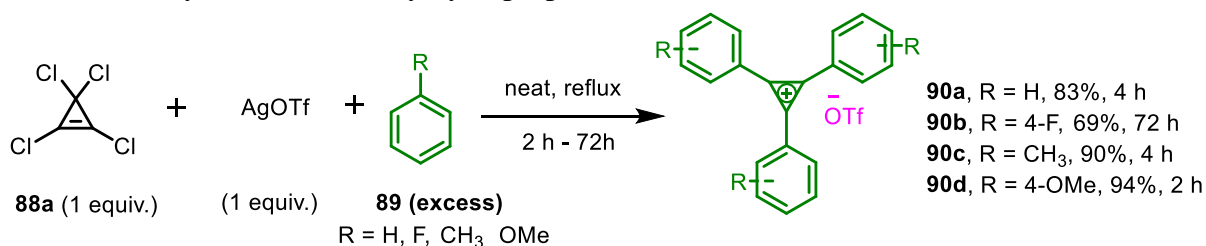
Although there are several reports on the catalytic applications of trityl and tropylium carbocations, surprisingly, the cyclopropenium carbocations have not been utilized as organic

Lewis acid so far in any fundamental organic transformations. Therefore, we became interested in exploring some of the cyclopropenium salts as organic Lewis acid in some fundamental organic transformations, especially, in reactions involving carbonyl activation.

4.4 Results and discussion

During the course of exploring the chemistry of cyclopropenium ions in the oxophilic activation through hydrogen bond donor catalysis,³⁷ we anticipated that a suitable substitution on the cyclopropenium ring could lead us to effective and efficient molecules that can act as organic Lewis acid catalysts. We envisioned that these cyclopropenium carbocations could activate the carbonyl group of carbonyl compounds through coordination between carbocation and the carbonyl group. In such cases, many fundamental organic transformations could be carried out using these cyclopropenium carbocation as an organic Lewis acid. With the proposed hypothesis, a variety of cyclopropenium ions (**90a-d**) with different aryl-substituents on the cyclopropane ring have been synthesized using a literature procedure (Scheme 13).³⁸

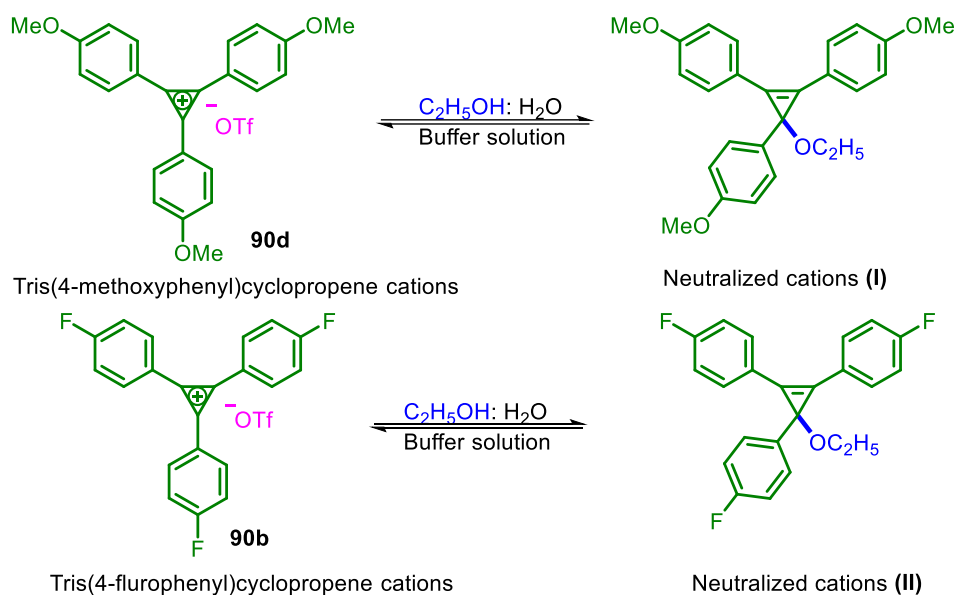
Scheme 13. Synthesis of tris(aryl)cyclopropenium salts.^a



^aAll reaction were carried out at 1.41 mmol scale of **88a**. yields reported are isolated yields.

4.4.1. Determination of the pK_a values of tris(aryl)cyclopropenium salts.

The UV spectra of the triarylcyclopropenyl cations are characterized by the absorption of light in the ultraviolet region, typically in the range of 200–400 nm. The exact position and intensity of the absorption bands depend on the substituents on the cyclopropenyl ring, and the solvent used. In 1961, Breslow and co-workers calculated the pK_a of **90a** and **90d** using UV-visible spectroscopy, and the values were found to be 2.7 and 6.40 in an aqueous EtOH solution.³⁹ To get hands-on experience in these experiments we have also repeated the experiments done by Breslow for the carbocation **90d** and followed the same procedure for **90b**. The following



Scheme 14. Neutralization of carbocation **90d** and **90b** in aqueous ethanolic solution. Buffer solutions used were freshly prepared in 23% aqueous ethanolic solution.

are the details of those experiments. The pK_a of **90d** and **90b** cations were determined in 23% aqueous ethanol (Scheme 13). For this purpose, we made a buffer solution in the range of pH 0.025 to 10. The cation (1 mg) was dissolved in 5.27 mL of 95% ethanol before being diluted with water to make it 10 mL. We created buffer or acid solutions by diluting 21.1 mL of 95% ethanol to 100 mL with water and 1 mL of the "50%" ethanolic cation solution to 10 mL with the "20%" ethanolic buffer solution. This created a medium that is referred to as "23% aqueous ethanol." Although less alcohol was sufficient for **90d**, preliminary experiments showed that this was the minimal amount of ethanol needed to prevent turbidity when **90d** was neutralized. The conventional method, which involves analyzing the ultraviolet spectra of each cation in 10–15 buffer or acid solutions spaced throughout a pH range of roughly one unit on either side of the pK_a , was adopted. The midpoint of the ensuing titration curve was taken as the pK_a . The absorbance at a wavelength that describes the cation was plotted against pH. The wavelengths used were 362 nm and 324 nm for tris(4-methoxyphenyl)cyclopropenyl cation and tris(4-fluorophenyl)cyclopropenyl cation, respectively. The spectra were recorded on the Carry 3500 UV-visible compact Peltier. The above-created solutions were analyzed in a 1-cm UV quartz cuvette. The tris(4-methoxyphenyl)cyclopropenyl cation's pK_a was found to be 6.39 (Figure 2 and Table 1) at normal concentration. However, interestingly, the tris(4-fluorophenyl)cyclopropenyl cation's pK_a was found to be 1.62 (Figure 3 and Table 2). The low

pK_a shows that **90b** has almost 4 times of Lewis acidic character in comparison to **90d**.

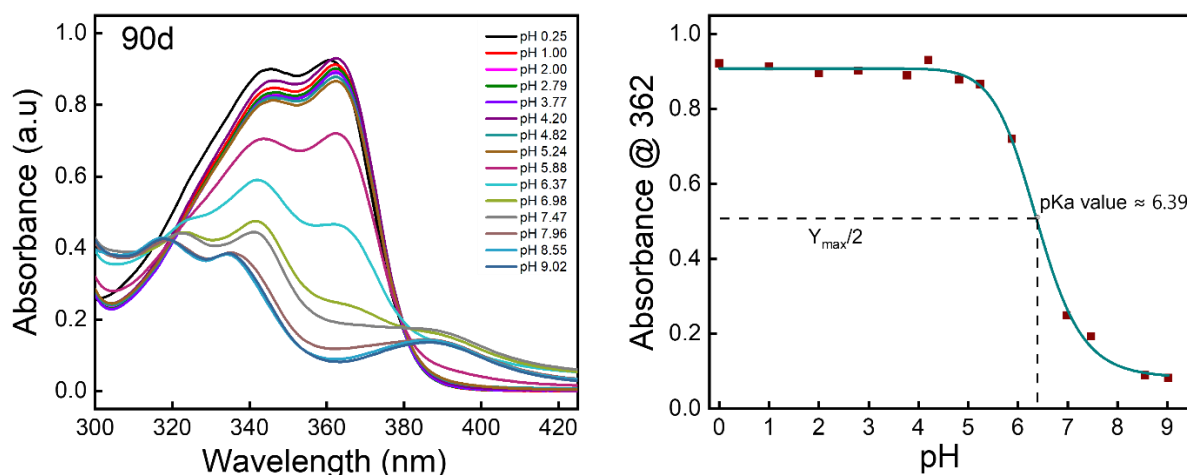


Figure 2. Ultraviolet absorption spectra of **90d** and neutralized cation **I** (Scheme 13) in 23% ethanol in water. The absorbance taken at 362 nm was plotted against the pH of the solution. From this, we can calculate pK_a , which corresponds to the pH value at half the maximum absorbance. The pK_a of **90d** calculated from this graph is 6.39.

Table 01. The absorbance value of **90d** at 362 using buffer solutions of pH 0.25–9.22.

pH	Absorbance @ 362 nm
0.25	0.92145
1.00	0.91347
2.00	0.89664
2.79	0.90234
3.77	0.89019
4.20	0.93061
4.82	0.87902
5.24	0.86668
5.88	0.7206
6.37	0.46674
6.98	0.24907
7.47	0.19343
7.96	0.11818
8.55	0.0898
9.22	0.0873

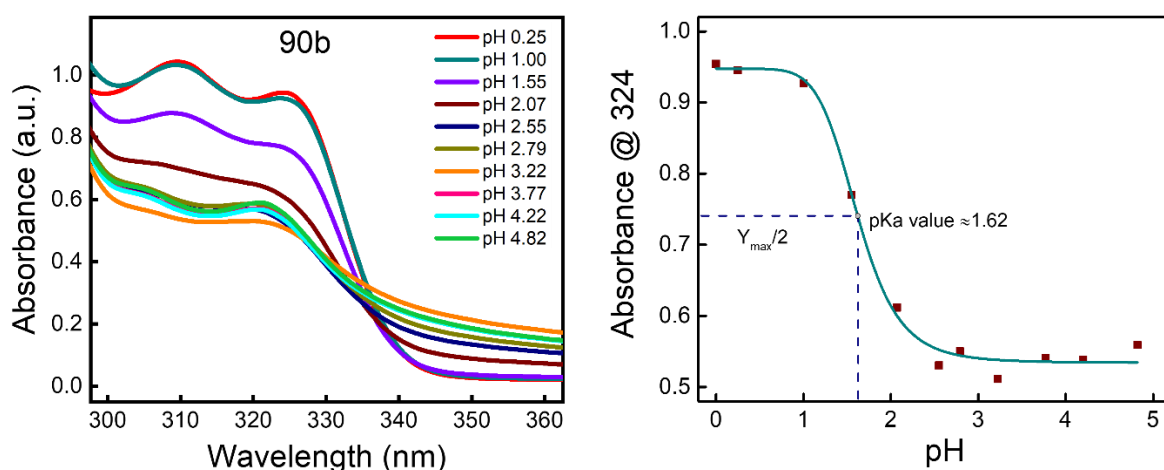


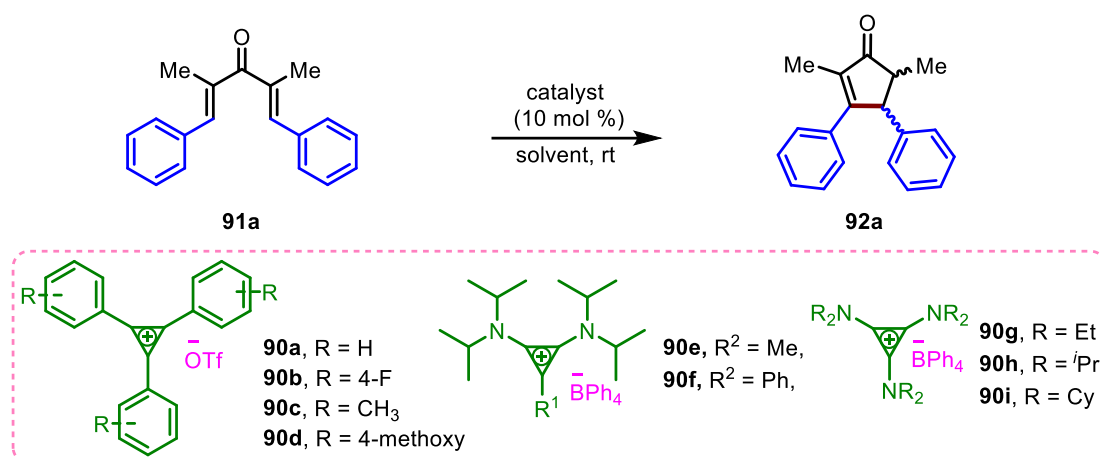
Figure 3. Ultraviolet absorption spectra of **90b** and neutralized cation **II** (Scheme 13) in 23% ethanol in water. The absorbance taken at 324 nm was plotted against the pH of the solution. The pK_a of **90b** calculated from this graph is 1.62.

Table 2. The absorbance value of **90b** at 324 using buffer solutions of pH 0.25–4.82.

pH	Absorbance @ 324 nm
0.25	0.94543
1.00	0.92669
1.55	0.76997
2.07	0.61155
2.55	0.53033
2.79	0.55004
3.22	0.51135
3.77	0.54058
4.20	0.53851
4.82	0.55907

4.4.2 Optimization study

It was clear from the pK_a measurement experiments that the cyclopropenium derivative **90b** has a pK_a of 1.62; so, we envisaged that this carbocation could be used as a Lewis acid catalyst in some of the fundamental organic transformations such as Nazarov cyclization as this reaction involves activation of the carbonyl group. In this regard, we started the optimization studies using a readily available symmetric tetra-substituted dienone **91a** as a model substrate. The outcomes of the optimization reactions are summarized in Table 3.

Table 3. Catalyst Screening and Optimization Study.^a

Entry	Catalyst	Solvent	Time	Yield of 92a ^b (%)	<i>dr</i> (<i>cis:trans</i>)
1	90a	THF	12 h	NR	
2	90a	1,4 Dioxane	12 h	NR	
3	90a	MeCN	12 h	<10	
4	90a	PhMe	12 h	NR	
5	90a	CHCl ₃	6 h	47	2:1
6	90a	CH ₂ Cl ₂	6 h	65	2:1
7	90a	1,2-DCE	6 h	53	3:1
8 ^c	90b	CH ₂ Cl ₂	15 min	92	3:1
9	90c	CH ₂ Cl ₂	12 h	60	1:1
10	90d	CH ₂ Cl ₂	12 h	42	1:1
11	90e	CH ₂ Cl ₂	12 h	NR	
12	90f	CH ₂ Cl ₂	12 h	NR	
13	90g	CH ₂ Cl ₂	12 h	>10	
14	90h	CH ₂ Cl ₂	12 h	NR	
15	90i	CH ₂ Cl ₂	12 h	NR	
16	90b	CHCl ₃	6 h	76	3:1
17	90b	1,2-DCE	6 h	83	3:1
18	90b	MeCN	12 h	70	2:1
19	90b	PhMe	12 h	27	2:1
20	90b	DMSO	16 h	67	2:1
21 ^d	90b	CH ₂ Cl ₂	1 h	83	3:1
22	NaOTf	CH ₂ Cl ₂	12 h	NR	
23	--	CH ₂ Cl ₂	12 h	NR	

^aAll reactions were carried out with **91a** (0.152 mmol), and 10 mol % of catalyst in 1 mL of solvent at room temperature. ^bIsolated yields. ^cOptimal condition. ^d5 mol % of catalyst was used. 1,2-DCE = 1,2-dichloroethane. DMSO = dimethyl sulfoxide. NR = No reaction

The optimization reactions were carried out with many cyclopropenium salts including the tris(aryl)cyclopropenium salts (**90a-d**). Initially, an experiment was carried out using **90a** as a catalyst in THF at room temperature; but no reaction was observed even after 12 h and the starting material **91a** remained as such (Entry 1, Table 3). The reaction was then performed in other solvents such as 1,4 dioxane, acetonitrile (ACN), and toluene. However, in those cases,

the formation of **92b** was not observed, except in MeCN, where **92a** was observed in <10%. Surprisingly, when the reaction was carried out in chlorinated solvents such as chloroform, dichloromethane and 1,2-dichloroethane, a drastic improvement in the formation of **92a** was observed (47, 65 and 53% yields, respectively) [Entries 5-7]. Interestingly, when tris(4-fluorophenyl)cyclopropenium salt **90b** was used as a catalyst, we observed a significant enhancement in the reaction rate and a great improvement in the yield of **92a** (up to 92% with $dr = 3:1\{cis:trans\}$) [Entry 8]. However, an opposite trend of reactivity was observed in the cases of reactions using electron-rich aryl-substituted cyclopropenium salts **90c** and **90d**; and **92a** was obtained in relatively lower reaction yields (60 and 42% yields, respectively), and poor diastereoselectivity ($dr = 1:1\{cis:trans\}$) in those cases (Entries 9 & 10]. Other bis(dialkylamino)-substituted cyclopropenium salts (**90e** and **90f**) and tris(dialkylamino)cyclopropenium salts (**90g-i**) were found to be ineffective for this transformation (Entries 11-15). Since the reaction worked well using **90b** in CH₂Cl₂ (Entry 8), a few other optimization experiments were carried out using this salt in other solvents (Entries 16-20); however, in those cases, the yield of **92a** was found to be inferior when compared to Entry 8. It was found that the reaction was also proceeding with 5 mol% of **90b** and in that case, **92a** was obtained in lower yield (83%) [Entry 21]. To understand whether the counter anion of **90b** (in this case, it is a triflate anion) plays any role in the Nazarov cyclization of **91a**, we performed a control experiment using sodium trifluoromethanesulfonate (NaOTf) as a catalyst in CH₂Cl₂ at room temperature (Entry 22). We presumed that there is a remote possibility that the triflate anion might get converted to TfOH, which could possibly catalyze the cyclization of **91a**. However, in this case, no product formation was observed even after 12 h which clearly shows that the counter anion (TfO⁻) is not involved in the catalytic process (Entry 22). The reaction did not proceed without the catalyst which clearly shows that a catalyst is required for this transformation (Entry 23).

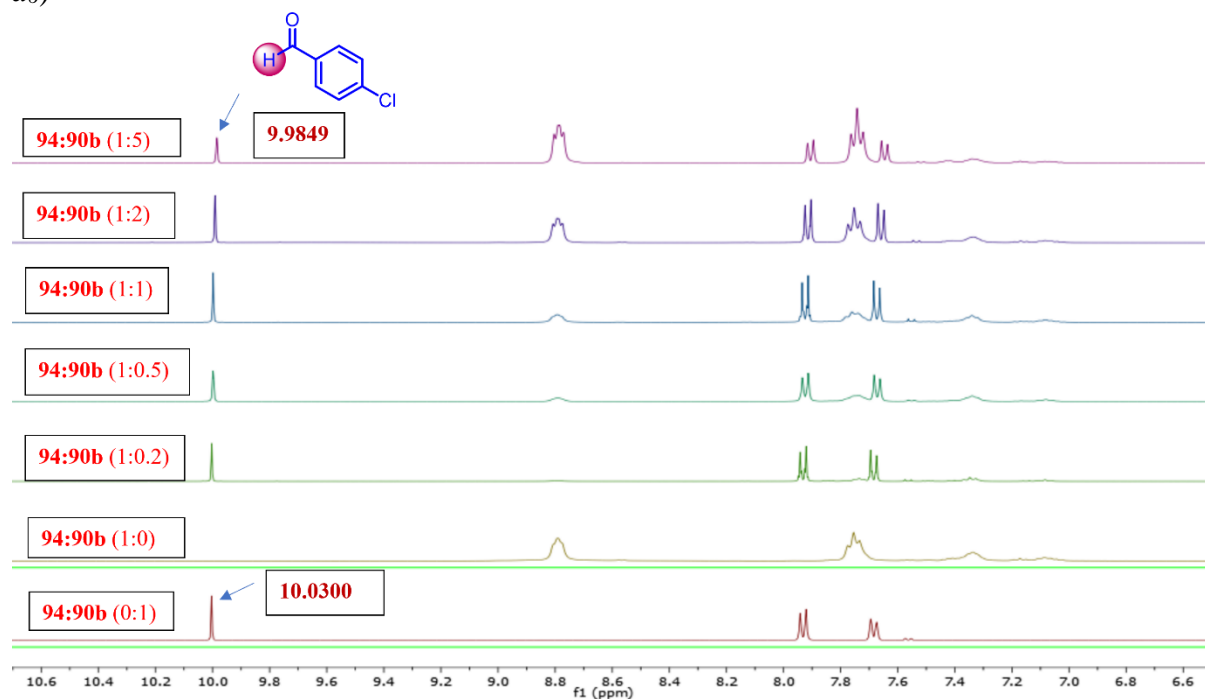
At this point, before moving to the substrate scope studies, we sought to understand the mechanism of this transformation. Based on the optimization studies (Table 3), we were partially convinced that the carbocation of the cyclopropene ring in **90b** behaves as an oxophillic Lewis acid in activating the carbonyl group of dienone **91a**. To confirm this concept, we have decided to perform a few control experiments based on NMR titration. We realized that it was not possible to perform NMR titration experiments between **90b** and **91a** as the Nazarov reaction of **91a** took place very fast (within 15 min). Therefore, since this reaction generally proceeds through carbonyl activation, to prove the concept, we thought of examining the complexation between **90b** and a model substrate such as an aryl-aldehyde or chalcone,

which closely resembles the structure of **91a**, through NMR titration experiments. We envisaged that these studies might provide some insights into whether the carbonyl group of **91a** is getting activated by **90b** or not in the actual Nazarov cyclization reaction. Thus, we have chosen chalcone **93** and *p*-chlorobenzaldehyde **94**, and as model substrates the NMR titration experiments with **90b**.

Initially, we performed the NMR titration between the catalyst **90b** and 4-chlorobenzaldehyde **94** in CDCl₃. However, since the catalyst **90b**, being a salt did not dissolve completely in CDCl₃ at higher concentrations. Therefore, the titration experiments were carried out in DMSO-*d*₆ in which **90b** was fully soluble even at high concentrations. Figure 4 shows the ¹H NMR spectra of pure **94**, pure **90b**, and mixture of **94** and **90b** at different concentrations. In pure form, the aldehyde proton (H-C=O) was observed at $\delta = 10.03$ ppm and, when the concentration of **90b** was increased gradually, there was a slight up-field shift in the chemical shift value of the aldehyde proton of **94**. At a higher concentration of **90b** (i.e., **94:90b** = 1:5), the chemical shift of the aldehyde proton was found to be $\delta = 9.985$ ppm. Not only the aldehyde proton, a slight up-field shifts in the *o*- and *m*-CH protons of the aryl groups were also observed. Although the difference in the chemical shift is not significant, this observation shows that there is a possible coordination between the carbonyl group of the aldehyde **94** and the catalyst **90b**. Similarly, the titration experiments between **90b** and **94** in DMSO-*d*₆ were observed using ¹³C NMR spectroscopy (Figure 5). In these cases, it was found that there was a slight up-field shift in the chemical shift of the carbonyl carbon of **94** (from $\delta = 192.187$ to 192.134 ppm). However, although there is a slight shift in the chemical shift, it seems to be negligible and therefore, we could not get much information in the ¹³C NMR titration experiments.

Further, the NMR titration experiments between the catalyst **90b** and chalcone **93** were carried out in DMSO-*d*₆. Figure 6 shows the ¹H NMR data for the titration between **90b** and **93**. The chemical shift of β -alkenyl carbon of the chalcone in pure form appeared at $\delta = 8.168$ ppm as a doublet. When the concentration of **90b** was increased gradually in the mixture, a slight and gradual up-field shift in the chemical shift of β -alkenyl carbon of the chalcone **93** was observed (from $\delta = 8.168$ to 8.127 ppm), which shows that there could be some kind of interaction between the C=O group of **93** and the catalyst **90b**. However, the ¹³C NMR analysis of the titration experiments revealed that the chemical shift of carbonyl carbon of **93** did not change much with increasing concentration of **90b** (from $\delta = 189.203$ to 189.120 ppm).

Figure 4. ^1H -NMR Titration of Catalyst **90b** and 4-Cl-Benzaldehyde **94** (400 MHz, $\text{DMSO-}d_6$)



□

Figure 5. ^{13}C -NMR Titration of Catalyst **90b** and 4-Cl-Benzaldehyde **94** (400 MHz, $\text{DMSO-}d_6$)

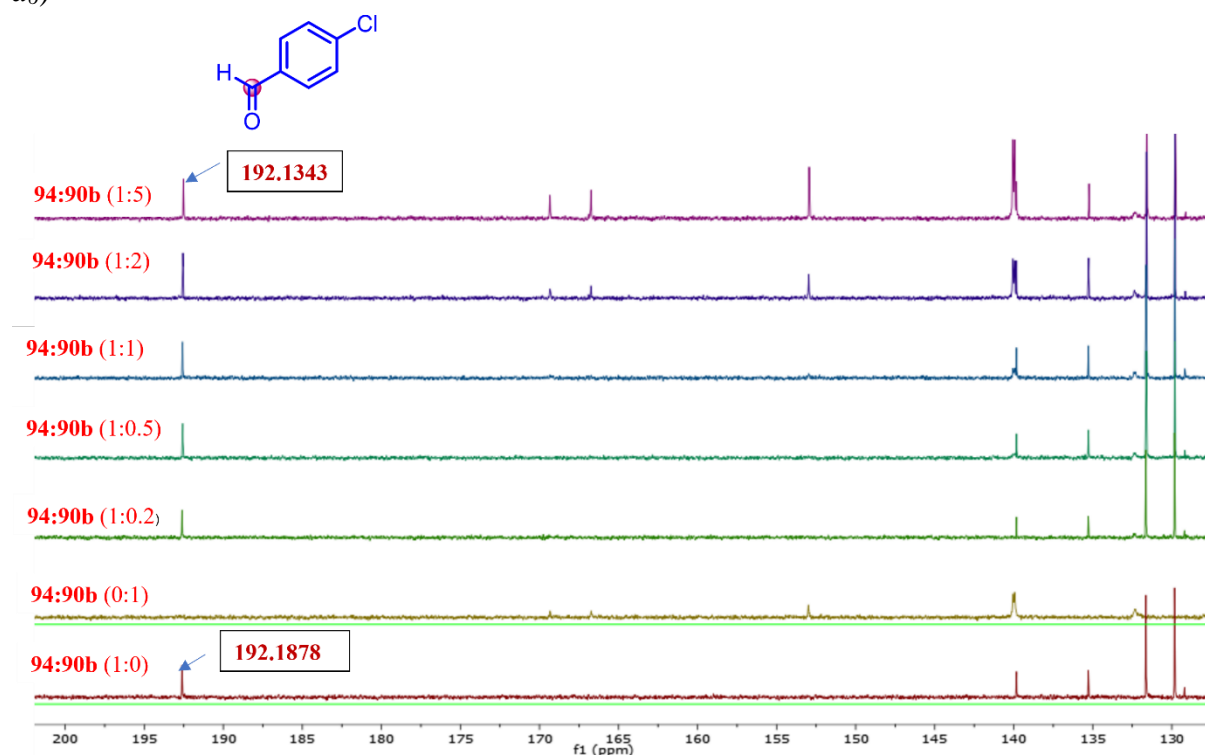


Figure 6. ^1H -NMR Titration of Catalyst **90b** and Chalcone **93** (400 MHz, $\text{DMSO-}d_6$)

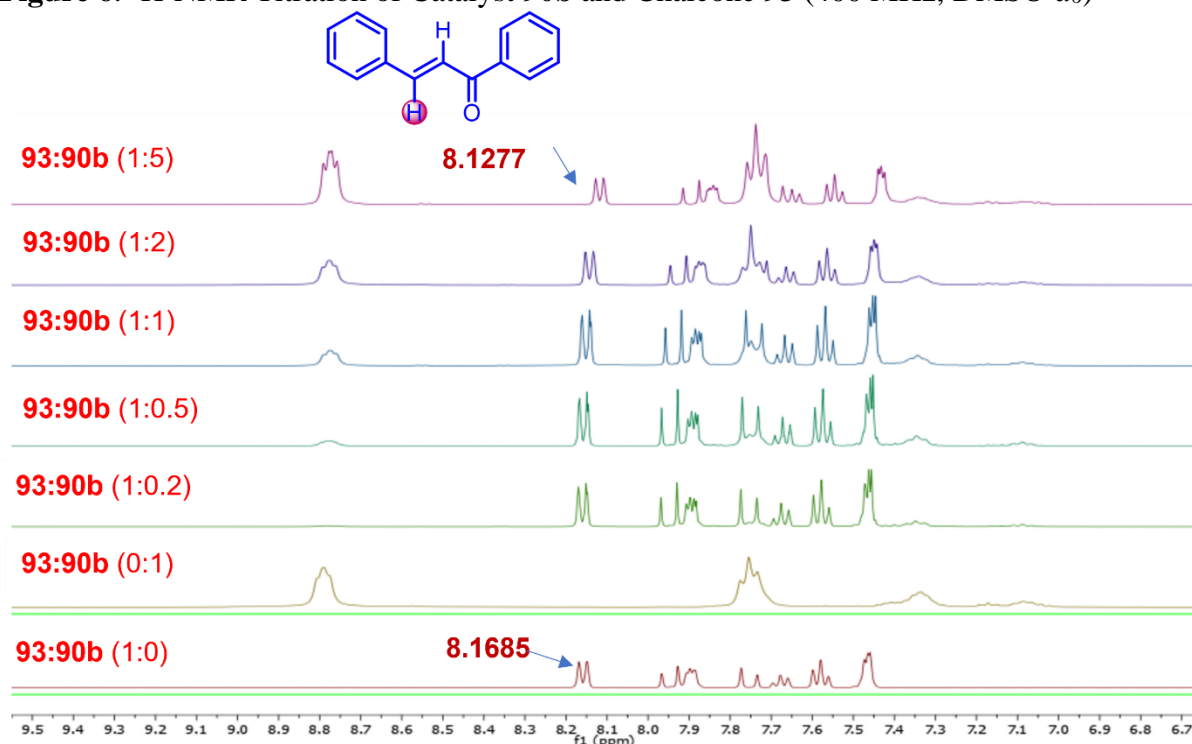
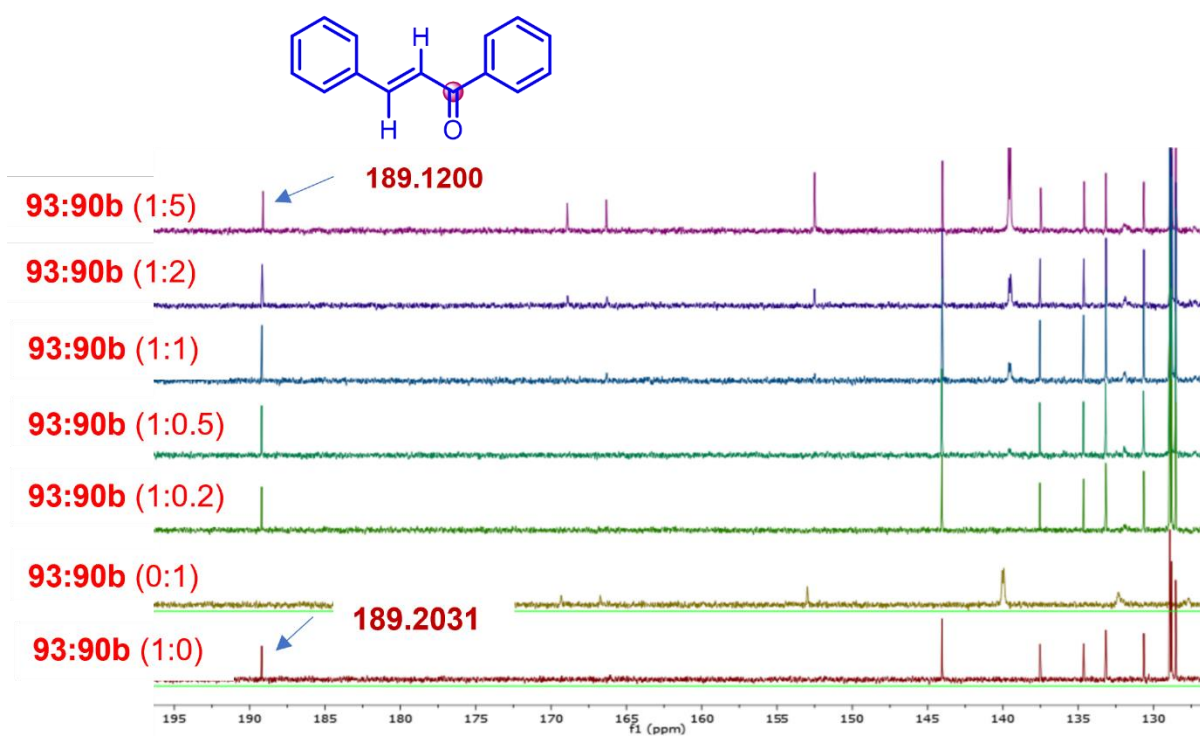


Figure 7. ^{13}C -NMR Titration of Catalyst **90b** and Chalcone **93** (400 MHz, $\text{DMSO-}d_6$)



Since we could not get solid proof on the exact mode of activation of the carbonyl compounds (**93** and **94**) by **90b** through NMR titration experiments, we were looking for other techniques that could provide some information on the interactions between the catalyst **90b** and the carbonyl group of **93/94**. X-ray photoelectron spectroscopy (XPS) is one of the most powerful techniques to detect defects, interactions between molecules, and hybridization in material chemistry, although researchers have not explored these methods in organic chemistry.⁴⁰ We thought that the XPS technique could be used to understand the coordination/complexation between **90b** and **93** or **94**. Figure 6(a) shows the XPS C-1s spectra of the cyclopropenium salt **90b**, 4-cholorobenzaldehyde **94**, and a mixture of both **90b** and **94**. The XPS binding energy data for C-C/C-H, C=C, and C-F bonds of **90b** are represented by peaks at 284.96 eV, 286.71 eV, and 291.91 eV, respectively. Similarly, in the case of the aldehyde **94**, the peaks at 284.59 eV, 286.19 eV, and 288.54 eV represent the C-C/C-H, C=C,

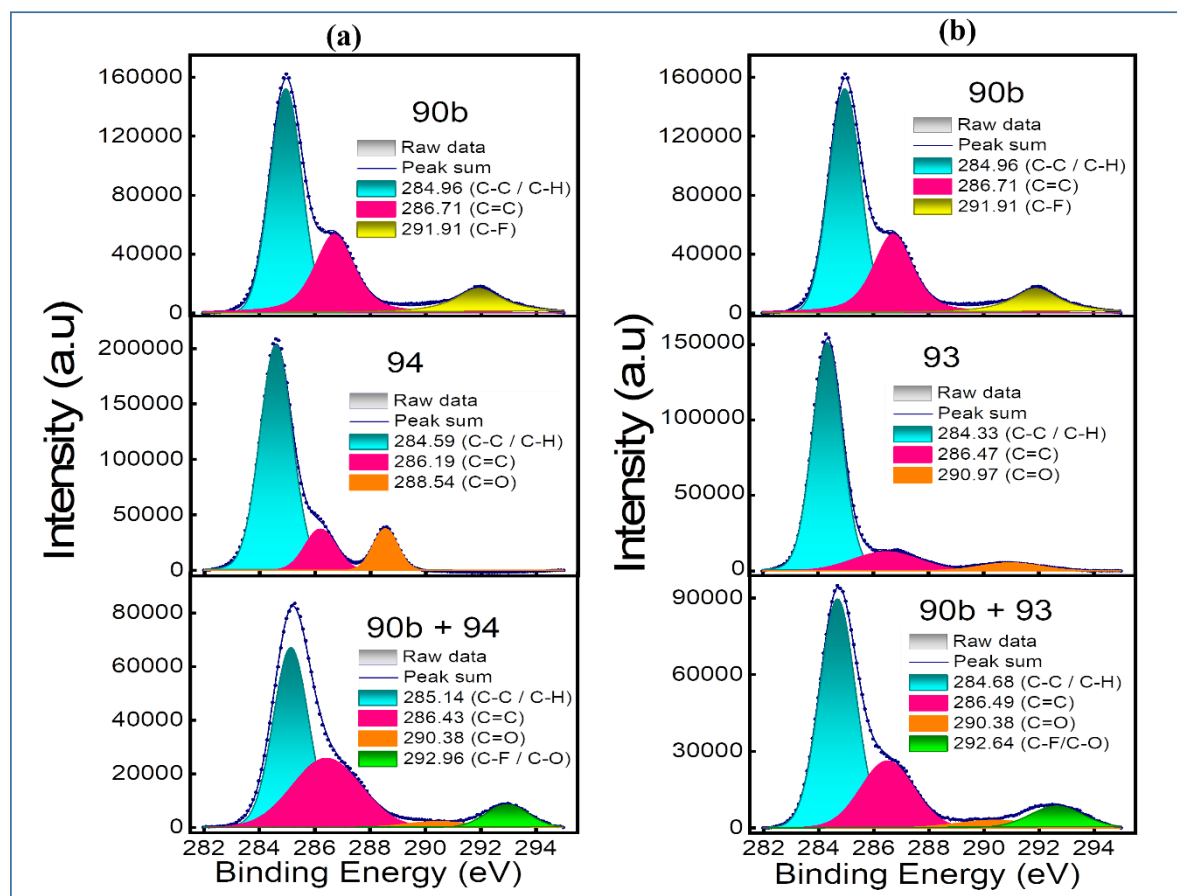


Figure 6. C_{1s} XPS spectra of **90b** and the carbonyl group (a) (i) catalyst **90b**; (ii) *p*-Cl benzaldehyde **94**; (iii) 1:1 mixture of **90b** and **94** (b) (i) catalyst **90b**; (ii) chalcone **93**; (iii) 1:1 mixture of **90b** and **93**.

and C=O bonds, respectively. The XPS C-1s spectra of the 1:1 mixture of **90b** and **94** have

some interesting data, as the peak corresponding to the C=O bond energy almost disappeared and a new peak appeared at 292.96 eV, which might be associated with the C-O interaction between **90b** and **94**. The disappearance of the carbonyl of **94** in XPS data for the mixture (**90b** + **94**) suggests that there is some kind of interaction between the carbonyl group of **94** and the catalyst **90b**.

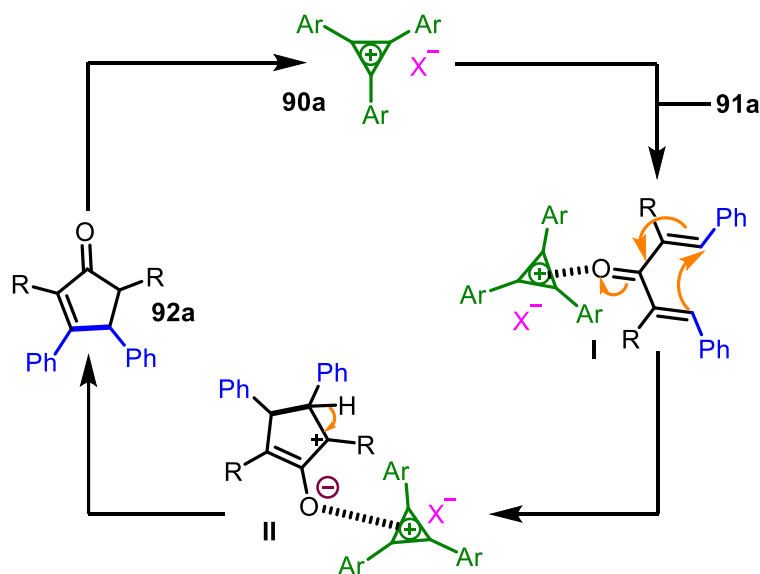
Similarly, the XPS analysis was also carried out for the mixture of chalcone **93** and the catalyst **90b**. Figure 6(b) shows the comparison of the XPS C-1s spectra of catalyst **90b**, chalcone **93**, and a mixture of both **90b** and **93**. The C-C/C-H, C=C, and C=O bonds of chalcone **93** are represented by peaks at 284.33 eV, 286.47 eV, and 290.97 eV, respectively. In this case of a 1:1 mixture of **90b** and **93**, the intensity of the C=O bond **93** was decreased, which clearly suggests that there is an interaction between the C=O group of **93** and the catalyst **90b**. The experimental data for the XPS analysis is given in Table 4.

Table 4. X-ray photoelectron spectroscopy (XPS) data comparison

Compounds	C-C/C-H	C=C	C=O	C-F/C-O
90b	284.96 eV	286.71 eV		291.91 eV
94	284.59 eV	286.19 eV	288.54 eV	
90b + 94	285.14 eV	286.43 eV	290.46 eV	292.96 eV
93	284.33 eV	286.47 eV	290.97 eV	
90b + 93	284.68 eV	286.49 eV	290.38 eV	292.64 eV

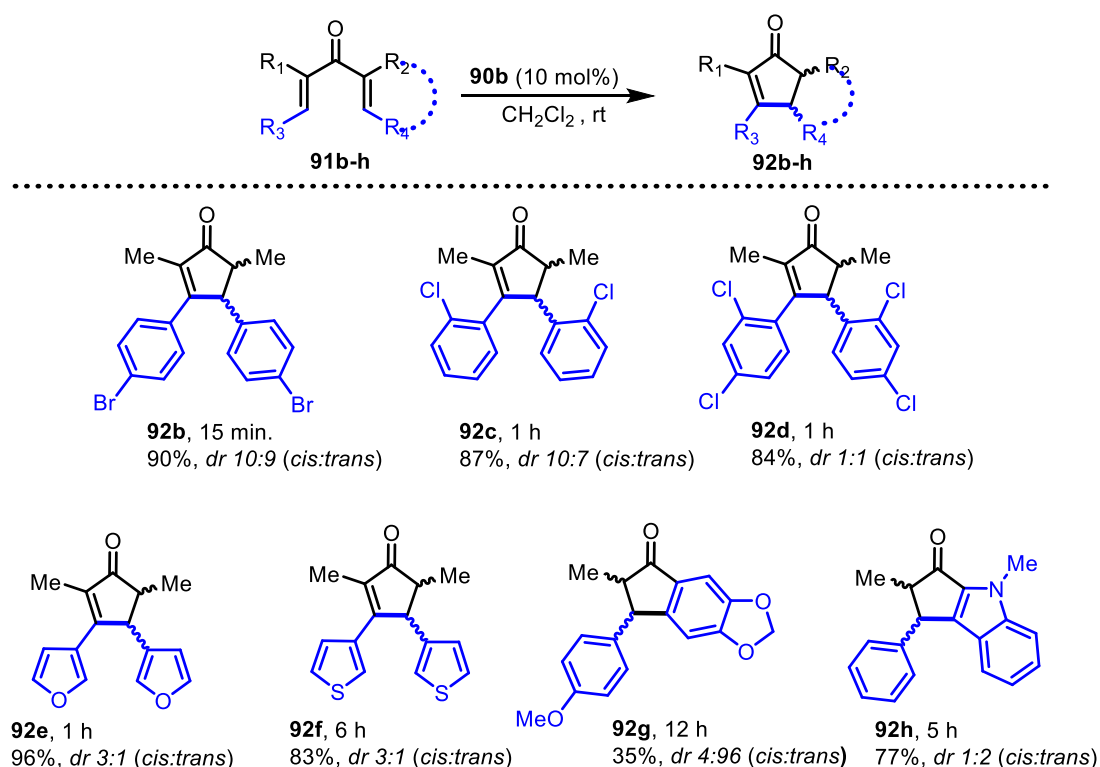
It is evident from the control experiment, NMR and XPS analysis that the cyclopropenium cation is indeed acting as an oxophilic Lewis acid catalyst in Nazarov cyclization of **91a**. Therefore, based on these observations, a plausible mechanism for this transformation has been proposed (Scheme 14). Initially, the dienone **91a** interacts with the catalyst **90b** through a reversible coordination complex **I** and promotes the intramolecular cyclization producing another complex **II**, which, after proton migration, generates the final product **92a**.

Scheme 14. Proposed mechanism for the Nazarov cyclization reaction



After having clarity in the mode of action of the catalyst **90b** on the Nazarov cyclization of **91a**, we examined the scope and limitation of this methodology using a wide range of enones (**91b-h**), and the results are summarized in Chart 1. The halo-substituted dienones **91b-d** produced the desired products **92b-d** in good yields and diastereoselectivity within a very short time (15 min. to 1 h). The dienones **91e** and **91f**, derived from furfural and 3-thiophenecarboxaldehyde, underwent the cyclization at a relatively less reaction rate and yielded the products **92e** and **92f** in 96 and 83% yields, respectively with *dr* 3:1 (*cis:trans*) after 6 h. However, the cyclization of unsymmetrical aryl vinyl ketone **91h** did not undergo complete conversion even after 12 hours, but produced the desired product **92h** in 35% yield with *dr* 4:96 (*cis:trans*). In the case of indole-based enone **91g**, the expected product **92g** was obtained in 77% yield with *dr* 1:2 (*cis:trans*). Interestingly, in the cases of **92h** and **92g**, *trans*-isomer was formed in major quantities.

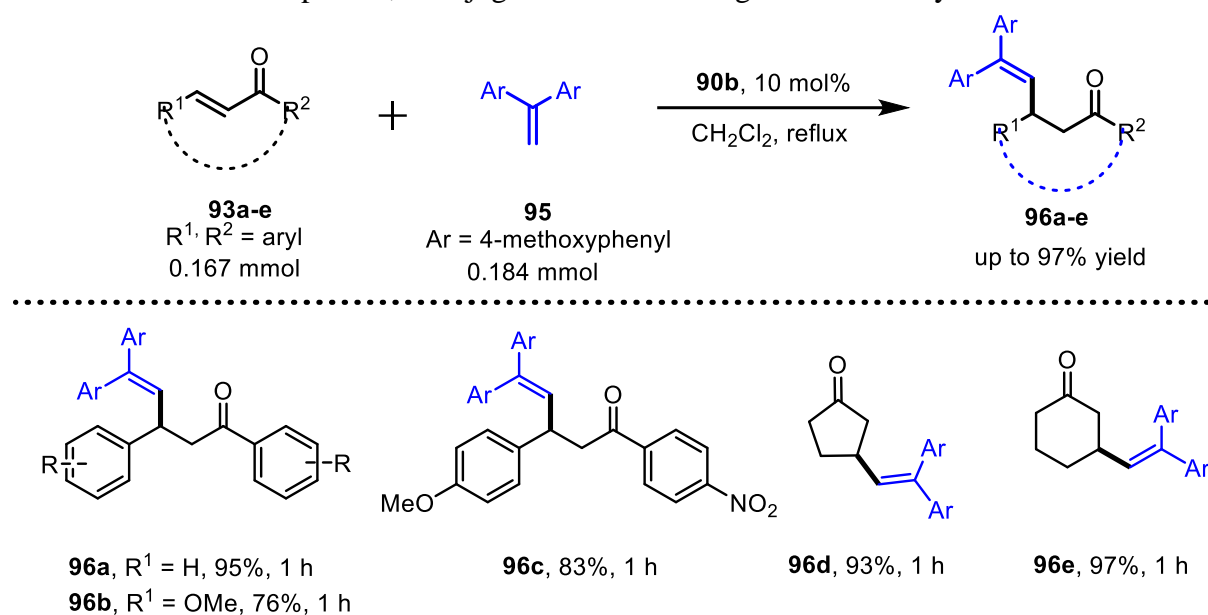
Chart 1. Substrate Scope of Nazarov Cyclization Reaction^a



^aAll reactions were carried out with **91b-h** in 40 mg scale in 1 mL of CH_2Cl_2 at room temperature. Yields represented are isolated yields. Diastereomeric ratios (*dr*) were calculated based on the ^1H NMR of the crude sample.

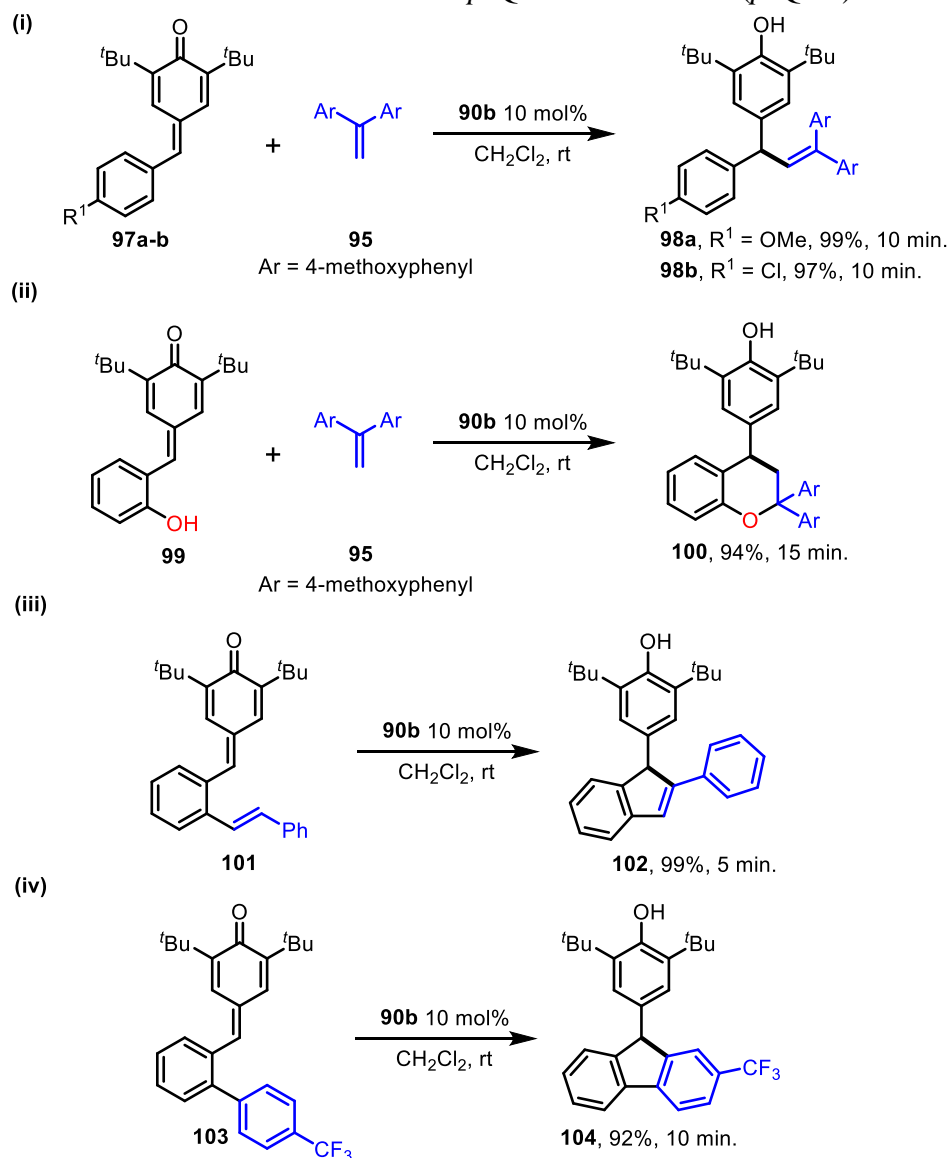
After proving the concept of ‘*carbocation catalysis*’ in the Nazarov cyclization, we intended to utilize the cyclopropenium carbocations as catalysts in other similar types of reactions. The intermolecular 1,4-conjugate addition of styrenes to enone systems⁴¹ is one such reaction that closely resembles the Nazarov cyclization. In this regard, an experiment involving the 1,4-addition of 1,1-diarylethylene **95** to chalcone **93a** was conducted in CH_2Cl_2 using **90b** as a catalyst at 40 °C. In this case, the expected 1,4-adduct **96a** was obtained in 95% yield within an hour (Chart 2). In the cases of other substituted chalcones such as **93b** and **93c**, the respective vinyolated products **96b** and **96c** were obtained in 76 and 83% isolated yields, respectively. Other enones such as cyclopentenone and cyclohexenone also reacted with **95** and gave the respective products **96d** and **96e** in 93 and 97% yields, respectively (Chart 2).

Chart 2. Substrate scope in 1,4 conjugated addition using **90b** as a catalyst^a



^aAll reactions were carried out with **93a-e** in 40 mg scale in 1 mL of CH_2Cl_2 at 40 °C.

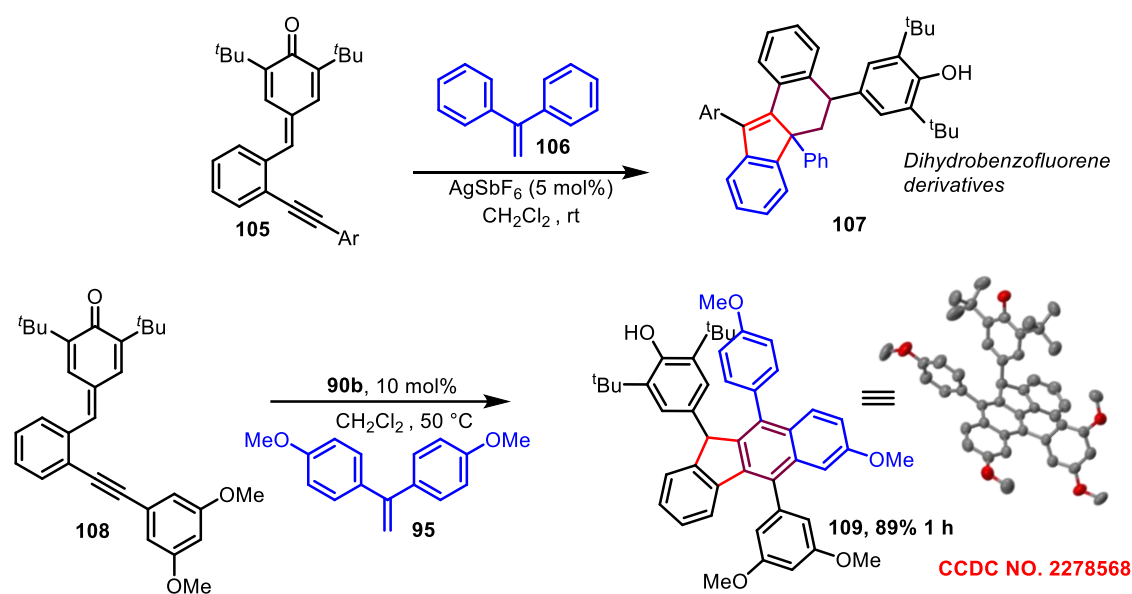
Later, since our research group has developed many metal as well as organocatalytic transformations of *p*-quinone methides (*p*-QMs) in the synthesis of carbocycles and heterocycles,⁴² we were interested in utilizing the cyclopropenium catalyst **90b** in the 1,6-conjugate addition reactions of different nucleophiles to *p*-QMs. Recently, our group has reported the $\text{Bi}(\text{OTf})_3$ catalyzed inter- and intramolecular hydroolefination of *p*-QMs to access a wide range of vinyl diarylmethane and indene derivatives, respectively.⁴³ So, we wanted to examine the catalytic activity of **90b** in the intermolecular hydroolefination of *p*-QMs with alkenes. In this regard, a couple of experiments were conducted for the intermolecular 1,6-conjugate addition of 1,1-diarylethylene **95** to two different *p*-QMs (**97a** & **97b**) and, in those cases, the expected vinyl diarylmethanes **98a** and **98b** were obtained in 99 and 97% isolated yields, respectively within 10 minutes [(i), Scheme 15]. When 2-hydroxyphenyl-substituted *p*-QM **99** was subjected to react with **95** using 10 mol% of **90b**, the dihydrocoumarin **100** was obtained in 94% yield [(ii), Scheme 15]. This reaction proceeds through the 1,6-conjugate addition of **95** to **99** followed by intramolecular trapping of the resulting carbocation by the hydroxyl group of **99**. Similarly, the intramolecular cyclization of 2-alkenyl-phenyl-substituted *p*-QM **101** and 2-aryl-phenyl-substituted *p*-QM **103** using 10 mol% of **90b** gave the corresponding indene **102** and fluorene **104** in 99 and 92% yields, respectively [(iii & iv), Scheme 15].

Scheme 15. Reactions of Various Substituted *p*-Quinone Methides (*p*-QMs)

All reactions were carried out in 40 mg of *p*-QMs in 1 mL of CH₂Cl₂ at room temperature.

We have recently reported an AgSbF₆ catalyzed synthesis of dihydrobenofluorene derivatives **107** through a cascade reaction between 2-alkynyl-phenyl-substituted *p*-QMs **105** and 1,1,-diphenylethylene **106** (Scheme 16).⁴⁴ We were interested in examining the same methodology using **90b** as a catalyst. Thus, a reaction was performed between 2-alkynyl-phenyl-substituted *p*-QM **108** and **95** using 10 mol% of **90b** in CH₂Cl₂ at room temperature. To our surprise, the expected dihydrobenzofluorene was not formed; instead, a densely functionalized 9-aryl fluorene derivative **109** was obtained with an 89% yield (Scheme 16).

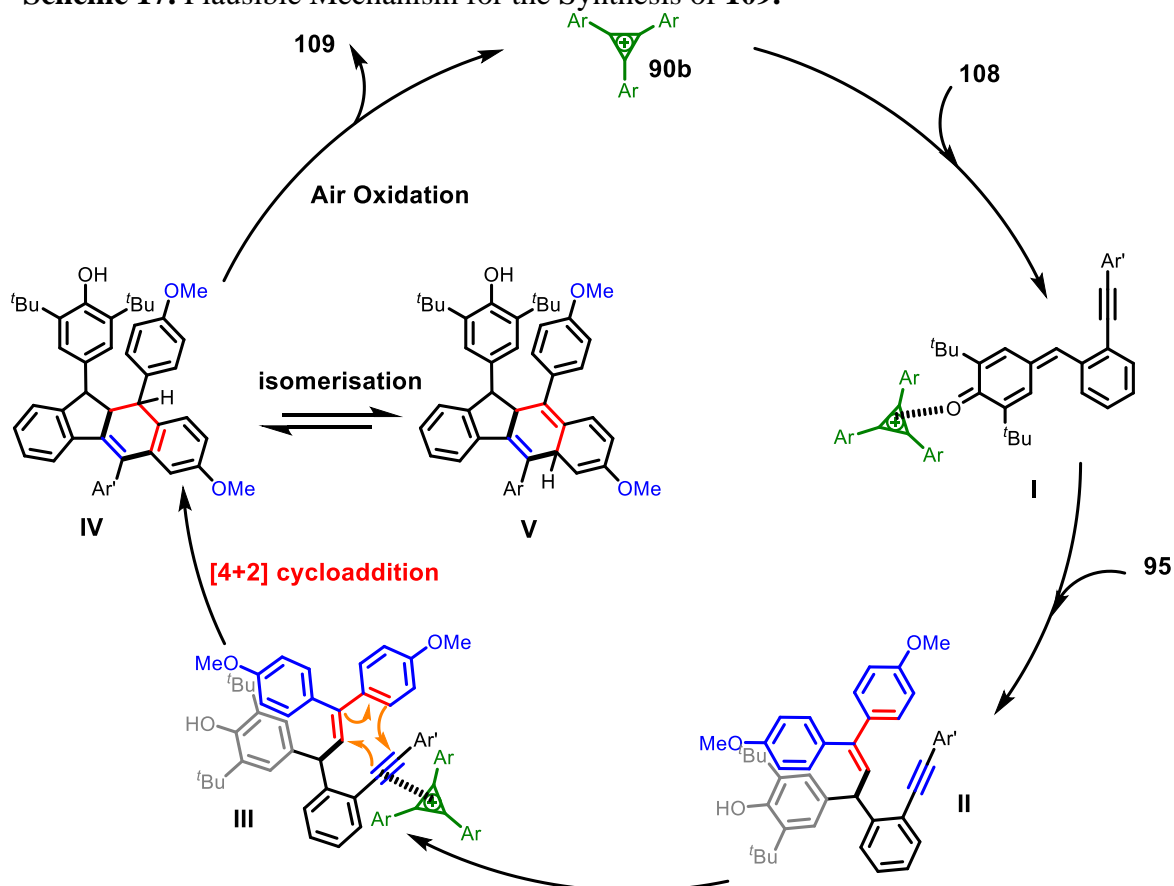
Scheme 16. The reaction of 2-alkynyl-phenyl-substituted *p*-QM with **95**



The reaction was carried out with **108** in 40 mg scale in 1.5 mL of CH_2Cl_2 at room temperature.

4.4.3 Reaction mechanism

Scheme 17. Plausible Mechanism for the Synthesis of **109**.



Initially, catalyst **90b** activates *p*-quinone methide **108** to complex **I** which, facilitate it for nucleophile **95** to attack in 1,6 fashion to generate the intermediate **II**, then alkynophylic activation by **90b** of **II** promotes the formal 4+2 cycloaddition reaction through complex **III** and generate another interesting intermediate **IV** which isomerize to intermediate **V** via 1,3 sigma tropic shift of proton. Later aerial oxidation furnished the final product **109**.

4.5 Conclusion

In conclusion, we have discovered, for the first time, that the tris(aryl)cyclopropenyl carbocation could be employed as an efficient organic Lewis acid catalyst for many fundamental and 100% atom-economical reactions such as Nazarov cyclization, 1,4- and 1,6-conjugate addition reactions leading to many useful small molecules under mild reaction conditions. Further catalytic applications of these carbocations in other organic transformations are currently under progress.

4.6 Experimental section

1. General methods

All reactions were carried out under an argon atmosphere in an oven-dried round-bottom flask. All the solvents were distilled before use and stored under an argon atmosphere. Most of the reagents and starting materials were purchased from commercial sources and used as such. All *p*-quinone methides⁴⁵ and triarylcyclopropenium salts **90a** to **90d** were prepared by following procedures reported in the literature.⁴⁶ Bis(dialkylamino)cyclopropenium salts **90e** and **90f** were prepared according to known procedures.⁴⁷ All chalcones were prepared according to the known literature procedure.⁴⁸ Melting points were recorded on the SMP20 melting point apparatus and are uncorrected. ¹H, ¹³C, and ¹⁹F spectra were recorded in CDCl₃ (400, 100, and 376 MHz respectively) on Bruker FT-NMR spectrometer. Chemical shift (δ) values are reported in parts per million relatives to TMS and the coupling constants (*J*) are reported in Hz. High-resolution mass spectra were recorded on Waters Q-TOF Premier-HAB213 spectrometer. FT-IR spectra were recorded on a Perkin-Elmer FTIR spectrometer. Thin layer chromatography was performed on Merck silica gel 60 F₂₅₄ TLC pellets and visualized by UV irradiation and KMnO₄ stain. Column chromatography was carried out through silica gel (100–200 mesh) using EtOAc/hexane as an eluent.

2. Preparation of the buffer solution

Stock solutions of pH below 3 were prepared by addition of HCl solution, while solutions

having a pH in the range of 3 to 7 were made using 0.1 M citric acid and 0.2 M Na₂HPO₄, Gomori's 50 ml procedure⁴⁹ was used to prepare the buffer solution, using 21.1 % of ethanol in water. Similar amounts of 50 ml of Gomori phosphate buffer were used to achieve pH values greater than 7, utilizing different ratios of 0.2 M NaH₂PO₄ and 0.2 M Na₂HPO₄ solutions. The pK_a of the triphenyl cation was calculated using the citrate-phosphate system and was found to be 4.35; a second calculation was done using the Gomori acetate buffer, which is composed of a mixture of 0.2 M acetic acid and 0.2 M sodium acetate, and the pK_a was found to be 3.34.³⁹

3. General General procedure of Nazarov reaction:

Anhydrous Dichloromethane (1.5 mL) was added to the mixture of tetrasubstituted *dienone* (0.152 mmol), and tris(4-trifluorophenyl)cyclopropenium **90b**, and the resulting suspension was stirred at room temperature. After the reaction was complete (based on TLC analysis), the reaction mixture was concentrated under reduced pressure. The residue was then purified through a silica gel column, using an EtOAc/Hexane mixture as an eluent, to get the pure product.

4. General procedure for the 1,6-conjugate addition of olefin to p-quinone methides:

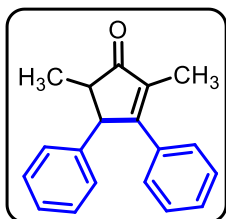
Anhydrous Dichloromethane (1.5 mL) was added to the mixture of *p*-quinonemethides (0.062 mmol), 4,4-(ethane-1,1-diyl)bis(methoxybenzene), (0.068mmol) and tris(4-trifluorophenyl)cyclopropenium **90b** and the resulting suspension was stirred at room temperature. After the reaction was complete (based on TLC analysis), the reaction mixture was concentrated under reduced pressure. The residue was then purified through a silica gel column, using an EtOAc/Hexane mixture as an eluent, to get the pure product.

5. General procedure for the 1,4-conjugate addition of olefin to chalcone:

Anhydrous Dichloromethane (1.5 mL) was added to the mixture of chalcone **94** (0.192 ml), **96a** 4,4-(ethane-1,1-diyl)bis(methoxybenzene), (0.211mmol) and tris(4-trifluorophenyl)cyclopropenium **90b** and the resulting suspension was stirred at room temperature. After the reaction was complete (based on TLC analysis), the reaction mixture was concentrated under reduced pressure. The residue was then purified through a silica gel column, using an EtOAc/Hexane mixture as an eluent, to get the pure product.

6. Characterisation of product

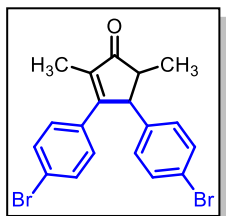
2,5-dimethyl-3,4-diphenylcyclopent-2-en-1-one (92a)⁵⁰



The reaction was performed at 0.152 mmol scale of **91a**; White solid, 92% yield, **m.p:** 128-130 °C; cis/trans ratio 3:1 R_f 0.25 (PE/Et₂O 9:1). **cis-2a** ¹H NMR (400 MHz) δ (ppm): 7.39–7.36 (m, 2H), 7.33–7.24 (m, 4H), 7.24–7.19 (m, 2H), 7.18–7.16 (m, 1H), 7.00 (br, s, 1H), 4.61–4.59 (m, 1H), 2.91 (quin, 1H, J = 7.4 Hz), 2.08 (d, 3H, J = 1.6 Hz), 0.75 (d, 3H, J = 7.5 Hz).

trans-2a ¹H NMR (400 MHz) δ (ppm): 7.33–7.24 (m, 5H), 7.23–7.19 (m, 2H), 7.15–7.11 (m, 1H), 7.09–7.06 (m, 2H), 3.98 (quin, 1H, J = 2.2 Hz), 2.41 (qd, 1H, J = 7.3, 2.8 Hz), 2.03 (d, 3H, J = 2.0 Hz), 1.36 (d, 3H, J = 7.4 Hz).

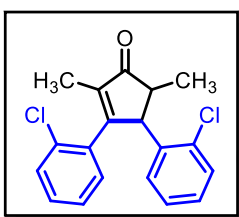
3,4-bis(4-bromophenyl)-2,5-dimethylcyclopent-2-en-1-one (92b)⁵⁰



The reaction was performed at 0.095 mmol scale of **91b**; R_f = 0.25 (10% EtOAc in hexane). White solid, **m.p:** 132-134 °C; 90% yield, cis/trans ratio 3:1 **cis-2a** ¹H NMR (400 MHz) δ (ppm): δ 7.46 (d, J = 8.6 Hz, 2H), 7.34 (d, J = 8.56 Hz, 2H), 7.22 (d, J = 8.56 Hz, 2H); 6.84 (s, b, 2H), 4.54 (m, 1H), 2.89 (quin, J = 7.52 Hz, 1H), 2.04 (d, J = 1.68 Hz, 3H), 0.74 (d, J =

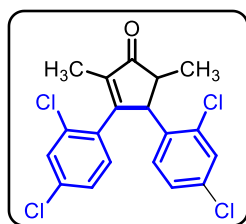
7.54 Hz, 3H);). **trans-2a** ¹H NMR (400 MHz) δ (ppm): 7.44 (d, J = 8.52 Hz, 2H), 7.33 (d, J = 8.4 Hz, 2H), 7.16 (d, J = 8.52 Hz, 2H); 3.89 (quin, J = 2.4 Hz, 1H), 2.33 (qd, J = 3.36 Hz, 1H), 1.99 (d, J = 2.04 Hz, 3H), 1.33 (d, J = 7.36 Hz, 3H);

3,4-bis(2-chlorophenyl)-2,5-dimethylcyclopent-2-en-1-one (92c)⁵⁰



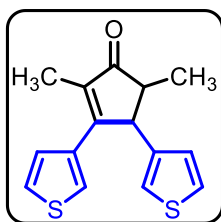
The reaction was performed at 0.120 mmol scale of **91c**; White solid, 88% yield, **m.p :** 109-110 °C; cis/ trans ratio 10/7. R_f 0.24 (PE/Et₂O 9:1). **trans** ¹H NMR (400 MHz) δ (ppm): 7.33 (d, 1H, J = 8.3 Hz), 7.22 (d, 1H, J = s 7.6 Hz), 7.18-7.10 (m, 4H), 7.06-7.02 (m, 2H), 4.74 (br s, 1H), 2.53 (br s, 1H), 1.77 (s, 3H), 1.41 (d, 3H, J = 6.9 Hz).

3,4-bis(2,4-dichlorophenyl)-2,5-dimethylcyclopent-2-en-1-one (92d)⁵⁰



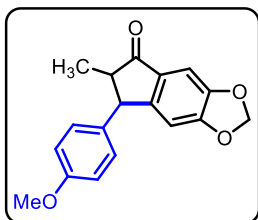
The reaction was performed at 0.10 mmol scale of **91d**; White solid, **m.p:** 130-131 °C; 84% yield, *cis/trans* ratio 1/1. **R_f** 0.41 (PE/Et₂O 9:1). *trans*-**2e** ¹H NMR (400 MHz) δ (ppm): 7.34 (dd, 1H, *J* = 7.9, 1.4 Hz), 7.20-7.12 (m, 4H), 7.04 (t, 1H, *J* = 7.9 Hz), 5.13-5.11 (m, 1H), 3.21 (qd, 1H, *J* = 7.4, 1.2 Hz), 1.68 (d, 3H, *J* = 1.7 Hz), 1.39 (d, 3H *J* = 7.6 Hz).

2,5-dimethyl-3,4-di(thiophen-3-yl)cyclopent-2-en-1-one (92e)⁵⁰



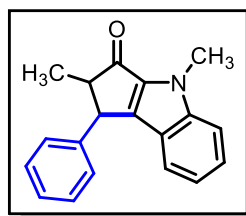
The reaction was performed at 0.146 mmol scale of **91e**, White solid; 83 % yield; **m.p:** 93-94 °C; *cis*-**2c** ¹H NMR (400 MHz) δ (ppm): 7.52-7.49 (m, 1H), 7.36 (d, 1H, *J* = 3.4 Hz), , 7.15-7.12 (m, 1H), 7.07-7.04 (m, 1H), 6.92-6.89 (m, 1H), 6.78 (d, 1H, *J* = 3.1 Hz), 4.85 (d, 1H, *J* = 7.2 Hz), 2.87 (quin, 1H, *J* = 7.2 Hz), 2.18 (d, 3H, *J* = 1.4 Hz), 0.89 (d, 3H, *J* = 7.6 Hz). *trans*-**2c** ¹H NMR (400 MHz) δ (ppm): 7.52-7.49 (m, 1H), 7.29 (d, 1H, *J* = 3.8 Hz), 7.15-7.12 (m, 1H), 7.07-7.04 (m, 1H), 6.92-6.89 (m, 1H), 6.86 (d, 1H, *J* = 3.4 Hz), 4.24 (br s, 1H), 2.49 (qd, 1H, *J* = 7.4 Hz, 2.4 Hz), 2.16 (d, 3H, *J* = 1.7 Hz), 1.34 (d, 3H, *J* = 7.6 Hz).

7-(4-methoxyphenyl)-6-methyl-6,7-dihydro-5H-indeno[5,6-d][1,3]dioxol-5-one (92f)⁵⁰



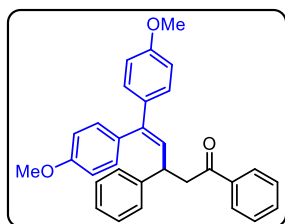
The reaction was performed at 0.135 mmol scale of **91f**; **R_f** = 0.2 (5% EtOAc in hexane); Colourless oil, 83% yield, *cis/trans* ratio 89/11. *trans* ¹H NMR (400 MHz) δ (ppm): 7.13 (s, 1H), 7.08-7.05 (m, 2H), 6.88-6.85 (m, 2H), 6.54 (s, 1H), 6.03 (s, 2H), 3.84 (d, 1H, *J* = 4.5 Hz), 3.80 (s, 3H), 2.57 (qd, 1H, *J* = 7.3, 4.5 Hz), 1.32 (d, 3H, *J* = 7.3 Hz)

(1R)-2,4-dimethyl-1-phenyl-1,4-dihydrocyclopenta[b]indol-3(2H)-one (92g)⁵⁰



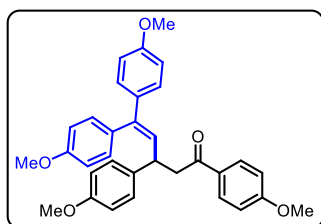
The reaction was performed at 0.150 mmol scale of **91g**; Pale yellow slid, 77% yield, **mp:** 117-118 °C; *cis/trans* ratio 1/2. **R_f** 0.21 (PE/EtOAc 95:5). *trans* ¹H NMR (400 MHz) δ (ppm): 7.43-7.40 (m, 2H), 7.38-7.36 (m, 1H), 7.34-7.22 (m, 4H), 7.10-7.05 (m, 2H), 4.80 (d, 1H, *J* = 6.5 Hz), 4.00 (s, 3H), 3.42-3.36 (m, 1H), 0.86 (d, 3H, *J* = 7.6 Hz *cis*- ¹H NMR (600 MHz) δ (ppm): 7.43-7.40 (m, 2H), 7.34-7.22 (m, 5H), 7.10-7.05 (m, 2H), 4.14 (d, 1H, *J* = 3.1 Hz), 3.99 (s, 3H), 2.87 (qd, 1H, *J* = 7.4, 2.9 Hz), 1.48 (d, 3H, *J* = 7.6 Hz).

5,5-bis(4-methoxyphenyl)-1,3-diphenylpent-4-en-1-one (96a)



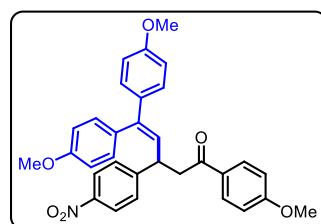
The reaction was performed at 0.192 mmol scale of **93a**; $R_f = 0.2$ (5% EtOAc in hexane); white solid (81.2 mg, 95% yield); m. p. = 110–113 °C; ^1H NMR (400 MHz, CDCl_3) δ 7.87 (d, $J = 7.3$ Hz, 2H), 7.54 (t, $J = 7.4$ Hz, 1H), 7.42 (t, $J = 7.4$ Hz, 2H), 7.32 (t, $J = 7.6$ Hz, 2H), 7.27 (d, $J = 7.04$ Hz, 2H), 7.22 (t, $J = 7.1$ Hz, 1H), 7.12 (d, $J = 8.7$ Hz, 2H), 6.99 (d, $J = 8.6$ Hz, 2H), 6.86 (d, $J = 8.6$ Hz, 2H), 6.79 (d, $J = 8.8$ Hz, 2H), 6.19 (d, $J = 10.2$ Hz, 2H), 4.24 – 4.18 (m, 1H), 3.85 (s, 3H), 3.79 (s, 3H), 3.43 (qd, $J = 6.72$ Hz, 2H), ^{13}C NMR (100 MHz, CDCl_3) δ 195.5, 159.0, 158.7, 144.4, 141.3, 137.1, 135.2, 133.0, 132.2, 130.9, 129.1, 128.8, 128.6, 128.56, 128.3, 127.4, 126.5, 113.6, 113.5, 55.36, 55.32, 46.5, 41.9; FT-IR (thin film, neat): 3638, 3440, 2959, 1759, 1732, 1601, 1436, 1368, 1316, 1259, 1177, 1156, 1036, 865, 700, 645 cm^{-1} ; HRMS (ESI): m/z calcd for $\text{C}_{31}\text{H}_{29}\text{O}_3$ $[\text{M}+\text{H}]^+$: 449.2111; found : 449.2115.

1,3,5,5-tetrakis(4-methoxyphenyl)pent-4-en-1-one (96b)



The reaction was performed at 0.149 mmol scale of **93b**; $R_f = 0.3$ (5% EtOAc in hexane); white solid (57.59 mg, 76% yield); m. p. = 110–114 °C; ^1H NMR (400 MHz, CDCl_3) δ 7.72 (d, $J = 7.76$ Hz, 2H), 7.18 (d, $J = 8.04$ Hz, 2H), 7.13 (d, $J = 8.6$ Hz, 2H), 7.07 (d, $J = 8.8$ Hz, 2H), 6.94 (d, $J = 8.6$ Hz, 2H), 6.83 (d, $J = 2.4$ Hz, 2H), 6.81 (d, $J = 2.4$ Hz, 2H), 6.75 (d, $J = 8.9$ Hz, 2H), 6.11 (d, $J = 10.24$ Hz, 1H), 4.13 – 4.06 (m, 1H), 3.83 (s, 3H), 3.78 (s, 3H), 3.77 (s, 3H), 3.31 (qd, $J = 7.64$ Hz, 2H), 3.39 (s, 3H), ^{13}C NMR (100 MHz, CDCl_3) δ 198.3, 159.0, 158.7, 158.1, 143.7, 140.8, 136.6, 135.4, 134.7, 132.3, 130.9, 129.5, 129.3, 128.6, 128.5, 114.1, 113.6, 113.5, 55.38, 55.35, 46.6, 41.3, 21.8; FT-IR (thin film, neat): 3387, 2960, 1760, 1732, 1595, 1436, 1371, 1236, 1121, 871, 757 cm^{-1} ; HRMS (ESI): m/z calcd for $\text{C}_{33}\text{H}_{33}\text{O}_5$ $[\text{M}+\text{H}]^+$: 509.2328; found : 509.2328.

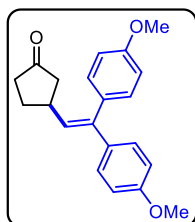
1,5,5-tris(4-methoxyphenyl)-3-(4-nitrophenyl)pent-4-en-1-one (96c)



The reaction was performed at 0.141 mmol scale of **93c**; $R_f = 0.2$ (5% EtOAc in hexane); yellow solid (61.3 mg, 83% yield); m. p. = 200–203 °C; ^1H NMR (400 MHz, CDCl_3) δ 8.13 (d, $J = 8.68$ Hz, 2H), 7.82 (d, $J = 8.8$ Hz, 2H), 7.35 (d, $J = 6.68$ Hz, 2H), 7.10 (d, $J = 8.8$ Hz, 2H), 6.96 (d, $J = 8.6$ Hz, 2H), 6.89 (d, $J = 4.0$ Hz, 2H), 6.87 (d, $J = 3.84$ Hz, 2H), 6.77 (d, $J = 8.9$ Hz, 2H), 6.1 (d, $J = 10.0$ Hz, 1H), 4.32 – 4.26 (m,

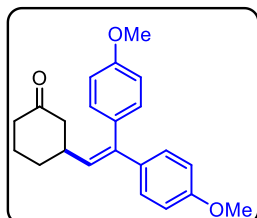
1H), 3.86 (s, 3H), 3.84 (s, 3H), 3.77 (s, 3H), 3.43 (qd, $J = 7.64$ Hz, 2H), ^{13}C NMR (100 MHz, CDCl_3) δ 196.0, 163.7, 159.3, 159.0, 152.4, 146.5, 142.7, 134.7, 131.8, 130.7, 130.5, 129.8, 128.6, 128.4, 127.4, 124.0, 113.9, 113.6, 55.6, 55.4, 55.32, 45.4, 41.7; FT-IR (thin film, neat): 3406, 2959, 2925, 2229, 1755, 1732, 1607, 1436, 1368, 1312, 1259, 1177, 1156, 1122, 1035 cm^{-1} ; HRMS (ESI): m/z calcd for $\text{C}_{32}\text{H}_{29}\text{NO}_6$ $[\text{M}-\text{H}]^+$: 524.2073; found : 524.2073.

3-(2,2-bis(4-methoxyphenyl)vinyl)cyclopentan-1-one (96d)



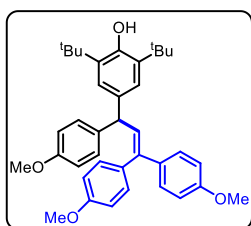
The reaction was performed at 0.487 mmol scale of **93d**; $R_f = 0.4$ (10% EtOAc in hexane); pale yellow gummy solid (146 mg, 93% yield); ^1H NMR (400 MHz, CDCl_3) δ 7.15 (d, $J = 8.7$ Hz, 2H), 7.09 (d, $J = 8.6$ Hz, 2H), 6.92 (d, $J = 8.6$ Hz, 2H), 6.81 (d, $J = 8.8$ Hz, 2H), 5.84 (d, $J = 9.6$ Hz, 2H), 3.84 (s, 1H), 3.79 (s, 1H), 2.99 – 2.88 (m, 1H), 2.40 – 2.30 (m, 2H), 2.14 – 2.03 (m, 3H), 1.83 – 1.72 (m, 1H); ^{13}C NMR (100 MHz, CDCl_3) δ 219.2, 159.1, 158.9, 141.7, 135.1, 132.5, 130.8, 129.8, 128.5, 113.8, 113.6, 55.4, 46.1, 38.5, 37.6, 30.9; FT-IR (thin film, neat): 3442, 2958, 1758, 1732, 1612, 1513, 1436, 1303, 1250, 1179, 1036, 838, 637 cm^{-1} ; HRMS (ESI): m/z calcd for $\text{C}_{21}\text{H}_{23}\text{O}_3$ $[\text{M}+\text{H}]^+$: 323.1647; found : 323.1647.

3-(2,2-bis(4-methoxyphenyl)vinyl)cyclohexan-1-one (96e)



The reaction was performed at 0.417 mmol scale of **93e**; $R_f = 0.4$ (10% EtOAc in hexane); pale yellow gummy solid (136 mg, 97% yield); ^1H NMR (400 MHz, CDCl_3) δ 7.15 (d, $J = 8.8$ Hz, 2H), 7.05 (d, $J = 8.6$ Hz, 2H), 6.89 (d, $J = 8.7$ Hz, 2H), 6.79 (d, $J = 8.8$ Hz, 2H), 5.79 (d, $J = 9.8$ Hz, 2H), 3.83 (s, 3H), 3.79 (s, 3H), 2.68 – 2.60 (m, 1H), 2.42 – 2.22 (m, 4H), 2.09 – 2.01 (m, 1H), 1.88 – 1.85 (m, 1H), 1.63 – 1.57 (m, 2H); ^{13}C NMR (100 MHz, CDCl_3) δ 211.1, 159.1, 158.8, 140.7, 135.2, 132.3, 130.6, 130.2, 128.5, 113.8, 113.6, 55.4, 48.2, 41.3, 39.5, 32.1, 25.1; FT-IR (thin film, neat): 3442, 2958, 1758, 1732, 1612, 1513, 1436, 1303, 1250, 1179, 1036, 838, 637 cm^{-1} ; HRMS (ESI): m/z calcd for $\text{C}_{22}\text{H}_{25}\text{O}_3$ $[\text{M}+\text{H}]^+$: 337.1804; found : 337.1804

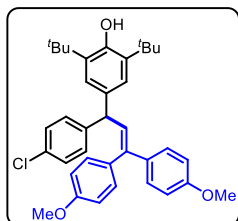
2,6-di-tert-butyl-4-(1,3,3-tris(4-methoxyphenyl)allyl)phenol (98a)



The reaction was performed on 0.123 mmol of **95a**; $R_f = 0.1$ (5% EtOAc in hexane); colorless gummy solid (68.8 mg, 99% yield); ^1H NMR (400 MHz, CDCl_3) δ 7.21 (d, $J = 8.84$ Hz, 2H), 7.12 (d, $J = 8.68$ Hz, 4H), 6.93 (s, 2H), 6.92 (d, $J = 8.7$ Hz, 2H), 6.85 (d, $J = 8.72$ Hz, 2H), 6.81 (d, $J = 8.9$ Hz, 2H), 6.38 (d, $J = 10.5$ Hz, 1H), 5.06 (s, 1H), 4.68 (d, $J = 10.5$ Hz, 1H), 3.89 (d, $J = 2.24$ Hz, 2H), 3.85 (s, 1H), 3.80 (s, 3H), 3.79 (s, 3H), 1.39 (s, 18H); ^{13}C

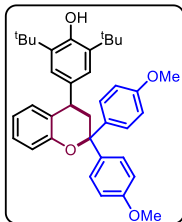
NMR (100 MHz, CDCl₃) δ 158.9, 158.8, 157.9, 152.1, 139.7, 137.2, 135.74, 135.47, 132.6, 131.2, 130.6, 129.5, 128.7, 125.0, 113.8, 113.7, 113.6, 55.40, 55.40, 49.5, 34.5, 30.5; FT-IR (neat): 3636 cm⁻¹; HRMS (ESI): m/z calcd for C₃₁H₃₇O₂ [M – H]⁻: 563.3161; found: 563.3164.

2,6-di-tert-butyl-4-(1-(4-chlorophenyl)-3,3-bis(4-methoxyphenyl)allyl)phenol (**98b**)



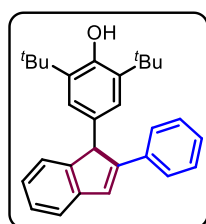
The reaction was performed on 0.122 mmol of **95b**; R_f = 0.1 (5% EtOAc in hexane); colorless gummy solid (67.3 mg, 97% yield); ¹H NMR (400 MHz, CDCl₃) δ 7.27 (d, J = 8.44 Hz, 2H), 7.20 (d, J = 8.48 Hz, 2H), 7.13 (d, J = 8.4 Hz, 2H), 7.09 (d, J = 8.68 Hz, 2H), 6.92–6.90 (m, 4H), 6.82 (d, J = 8.88 Hz, 2H), 6.35 (d, J = 10.5 Hz, 2H), 5.09 (s, 1H), 4.79 (d, J = 10.5 Hz, 1H), 3.85 (s, 1H), 3.80 (s, 3H), 3.79 (s, 3H), 1.39 (s, 18H); ¹³C NMR (100 MHz, CDCl₃) δ 158.9, 158.9, 152.3, 143.7, 140.5, 135.9, 135.4, 134.8, 132.4, 131.8, 131.1, 129.9, 129.7, 128.7, 128.6, 124.9, 113.8, 113.7, 113.6, 55.5, 55.4, 49.5, 34.5, 30.5; FT-IR (neat): 3636 cm⁻¹; HRMS (ESI): m/z calcd for C₃₁H₃₇O₂ [M – H]⁻: 667.2666; found: 667.2668.

4-(2,2-bis(4-methoxyphenyl)chroman-4-yl)-2,6-di-tert-butylphenol (**100**)



The reaction was performed on 0.129 mmol of **95c**; R_f = 0.2 (5% EtOAc in hexane); colorless gummy solid (66.7 mg, 94% yield); ¹H NMR (400 MHz, CDCl₃) δ 7.47–7.44 (m, 4H), 7.19–7.12 (m, 2H), 7.0 (s, 1H), 6.89 (t, J = 9.32 Hz, 2H), 6.77 (t, J = 6.70 Hz, 2H), 6.71 (d, J = 7.52 Hz, 2H), 5.12 (s, 1H), 3.84 (d, J = 3.68, 1H), 3.79 (d, J = 1.64 Hz, 1H), 3.07 (dd, J = 5.16, 5.2 Hz, 1H), 2.67 (t, J = 13.2 Hz, 2H), 1.45 (s, 18H); ¹³C NMR (100 MHz, CDCl₃) δ 158.7, 158.8, 154.3, 152.5, 138.8, 136.2, 136.0, 134.7, 129.7, 127.6, 127.5, 127.2, 126.1, 125.4, 120.3, 117.1, 114.0, 113.6, 81.7, 55.4, 53.5, 42.0, 40.1, 34.5, 30.5; FT-IR (neat): 3636 cm⁻¹; HRMS (ESI): m/z calcd for C₃₅H₃₇O₂ [M – H]⁻: 449.3005; found: 449.3004.

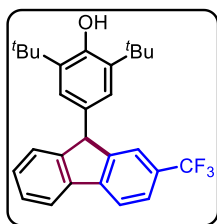
2,6-di-tert-butyl-4-(2-phenyl-1H-inden-1-yl)phenol (**102**)⁴²



. The reaction was performed on 0.10 mmol of **95d**; R_f = 0.4 (5% EtOAc in hexane); white solid (39.2 mg, 99% yield); mp = 170–172 °C; ¹H NMR (400 MHz, CDCl₃) δ 7.50–7.48 (m, 2H), 7.41 (d, J = 7.5 Hz, 1H), 7.30–7.23 (m, 5H), 7.20–7.12 (m, 2H), 6.91 (s, 2H), 4.99 (s, 1H), 4.92 (s, 1H), 1.33 (s, 18H); ¹³C NMR (100 MHz, CDCl₃) δ 152.5, 150.5, 149.5, 143.3, 135.9, 135.8, 130.1, 128.4, 127.9, 127.2, 127.0, 126.8, 125.3, 124.6, 123.9, 121.1, 56.3, 34.4, 30.5;

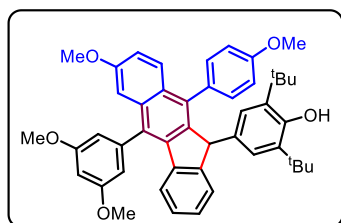
FT-IR (neat): 3636 cm⁻¹

2,6-di-tert-butyl-4-(2-(trifluoromethyl)-9H-fluoren-9-yl)phenol (104)



The reaction was performed at 0.091 mmol scale of corresponding 2-bromo phenyl-substituted p-quinone methide **95e**; R_f = 0.4 (5% EtOAc in hexane); orange solid (37.11 mg, 92% yield); mp = 146–148 °C; ¹H NMR (400 MHz, CDCl₃): δ 7.87 (d, J = 7.8 Hz, 1H), 7.84 (d, J = 7.2 Hz, 1H), 7.65 (d, J = 9.6 Hz, 1H), 7.43–7.40 (m, 2H), 7.36–7.32 (m, 1H), 6.88 (s, 2H), 5.13 (s, 1H), 5.03 (s, 1H), 1.38 (s, 18H); ¹³C{¹H} NMR (100 MHz, CDCl₃): δ 153.0, 148.9, 148.5, 139.4, 136.3, 130.7, 128.4, 127.5, 126.1 (d, J_{C-F} = 276.1 Hz), 125.7, 124.6, (d, J_{C-F} = 3.84 Hz), 122.6 (d, J_{C-F} = 4.05 Hz), 120.6, 120.0, 54.5, 34.5, 30.4; ¹⁹F NMR (376 MHz, CDCl₃): δ -115.3; IR (neat): 2956, 1613, 1551, 1470, 1254, 762 cm⁻¹; HRMS (ESI) m/z: calcd for C₂₇H₃₀FO [M + H]⁺, 339.2243; found, 339.2248.

2,6-di-tert-butyl-4-(5-(3,5-dimethoxyphenyl)-7-methoxy-10-(4-methoxyphenyl)-11H-benzo[b]fluoren-11-yl)phenol (109)



The reaction was performed at 0.088 mmol scale of corresponding 2-alkynylphenyl-substituted p-quinone methide; R_f = 0.4 (5% EtOAc in hexane); orange solid (54.26 mg, 89% yield); mp = 146–148 °C; ¹H NMR (400 MHz, CDCl₃): δ 7.45 (d, J = 9.0 Hz, 1H), 7.31 (dd, J = 2.0 Hz, J = 2.0 Hz, 1H), 7.16–7.11 (m, 2H), 7.07–6.96 (m, 3H), 6.72–6.67 (m, 4H), 6.55 (dd, J = 3.0 Hz, J = 2.6 Hz, 1H), 6.43 (dd, J = 2.0 Hz, J = 2.0 Hz, 1H), 6.34 (s, 2H), 5.04 (s, 1H), 4.87 (s, 1H), 3.89 (s, 3H), 3.85 (s, 3H), 3.83 (s, 1H), 5.13 (s, 3H), 3.75 (s, 3H), 1.23 (s, 18H); ¹³C{¹H} NMR (100 MHz, CDCl₃): δ 161.7, 158.2, 157.3, 151.8, 150.5, 143.3, 141.5, 140.1, 137.2, 135.9, 135.2, 134.2, 132.6, 131.6, 131.1, 130.4, 128.2, 127.6, 126.9, 125.7, 124.9, 123.8, 117.0, 113.4, 113.2, 108.3, 107.7, 105.5, 100.4, 55.7, 55.66, 55.4, 55.0, 34.1, 30.3; IR (neat): 2956, 1613, 1551, 1470, 1254, 762 cm⁻¹; HRMS (ESI) m/z: calcd for C₂₇H₃₀FO [M + H]⁺, 693.3575; found, 693.3575.

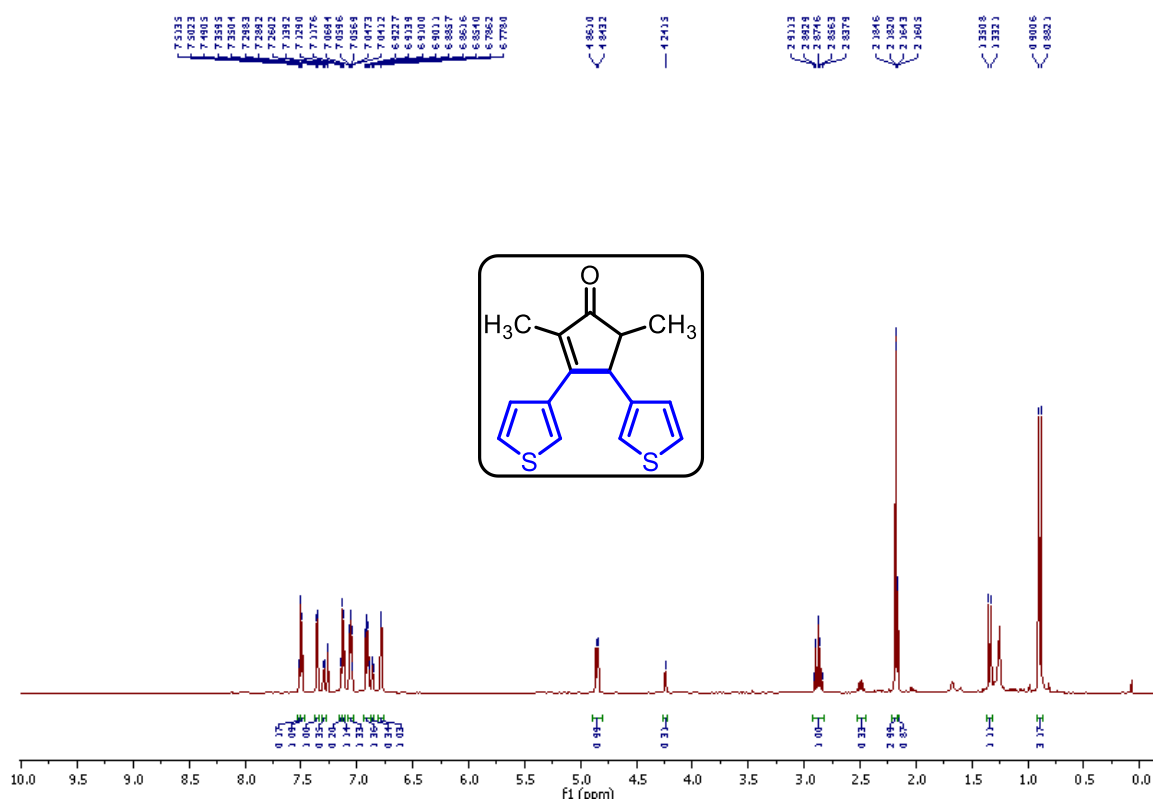
Chemical Structure: 1,2-diphenyl-3-methyl-4-penten-3-one

¹H NMR Spectrum (CDCl₃):

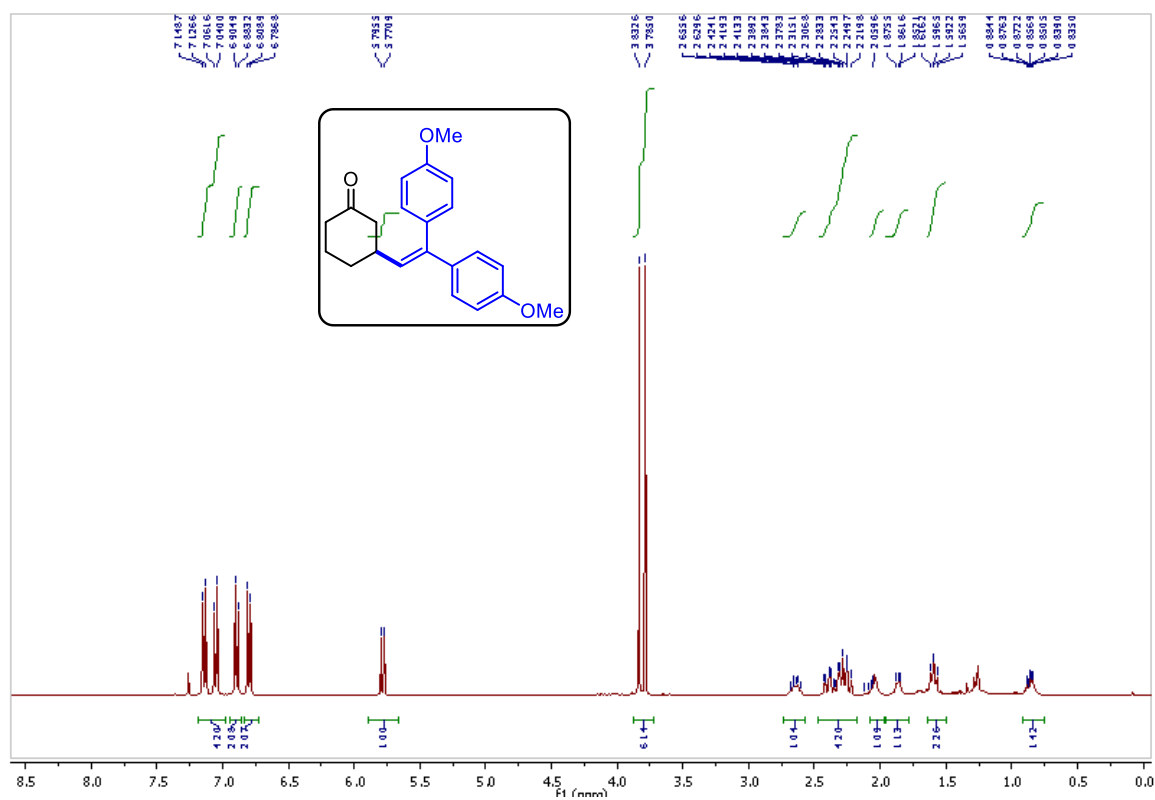
Peak List (ppm): 7.863, 7.861, 7.857, 7.853, 7.851, 7.849, 7.847, 7.843, 7.839, 7.835, 7.831, 7.827, 7.823, 7.819, 7.815, 7.811, 7.807, 7.803, 7.799, 7.795, 7.791, 7.787, 7.783, 7.779, 7.775, 7.771, 7.767, 7.763, 7.759, 7.755, 7.751, 7.747, 7.743, 7.739, 7.735, 7.731, 7.727, 7.723, 7.719, 7.715, 7.711, 7.707, 7.703, 7.699, 7.695, 7.691, 7.687, 7.683, 7.679, 7.675, 7.671, 7.667, 7.663, 7.659, 7.655, 7.651, 7.647, 7.643, 7.639, 7.635, 7.631, 7.627, 7.623, 7.619, 7.615, 7.611, 7.607, 7.603, 7.599, 7.595, 7.591, 7.587, 7.583, 7.579, 7.575, 7.571, 7.567, 7.563, 7.559, 7.555, 7.551, 7.547, 7.543, 7.539, 7.535, 7.531, 7.527, 7.523, 7.519, 7.515, 7.511, 7.507, 7.503, 7.499, 7.495, 7.491, 7.487, 7.483, 7.479, 7.475, 7.471, 7.467, 7.463, 7.459, 7.455, 7.451, 7.447, 7.443, 7.439, 7.435, 7.431, 7.427, 7.423, 7.419, 7.415, 7.411, 7.407, 7.403, 7.399, 7.395, 7.391, 7.387, 7.383, 7.379, 7.375, 7.371, 7.367, 7.363, 7.359, 7.355, 7.351, 7.347, 7.343, 7.339, 7.335, 7.331, 7.327, 7.323, 7.319, 7.315, 7.311, 7.307, 7.303, 7.299, 7.295, 7.291, 7.287, 7.283, 7.279, 7.275, 7.271, 7.267, 7.263, 7.259, 7.255, 7.251, 7.247, 7.243, 7.239, 7.235, 7.231, 7.227, 7.223, 7.219, 7.215, 7.211, 7.207, 7.203, 7.199, 7.195, 7.191, 7.187, 7.183, 7.179, 7.175, 7.171, 7.167, 7.163, 7.159, 7.155, 7.151, 7.147, 7.143, 7.139, 7.135, 7.131, 7.127, 7.123, 7.119, 7.115, 7.111, 7.107, 7.103, 7.099, 7.095, 7.091, 7.087, 7.083, 7.079, 7.075, 7.071, 7.067, 7.063, 7.059, 7.055, 7.051, 7.047, 7.043, 7.039, 7.035, 7.031, 7.027, 7.023, 7.019, 7.015, 7.011, 7.007, 7.003, 6.999, 6.995, 6.991, 6.987, 6.983, 6.979, 6.975, 6.971, 6.967, 6.963, 6.959, 6.955, 6.951, 6.947, 6.943, 6.939, 6.935, 6.931, 6.927, 6.923, 6.919, 6.915, 6.911, 6.907, 6.903, 6.899, 6.895, 6.891, 6.887, 6.883, 6.879, 6.875, 6.871, 6.867, 6.863, 6.859, 6.855, 6.851, 6.847, 6.843, 6.839, 6.835, 6.831, 6.827, 6.823, 6.819, 6.815, 6.811, 6.807, 6.803, 6.799, 6.795, 6.791, 6.787, 6.783, 6.779, 6.775, 6.771, 6.767, 6.763, 6.759, 6.755, 6.751, 6.747, 6.743, 6.739, 6.735, 6.731, 6.727, 6.723, 6.719, 6.715, 6.711, 6.707, 6.703, 6.699, 6.695, 6.691, 6.687, 6.683, 6.679, 6.675, 6.671, 6.667, 6.663, 6.659, 6.655, 6.651, 6.647, 6.643, 6.639, 6.635, 6.631, 6.627, 6.623, 6.619, 6.615, 6.611, 6.607, 6.603, 6.599, 6.595, 6.591, 6.587, 6.583, 6.579, 6.575, 6.571, 6.567, 6.563, 6.559, 6.555, 6.551, 6.547, 6.543, 6.539, 6.535, 6.531, 6.527, 6.523, 6.519, 6.515, 6.511, 6.507, 6.503, 6.499, 6.495, 6.491, 6.487, 6.483, 6.479, 6.475, 6.471, 6.467, 6.463, 6.459, 6.455, 6.451, 6.447, 6.443, 6.439, 6.435, 6.431, 6.427, 6.423, 6.419, 6.415, 6.411, 6.407, 6.403, 6.399, 6.395, 6.391, 6.387, 6.383, 6.379, 6.375, 6.371, 6.367, 6.363, 6.359, 6.355, 6.351, 6.347, 6.343, 6.339, 6.335, 6.331, 6.327, 6.323, 6.319, 6.315, 6.311, 6.307, 6.303, 6.299, 6.295, 6.291, 6.287, 6.283, 6.279, 6.275, 6.271, 6.267, 6.263, 6.259, 6.255, 6.251, 6.247, 6.243, 6.239, 6.235, 6.231, 6.227, 6.223, 6.219, 6.215, 6.211, 6.207, 6.203, 6.199, 6.195, 6.191, 6.187, 6.183, 6.179, 6.175, 6.171, 6.167, 6.163, 6.159, 6.155, 6.151, 6.147, 6.143, 6.139, 6.135, 6.131, 6.127, 6.123, 6.119, 6.115, 6.111, 6.107, 6.103, 6.099, 6.095, 6.091, 6.087, 6.083, 6.079, 6.075, 6.071, 6.067, 6.063, 6.059, 6.055, 6.051, 6.047, 6.043, 6.039, 6.035, 6.031, 6.027, 6.023, 6.019, 6.015, 6.011, 6.007, 6.003, 5.999, 5.995, 5.991, 5.987, 5.983, 5.979, 5.975, 5.971, 5.967, 5.963, 5.959, 5.955, 5.951, 5.947, 5.943, 5.939, 5.935, 5.931, 5.927, 5.923, 5.919, 5.915, 5.911, 5.907, 5.903, 5.899, 5.895, 5.891, 5.887, 5.883, 5.879, 5.875, 5.871, 5.867, 5.863, 5.859, 5.855, 5.851, 5.847, 5.843, 5.839, 5.835, 5.831, 5.827, 5.823, 5.819, 5.815, 5.811, 5.807, 5.803, 5.799, 5.795, 5.791, 5.787, 5.783, 5.779, 5.775, 5.771, 5.767, 5.763, 5.759, 5.755, 5.751, 5.747, 5.743, 5.739, 5.735, 5.731, 5.727, 5.723, 5.719, 5.715, 5.711, 5.707, 5.703, 5.699, 5.695, 5.691, 5.687, 5.683, 5.679, 5.675, 5.671, 5.667, 5.663, 5.659, 5.655, 5.651, 5.647, 5.643, 5.639, 5.635, 5.631, 5.627, 5

[illegible]

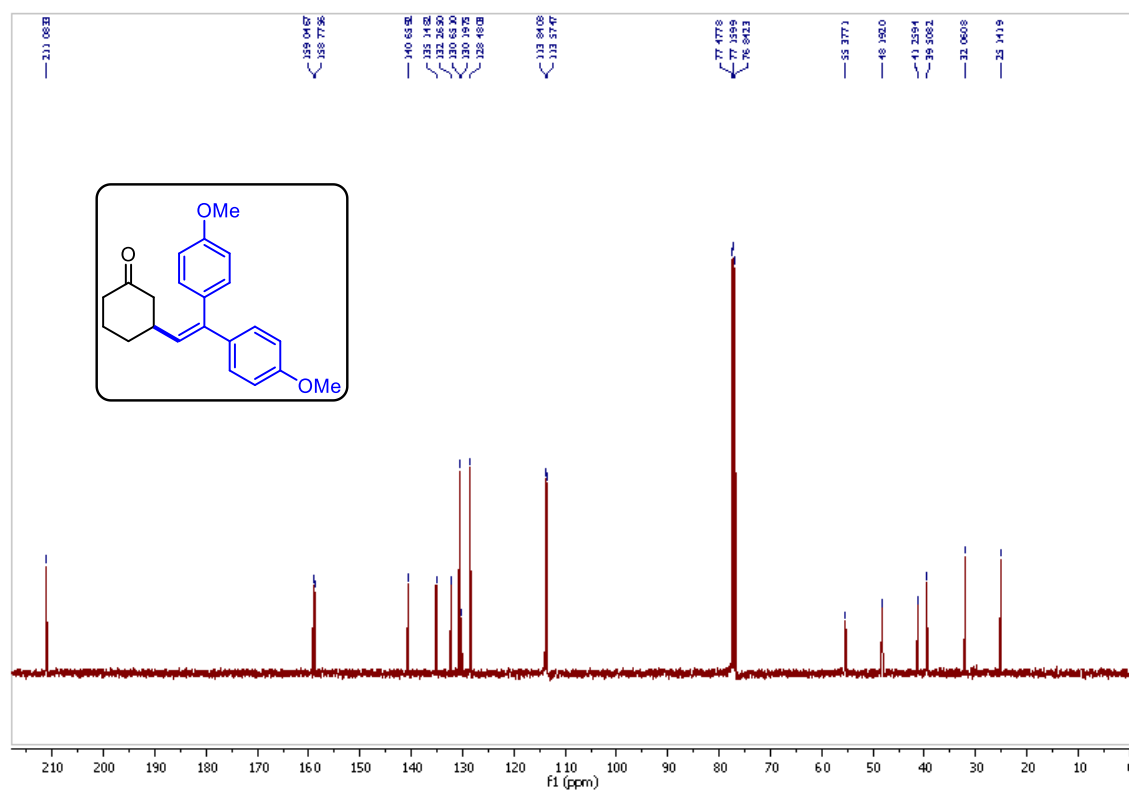
¹H NMR spectrum of **92e** (trans)



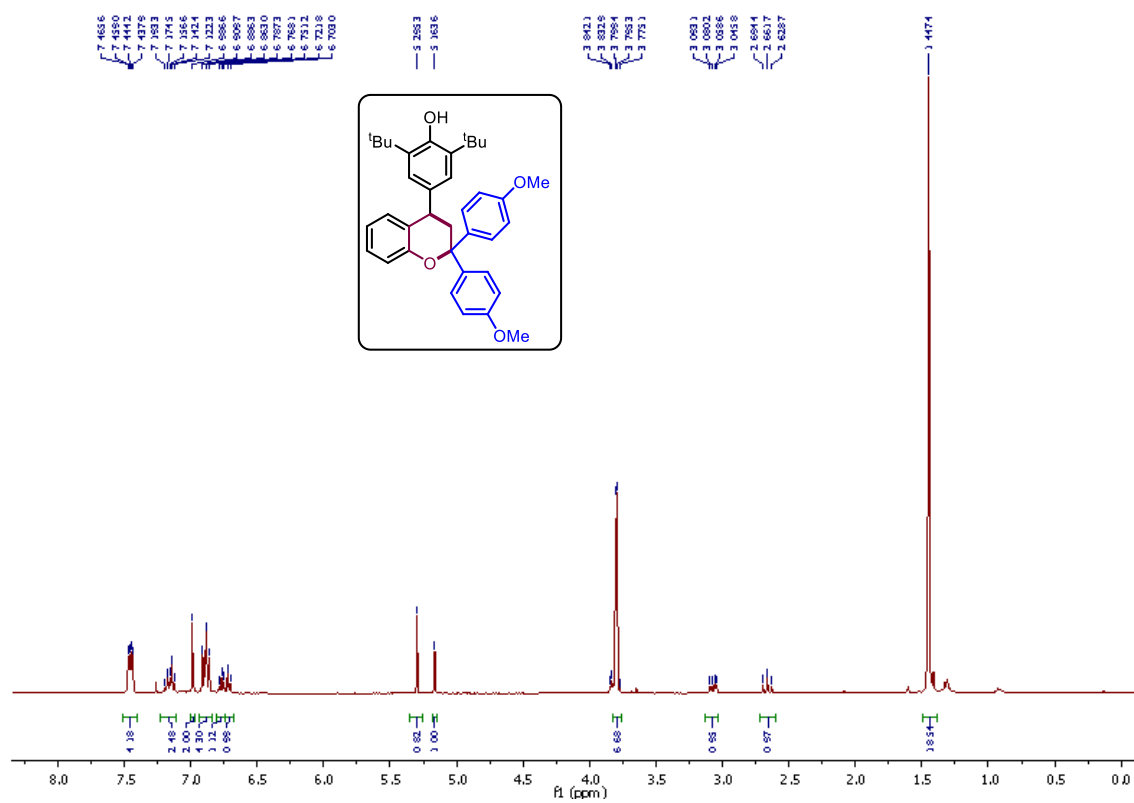
¹H NMR spectrum of **96e**

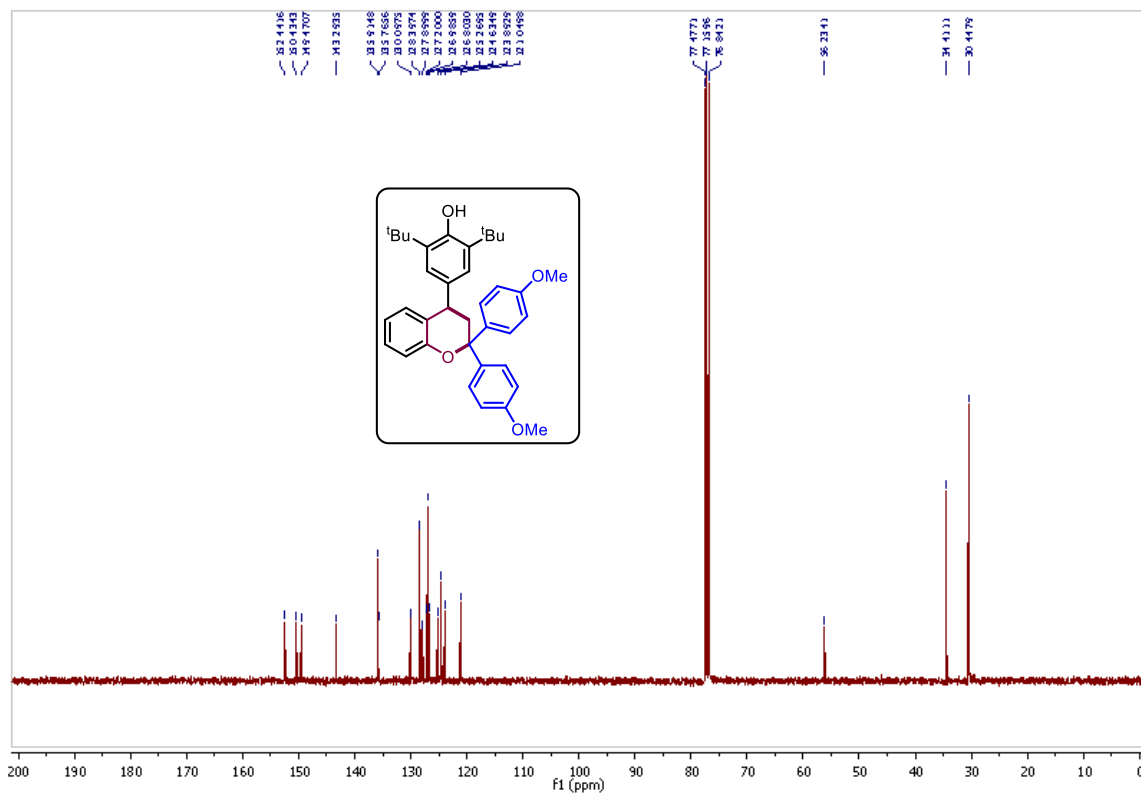
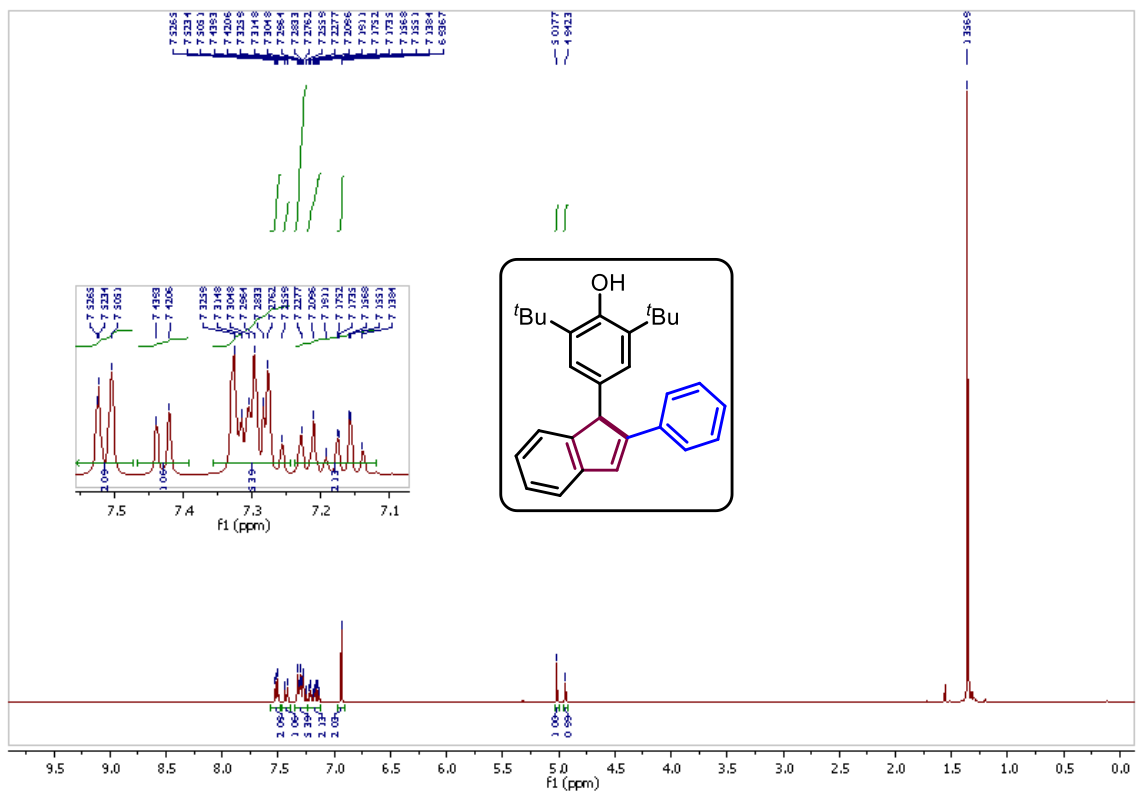


^{13}C NMR spectrum of **96e**

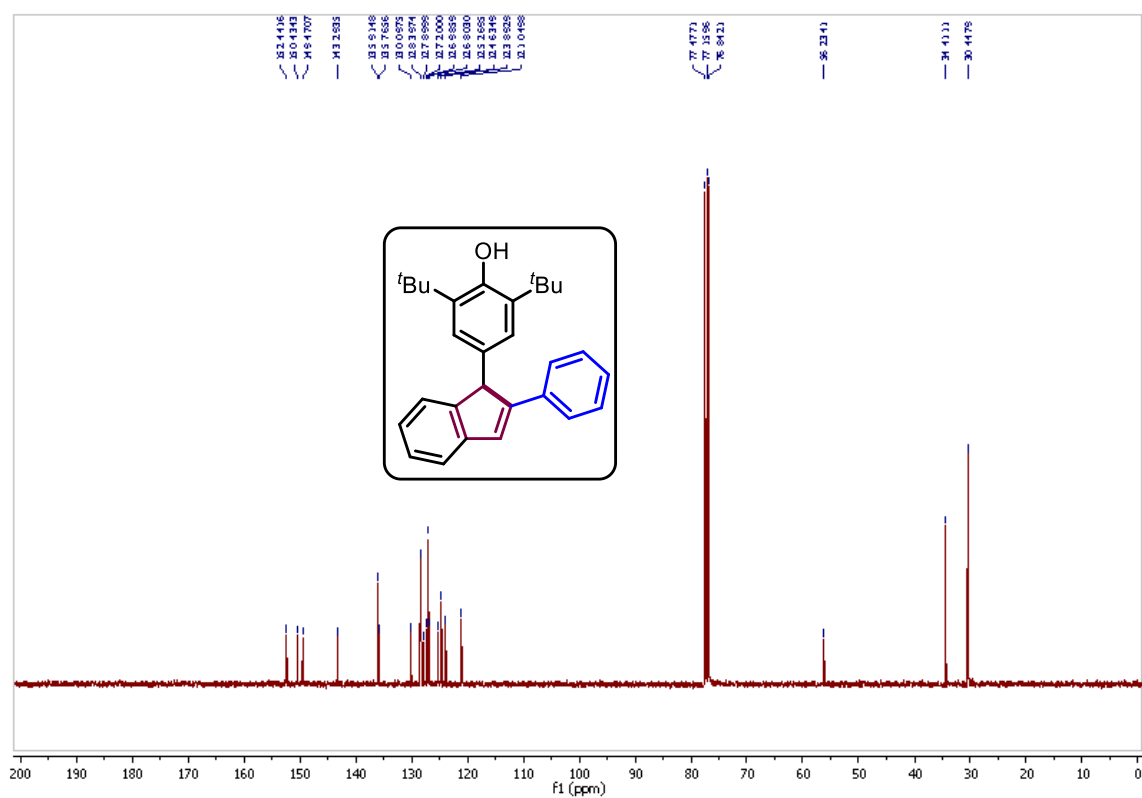


^1H NMR spectrum of **100**

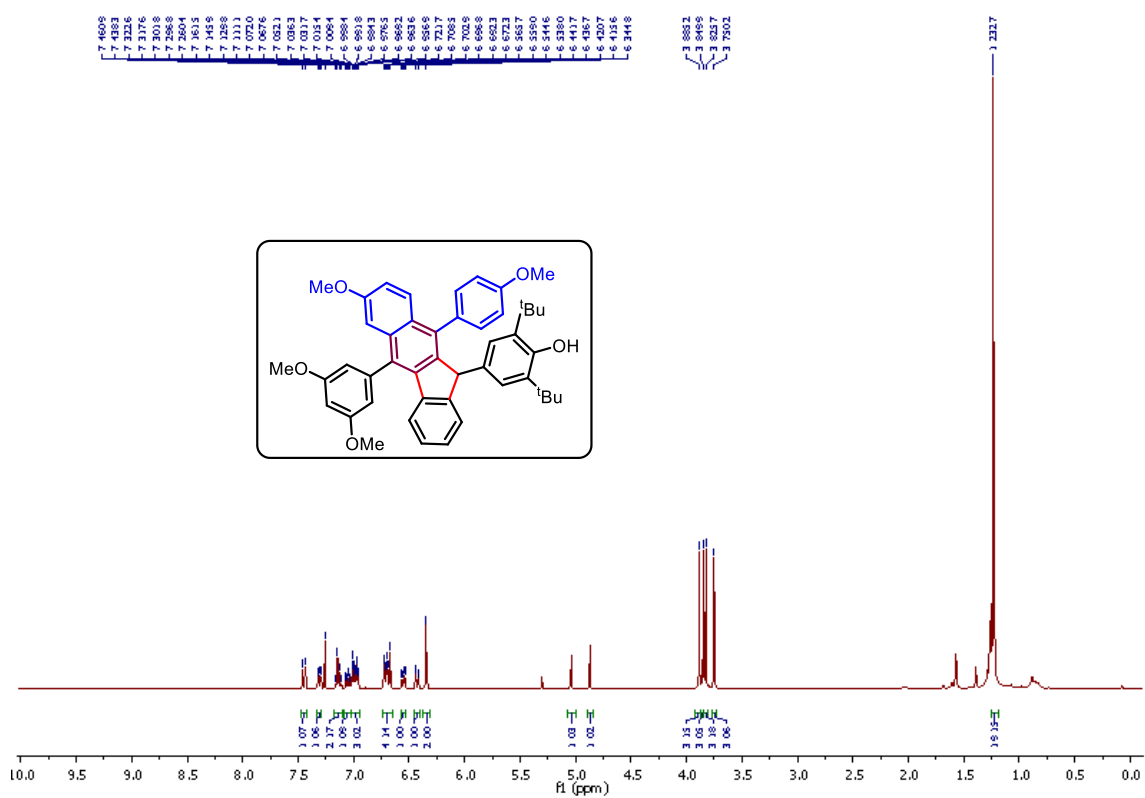


^{13}C NMR spectrum of **100**¹H NMR spectrum of **102**

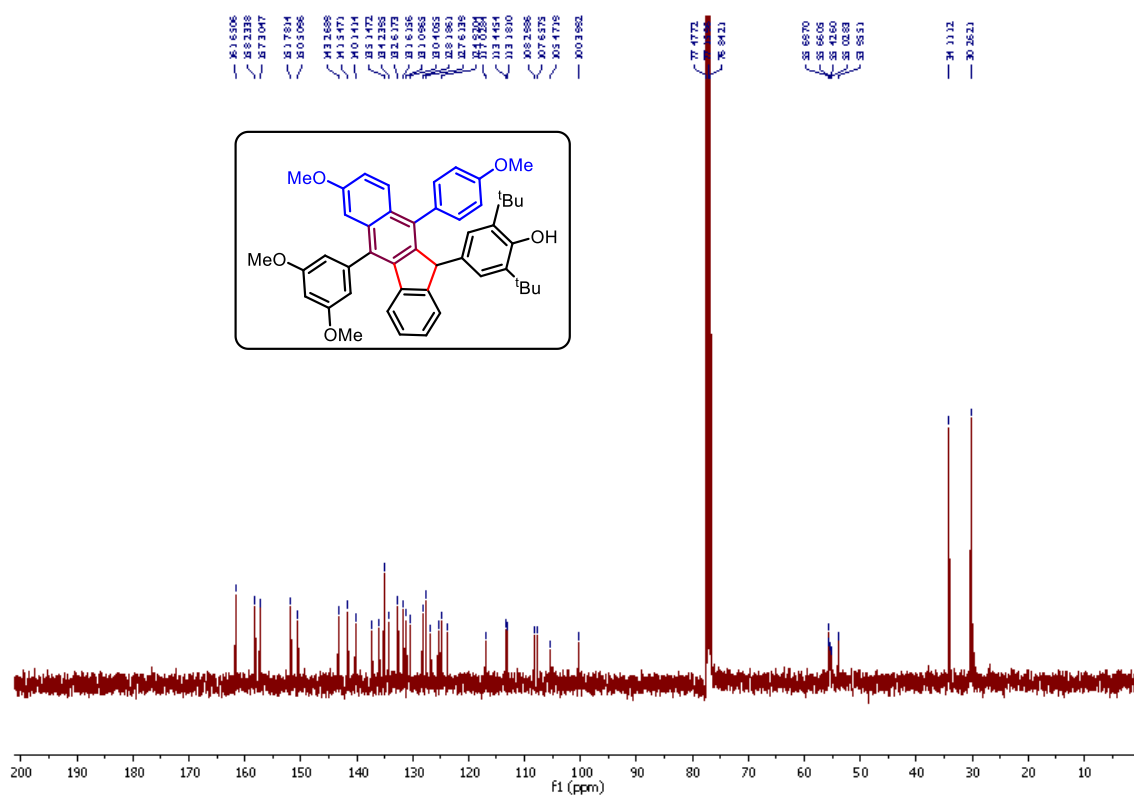
^{13}C NMR spectrum of **102**



^1H NMR spectrum of **109**

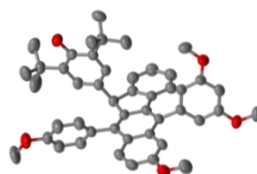
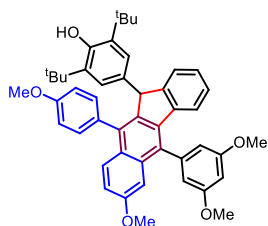


¹³C NMR spectrum of **109**



X-ray crystallographic analysis for compound 109

Identification code	109
Empirical formula	C ₄₇ H ₄₈ O ₅
Formula weight	692.85
Temperature/K	298.0(1)
Crystal system	monoclinic
Space group	I2/a
a/Å	18.9123(18)
b/Å	11.2310(10)
c/Å	36.841(3)
$\alpha/^\circ$	90.00
$\beta/^\circ$	99.090(8)
$\gamma/^\circ$	90.00
Volume/Å ³	7726.9(12)
Z	8
$\rho_{\text{calc}}/\text{cm}^3$	1.191
μ/mm^{-1}	0.076
F(000)	2960.0
Crystal size/mm ³	0.2 × 0.2 × 0.2
Radiation	Mo K α (λ = 0.71073)
2 θ range for data collection/ $^\circ$	4.94 to 65.64
Index ranges	-28 ≤ h ≤ 26, -15 ≤ k ≤ 14, -55 ≤ l ≤ 49
Reflections collected	46834
Independent reflections	13695 [R _{int} = 0.1300, R _{sigma} = 0.1821]
Data/restraints/parameters	13695/0/480
Goodness-of-fit on F ²	0.899
Final R indexes [I ≥ 2 σ (I)]	R1 = 0.0915, wR2 = 0.2229
Final R indexes [all data]	R1 = 0.2790, wR2 = 0.3477
Largest diff. peak/hole / e Å ⁻³	0.32/-0.31



CCDC NO. 2278568

4.7 References: -

- (1) Clayden, J.; Greeves, N.; Warren, S. *Organic Chemistry*; OUP: Oxford, **2012**, 254.
- (2) Olah, G. A.; Prakash, G. K. *Carbocation Chemistry*; Wiley: Hoboken, NJ, **2004**.
- (3) Merling, G. Ueber Tropin. *Berichte der deutschen chemischen Gesellschaft* **1891**, 24, 3108.
- (4) Sereda, O.; Tabassum, S.; Wilhelm, R. *Top. Curr. Chem.* **2009**, 291, 349.
- (5) Capaldo, L.; Quadri, L. L.; Ravelli, D. *Angew. Chem. Int. Ed.* **2019**, 58, 17508.
- (6) Mei, L.; Gianetti, T. *Synlett.* **2021**, 32, 337.
- (7) Naidu, V. R.; Ni, S.; Franzén, J. *ChemCatChem* **2015**, 7, 1896.
- (8) Bah, J.; Franzén, J. *Chem. Eur. J.* **2014**, 20, 1066.
- (9) Xiao, W.; Wu, J. *Chinese Chem. Lett.* **2021**, 32, 2751.
- (10) Lyons, D. J. M.; Crocker, R. D.; Enders, D.; Nguyen, T. V. *Green Chem.* **2017**, 19, 3993.
- (11) Pommerening, P.; Mohr, J.; Friebel, J.; Oestreich, M. *Eur. J. Org. Chem.* **2017**, 2017, 2312.
- (12) Zhang, Q.; Lv, J.; Li, S.; Luo, S. *Organic Letters* **2018**, 20, 2269.
- (13) Zhang, Q.; Lv, J.; Luo, S. *Beilstein J. Org. Chem.* **2019**, 15, 1304.
- (14) Ludwig, J. R.; Zimmerman, P. M.; Gianino, J. B.; Schindler, C. S. *Nature* **2016**, 533, 374.
- (15) Ludwig, J. R.; Phan, S.; McAtee, C. C.; Zimmerman, P. M.; Devery, J. J. I. I.; Schindler, C. S. *J. Am. Chem. Soc.* **2017**, 139, 10832.
- (16) McAtee, C. C.; Riehl, P. S.; Schindler, C. S. *J. Am. Chem. Soc.* **2017**, 139, 2960.
- (17) Groso, E. J.; Golonka, A. N.; Harding, R. A.; Alexander, B. W.; Sodano, T. M.; Schindler, C. S. *ACS Catal.* **2018**, 8, 2006.
- (18) Ma, L.; Li, W.; Xi, H.; Bai, X.; Ma, E.; Yan, X.; Li, Z. *Angew. Chem. Int. Ed.* **2016**, 55, 10410.
- (19) Tran, U. P. N.; Oss, G.; Pace, D. P.; Ho, J.; Nguyen, T. V. *Chem. Sci.* **2018**, 9, 5145.
- (20) Ni, S.; Franzén, J. *Chem. Commun.* **2018**, 54, 12982.
- (21) Mann, J. S.; Mai, B. K.; Nguyen, T. V. *ACS Catal.* **2023**, 13, 2701.
- (22) Ni, S.; El Remaily, M. A. E. A. A.; Franzén, J. *Adv. Syn. Catal.* **2018**, 360, 4204.
- (23) Hussein, M. A.; Huynh, V. T.; Hommelsheim, R.; Koenigs, R. M.; Nguyen, T. V. *Chem. Commun.* **2018**, 54, 12970.
- (24) Shang, W.; Duan, D.; Liu, Y.; Lv, J. *Org. Lett.* **2019**, 21, 8013.

- (25) Rekha; Sharma, S.; Singh, G.; Anand, R. V. *ACS Org. Inorg. Au* **2022**, 2, 186.
- (26) Liu, J.; Xu, J.; Li, Z.; Huang, Y.; Wang, H.; Gao, Y.; Guo, T.; Ouyang, P.; Guo, K. *Eur. J. Org. Chem.* **2017**, 2017, 3996.
- (27) Patterson, W. J.; Lucas, K.; Jones, V. A.; Chen, Z.; Bardelski, K.; Guarino-Hotz, M.; Brindle, C. S. *Eur. J. Org. Chem.* **2021**, 48, 6737.
- (28) Zhu, W.; Sun, Q.; Wang, Y.; Yuan, D.; Yao, Y. *Org. Lett.* **2018**, 20, 3104.
- (29) Oss, G.; Ho, J.; Nguyen, T. V. **2018**, 29, 3974.
- (30) Jin, H.; Rudolph, M.; Rominger, F.; Hashmi, A. S. K. *ACS Catal.* **2019**, 9, 11663.
- (31) Rulev, Y. A.; Gugkaeva, Z. T.; Lokutova, A. V.; Maleev, V. I.; Peregudov, A. S.; Wu, X.; North, M.; Belokon, Y. N. *ChemSusChem* **2017**, 10, 1152.
- (32) Omoregbee, K.; Luc, K. N. H.; Dinh, A. H.; Nguyen, T. V. *J. Flow Chem.* **2020**, 10, 161.
- (33) Doan, S. H.; Hussein, M. A.; Nguyen, T. V. *Chem. Commun.* **2021**, 57 8901.
- (34) Mei, L.; Moutet, J.; Stull, S. M.; Gianetti, T. L. *J. Org. Chem.* **2021**, 86, 10640.
- (35) Stull, S. M.; Mei, L.; Gianetti, T. L. *Synlett.* **2021**, 33, 1194.
- (36) Ton, N. N. H.; Mai, B. K.; Nguyen, T. V. *J. Org. Chem.* **2021**, 86, 9126.
- (37) Ranga, P. K.; Ahmad, F.; Nager, P.; Rana, P. S.; Anand, R. V. *J. Org. Chem.* **2021**, 86, 50494.
- (38) Weiss, R.; Kölbl, H.; Schlierf, C. *J. Org. Chem.* **1976**, 41, 2262.
- (39) Breslow, R.; Chang, H. W. *J. Am. Chem. Soc.* **1961**, 83, 2375.
- (40) Sivaranjini, B.; Mangaiyarkarasi, R.; Ganesh, V.; Umadevi, S. *Scientific Reports*, **2018**, 8, 8888.
- (41) (a) Ho, C.-Y.; Ohmiya, H.; Jamison, T. F. *Angew. Chem., Int. Ed.* **2008**, 47, 1890. (b) Ogoshi, S.; Haba, T.; Ohashi, M. *J. Am. Chem. Soc.* **2009**, 131, 10346. (c) Zhao, C.; Toste, F. D.; Bergman, R. G. *J. Am. Chem. Soc.* **2011**, 133, 1078. (d) Okamoto, K.; Tamura, E.; Ohe, K. *Angew. Chem., Int. Ed.* **2013**, 52, 10636. (e) Li, K.; Wan, Q.; Kang, Q. *Org. Lett.* **2017**, 19, 3300.
- (42) (a) Reddy, V.; Anand, R. V. *Org. Lett.* **2015**, 17, 3390. (b) Jadhav, A. S.; Anand, R. V. *Org. Biomol. Chem.* **2017**, 15, 56. (c) Jadhav, A. S.; Pankhade, Y. A.; Anand, R. V. *J. Org. Chem.* **2018**, 83, 8606.
- (43) Goswami, P.; Anand, R. V. *Chemistry Select* **2016**, 1, 2556.
- (44) Jadhav, A. S.; Pankhade, Y. A.; Hazra, R.; Anand, R. V. *J. Org. Chem.* **2018**, 83 10119.
- (46) (a) Reddy, V.; Anand, R. V. *Org. Lett.* **2015**, 17, 3390. (b) Chu, W.-D.; Zhang, L.-F.; Bao, X.; Zhao, X.-H.; Zeng, C.; Du, J.-Y.; Zhang, G.-B.; Wang, F.-X.; Ma, X.-Y.; Fan,

- C.-A. *Angew. Chem. Int. Ed.* **2013**, 52, 9229.
- (47) Holschumacher, D.; Hrib, C. G.; Jones, P. G.; Tamm, M. *Chem. Commun.* **2007**, 3661.
(b) Wilde, M. M. D.; Gravel, M. *Angew. Chem. Int. Ed.* **2013**, 52, 12651.
- (48) Elkanzi, N. A.; Hrichi, H.; Alolayan, R. A.; Derafa, W.; Zahou, F. M.; Bakr, R. B. *ACS Omega.* **2022**, 7, 27769.
- (49) Colowick, S. P. NO KAPLAN Method in Enzymology. Academic Press, New York **1955**.
- (50) (a) Pellissier, H. *Tetrahedron* **2005**, 61, 6479. (b) Nejrotti, S.; Iannicelli, M.; Jamil, S. S.; Arnodo, D.; Blangetti, M.; Prandi, C. *Green Chem.* **2020**, 22, 110.

CURRICULUM VITAE

Mr. Pavit Kumar Ranga

Department of Chemical Science, Indian Institute of Science Education and Research, Mohali
E-mail: pavitranga32@gmail.com

Mob: +91-8837534525

Experimental Organic Chemistry Skill:

- Firsthand experience in setting up a synthetic organic chemistry lab and designing projects.
- Good knowledge of organic, organocatalysts chemistry [Cyclopropenium ion, Bis(amino)cyclopropenylidene {BACs} *N*- heterocyclic carbene and chiral phosphoric acid catalysis].
- Good knowledge and hands-on experience in continuous flow microreactor.
- Experience in the isolation, purification, and characterization of a wide range of organic compounds by modern chromatographic and spectroscopic (IR, NMR, and HRMS) techniques. Proficiency in handling IR, 400 MHz NMR, and HPLC.
- Excellent practical skills in handling air/moisture sensitive reagents/reactions and milligram/gram scale reactions.
- Excellent knowledge of Windows family operating system with good command of Microsoft Word and PowerPoint, software packages including ChemDraw, expertise in E-notebook writing, Sci-Finder usage for searching literature/patents and handling NMR software's Top Spin, Mnova, and spin works).
- Guided undergraduate students and research associates extensively and mentored them in formulating their projects.

Research Expertise: Natural product synthesis, Organometallic Chemistry, and Continuous flow chemistry.

- **2016 –: Ph. D. in Synthetic Organic Chemistry**, Department of Chemical Sciences, Indian Institute of Science Education and Research (IISER) Mohali,

140306, Punjab, India.

- **Thesis Title:** “Cyclopropenium Ions Catalyzed Organic transformations and their application in total synthesis of resveratrol-derived natural products”
 - **Ph.D. Thesis Supervisor:** Prof. R. Vijaya Anand
- **2014 - 2016: Project Assistant, Regional Centre of Biotechnology (LNCB Lab),** Faridabad, India. **P.I :** Prof. Avinash Bajaj
- **2011 – 2013: M.Sc. in Chemistry, Kurukshetra University,** Kurukshetra, 136119, India with **First Class.**
- **2008 – 2011: Bachelor of Science, Government P.G. College (KUK),** Hisar, India with **First Class.**

- Awarded **Senior Research Fellowship** and **Junior Research Fellowship** (MHRD Fellowship) from the Indian Institute of Science Education and Research (IISER) Mohali from August 2016 to July 2021.
- Qualified Graduate Aptitude Test in Engineering (**GATE**) examination held on year **2014.**
- Qualified **CSIR-NET** with all India 59th rank in **CSIR-UGC NET** (Council of Scientific and Industrial Research-University Grants Commission National Eligibility Test) examination held on June 2013.
- Qualified IIT-JAM held in year **2011.**

1. **Ranga, P. K.;** Ahmad, F.; Nager, P.; Rana, P. S.; Anand, R. V. Bis(amino)cyclopropenium Ion as a Hydrogen-Bond Donor Catalyst for 1,6-Conjugate Addition Reactions. *J. Org. Chem.* **2021**, 86, 4994–5010.
2. **Ranga, P. K.;** Ahmad, F.; Singh, G.; Tyagi, A.; Anand, R. V. "Recent Advances in the Organocatalytic Applications of Cyclopropene- and Cyclopropenium-based Small Molecules" *Org. Biomol. Chem.* **2021**, 19, 9541 – 9564.
3. **Ranga, P. K.;** Ahmad, F.; Fatma, S.; Kumar, A.; Wadhawe, A.B.; Saini, P.; Kumar, V.; Anand, R. V. “Tris-arylcyclopropenium carbocation as a highly promising organocatalyst

in fundamental organic transformation such as Nazarov cyclization conjugate addition reactions and inter & intramolecular CAM reaction.” (*manuscript under preparation*)

4. **Ranga, P. K.;** Ahmad, F.; Fatma, S.; Kumar, A.; Wadhwa, A.B.; Saini, P.; Kumar, M.; Anand, R. V. “BACs. Catalyzed intramolecular cyclization through umpolung of aldehyde followed by 1,6 conjugate addition reaction: excess to various resveratrol based natural products.” (*manuscript under preparation*)
5. Ahmad, F.; **Ranga, P. K.;** Fatma, S.; Pankhade, Y. A.; Gauda, A.; Anand, R. V. “Pd(II)-catalyzed annulation of terminal alkynes with 2-pyridinyl-substituted *p*-quinone methides: direct access to indolizines” *Chem. Commun.* **2022**, 58, 13238 – 13241.
6. Ahmad, F.; **Ranga, P. K.;** Fatma, S.; Kumar, A.; Anand, R. V. “Cu(II)-Catalyzed [3+2]-Annulation of 2-Pyridinyl-substituted *p*-Quinone Methides with Enaminones: Access to Functionalized Indolizine Derivatives” (*Manuscript submitted*)

-
- Presented a poster on “*Bis(amino)cyclopropenium Ion as a Hydrogen-bond Donor Catalyst for 1,6-Conjugate Addition Reactions*” **Ranga, P. K.;** Anand, R. V. in the *International Conference On Advancing Green Chemistry: Building A Sustainable Tomorrow* held at University of Delhi, India (3-4th October, 2017)
 - Presented a poster on “*Bis(amino)cyclopropenium Ion as a Hydrogen-bond Donor Catalyst for 1,6-Conjugate Addition Reactions*” **Ranga, P. K.;** Anand, R. V. in the *15th Junior National Organic Symposium (J-NOST)* held at CSIR- Indian Institute of Chemical Technology, Hyderabad, India (28-1st December, 2018).
 - Participated in the *Recent Advances In Organic And Bioorganic Chemistry (RAOBC)* held at the Department of Chemical Sciences, Indian Institute of Science Education and Research (IISER) Mohali, S. A. S. Nagar, India (22-24th March, 2019).